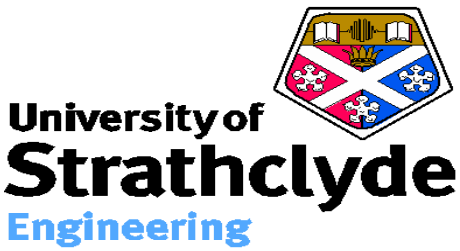

Dynamic Coupling of Air Culvert Air Conditioning Hybrid Cooling System in Buildings

A thesis submitted in fulfillment of the requirements for the Degree of Doctor of Philosophy

Ahmad Qatnan Alanezi B.Sc. M.Sc.

Department of Mechanical & Aerospace Engineering
Energy Systems Research Unit
Glasgow, United Kingdom
August 2012

Dedicated to My

Parents, *Qatnan and Qutna*
Wife, *Hanadi*
And Children, *Abdullah, Mohammed, Khaled and Bader*

COPYRIGHT DECLARATION

Acknowledgments

From the bottom of my heart I thank Allah (أالله) (SWT) for enlightening my heart and granting me with strength to be able to finish this PhD degree enjoying every moment of it.

I am genuinely grateful to my supervisor, Professor Joe Clarke, whose encouragement, guidance and support enabled me to develop an understanding of this research.

Distinguished appreciation goes to the Public Authority of Applied Education and Training (PAAET) in Kuwait for sponsoring me throughout the dissertation.

Special thanks are extended to Mr. Bobby McQueen and Mr. Jim Smith from Glasgow City Council for providing valuable data and information on the air culvert at Drumchapel Sports Centre. It is my pleasure to mention the following persons from ESRU, who helped me to acquire essential modelling knowledge: Dr. Aizaz Samuel, Dr. Alaa Al-Mosawi, Dr. Georgios Kokogiannakis, Dr. John Hand and Dr. Paul Strachan.

I gratefully thank my parents, my wife, and my children, to whom this work is dedicated, for their love and support.

Table of Contents

List of Figures

List of Tables

List of Abbreviations

A/C	Air-Conditioning
AHU	Air Handling Unit
ANSI	American National Standards Institute
ASHRAE	American Society of Heating, Refrigeration, and Air-Conditioning
BP	British Petroleum
CAD	Computer Aided Design
CAV	Constant Air Volume
CFD	Computational Fluid Dynamics
CIBSE	Chartered Institution of Building Services Engineers
CO_2	Carbon dioxide
CPU	Central Processing Unit
CV	Control Volume
D	Dimensional
DX	Direct expansion
EAHE	Earth-to-Air Heat Exchanger
ESP-r	Environmental System Performance – research
ESRU	Energy Systems Research Unit
EU	European Union
GCC	Gulf Cooperation Council
GDP	Gross Domestic Product
GHG	Greenhouse Gas
GW	Giga-Watt
HCFC	Hydro-Chlorofluorocarbon
HVAC	Heating, Ventilation, and Air-Conditioning

I	Input
IAQ	Indoor Air Quality
IEA	International Energy Agency
kW	Kilo-Watt
kWh	Kilo-Watt-hour
MEW	Ministry of Electricity and Water
Mt	Mega-tonnes
mtoe	million tonnes of oil equivalent
MWh	Mega-Watt-hour
O	Output
O_3	Ozone
PCMs	Phase Change Materials
PID	Proportional Integral Derivative
PV	Photovoltaic
R^2	Coefficient of determination
TRNSYS	Transient System Simulation Program
TWh	Tera-Watt-hour
UAE	United Arab Emirates
UK	United Kingdom
UN	United Nations
USA	United States of America
VAV	Variable Air Volume
W	Watt
WBCSD	World Business Council for Sustainable Development

Nomenclature

A	Area [m^2]
c_p	Specific heat capacity at constant pressure [J/kg·K]
COP	Coefficient of Performance [-]
D	Diameter [m]
h	Enthalpy [kJ/kg]
h_c	Convective heat transfer coefficient [$W/m^2 \cdot K$]
H	Height [m]
k	Thermal conductivity [W/m·K]
L	Length [m]
$\dot{m}$	Mass flow rate [kg/s]
NP	Number of People [-]
NTU	Number of Transfer Units [-]
Nu	Nussalt Number [-]
p	Pressure [Pa]
P	Power [W]
PPD	Percentage of People Dissatisfied [%]
Pr	Prandtl Number [-]
Q	Heat [J]
R	Thermal resistance [m^2K/W]
Re	Reynolds Number [-]
RH	Relative humidity [%]
T	Temperature [°C]
U	Overall heat transfer coefficient [$W/m^2.K$]

V	Velocity [m/s]
$\dot{V}$	Volume flow rate [m^3/s]
w	Width [m]

Greek Symbols

ω	Humidity ratio [kg/ (kg dry air)]
ρ	Density [kg/m^3]
α	Thermal diffusivity [m^2/s]
v	Kinematic viscosity [m^2/s]
ε	Culvert temperature effectiveness [-]
f	Friction factor [-]
δ	Culvert wall thickness [m]
Δ	Change [-]
η	Fan efficiency [-]

Subscripts

a	Air
ama	annual mean ambient
amb	Ambient air
d	Dew-point
db	Dry-bulb
e	Moist air entering the cooling coil
E	Entrance
g	Ground
h	Hydraulic
hag	high annual ground

in	Indoor
L	Latent
lag	low annual ground
oc	Outlet air of culvert
p	Apparatus dew point
s	Standard
S	Sensible
v	Ventilation
w	Culvert internal wall
wb	Wet-bulb

Abstract

Active and passive cooling methods have been the subject of much investigation. Nevertheless, there remains a significant opportunity to utilise the so-called 'responsive building elements' and to arrange for cooperative deployment with downsized, conventional HVAC systems. The integration of an air culvert with an active cooling system along with associated control is the subject of this thesis. The issues studied within this thesis are as follows.

- The quantification of air culvert thermal efficacy.
- The elaboration of an integrated system design method that accounts for the transient interaction between the air culvert and the air conditioning systems.
- The requirement for hybrid system control when deployed within different climates.

The ESP-r system was adopted within the present work. A ground temperature model was established for the hot/dry climate location selected and validated against measured soil temperature profiles. A culvert model was derived and verified empirically and by inter-model comparison. Results showed that the ESP-r model can robustly quantify the thermal performance of an air culvert. The culvert was then coupled to a residential villa situated in the hot/arid climate domain and its contribution explored. A constant air volume air-conditioning system was then linked to the culvert-building model and used to research approaches to the control of such a hybrid cooling system. A general control strategy was then devised corresponding to specific objectives and constraints. Results confirmed that the final control set-up can be implemented for a culvert/HVAC hybrid cooling system regardless of climate type, with cooling load matching in excess of 85% keeping indoor resultant temperatures within comfort threshold limits.

The project conclusion is that a culvert may be deployed in a manner that allows significant down-sizing of conventional cooling plant, thereby achieving both capital and running costs savings without appreciable loss of amenity.

Chapter 1 : Introduction

Energy demand is reviewed and the energy consumption of buildings due to active cooling measures in high per capita energy consumption regions is emphasized. The significance of acquiring hybrid cooling systems for buildings in hot-arid climates is highlighted.

1.1 Worldwide Energy Overview

Energy consumption has increased dramatically in the early 20th century due to the industrial revolution. Industry, transportation and buildings are the main energy consuming sectors worldwide. Buildings account for nearly 50% of the energy consumed in developed countries (Harris & Elliot 1997) and this figure will be approached in developing countries in future as their economies grow. From an economic perspective, the energy supply must match or exceed demand so that the price of energy does not escalate. Another issue, however, is that those increasingly stringent environmental standards have to be met. Therefore, solving the growing energy dilemma will require new, clean energy supplies and a radical reduction in energy demand.

1.1.1 Energy Demand Side

"*The global energy demand quadrupled between 1950 and 2000 and is likely to be doubled or tripled by 2050*" is one of the key remarks made by WBCSD (2004). The two essential reasons behind this energy increase in 1950-2000 were population growth (56% increase) and increasing GDP (260% growth). The world's population is expected to increase by 50% in the first half of the 21st Century, reaching 9 billion by 2050 as reported by the UN population division (2001). GDP in GCC[1] is expected to increase exponentially in the coming years as oil prices rise due to shortage in oil reserves elsewhere alongside a more global demand for this commodity. Energy demand in GCC will be increasing and especially for cooling of buildings as a response to the expected population increase and economic growth.

[1] GCC is a council that includes Bahrain, Kuwait, Oman, Qatar, Saudi Arabia, and U.A.E.

The energy required to cool and heat buildings is approximately 7% of the total world energy consumption and this can be reduced by around 2.5% if buildings are efficiently designed (Agrawal 1988). Due to an increase in the standard of living, reduction in the cost of air-conditioning, and urban heat island effects, there is a growth in building cooling even in temperate and cool regions. Watkins et al. (2002) reported a heat island intensity for London of 7ºC during summer time. This requires the use of mechanical cooling particularly in modern commercial buildings where internal heat sources dominate and window opening is not possible (Jenkins 2009). Building cooling energy consumption in EU countries was about 1.9TWh in 1990 and it is expected to surpass 44TWh by 2020 (Adnot 1999). The corresponding CO_2 emissions would then rise from 0.516Mt to 18.1Mt over the same period.

1.2 Cooling of Buildings in Hot/Arid Regions

Peel et al. (2007) reported that hot/dry climate regions represent approximately 14% of the earth land. Buildings in such climates in the Northern hemisphere require the use of mechanical cooling continuously from April to November in order for occupants to be thermally comfortable. Cooling degree days in Kuwait from June 1 2010 until May 31 2011 equated to 3765°Cday.yr^{-1} for a base temperature of 18°C (BizEE Software 2011). Table 1.1 shows that Kuwait and all GCC countries accounted, respectively, for 0.24% and 2.76% of the global energy consumption for the year 2006, with only 0.043% and 0.6% of the world population residing in Kuwait and GCC regions respectively. GCC is the world's highest per capita[2] energy consumption region due to the excessive use of active cooling: for example, Kuwait consumes 16.7MWh compared to the world average of 2.8MWh. In the UK and EU the corresponding figure is 6.1MWh and 6.3MWh respectively (IEA 2008). Energy performance and the environmental consequences of buildings in the GCC region are disturbing. According to AboulNaga and Elsheshtawy (2001), the average cooling energy consumption in domestic UAE buildings is 213kWh/m^2/yr whereas the existing residential building cooling energy consumption profile in the GCC region stretches to 250kWh/m^2/yr. Hence, it is of a paramount importance in

[2]Energy per capita is the division of total energy consumption by the population.

this part of the world to use energy efficiently because conventional energy supply facilities are expensive and give rise to environmental impact. The only renewable energy source that can be used at the large scale in the GCC region is solar energy. However, the efficiency of converting solar energy into electricity is reduced during the summer season in GCC because of the high ambient temperature. Moreover, money spent on energy conservation usually gives better long-term benefit than money spent on increased power generation and energy supply capacity enhancement as concluded by Beggs (2009).

Table 1.1: World energy consumption in 2006 (BP 2007).

Region	Energy consumption (mtoe)	Percentage of world (%)
Kuwait	25.6	0.24
GCC States	300	2.76
South & Central America	528.6	4.86
North America	2803	25.77
Europe & Eurasia	3027.2	27.83
Africa	324.1	2.98
Asia Pacific	3641.5	33.47

1.2.1 Methods for Cooling of Buildings

Refrigeration has several uses one of which is air conditioning. Vapour compression systems are preferred for air conditioning systems due to their comparatively high COP, simplicity of operation, cost-effectiveness and low maintenance (Cengel & Boles 2006). All-air, all-water and air-water systems are the air conditioning types available. CAV and VAV approaches can be incorporated in single-zone, multi-zone, double-duct, and reheat systems, with more energy efficiency but less IAQ due to poor ventilation of the VAV systems over their CAV counterparts (Wang et al. 2000). A single-zone, all-air CAV A/C system is selected in the present work to contribute to the hybrid cooling system since it is the A/C type commonly used in small residences (ASHRAE Handbook 2004): its sensible and latent cooling load is transported by air and is thus compatible with an air culvert, the passive cooling device studied in this thesis. A CAV system is straightforward, with no complications in use, and its implementation is cheap in contrast to the VAV air-conditioning system. However, the latter system can save more energy because it regulates the air volume flow rate entering a building zone. The higher the ambient

air temperature and solar insolation there is, the more the need for mechanical cooling will be, which puts an added burden on the electricity grid, particularly during summer peak conditions. The fact that a mechanical cooling system introduces little fresh air to the indoors, to save energy, also raises IAQ problems. The impact of active cooling systems on the environment is worrying where HCFCs give rise to GHG emission. Dependence on mechanical cooling systems is costly in the long run since they use the peak time electricity even during summer non-peak times where the A/C plant should operate at part-load; nevertheless, it cycles on and off, operating at full load to satisfy the building cooling set-point air temperature. In summary, the limitations of active cooling systems are as follows.

1. Peak electricity load increase.
2. Environmental impact due to global warming.
3. Increased long-term cost.
4. IAQ issues.

It is widely perceived that the indoor comfort of buildings is accomplished at the expense of increased energy consumption due to active cooling utilization; passive cooling contributes to reducing or eliminating this expense. Buildings can be cooled by passive schemes through heat discharge to natural heat sinks such as the ambient air, sky and soil. The appropriateness of any passive cooling system not only depends on the indoor conditions but also on the building type and the site microclimate. Passive heating systems invariably contribute to the comprehensive thermal efficacy of a building; conversely, erroneous selection of a passive cooling approach may seriously exacerbate these same conditions. In hot climates, occupants are acclimatized to warmer environments and this fact will dictate the climate boundaries under which a particular passive cooling system can be applied (Santamouris & Asimakopoulos 1996). Ventilation cooling, desiccant cooling, evaporative cooling, radiant cooling and ground cooling are the main passive cooling techniques. Ground air cooling is the passive cooling mechanism selected for this thesis. There are two ways to integrate ground air cooling into a building: direct and indirect. The former method requires that the building be fully or partially built underground and it is appropriate to hot-arid climates with moderate winters because high heat loss rates are associated with this method during winter (Santamouris &

Asimakopoulos 1996). The latter approach pre-cools the air entering the building by incorporating culverts. They can be applied in open or closed loop mode; when the culvert inlet and outlet are positioned within the building the approach is termed closed loop, but when the ambient air is drawn directly through the inlet by a fan passing across the culvert, it is termed an open loop as depicted in Figure 1.1. The closed loop scenario has lost impetus versus its open loop counterpart as fresh air requirements are compromised. The indirect, open loop air culvert is the passive cooling technique used in the hybrid cooling system studied in this thesis.

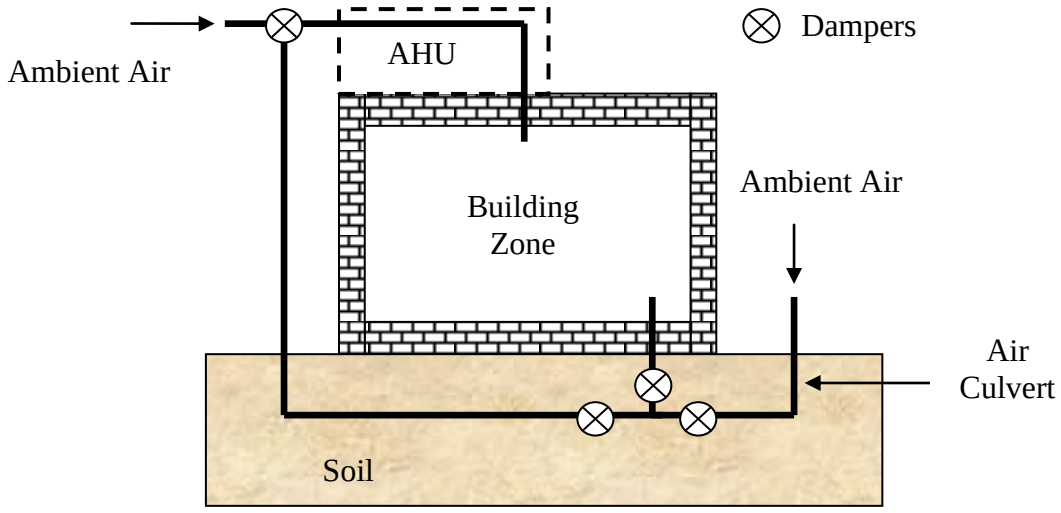

Figure 1.1: An air culvert air conditioning hybrid cooling system coupled to a building.

1.3 Hybrid Cooling Systems

Passive cooling alone can not yield indoor thermal comfort if the climate is hot, while providing thermal comfort for a space by only active cooling is an energy intensive process. On the other hand, hybrid cooling approaches employ combinations of passive and active systems to reduce energy consumption. They comprise two or more cooling technologies in a manner that overcomes the limitations of any one approach. Active cooling and some passive cooling methods have been extensively studied throughout the years and have reached a level of maturity. However, there is still a huge potential to improve the so-called ’responsive building elements ‘and arrange for their integration with conventional HVAC systems. Responsive building elements include advanced integrated façades, thermal

mass activation, earth coupling, dynamic insulation and PCMs (IEA 2009). The inclusion of a passive cooling technique for hot/dry climate linked with a responsive building element such as an air culvert, within a hybrid approach, offers a lower cost solution to the cooling of buildings. An air culvert is an earth coupling facility that is commonly termed EAHE in the literature; it consists of several sections or ducts of an optimum length buried underground at a reasonable depth to utilize the thermal inertia of the soil to behave as a heat sink in summer and a heat source in winter. It works such that the ambient air (Figure 1.1) is drawn into culvert sections by a fan; the incoming air exchanges heat with the soil and the treated air is supplied to a building zone or AHU. Even when such a hybrid cooling system is used, it does not necessarily result in a high cooling energy consumption reduction. This requires proper control addressing issues such as the nature of the coupling between the active and passive components, and the switching of these components as a function of ambient and building conditions.

The transient interaction between the building thermal subsystems (building zone, AHU and air culvert) against damper control is a complex process. The dampers are to be switched on/off based on a control algorithm that dictates which air source should supply the AHU (ambient air or that coming off culvert) and whether the culvert, A/C system or some combination of these shall operate. The interaction between a building, its A/C plant and the air flow network representing the air culvert, along with the control of such technical domains, can be represented as rigorously to reality as possible by an integrated building energy simulation tool. A simulation program, ESP-r, has been used in the present work. Within this tool, the user is able to address the interaction between a building's thermal capacity measured in hours and the dynamic response of the A/C plant and control system measured in minutes or less (Winkelmann & Clarke 1986). ESP-r has the ability to couple several domains in an integrated manner: domains in the present work include space thermal flows, culvert air flow, HVAC energy conversions and control action. The user can select which domains are to be appraised depending on the analysis requirement. Each domain is handled mathematically by a separate solver, but the solution for all solvers is coordinated to ensure a simultaneous solution. Figure 1.2 depicts how the selected domains for this thesis are interrelated within ESP-r.

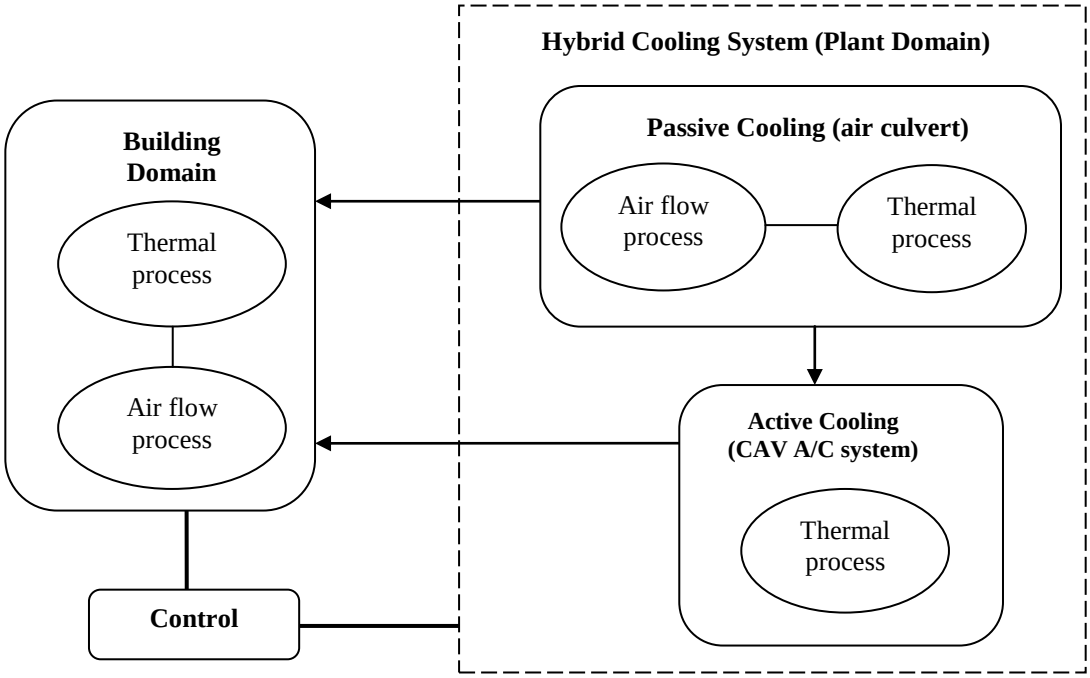

Figure 1.2: Coupling of the research-related technical domains in ESP-r.

1.4 Thesis Objectives & Outline

The objectives of this thesis are.

- To use the integrated whole building energy simulation tool, ESP-r, to construct a novel control strategy that will harmonize the use of an air culvert when coupled to a CAV all-air A/C system in a residential building located in a hot/dry climate. The aim is to lower the active cooling energy consumption and peak cooling load considerably.
- Afterwards, this regional control strategy for hot/dry climate will be generalized to any climate to enhance the air culvert technology transfer and establish a discipline for best practice. This general control algorithm is able to predict how much modularized sensible cooling load is required, versus culvert passive cooling contribution, on the basis of ambient air and ground temperatures that change with location.

Chapter 1 has considered the importance of cooling of buildings against the totality of global energy consumption and introduces the potential role of hybrid cooling systems. Approaches to the cooling of buildings are revised in Chapter 2

where active cooling techniques are reviewed, passive approaches considered, and the use of an air culvert justified in terms of its significant potential contribution. A literature review of culverts and an overview of how the AHU and air culvert can be modelled by ESP-r are also presented. Chapter 3 details the extents to which an air culvert may be used in free-standing mode to, in part, satisfy the cooling loads of a building in a hot climate region with and without building cooling energy efficiency measures. It introduces the ESP-r air culvert model and describes its verification by empirical testing and inter-model comparison. It also details the results from a parametric study to optimise the air culvert's design parameters. Chapter 4 discusses the deployment of a single-zone, CAV A/C system and the identification of a coupling strategy with the air culvert. Chapter 5 describes how the global control strategy for such a hybrid system was generated and details the general control algorithm for different climate zones. Finally, conclusions and future work are given in Chapter 6.

Chapter 2 : Approaches to Cooling of Buildings

This chapter appraises active and passive cooling methods as considered in this thesis. A/C types are reviewed with an emphasis on all-air A/C system as this is the active cooling type selected to comprise the hybrid cooling system with air culvert since both mechanisms employ air as the cooling exchange medium. The outcome from a literature review of air-culverts both theoretically (simplified and complex models) and experimentally is presented along with results from parametric studies.

2.1 Active Cooling

Vapour compression is the most common refrigeration cycle incorporated in air conditioning systems. The cycle starts with evaporation of the refrigerant in the cooling coil. Compression raises the pressure of the refrigerant under constant entropy. The vapour gets hot, and is cooled before condensation starts. Thereafter, the liquid flows from the condenser to the expansion valve; if some vapour is present there, it can cause excessive pressure drop and a reduction in the performance of the system. Some degree of sub-cooling is therefore necessary to ensure 100% liquid flow. This sub-cooling can occur in the condenser, and further cooling of the liquid can take place between the condenser and the valve. The pressure is reduced in an expansion device, and the refrigerant is returned to original condition. The steady-state processes stated above, and listed below, are actually transient in practical refrigeration systems and can be best simulated in transient integrated energy simulation tools.

Evaporation: Isobaric heat extraction in the cooling coil.

Compression: Isentropic compression of saturated vapour in compressor.

Condensation: Isobaric heat rejection in condenser.

Expansion: Isenthalpic expansion of saturated liquid in expansion valve.

A/C systems provide a comfortable indoor environment for occupants while the external weather conditions are continuously alternating; the controlled comfort parameters include air temperature, air relative humidity, and air motion. These systems incorporate the vapour-compression thermodynamic refrigeration cycle, which provides the required cooling capacity based on the expected peak load, not

the partial load. This leads to a lower overall operating efficiency. That is why A/C modularization should be considered to reduce this problem, especially with CAV systems where the single-zone version is widely used in small buildings due to its simplicity and functionality.

Air can be cooled directly (DX) by the refrigerant or indirectly where air is cooled by chilled water produced by a refrigerant in a chiller. DX systems are more efficient than chilled water systems because the cooling process occurs without a secondary cooling medium. DX systems suit residential buildings where the pressure drop inside the refrigeration piping is small because the distance between the condenser and AHU is small. In large buildings, such as hotels, airports, shopping malls and high-rise buildings, the distance between the condenser and AHU is high and, accordingly, the pressure drop inside the refrigerating tubing is also high. This pressure loss can sometimes increase up to the point where the refrigerant is not able to reach the AHU, leading to a complete system malfunction. The alternative then for large buildings, either multi-storey or horizontally arranged, is to use chilled water refrigeration systems. These systems have no pressure drop problem because the pump provides high capacity at low initial and operating costs (Ananthanarayanan 2005).

Figure 2.1 shows the cooling and dehumidification processes where air temperature and air specific humidity at point ‘e’ in the psychometric chart are decreased due to the fact that moist air keeps passing through the cooling coil until air temperature reaches the dew-point temperature at point ‘d’. The moist air temperature then reduces below the dew-point temperature until it reaches the apparatus dew-point at point ‘p’. When this occurs, condensate from the moist air entering the cooling coil is drained out; the relative humidity however is increased during the process. Latent and sensible cooling loads are quantified by equations 2.1 and 2.2 respectively. Typically, these loads are calculated on the basis of steady-state considerations based on the psychometric chart as shown in Figure 2.1 whereas, if determined transiently, the results would be more representative of the reality. In chapter 4, the AHU cooling coil load derived from the psychometric chart is compared with predictions from a CAV A/C system as modelled in ESP-r. Air conditioning systems are classified into two categories: packaged or central. Types of

packaged systems are single-package and split-package and in both systems the components are assembled at the factory. All components of single package units, such as window A/C systems, are placed in housing and fitted in a slot modified in the room's wall; they provide a cooling capacity of 0.5-2 tons. Split-package units comprise two housings, one located indoors and the other outdoors. The outdoor compartment includes the compressor, condenser and expansion valve, while the indoor housing contains the cooling coil and a fan; such systems provide a cooling capacity of 1.5-25 tons. The other system is called central because the cooling agent is transported from one central location to different parts of the building and vice versa carrying both thermal (sensible) and moisture-related (latent) energy (Ameen 2006).

$$Q_L = \dot{m}_a(h_d - h_p) \qquad 2.1$$

$$Q_S = \dot{m}_a(h_e - h_d) \qquad 2.2$$

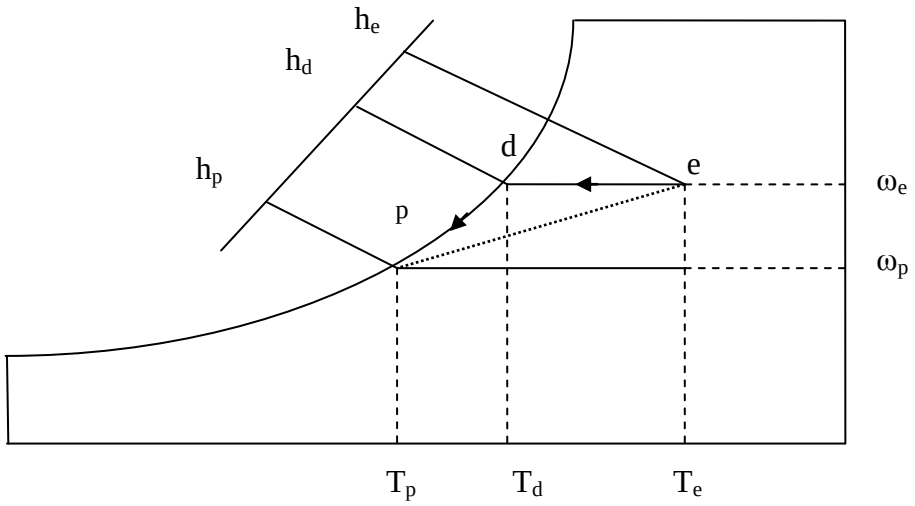

Figure 2.1: Psychometric chart of cooling and dehumidification processes.

All central A/C systems consist of four sub-systems: source, distribution, delivery and control (Grondzik 2007). The source sub-system has already been reviewed, which is the refrigeration thermodynamic cycle (vapour compression) but simulating its performance has not been studied because it is outside the scope of this thesis; only the cooling coil performance is considered. The control sub-system, such as scheduling, optimum start/stop, night setup, PID control loops, minimum outside

air control, dead band control, duty cycling, free cooling, enthalpy cycle, space set-point reset and night purge, has been extensively studied over the years. The distribution and delivery sub-systems of the central A/C system however are concerned with the central A/C types, which are all-air, all-water and air-water. A single-zone, all-air CAV air conditioning system is used in chapter 4 to study its interaction with an air culvert and the building when all are coupled.

In all-air systems, sensible and latent cooling, as well as humidification if required, is supplied by the AHU to different localities in the building and the same air returns to the AHU with no extra cooling or humidification required in the space being air conditioned. The most likely components of an AHU are the air filter, mixing box, humidifier if required, cooling coil, heating coil (optional), and a fan (supply and return). All-air systems can closely control both temperature and humidity, however they consume too much energy to move air and they require large air ducting; they may be CAV or VAV. The principle upon which the single-zone version of all-air CAV operates relies on the fact that air is supplied to a space at a constant volume flow rate with the supply air temperature being varied according to the space cooling load. Single-zone, all-air CAV systems are energy efficient compared to other CAV, all-air types such as reheat; they can be represented by simple control, and they are conveniently modifiable to include free cooling. However, their deficiency is that they respond only to one space condition criteria and humidity control is not achievable. Thus, their utilization is limited to better thermal zoning situations where no or little load variations occur throughout the space and humidity control is not vital (Grondzik 2007).

2.1.1 A/C Plant Representation in ESP-r

The performance of the vapour compression refrigeration system deteriorates in real operating conditions due to irreversibility (exergy destruction) initiated both internally and externally (Grazzini 1993). Internal exergy losses occur in the compressor, and entropy increases due to friction whereas it is assumed constant in the system theoretical optimization. External irreversibility occurs due to heat exchange between air and refrigerant in the condenser. When air is conditioned, a space has to be cooled from an initial temperature to a final set-point temperature by

DX or indirect contact with a cooling coil. Because of the air temperature continuous decrease over the cooling coil, the conditions surrounding the cooling coil do not remain steady and the complete system operates under transient conditions. Further, the transient simulation of an air conditioning system becomes more vital when control issues are addressed. Winkler (2009) has stated that "*Transient simulation of vapour compression systems has been most commonly used in the area of control algorithm development. Since vapour compression systems tend not to operate in steady state for significant periods of time and controls are inherently time dependent, transient simulation and/or experiments are required to design optimized control strategies*". This thesis is not concerned with the simulation of the vapour compression cycle. Instead, how the A/C plant components interact with the other systems (through cooling coil) is modelled in a transient manner. ESP-r (Clarke 1977) is the research method that was adapted in this thesis to model the transient heat exchange in the AHU cooling coil. ESP-r is an integrated energy modelling program for the simulation of the thermal energy and fluid flows within a combined building and plant systems when restrained to a user-defined control action. It is a detailed transient thermal simulation program which aims to imitate the real world as exhaustively as possible, combining building, plant and mass flow simulation. The underlying theory behind ESP-r and its implementation is comprehensively detailed elsewhere in (Aasem 1993; Clarke 2001; Hand 1998; Hensen 1991; Kelly 1998; MacQueen 1997; Nakhi 1995; Negrao 1995); the technical domains used in this thesis are explained where applicable. The ESP-r system applies one fundamental modelling theorem to all prospects of the building. Clarke (2001) defined model formulation in ESP-r as follows: "*The continuous building/plant system is made discrete by the placement of 'nodes' at pre-selected points of interest. These nodes represent homogeneous or non-homogeneous physical volumes corresponding to room air, opaque and transparent boundary surfaces, constructional elements, plant component parts, renewable energy components, room contents and so on. For each node in turn, and in terms of all surrounding nodes representing regions deemed to be in thermodynamic contact, conservation equations are developed to represent the nodal condition and the inter-nodal transfers of energy, mass and momentum. The entire equation-set is solved simultaneously for successive time steps to obtain the*

future time-row nodal state variables as a function of the present time-row states and prevailing boundary conditions at both time-rows". This technique ensures that all regions of the building are appropriately connected in a manner that respects the spatial and temporal integrity. Equation 2.3 exemplifies how a solution in ESP-r is generated. Here **A** represents a dispersed matrix of future time-row coefficients of the nodal temperature or heat injection terms of the conservation equations, **B** corresponds to the matrix established at the present time-row, **C** defines a vector of known boundary excitations relating to the present and future time-rows, **θ** is a vector of nodal temperatures and heat injections, n + 1 referring to the future time-row, and n to the present time-row.

$$\mathbf{A}\boldsymbol{\theta}_{n+1} = \mathbf{B}\boldsymbol{\theta}_{n} + \mathbf{C} \qquad 2.3$$

The A/C plant network in ESP-r can be represented with a detailed component system. The A/C plant may then be simulated dynamically by the technique described above. For example, the AHU shown in Figure 4.1 and its coupling with the building zone can be simulated in ESP-r by using components that are already integrated in ESP-r such as a mixing box, ducts, humidifier and cooling coil and so on. These components are then connected to one another as appropriate. Then, at every component node, conservation equations are extracted and solved simultaneously to calculate component node temperature, first phase (dry air) and second phase (vapour) mass flow rates at each time-step. A single-zone, CAV air conditioning system and its coupling with an air culvert and building along with their control systems is described in Chapter 4.

2.2 Indirect Ground Air Cooling

The high thermal capacity of the soil allows the temperature below a specific depth to remain constant throughout the year; a temperature that is near the annual average ambient temperature. In summer, the soil would act as a heat sink because the ambient temperature is higher than the ground temperature, whereas in winter the earth serves as a heat source. It will be seen in the next chapter how ground temperature varies at different depths with a decrease of the sinusoidal effect as the depth is increased. Due to drilling costs and site constructional restrictions, a

pipe/duct depth where the ground temperature is constant throughout the year would be unachievable from an economic and practical point of view. Ground temperatures can be calculated from equation 3.1 (Kasuda and Archenbach 1965). Wu and Nofziger (1999) confirmed that the ground temperature model underestimates measured values by 2°C, they modified the Kasuda and Archenbach (1965) model such that its outcome would agree well with measured data; this issue is discussed in section 3.1.1. Air culvert as concluded by Akridge (1982), it posses some limitations in hot/humid climates due to condensation that infrequently exists in hot/dry climate. The advantage in using culverts is that the higher the ambient temperature is the higher the culvert cooling capacity would be given that the ground temperature is relatively low compared to the annual average ground temperature. The thermal performance of an air culvert depends on several factors; these factors include the following.

1. Temperature and relative humidity of the inlet (ambient) air.
2. Soil temperature.
3. Heat exchange surface area.
4. Air flow rate.
5. Convective heat transfer between the flowing air and internal pipe/duct surface.

The above parameters were studied in the present work to produce a parametric priority list as presented in section 3.4. This list allows the culvert thermal efficacy to be maximised for both cooling and heating season operation. The first parameter in that list is able to reduce both the annual cooling energy and peak cooling load drastically as will be seen in Chapter 4. The air culvert was selected as the passive cooling technique that suits the hot/dry climate in order to compose the hybrid cooling system with the single-zone CAV, all-air air-conditioning system for use in residential building applications. The next section presents the result of a literature review of air culverts in terms of how their thermal performance may be assessed both theoretically and experimentally.

2.2.1 Air Culvert

Research into culverts has focused mainly on analytical and numerical models to predict the culvert outlet air temperatures, along with a few experimental measurements where little consideration was given to the control strategies of culvert/building and their coupling with active cooling in the transient domain. Some researchers have studied the control aspect but only from the perspective of simple daily and seasonal operation.

2.2.1.1 Simplified Solution

Simplified culvert models have emerged over the years (Chen et al. 1983; Elmer & Schiller 1981; Levit et al. 1989; Rodriguez et al. 1988; Santamouris & Lefas 1986; Schiller 1982; Seroa da Motta & Younf 1985; Sodha et al. 1984). The culvert in these models was divided into elements and the air temperature at the outlet was calculated by applying the steady-state heat diffusion partial differential equations 2.4 or 2.5 depending on the coordinate system used and dimensionality of the model along with variable states of thermal conductivity. All models assumed a 1-D steady-state characterization except Schiller's (1982) 2-D steady-state model and the 3-D steady-state model by Chen et al. (1983). All models account only for convection heat transfer where the culvert's wall temperature was assumed constant, whereas the Schiller model considered both convection and conduction heat transfer although these were not handled simultaneously. Only Schiller considered variable thermal conductivity whereas the other models considered the soil to be isotropic and homogeneous. Figure 2.2 illustrates the two heat transfer modes involved in these simplified culvert models, namely conduction and convection. After the culvert outlet air temperature is calculated, the result is inserted into equation 2.6 for convective heat flux only or equation 2.7 for convective and conductive heat flux.

$$\frac{\partial}{\partial x}\left(k\frac{\partial T}{\partial x}\right)+\frac{\partial}{\partial y}\left(k\frac{\partial T}{\partial y}\right)+\frac{\partial}{\partial z}\left(k\frac{\partial T}{\partial z}\right)=0 \qquad 2.4$$

$$\frac{1}{r}\frac{\partial}{\partial r}\left(rk\frac{\partial T}{\partial r}\right)+\frac{1}{r^2}\frac{\partial}{\partial \emptyset}\left(k\frac{\partial T}{\partial \emptyset}\right)+\frac{\partial}{\partial z}\left(k\frac{\partial T}{\partial z}\right)=0 \qquad 2.5$$

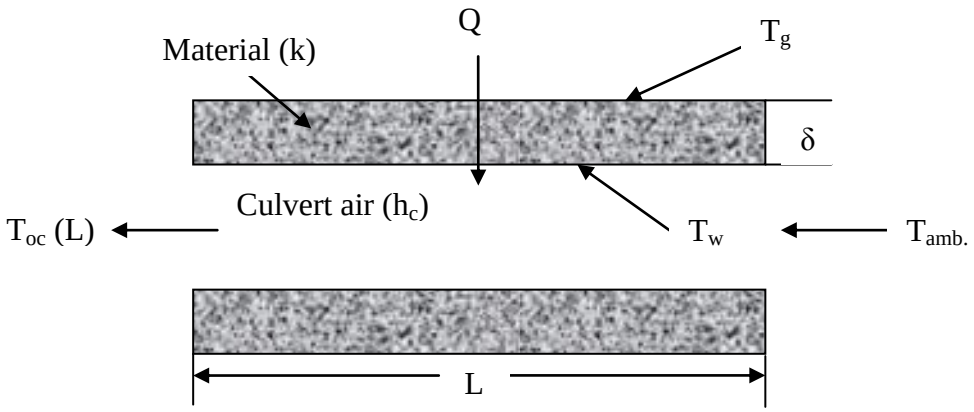

Figure 2.2: Conduction and convection in a simplified culvert example.

$$Q = \left(\frac{T_w - T_{oc}(L)}{1/h_c A}\right) \qquad 2.6$$

$$Q = \frac{\left(T_g - T_{oc}(L)\right)}{\left(\frac{\delta}{kA} + 1/h_c A\right)} \qquad 2.7$$

Argiriou et al. (1992) undertook a sensitivity analysis to compare how those simplified models would react to different depths, lengths, diameters and air velocities. It was found that the outlet air temperature in all models increased linearly as depth is decreased. The culvert outlet air temperature for all models increased rapidly when the velocity of the air inside the culvert is increased up to about 6m/s after which it becomes nearly constant. Schiller's (1982) model predicted the highest temperature although it was claimed that the value was within an acceptable range. Argiriou et al. (1992) claimed that the culvert outlet air temperature drops rapidly when the length of the culvert is increased and it tends nearly to a constant value after a length of about 50m. The outlet air temperature increases rapidly with radius up to 0.15m, but for values higher than 0.20m, the outlet temperature remains practically constant. Argiriou et al. (1992) concluded that all models investigated compared well with and showed good agreement with experimental data, with the percentage error for all models regarding upper and lower measurements limits being 3% and 4.7% respectively. The corresponding values for the Schiller's (1982) model were 10.3% to 13.9% respectively. Steady-state models other than those studied by Argiriou et al. (1992) have recently emerged. Athienitis & Santamouris (2002), De Paepe & Janssens (2003), Ghosal & Tiwari (2006), Loveday et al. (2006), Serres et

al. (1997) and Tiwari et al. (1993) all considered that culvert's inside surface temperature is constant throughout the pipe length in order to evaluate the outlet temperature. Other assumptions or thermal resistance treatments were varied from one model to another. Serres et al. (1997) considered that the ground temperature is constant throughout the year whereas Athienitis & Santamouris (2002), De Paepe & Janssens (2003), Ghosal & Tiwari (2006), Loveday et al. (2006) and Tiwari et al. (1993) assumed that the ground temperature follows a sinusoidal pattern without assessing the culvert's impact on the ground temperature. The ground temperature model used in most cases is that developed by Kasuda and Archenbach (1965) as represented by equation 3.1. The analytical model presented by Hollmuller (2003) accounted for the culvert impact on ground temperature where the culvert was subjected to both isothermal and adiabatic boundary conditions. All models were validated against theoretical models and sometimes against experimental results. Four steady-state culvert models were selected for inter-comparison with the ESP-r air culvert model presented in chapter 3.

- **(Loveday et al. 2006):** These researchers assumed internal surface temperature uniformity within the culvert to generate a steady-state model that calculates the culvert outlet air temperature. They included the effect of the additional heat incurred by the fan power consumption on the culvert outlet air temperature as illustrated by equation 2.8. Results from their model showed good agreement with two experimental studies (Shingari 1995) and (Dhaliwal & Goswami 1984) and one theoretical model (Mihalakakou et al. 1995).

$$T_{oc}(x) = T_a - (T_a - T_g)\varepsilon + \frac{\Delta p}{\eta \rho c_p} \qquad 2.8$$

- **(Athienitis & Santamouris 2002):** They assumed that since the ground temperature changes only when culvert is continuously used over long periods, the soil temperature may be assumed constant for intermittent heating or cooling over several hours since the soil can recover its previous conditions during the off-period. Thus, a uniform temperature was assumed for the inner surface of the culvert where an analytical model giving an

exponential relationship of culvert outlet air temperature with distance from the culvert inlet was attained as represented by equation 2.9. Comparison with experimental data by Goswami and Ileslamlou (1990) indicated good agreement.

$$T(x) = T_g + \left(T_{amb.} - T_g\right)e^{-x/a} \qquad 2.9$$

- **(De Paepe & Janssens 2003):** The inside wall temperature of the culvert was considered to be constant and equal to that of the ground due to the fact that the contact between the culvert external surface and earth was considered to be perfect and the conductivity of the soil was assumed high compared to the surface resistance. This model was used to develop a straightforward culvert design method based on the maximum specific pressure drop (hydraulic performance) calculable for the given effectiveness (thermal performance) to be realized where three parameters are optimized: length, diameter and number of parallel tubes incorporated.
  - **Thermal performance**: Culvert effectiveness was calculated from equation D.9; the researchers confirmed that the culvert length is an independent parameter affecting NTU where there is linear relation between them. Nevertheless, the thermal performance per unit length (NTU/L) depends only on the culvert diameter and its air volumetric flow rate as illustrated in equation D.11. They reported that long culvert ducts with small diameter and low flow rate produce better effectiveness but due to long ducts with small diameter the pressure drop inside the culvert is increased requiring higher fan power consumption. They recommended having parallel ducts of small diameter over which the air flow rate is distributed to accommodate the higher flow rate requirement.
  - **Hydraulic performance**: They added that the effect of the culvert's length on the pressure drop, as shown from equation D.12, is linear as well with hydraulic performance per unit length being ($\Delta p/L$). Both culvert diameter and culvert air flow rate have a simultaneous effect on the pressure drop where small flow rate and large diameter combination produces small pressure drop system which concludes that using side by side tubes with large diameter would be beneficial. Now, this finding clashes with the thermal requirement mentioned earlier of a

small diameter. However, having more tubes aligned laterally is useful on both fronts thermal and hydraulic performance.

Thus, they concluded that the deciding factor is the culvert length and diameter combination in order to optimize the air culvert performance. The need is to determine the specific pressure drop needed for the given culvert effectiveness. Equation D.13 calculates the maximum specific pressure drop in the system. It is derived such that the minimum culvert thermal effectiveness at the desired culvert outlet air temperature is calculated from equation D.10 after which it is inserted into equation D.9 to get the minimum NTU. Knowing the maximum allowable pressure loss it is possible to determine the maximum specific pressure drop (J_{max}) for use to limit both diameter and volumetric flow rate to certain values leading to the selection of the suitable diameter and maximum number of tubes where the culvert's length is specified by equation D.11 based on the minimum NTU. Culvert outlet air temperature is calculated using equation 2.10.

$$T_{oc}(x) = T_g + (T_{amb.} - T_g)e^{-NTU} \qquad 2.10$$

- **(Rodriguez et al. 1988):** This model, which calculates the culvert outlet air temperature as shown from equation 2.11, is based on the assumption that the temperature of the external wall of the pipe is maintained constant during the process and, therefore, the inside culvert wall temperature is constant.

$$T_{oc}\,(x) = T_g + (T_a - T_g)e^{\left(\frac{-4h_c x}{\rho c_p V D}\right)} \qquad 2.11$$

2.2.1.2 Complex Modelling

Despite the fact that steady-state models signify the evidence that heat is exchanged and stored in culvert, they can not provide a holistic culvert performance assessment in that they are unable to evaluate the transient culvert thermal and hydraulic performances especially when the fluctuation in ambient temperatures increases. Even though exact analytical solutions are possible, they are rarely encountered in realistic systems. Hence, numerical integration has become an important mathematical tool when appraising complex systems such as air culverts.

Culvert transient modelling advocates claim that steady-state models lack the quantification of latent heat transfer between air and culvert wall and therefore the humidity of the culvert outlet air cannot be determined, which would affect outlet air temperatures. Further, most of these steady-state models do not take frictional losses and pressure drops into account and also consider an axial symmetry for the heat flowing into the ground assuming that soil thermal stratification is non-existent and that the inside culvert wall temperature is constant. So, to eliminate these assumptions, a transient heat conduction model should be utilized. Equations 2.12 and 2.13 represent such a 3-D transient energy model with either constant or variable thermal conductivity for rectangular and spherical coordinates respectively. For moisture effects, a mass equation is generated and moisture terms are added to the energy equation. Two spatial boundary conditions for every direction and one temporal initial condition are also required.

$$\frac{\partial}{\partial x}\left(k\frac{\partial T}{\partial x}\right)+\frac{\partial}{\partial y}\left(k\frac{\partial T}{\partial y}\right)+\frac{\partial}{\partial z}\left(k\frac{\partial T}{\partial z}\right)=\rho c_p\frac{\partial T}{\partial t} \qquad 2.12$$

$$\frac{1}{r}\frac{\partial}{\partial r}\left(rk\frac{\partial T}{\partial r}\right)+\frac{1}{r^2}\frac{\partial}{\partial \emptyset}\left(k\frac{\partial T}{\partial \emptyset}\right)+\frac{\partial}{\partial z}\left(k\frac{\partial T}{\partial z}\right)=\rho c_p\frac{\partial T}{\partial t} \qquad 2.13$$

However, unlike the steady-state solutions, due to the complexity involved, transient solutions require the use of numerical methods to arrive at an approximate solution. Numerical models based on finite element or finite difference methods have been utilised in culvert numerical modelling. Mihalakakou et al. (1994) developed a 2-D transient, implicit culvert numerical model based on coupled energy and mass transfer equations on a single pipe. Bojic et al. (1997), Giardina (1995), Huber & Remund (1996) and Kumara et al. (2003) all studied single pipe based on transient numerical models. Some of these models have been incorporated in energy modelling programs: for example, Mihalakakou et al. (1994) developed their culvert model in the modular energy modelling program TRNSYS. All models were calibrated against monitored results and showed good agreement. Badescu (2007), Boulard et al. (1989), De Paepe (2002), Gauthier et al. (1997), Gygli & Fort (1994) and Thiers & Peuportier (2008) investigated multiple pipes based on 2-D and 3-D transient conduction and changing boundary conditions, with the possibility to

consider the non-homogeneity and non-isotropy of the soil along with condensation and evaporation effects. Hollmuller and Lachal (2001) developed a fully transient, 3-D, finite difference, control volume model with adiabatic boundary condition and several issues were examined such as complex geometries, more ground features, moisture effects, pressure drops, and culvert air flow direction control. However, Hollmuller and Lachal (2001) emphasized that their model needs high computation time due to the extensive meshing required in order to precisely describing the culvert thermal efficacy. Moreover, Hollmuller and Lachal (2005) concluded that "*when validation of EAHE numerical models against monitoring is ever carried out, latter in all cases remains limited to a few hours or days and does generally not concern real scale installations, thereby not providing necessary proof of robustness one would expect*". Here comes the need for a transient numerical energy modelling program based on finite difference control volume technique accommodating all real-world energy flow paths in order to veraciously appraise for culvert outlet air temperature. The heat transfer mode dominating heat exchange in the culvert is convection/advection followed by conduction and thermal radiation between surfaces. Since culvert length is large compared to wall thickness, a 1-D transient conduction model is accurate enough to assess the culvert's thermal performance. 3-D transient conduction is only required where phenomenon such as thermal bridging is present (Nakhi 1995); this is usually minimal in a culvert due to the convection and advection domination.

2.2.1.3 Physical Projects

Air culverts are not popular in real projects and are rarely incorporated in buildings. This is due to a variety of reasons: lack of expertise, climate constraint, site restrictions, initial costs etc. They have been installed in residential and office buildings in Europe, the USA and Pacific Asia. Tjelflaat (2002) studied a culvert providing ventilation for a single-storey school in Norway where the air flow rate depends on natural driving forces during cool periods: a wind tower for inward flow with the stack effect associated with a thermal chimney driving the outward flow. During hot periods, forced ventilation is enforced to utilize the thermal mass of the earth. Large cross-sectional culverts have been adopted recently to reduce the pressure drop and reduce fan power consumption. However, large air culverts trigger

enormous complications in terms of predicting culvert thermal efficacy due to the complicated convective heat flux treatment since the flow inside the duct is far from being fully turbulent. Wachenfeldt (2003) revealed a discrepancy between culvert simulation results and those measured in an air culvert ventilating a school in Grong, Norway. The reason was because the average convective heat transfer coefficient was not handled properly in the simulations. Figure 2.3 illustrates the difference between a fully developed turbulent convective heat transfer regime and the measured counterparts along with the recommended curve-fitted values. Pfafferott (2003) studied 3 air culvert projects for office buildings in Germany - DB Netz AG (Hamm), Fraunhofer ISE (Freiburg), Lamparter Office (Weilheim) - where the thermal performance of culverts at the different locations was calculated; the COP for the 3 facilities respectively were 88, 29, and 380. In the USA, Akridge (1982), Akridge & Benton (1981), Dhaliwal & Goswami (1984) and Francis (1981) all conducted experimental modelling and compared results with monitored data. Akridge (1982), for example, concluded that there were culvert limitations in hot/humid climates. He also claimed that the soil can provide sensible cooling effectively whereas latent cooling is rarely satisfied. In India, Sodha et al. (1985) evaluated an air culvert ventilating a hospital complex while Sawhney et al. (1999) examined an experimental culvert with cooling COP of 3.35.

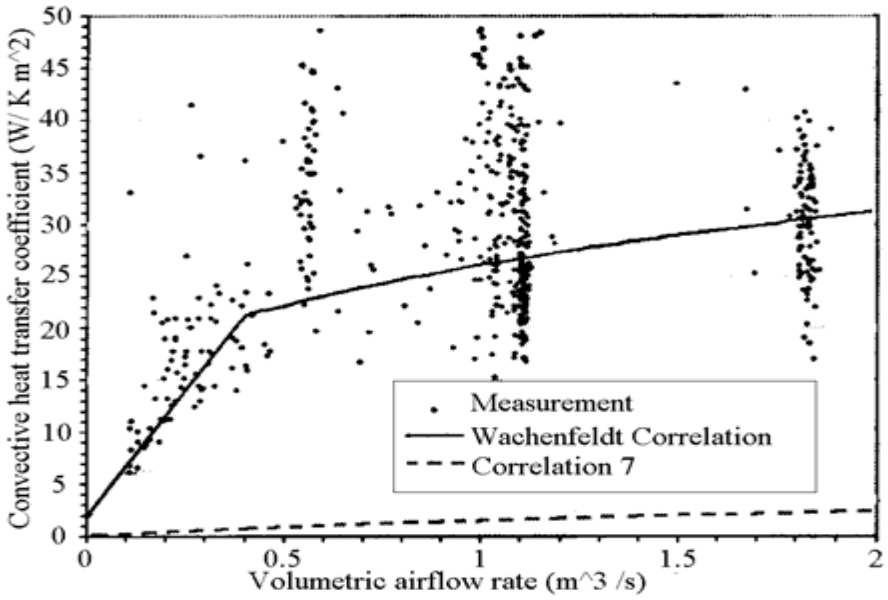

Figure 2.3: Convective heat transfer coefficient against flow rate in large cross-sectional culverts (Wachenfeldt 2003).

2.2.2 Control of Air Culverts

Tjelflaat (2002) practiced a control strategy for culvert coupling with a building such that the pre-heating supply air temperature set-point in the heating season is 19 °C. When the hot period starts, the pre-heating is shut-off and the supply air temperature floats freely to take advantage of the culvert thermal mass. Tjelflaat (2002) added that the supply air temperature down to 17°C in the warm season did not cause discomfort and concluded *"It is important that all aspects of energy use are evaluated simultaneously, and a good simulation tool with realistic input data is very valuable".* Thiers and Peuportier (2008) studied the control of culvert and other supplementary heating and cooling services based on daily and seasonal operation. Tombazis et al. (1990) studied a hybrid cooling system in a hotel that consisted of AHU and culvert along with natural ventilation. They made a control strategy for such a coupling that could capitalize on the energy efficiency since an unwanted temperature increase could be experienced when cooling provided by culvert is not properly controlled. They outlined a control strategy that took into consideration the three cooling systems: conventional air-conditioning, culvert and natural ventilation; the control strategy is illustrated in Figure 2.4. The relevant control strategy indicates that when T_{in} exceeds 26°C, the control routine checks if T_{oc} is less than T_{amb}. In order for the air culvert to operate, $(T_{oc} - T_{amb})$ must be larger than 2°C so that the cooling capacity produced is more than the electricity consumed by the ventilation system. Otherwise, if T_{amb} is less than 24°C, ventilation is enforced; if not, conventional air-conditioning is utilized. When $(T_{oc} - T_{amb})$ is more than 2°C, the control algorithm will check$(T_{oc} - T_{in})$. If T_{in} is higher than T_{oc} and T_{oc} is greater than 28°C then the culvert supplies the AHU with pre-cooled air. However, if T_{oc} is lower than 28°C then the culvert supplies the building directly with pre-cooled air. In order to determine the number of exchangers required to supply air through the culvert, the control strategy checks the mass flow rate required to ventilate the building. This hybrid cooling system control strategy suits only the culvert design parameters (culvert fan operates when $(T_{oc} - T_{amb})$ is larger than 2°C) and multi-chiller control is not approached. This 2°C temperature difference condition is relatively high but is inevitable due to the high ventilation rate the culvert has to provide to the hotel.

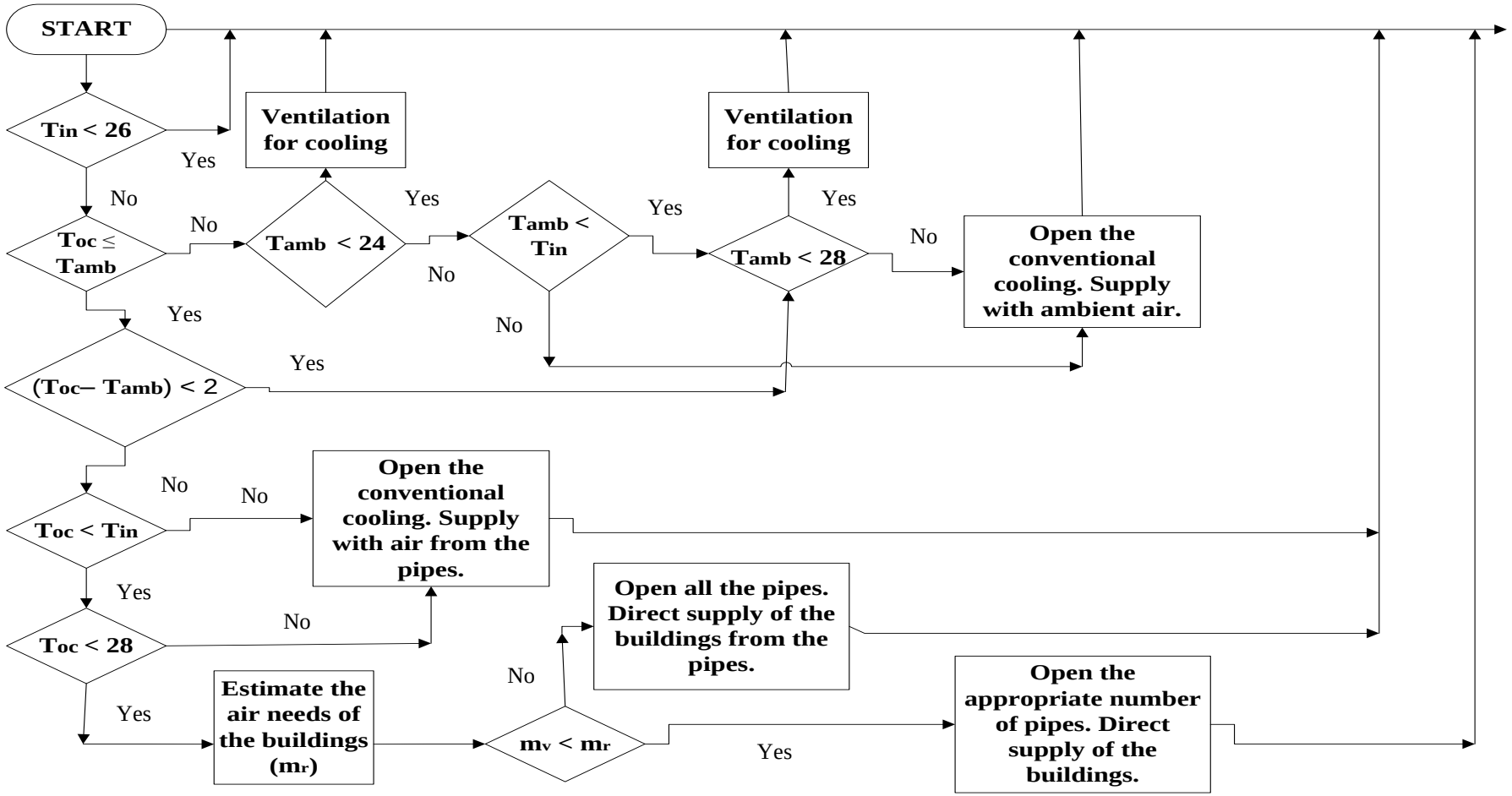

Figure 2.4: Coupling control strategy of culvert with A/C and ventilation (Tombazis et al. 1990).

Residential buildings require less ventilation than commercial facilities and therefore a smaller temperature difference is possible between the culvert outlet and ambient condition to activate the culvert fan; this is justified in section 4.3. It can be controlled by imposing the rule that in order to switch on the fan, the culvert's cooling capacity has to be larger than the fan power. Thus, a general control strategy for the A/C air culvert hybrid sensible cooling system is presented in chapter 5 that includes a multi-chiller control for any climate and is applicable for any culvert design parameters. The hybrid sensible cooling system is used in the general control strategy because most of the culvert cooling is sensible and the A/C sensible cooling is modularized. A hot/dry climate requires more sensible than latent cooling while the opposite is true in a hot/humid climate. So, when the general hybrid sensible cooling system control strategy is incorporated in a hot/humid climate care should be taken to provide latent cooling through means other than the general controller.

2.3 ESP-r Modules

ESP-r is the research method used in this thesis; it consists of three main modules for Project Management, Simulation, and Results Analysis. Figure 2.5 shows how the user interface includes both the Project Management and the Results Analysis modules while the Simulator is located at the heart of the system receiving its data model and returning its performance predictions.

- **Project Manager**

The Project Manager controls the model definition process, simulation engine invocation, and the results analysis. It offers an interactive, graphical interface that provide model building facilities related to site conditions, building form and fabric, HVAC & renewable energy systems, air flow, electrical networks and control systems. It also provides access to standard data relating to material properties, constructions, optical properties, plant components, weather collections and the like. The Project Manager gives partial instances of the data model to The Simulator and can also exchange data with external applications such as Radiance for lighting simulation or CAD packages for importing/exporting geometry.

- **Simulator**

The data model, as if exists at any point in time, is passed to the Simulator where solvers appropriate to the active model domains are activated. The active solvers then co-operate to attain a simultaneous solution of the given problem, which may comprise a building in whole or part depending on the design question in hand. For example, in the present context this might comprise a culvert-only model with prescribed boundary conditions, which can later be replaced by a building and HVAC representation.

- **Results Analysis**

The Simulator produces a database comprising CV state variables (temperature, pressure *etc*.) and inter-CV flows (heat, moisture, electricity *etc*.) at each simulation time step. These results maybe tabulated, graphed or statistically analysed in order to quantify performance and explore the inherent causal relationships prior to making decisions on appropriate design changes.

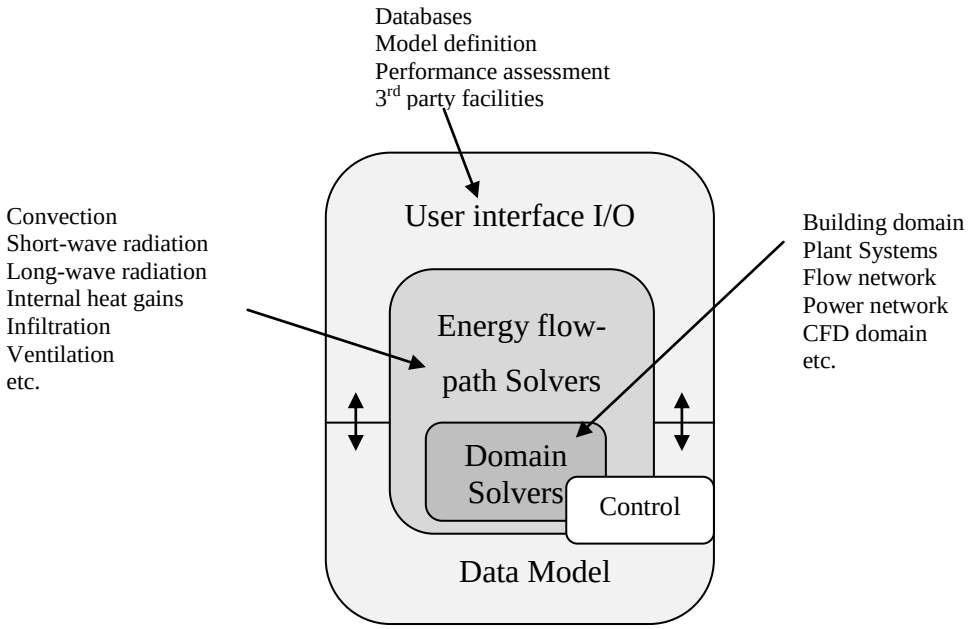

Figure 2.5: ESP-r capsule (Hand 1998).

2.3.1 Air Culvert Representation in ESP-r

Energy flow paths such as convection, advection, conduction, radiation and heat storage are encountered within the air culvert, thus their quantification can only be represented meticulously in an integrated building energy modelling simulation tool such as ESP-r. All energy flow paths are represented in ESP-r by mathematical models that are coupled and solved simultaneously. The culvert in ESP-r is represented as several zones (to account for the horizontal temperature distribution) with a connected air flow network (to account for the pressure drop).

2.3.1.1 Culvert Nodal Energy Balances in ESP-r

In order for the culvert outlet air temperature to be accurately assessed, the following heat transfer mechanisms as shown in Figure 2.6 have to be represented.

1. Convection between the flowing air and the culvert internal surfaces.
2. Advection due to ventilated air flowing from one culvert tube to another.
3. Conduction between the ground and the culvert external surfaces.
4. Long-wave radiation between culvert internal surfaces.

The culvert energy coefficient matrices A, B and C in equation 2.3 are extracted from energy flow path balance equations for the culvert intra-constructional nodes, culvert internal surface nodes and the culvert air nodes. The only heat transfer mode acting on the culvert intra-constructional node is transient conduction with neighbouring nodes. Due to the involvement of more than one heat transfer mechanism, the two heat balance equations of the culvert internal surface node and the culvert air node are elaborated next as reflected on by Beausoleil-Morison (2000) and Clarke (2001).

- **Culvert internal surface node**

Figure 2.7 depicts the heat balance on an internal surface node in ESP-r with equation 2.14 representing the heat storage in the control volume (CV). Relating that to an air culvert, T_{I-1} and T_I in equation 2.15 refer to the present time-row ground and culvert internal surface temperatures respectively. The second term in equation 2.14 is zero since there is no solar radiation absorbed in CV I and no casual heat gains are produced inside the culvert. The long-wave radiation into CV I is calculated by

equation 2.16, where N is the number of internal surfaces surrounding internal surface I and $h^t_{r,s\rightarrow I}$is a linearized radiation heat transfer coefficient (W/m^{2}K) that is recalculated at each time step as a function of inter-surface view factors. T^t_s and T^t_I refer respectively to the present time-row temperatures of the surrounding surfaces and surface I. Convection within the CV, as expressed in equation 2.17, represents the heat exchange between a culvert air node and its adjacent internal surface at the present time-row, where $h^t_{c,I}$is the convection heat transfer coefficient (W/m^{2}K) between the surface *I* and the air node I+1. The convective heat transfer coefficient is re-evaluated at each time step. Each culvert air node is treated as homogeneous and represented a single temperature and pressure.

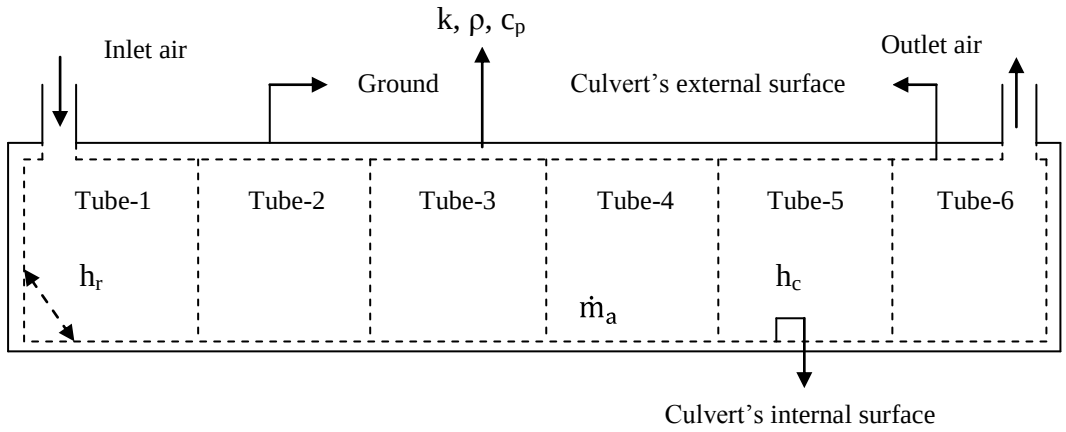

Figure 2.6: Air culvert heat transfer mechanisms in the transient domain.

$$\begin{aligned}\text{Heat storage in CV} \\ &= \{\text{Conduction into CV} + \text{Heat sources within CV} \\ &+ \text{Longwave radiation into CV} + \text{Convection into CV}\}\end{aligned} \qquad 2.14$$

where,

$$\text{Conduction into CV} = \frac{k_{I-1}\Delta y\Delta z}{\Delta x_{I-1}}(T^t_{I-1} - T^t_I) \qquad 2.15$$

$$\text{Longwave radiation into CV} = \sum_{s=1}^{N} h^t_{r,s\rightarrow I}\Delta y\Delta z(T^t_s - T^t_I) \qquad 2.16$$

$$\text{Convection into CV} = h_{c,I}^{t}\Delta y\Delta z(T_{I+1}^{t} - T_{I}^{t}) \qquad 2.17$$

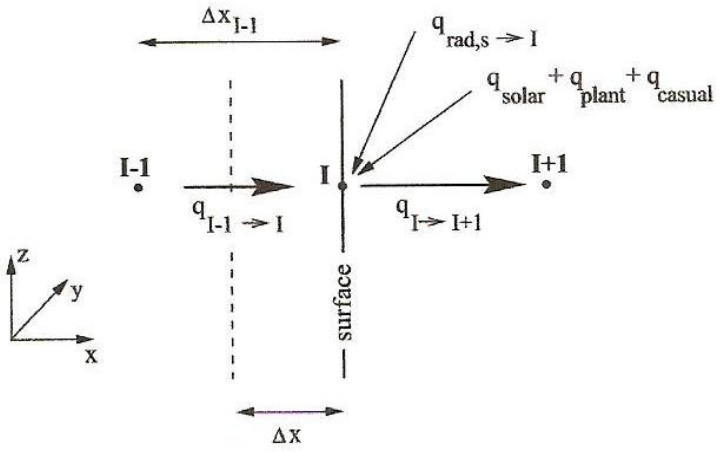

Figure 2.7: Heat balance at an internal surface node (Beausoleil-Morrison 2000).

- **Culvert air node**

Figure 2.8 depicts the representation of the heat balance at an air node in ESP-r, with equation 2.18 representing the heat stored in the CV. N refers to the number of culvert internal surfaces, A_S is the culvert surface area (m^2), $h_{c,S}^{t}$ is handled the same way as for the culvert internal surface node, T_S is the culvert internal surface temperature, and T_I the culvert air temperature. There are no heat sources within a culvert air CV. Advection thermal energy exchange with a culvert air CV due to air flow from an up-stream CV is included in equation 2.20, where M is the number of culvert CVs supplying air to CV I and $\dot{m}_{J\to I}^{t}$ refers to the air mass flow rate from CV J to CV I (kg/s) at the present time-row and T_J^t and T_I^t respectively represent the present time-row temperatures of the air nodes in culvert CVs J and I. Advection heat transfer into the culvert tube control volume I due to infiltrated ambient air is also included in equation 2.21, where $\dot{m}_{o\to I}^{t}$ is the infiltration rate from ambient (kg/s) at the present time-row and T_o^t and T_I^t respectively represent the present time-row temperatures of the ambient and culvert air CV. There are several ways to calculate the mass flow rates as used in equations 2.20 and 2.21; for example, they may be assigned fixed values, controlled as a function of some sensed condition, or calculated via a flow network or CFD model.

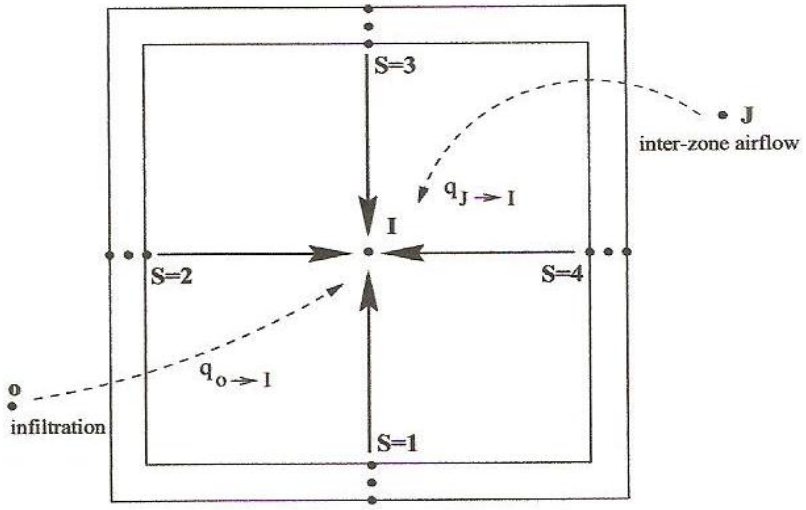

Figure 2.8: Energy balance at culvert air node (Beausoleil-Morrison 2000).

$$\begin{aligned}\text{Heat storage in CV} &= \{\text{Convection into CV} + \text{Heat sources within CV} \\ &+ \text{Advection into CV by ventilation} \\ &+ \text{Advection into CV by infiltration}\}\end{aligned} \tag{2.18}$$

where,

$$\text{Convection into CV} = \sum_{S=1}^{N} h_{c,S}^{t} A_S (T_S^t - T_I^t) \tag{2.19}$$

$$\text{Advection into CV by ventilation} = \sum_{J=1}^{M} \dot{m}_{J\to I}^{t}\, c_p \left(T_J^t - T_I^t\right) \tag{2.20}$$

$$\text{Advection into CV by infiltration} = \dot{m}_{o\to I}^{t} c_p (T_o^t - T_I^t) \tag{2.21}$$

In ESP-r, the simulation model can comprise a building that consists of one or more zones which have geometric, operational and constructional attributes as mandatory files. The mandatory files embrace the least descriptive data required to develop the differential equation coefficient sets for the simulation commencement. However, to increase the simulation accuracy, additional descriptions may be added to enable a more detailed treatment of convective and radiative heat transfer. An air flow network can also be added to model temporal air flow in the culvert. A plant

system may then be defined as a collection of connected components and this system connected to the flow network to represent combined heat and mass transfer. Via ESP-r's Project Manager, model modifications can be applied to enable parametric investigations in order to determine the impact of principal design parameters.

2.4 Concluding Remarks

Chapter 1 emphasised that the annual cooling energy consumption and peak cooling power in a hot/dry climate are substantial. The need therefore is to minimize those consumptions through hybrid cooling system. Chapter 2 confirmed that a single-zone, CAV air-conditioning system and air culvert may be brought together to create such a hybrid cooling system. An air culvert was chosen because it can accommodate well a hot/arid climate while its synergy with active cooling has rarely been studied. The single-zone, CAV air-conditioning system type was selected because it is the most commonly used configuration in residential units and its cooling exchange medium is the same as that of the culvert. Chapter 2 has presented the results from a literature review of air culverts and how they are modelled in a dynamic manner within the ESP-r system.

Chapter 3 : Air Culvert

A soil temperature distribution analysis has been conducted since it is vitally linked with ground coupling of the culvert and a verified ground temperature model is produced for a hot/arid climate. An air culvert model is constructed in ESP-r and its performance verified empirically and by inter-model comparison. The chapter then explores how much of the time the culvert can usefully maintain a suitable indoor environment and how this contribution might be improved by the implementation of energy saving measures.

3.1 Air Culvert Definition

Section 3.2 discusses the culvert model as simulated in ESP-r, which consists of an air flow network that is linked to zones situated at a depth selected to utilize the soil's thermal inertia while keeping installation costs low. The values assigned to the various culvert design parameters and operating conditions are discussed in the sensitivity analysis section presented later in this chapter. The culvert model operates such that the ambient air is induced by a fan. This ambient air exchanges heat with the soil (gain/loss) depending on the temperature difference with the surrounding ground. Air is passed from one culvert section to another until it reaches the outlet of the last section. The air culvert model requires an accurate prediction of the temporal ground temperature as a boundary condition.

3.1.1 Ground Temperature Profile

Saudi Arabia is the largest GCC country in terms of both area and population. The climate of Saudi Arabia's capital, Riyadh (hot/dry), was used in the present research to ensure that the project's results would have the greatest impact. Unfortunately, there was no measured ground temperature data for Riyadh; the only data available being for neighbouring Kuwait. The approach adopted was therefore to validate the ground temperature model against the measured values for Kuwait, and then substitute Riyadh climate data in the model for use in the present work. The US Department of Energy (DOE) offers annual weather files for more than 2000 international locations. Figure 3.1 shows the ground temperature profiles calculated

for Riyadh and Kuwait weather files. The two profiles are in agreement except for the late summer period when the Riyadh temperatures lag those of Kuwait due to a slight ambient temperature increase in Kuwait (the maximum ambient temperatures of the selected weather data were 49.7°C and 46°C for Kuwait and Riyadh respectively). It may be concluded that the cooling and heating potential of an air culvert utilized in Kuwait, or for a similar climate zone elsewhere, is approximately equal to that found in Riyadh. The DOE calculation assumed a thermal diffusivity of 2.71 x 10^{-8} m^2/s for all world locations, which leads to an inaccurate ground temperature calculation since this value will change from one location to another according to the climate type. For example, Al-Ajmi et al. (2002) estimated an average value of 1.06 x 10^{-6} m^2/s for Kuwait based on measured soil temperatures at a depth of 4 m; the DOE ground temperatures were therefore recalculated using this value. The mathematical model shown in equation 3.1 for estimating the soil subsurface temperature was derived by Kasuda and Archenbach (1965) with the cosine expressed in radians. T_m, A_s, z, t, t_0, and α refer respectively to the mean annual ground temperature at (z = 0 m) in °C, the annual temperature amplitude at the surface (z=0 m) in °C, the ground depth in m, the year-day, the phase constant (day of the year when the lowest ambient air temperature occurs), and the thermal diffusivity of the soil (m^2/day).

$$T_g = T_m - A_s e^{-z\sqrt{\pi/365\alpha}} \cos\left\{2\pi/365\left[t - t_0 - \frac{z}{2}\sqrt{365/\pi\alpha}\right]\right\} \qquad 3.1$$

The assumptions that were employed in the derivation of this model are.

1. A sinusoidal temperature variation at the soil surface, z = 0.
2. At an infinite depth, the soil temperature is constant and is equal to the annual average ambient air temperature.
3. The thermal diffusivity is constant throughout the soil profile for all the year.

For 1995 in Kuwait, the mean annual ambient temperature, annual temperature amplitude and the day number of the lowest ambient temperature (26.2°C, 13.1°C and 36 respectively) were inserted in equation 3.1 to produce the ground temperature profile as shown in Figure 3.2 for different depths. This figure illustrates that the soil temperature throughout the year is sinusoidal when the culvert

is buried close to the ground surface. This sinusoidal shape is dampened with increasing depth; this issue is revisited in the sensitivity analysis section.

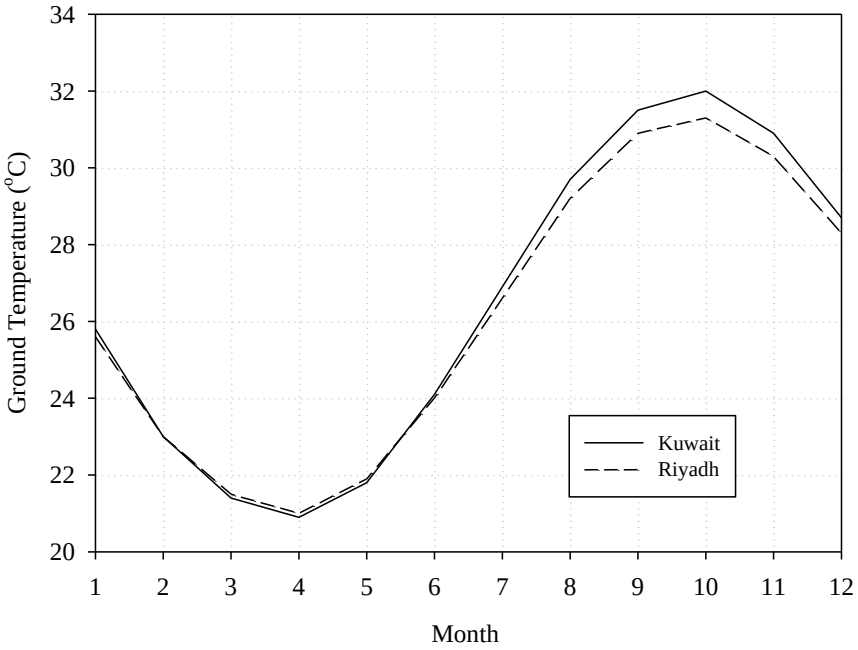

Figure 3.1: Ground temperature profile for two locations at a depth of 4m as listed by DOE.

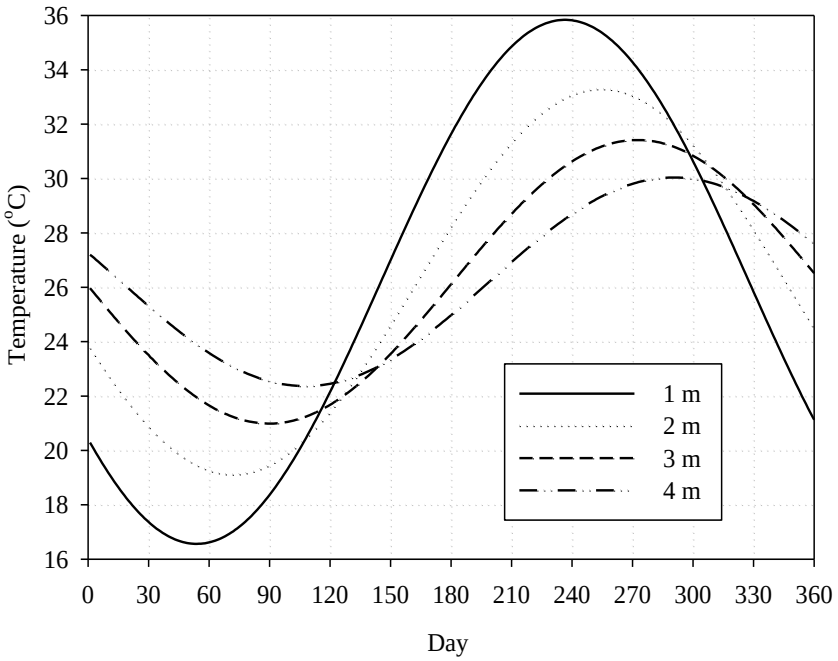

Figure 3.2: Theoretical daily ground temperature profile for Kuwait at different depths.

Figure 3.3 shows a comparison of Kuwait average monthly soil temperatures at a depth of 4m using the above mathematical model against measured data at the same depth. There is little agreement between the theoretical and measured values. One possible reason for the disagreement could be errors in monitoring equipment: it is unlikely that the measured monthly mean ground temperature, as displayed in Table 3.1, would increase from 25°C in December to 29°C in January since the soil in January at this depth is operating as a heat source resulting in a decrease in ground temperature at this time. Moreover, the clay and average water content of each soil layer is accounted for in the measured reading automatically but not in the model where the thermal diffusivity is assumed to be constant throughout the year.

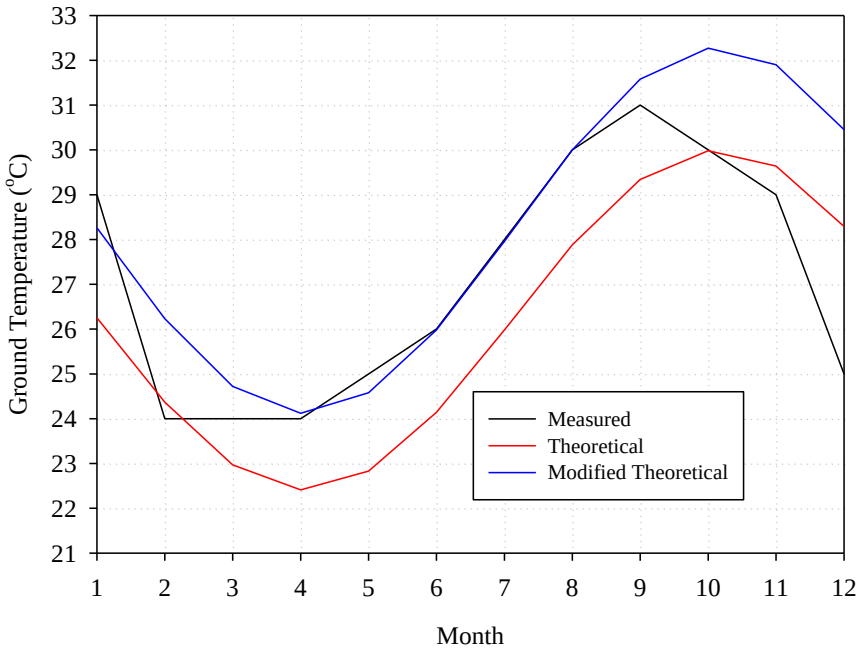

Figure 3.3: Monthly ground temperatures of Kuwaiti soil at a depth of 4m.

Wu & Nofziger (1999) reported that the ground temperature model stated above consistently underestimated soil temperatures by about 2°C. They confirmed that a good estimate of the temperature under bare soils can be obtained using this model by simply increasing the maximum and minimum mean air temperatures by 2°C when defining the model parameters. Jiménez et al. (2005) reported that for a hot/dry climate, the soil water content of a covered soil is 1.6 times higher than that of the bare soil. The thermal diffusivity increases with an increase of moisture in the surface layers, and the soil temperature decreases. In winter, the thermal diffusivity is

less, because the soil is getting drier and thus the soil temperature is higher. The diffusivity used in the ground temperature calculations represents mainly the period of hot season from April to November for a bare Kuwait soil. Therefore, in order to get the modified numerical solution, T_m and A_s have been changed respectively to 28.2°C and 15.1°C and calculations were performed again yielding the results given in Table 3.1. The dotted line representing the theoretical soil temperature model in Kuwait, as presented in Figure 3.3, does not show compliance with the measured values during the hot season being 2°C less than the measured values. But, for the winter season this is not the case, this could be due to the lower diffusivity in winter which is not accounted for in the numerical ground temperature calculation or due to incorrect temperature measurement. On the other hand, the dashed line representing the modified theoretical ground temperature model (by increasing maximum and minimum mean air temperatures by 2°C) in Figure 3.3 shows full agreement with the measured values during the cooling season in Kuwait with little improvement in the heating season agreement. In conclusion, the modified theoretical ground temperature model can predict well the soil temperatures in the cooling season with an acceptable margin of error for the heating season. Hence, it was decided to use the modified numerical ground temperature model to predict the soil temperature profile of Riyadh climate.

Table 3.1: Monthly ground temperatures in °C of Kuwaiti soil at 4m depth.

Month	Measured	Theoretical	Modified Theoretical
Jan.	29	26.25	28.26
Feb.	24	24.37	26.23
Mar.	24	22.97	24.72
Apr.	24	22.41	24.12
May	25	22.83	24.58
Jun.	26	24.14	25.98
Jul.	28	25.98	27.96
Aug.	30	27.88	30.00
Sep.	31	29.34	31.58
Oct.	30	29.98	32.27
Nov.	29	29.64	31.90
Dec.	25	28.29	30.45

3.1.1.1 Monthly Soil Temperature Profile for the Hot/arid Climate

The monthly maximum mean ambient temperature in Riyadh is 36.4°C and the monthly minimum mean ambient temperature is 14°C. T_m, A_s, and t_0 of the Riyadh climate set as required by the modified numerical ground temperature model are as follows.

1. Monthly maximum mean ambient temperature 38.4°C.
2. Monthly minimum mean ambient temperature 16°C.
3. February 9th marks the lowest ambient surface temperature at 4°C.
4. T_m is (38.4 + 16)/2 = 27.2°C.
5. A_s is (27.2/2) = 13.6°C.
6. t_0 is (31 + 9) = 40 days.
7. α is as measured in Kuwait (0.0912 m^2/day).
8. Inserting these values into equation 3.1 gives the modified theoretical ground temperature model, equation 3.2, for Riyadh as a function of ground depth and day of the year:

$$T_g = 27.2 - 13.6e^{-0.31z}\cos\{2\pi/365[t - 40 - 17.9z]\} \qquad 3.2$$

The modified monthly ground temperature profile of Riyadh at a depth of 3m is given in Table 3.2. This profile was assigned to the ESP-r air culvert model via the model context feature of the Project Manager. It is important to state that culvert operation impact on ground temperature has neither been quantified theoretically nor done experimentally, but it was estimated as will be seen in the sensitivity analysis section.

Table 3.2: Modified monthly soil temperature profile in °C at a depth of 3 m in Riyadh.

Jan.	Feb.	Mar.	Apr.	May	Jun.	Jul.	Aug.	Sep.	Oct.	Nov.	Dec.
26	23.58	22.11	21.96	23.17	25.44	28.16	30.64	32.22	32.49	31.38	29.01

3.2 Air Culvert Model in ESP-r

The air culvert was represented via rectangular zones and an air flow network as shown in the 'quality assurance report' given in Appendix B. In the defined

network, air flows from one rectangular zone to another via components that represent the pressure drop. Six zones are employed, each of 10m length, to transfer air from the inlet (ambient) to outlet (building zone or AHU). The perspective view shown in Figure 3.4 depicts the ESP-r air culvert model; only four sections are shown here to illustrate how the culvert is constructed. The model outputs (temperature, pressure and velocity) for each section (node) are available through the Results Analysis module on conclusion of the simulation.

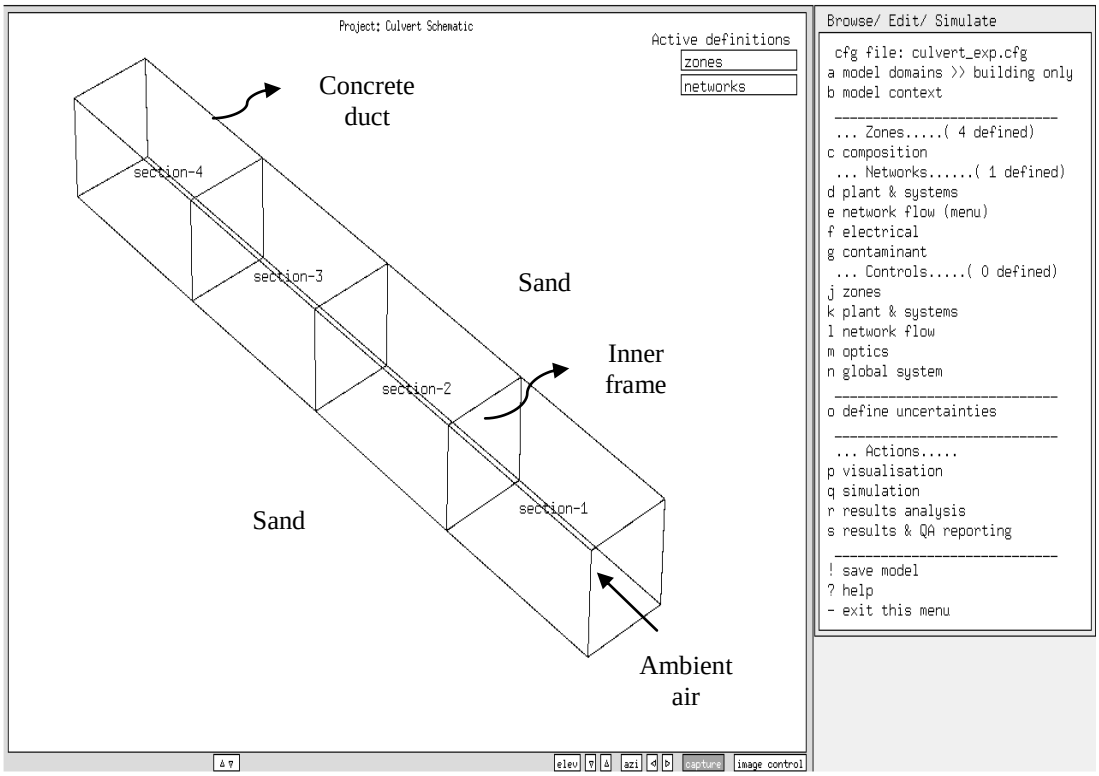

Figure 3.4: Culvert model perspective view as represented in ESP-r.

Two constructions were applied to this model; one to represent the earth side (sand) around the rectangular concrete duct and another to represent the inner frame that joins one section to another (Figure 3.4). The earth side construction, from outside, comprises 1m of sand, 10cm of gravel, and 10cm of heavy mix concrete. Four sand layers were included to more effectively represent earth around culvert sections helping quantifying heat flux better. The inner frame, from outside, comprises 4mm aluminium (grey coated), 80mm glass fibre quilt and 4mm aluminium (grey coated). The thermo-physical properties of these materials are given in the quality assurance report of Appendix B, but for easy access they are listed here in Table 3.3.

Table 3.3: Thermophysical properties of culvert constructions.

No	Construction	Material	l (m)	k (W/mK)	ρ (kg/m^3)	c_p (J/kgK)
1	Earth side	Common earth	0.250	1.28	1460	879
		Common earth	0.250	1.28	1460	879
		Common earth	0.250	1.28	1460	879
		Common earth	0.250	1.28	1460	879
		Gravel	0.100	0.52	2050	184
		Concrete	0.100	1.40	2100	653
2	Inner frame	Aluminium (gray coted)	0.004	210	2700	880
		Glass fibre quilt	0.08	0.04	12	840
		Aluminium (gray coted)	0.004	210	2700	880

3.2.1 Air Culvert Design

The air culvert design and performance parameters were derived as follows.

1. What is the ventilation rate that the air culvert should provide?

$$\dot{V}_v = NP(\dot{V}_s) \qquad 3.3$$

If 5 people occupy a building, each requiring 16l/s when 25% smoke is allowed (CIBSE Guide B 2005), then equation 3.3 gives the required air volume flow rate of 0.08m^3/s. This quantity may be reduced to 8l/s per person where no one smokes. The minimum required ventilation air flow rate given by ANSI/ASHRAE Standard 62.1 (2007) is 7.5l/s per person.

2. What is the required air velocity inside the culvert?

According to CIBSE Guide B (2005), for an efficient heat transfer exchange within the culvert without high pressure drop, an air speed of 2m/s suggested. This

means that when the air volume flow rate during the design phase is changed, the diameter would need to change to maintain the air speed at 2m/s or less. This issue is discussed further in the sensitivity analysis section.

3. What is the diameter of the culvert?

   Equation 3.4 yields a diameter of 0.23 m.

4. What is the convective heat transfer coefficient?

$$D = 2\sqrt{\frac{\dot{V}_v}{\pi V}} \qquad 3.4$$

With D = 0.23m, V= 2m/s, and v of air at 20°C = 0.0000151m^2/s, Re (from equation 3.5) is 29934. It is assumed that common properties such as v, α, ρ, k and c_p are slightly varied when temperature is within 0-50°C at atmospheric pressure. Thus, using values of those properties at randomly selected temperature say 20°C was considered. Obviously this is a turbulent flow regime but is this turbulent flow fully developed? Equation 3.6 (White 1987) produces an entrance length of 5.54m, which is below the culvert's length of 60m, hence turbulent flow is fully developed from 5.54m until 60m and therefore relevant empirical convective heat transfer coefficient correlations may be used from length 5.54m and on. But α of air at 20°C is 0.000019 m^2/s, thus Pr from equation 3.7 is 0.795. Now, $0.5 \leq Pr \leq 2000$, $3000 \leq Re \leq 5 \times 10^6$, and $L/D \geq 10$, therefore Nu is 75.6 from equation 3.8 (Gnielinski 1976) where f is calculated to be 0.0237 from equation 3.9 (Petukhov et al. 1970). With D = 0.23 m, k of air at 20°C = 0.0257 W/mK, h_c from equation 3.10 is 8.6 W/m^{2}K. The selected parameters are listed in Table 3.4 where the modified monthly ground temperature profile used is shown in Table 3.2. The next section addresses the calibration of the ESP-r culvert model prior to use.

Table 3.4: Selected parameters used in the culvert thermal analysis.

L (m)	D (m)	$\dot{V}$ (m^3/s)	h_c (W/m^2.K)
60	0.23	0.08	8.6

$$\mathrm{Re} = \frac{\mathrm{VD}}{\mathrm{v}} \quad 3.5$$

$$\mathrm{L_E} = 4.4\mathrm{DRe}^{1/6} \quad 3.6$$

$$\mathrm{Pr} = \alpha/\mathrm{v} \quad 3.7$$

$$\mathrm{Nu} = \frac{(\frac{f}{8})(\mathrm{Re_D} - 1000)\mathrm{Pr}}{1 + 12.7\sqrt{(\frac{f}{8})}\left(\mathrm{Pr}^{2/3} - 1\right)} \quad 3.8$$

$$f = (0.79 \ln \mathrm{Re_D} - 1.64)^{-2} \quad 3.9$$

$$\mathrm{h_c} = \mathrm{Nuk/D} \quad 3.10$$

3.2.2 Model Calibration and Verification

In order to give credibility to the ESP-r air culvert model, it was compared with the results from other programs and measured culvert data. In the former case, the inter-comparison required that the internal surface temperature be held constant because that was an assumption imposed by the other programs. The programs used in the study were produced by Athienitis & Santamouris (2002), De Paepe & Janssens (2003), Loveday et al. (2006) and Rodriguez et al. (1988). In the latter case, monitored data for a 1 year period was obtained for a culvert supplying air to a Sports Centre in Glasgow.

3.2.2.1 Inter-model Comparison

The selected parameters displayed in Table 3.4 and Table 3.2 were inserted in equations 2.8, 2.9, 2.10 and 2.11 and to derive the culvert outlet air temperatures for the four steady-state models selected. Loveday et al. (2006) was selected because as mentioned in the literature review that the authors included for the heat produced by the fan and its impact on culvert outlet air temperature. De Paepe & Janssens (2003) as stated in the literature review studied both hydraulic and thermal performances of culvert. These two models considered different aspects that usually encountered in culvert but they studied it in the steady state case. The other two models were used to

confirm results generated from the former two models. The variables used in those equations and how to compute them are supplied in Appendix D. The ESP-r air culvert model was modified to align with the assumptions made by these models; namely, the culvert internal wall temperature is kept constant throughout the simulation, and weather parameters such as relative humidity, wind speed and direction along with diffuse solar radiation were set to zero in the ESP-r weather boundary condition. A summer peak day was simulated in ESP-r and the hourly outlet air temperature was compared to the corresponding results from the four comparison programs.

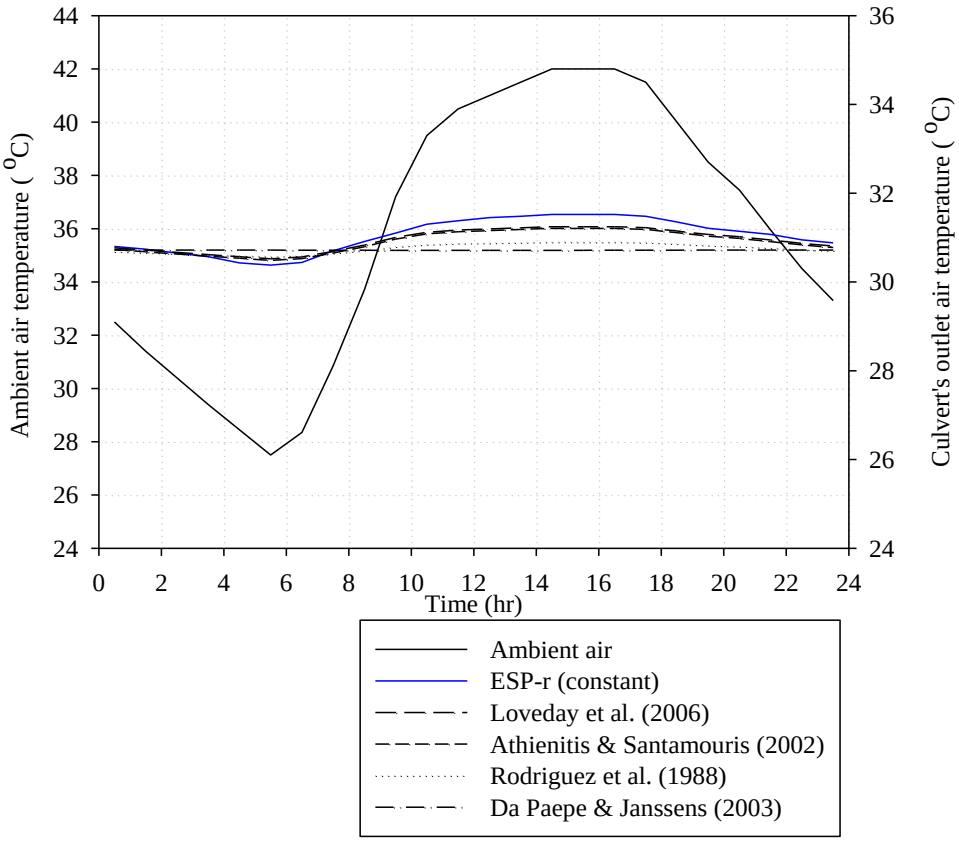

Figure 3.5: Culvert outlet air temperature using different models.

Figure 3.5 shows that the ESP-r solution under constant assumptions agrees well with the 4 comparative solutions with all results lying within a ±2% error band of (Loveday et al. 2006) solution. This agreement confirms the ESP-r predictions under steady-state conditions.

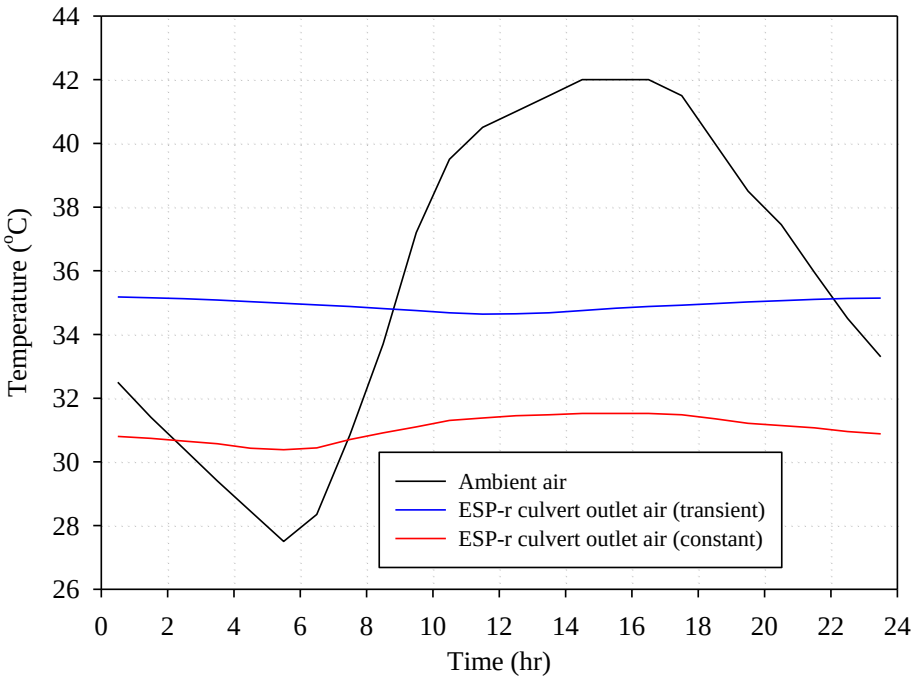

Figure 3.6: Culvert outlet air temperature from the ESP-r model.

Figure 3.6 depicts the clear difference between the two ESP-r solutions corresponding to the transient and steady-state cases. The steady-state solution follows the ambient air temperature profile, which indicates that the culvert performance worsens during the summer peak time. In the transient case, the culvert thermal efficacy improves marginally at the summer peak. Further, a steady-state model overestimates the culvert thermal performance in a manner that would lead an A/C system designer to conclude that a smaller auxiliary cooling system is required. This becomes vital when constructing a control strategy that couples culvert, A/C system and building. For example, Figure 3.6 shows that the steady-state solution suggests that the culvert outlet air must be supplied to the AHU of the A/C system from midnight until 2 A.M. and from 7 A.M. until midnight since the culvert outlet air temperature is less than the ambient air temperature. However, the transient solution in the same figure shows that from midnight until 9 A.M. the culvert outlet air temperature is higher than the ambient air temperature and therefore the air from outdoors should be introduced to the AHU, whereas from 9 A.M. until 10 P.M. the AHU receives the air from the culvert and ambient air from 10 P.M. until midnight. Consequently, it was concluded that ESP-r can robustly quantify the air culvert's

thermal performance and therefore assist with the identification of a control strategy for the hybrid system developed in chapter 4. It is known that the longer the culvert is at any reasonable depth, the closer will the temperature of flowing air get to the ground temperature. On the other hand the construction cost of the culvert will increase as will the energy losses associated with the friction induced pressure drop. Referring to Figure 3.7, the four steady-state culvert solutions predict that the longer the tube, the more the culvert's outlet temperature will decrease until it reaches the ground temperature value after about 60 m. The ESP-r transient solution in Figure 3.7 relates to this latter effect (system pressure drop) and shows that the culvert's outlet air temperature cannot reach the ground temperature no matter the length of the culvert. This is because, as the culvert gets longer, the existing fan static pressure is unable to provide the required flow rate. Now, in the steady state case to correspond for such situation, the fan capacity must therefore be increased to drive air through the lengthier culvert. Then, other culvert parameters must be changed, such as the diameter and convective heat transfer coefficient, to correspond to the new fan flow rate which will then act to demolish the attainable air temperature drop. However, the ESP-r air culvert transient model (Figure 3.7) can assess the actual air temperature drop because the pressure drop is quantified simultaneously at every node helping in assessing the accurate node's air temperature. The referenced figure shows the wide margin between the transient and steady state solutions requiring the need of quantifying culvert thermal performance transiently. In the present case, the optimum length was considered to be the length after which the further reduction in culvert outlet air temperature would be less than 1%. Culvert outlet air temperatures calculated for different diameters, with associated convective heat transfer coefficients at different lengths are shown in Table 3.5. These results indicate an optimum length of 40 m when a smaller diameter culvert is used. Beyond the 40m length, culvert thermal performance will not improve as the culvert outlet air temperature depression is minimal. When a larger culvert diameter is employed, the optimum length increases to 50-60m. The influence of the culvert length and diameter on thermal efficacy, along with the corresponding treatment of the convective heat transfer coefficient, is visited again in the sensitivity analysis section.

Table 3.5: Optimum culvert length for different diameters at summer peak.

Length (m)	Diameter (m)		Outlet air temperature (°C)		Difference in outlet air temperature (%)	
	D1	D2	$T_{oc\_}1$	$T_{oc\_}2$	$\Delta T_{oc\_}1$	$\Delta T_{oc\_}2$
10	0.23	0.67	39.11	36.85	-6.8	-12.2
20	0.23	0.67	37.18	34.39	-4.9	-6.7
30	0.23	0.67	35.94	33.28	-3.3	-3.2
40	0.23	0.67	35.36	32.48	-1.6	-2.4
50	0.23	0.67	35.12	32.07	-0.7	-1.3

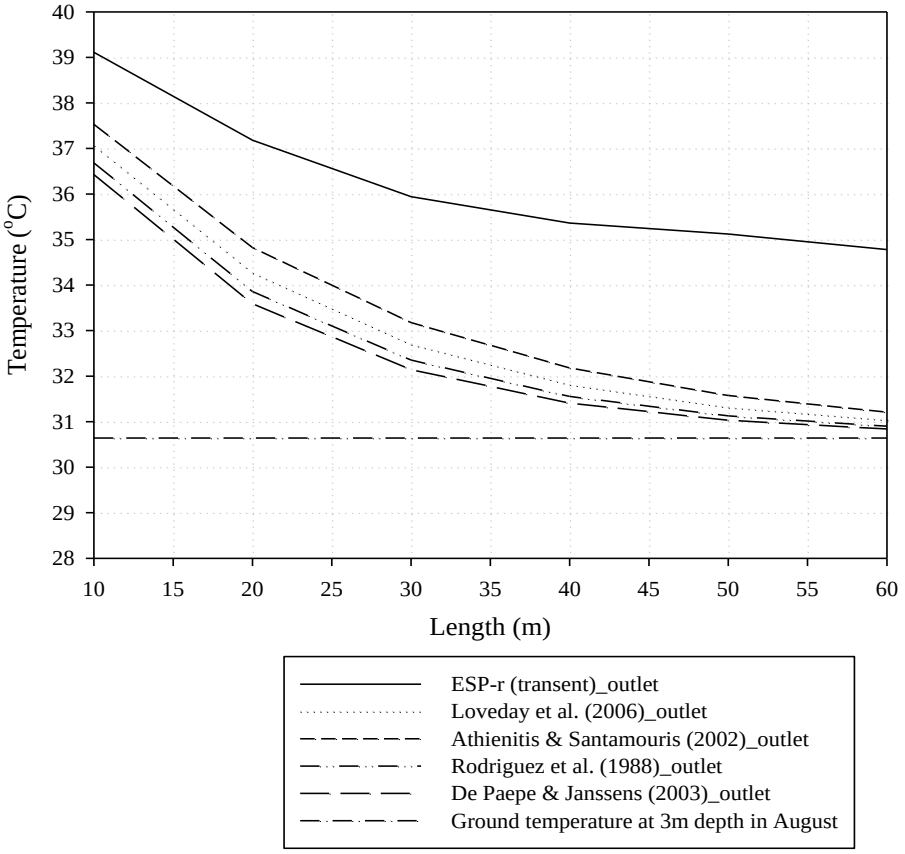

Figure 3.7: Culvert outlet air temperatures for the Riyadh summer peak condition under several culvert lengths and for different models.

3.2.2.2 Empirical Calibration

It was not possible to locate an existing culvert with the same parameters as identified above. Instead, an existing culvert was located and modelled in ESP-r in order to verify the modelling approach in principle. The Drumchapel Sports Centre in Glasgow employs an air culvert for cooling and has been monitored by Glasgow City Council's Management and Regeneration Services Department since its

installation in 2001. A visit was made to the site and interviews conducted with operations staff. These staff confirmed that measurement over a 10 year period conformed to a monitoring specification established by the ESRU group for use in a study conducted shortly after culvert commissioning. Figure 3.8 and Figure 3.9 represent the 2 rooms receiving culvert air (dance studio and fitness suite) and the linked culvert schematic. Figure 3.10 shows the culvert in the early stages of its construction. Four temperature sensors are positioned to take readings of the primary and secondary culvert air temperatures; the positions of these sensors are laid out in Figure 3.9 (green box for primary and red box for secondary). While access into the primary culvert was possible, this was not the case with the secondary culvert and so measuring the secondary culvert outlet air temperature was not possible. As explained in the literature review that culverts are validated for couple of hours or days at the most and never verified for longer periods, a week for example. To address this problem, Glasgow Council supplied monitored data for a 1-year period from which a sequential 8-day selection was made for validation purposes as listed in Table 3.6. The culvert is controlled such that when the indoor air temperature set-point in the dance studio and fitness suite (Figure 3.8) exceeds 16°C, separate fans direct culvert air (Figure 3.11) to the dance studio ($1.2m^3/s$) and fitness suite ($0.9m^3/s$) recommended by the design consultant. The incoming air is cooled after exchanging heat with the soil and delivered to the two zones as depicted in Figure 3.9. The culvert is 80m long (40m for each room with a 20m split between the primary and secondary culverts), with height and width of 1.8m and 1.5m respectively and constructed from concrete with a 0.4m thickness. The culvert was simulated in ESP-r with a volumetric flow rate to the fitness suite of $0.74m^3/s$ based on a monitored air velocity of 0.35m/s. The ground temperature was calculated from the equation 3.11 model, with a thermal diffusivity of $0.05m^2/day$ (NERC 2010). To estimate a value for the convective heat transfer coefficient, a flow characterization was undertaken. Using equation 3.6, the entrance length after which a fully developed turbulent flow should be imposed was about 42m whereas the culvert's length was 40m. Thus, the use of Nusselt Number correlations for fully developed turbulent flow to calculate the convective heat transfer coefficient would have been misleading.

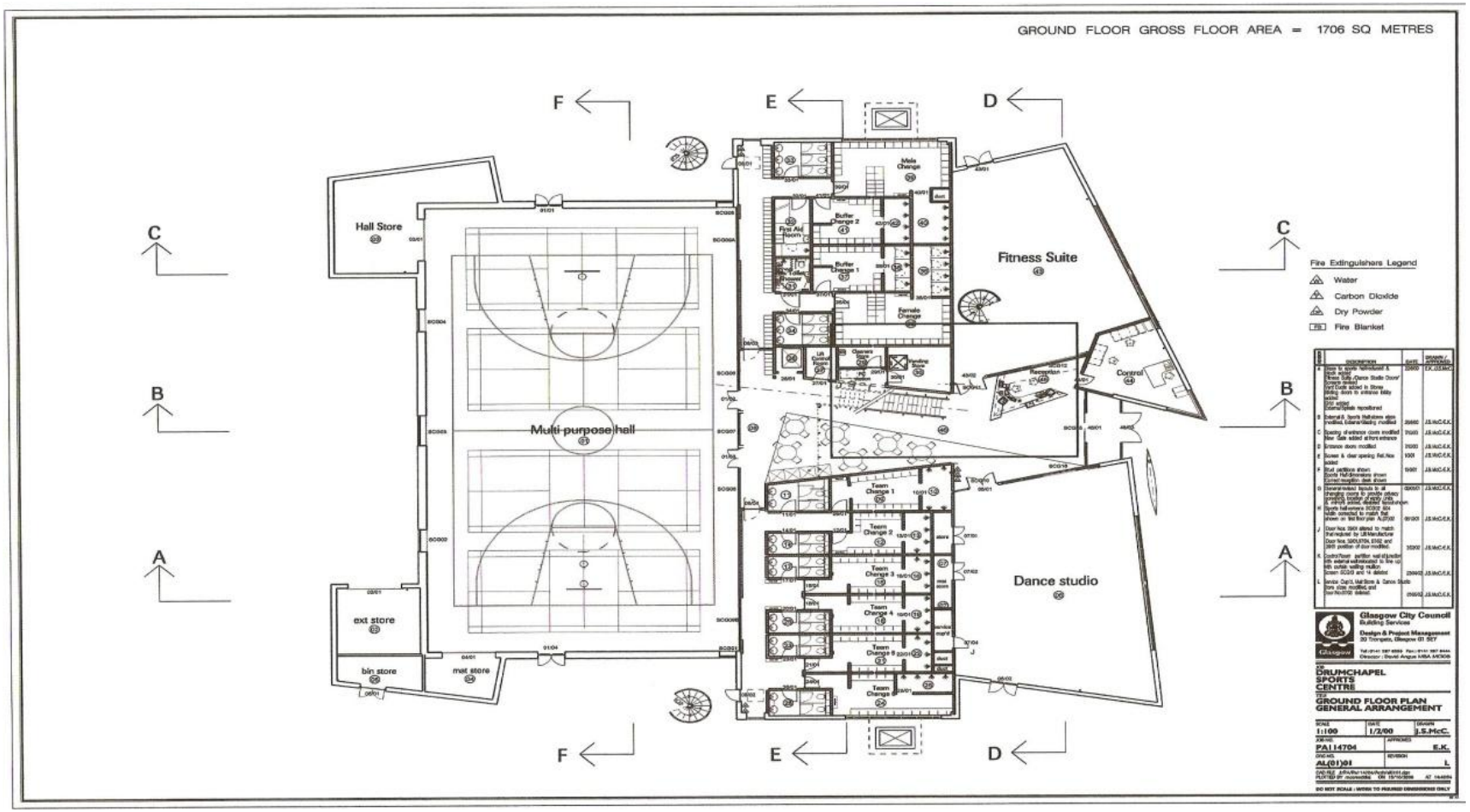

Figure 3.8: Drawing of Drumchapel Sports Centre (Glasgow City Council Building Services 2000).

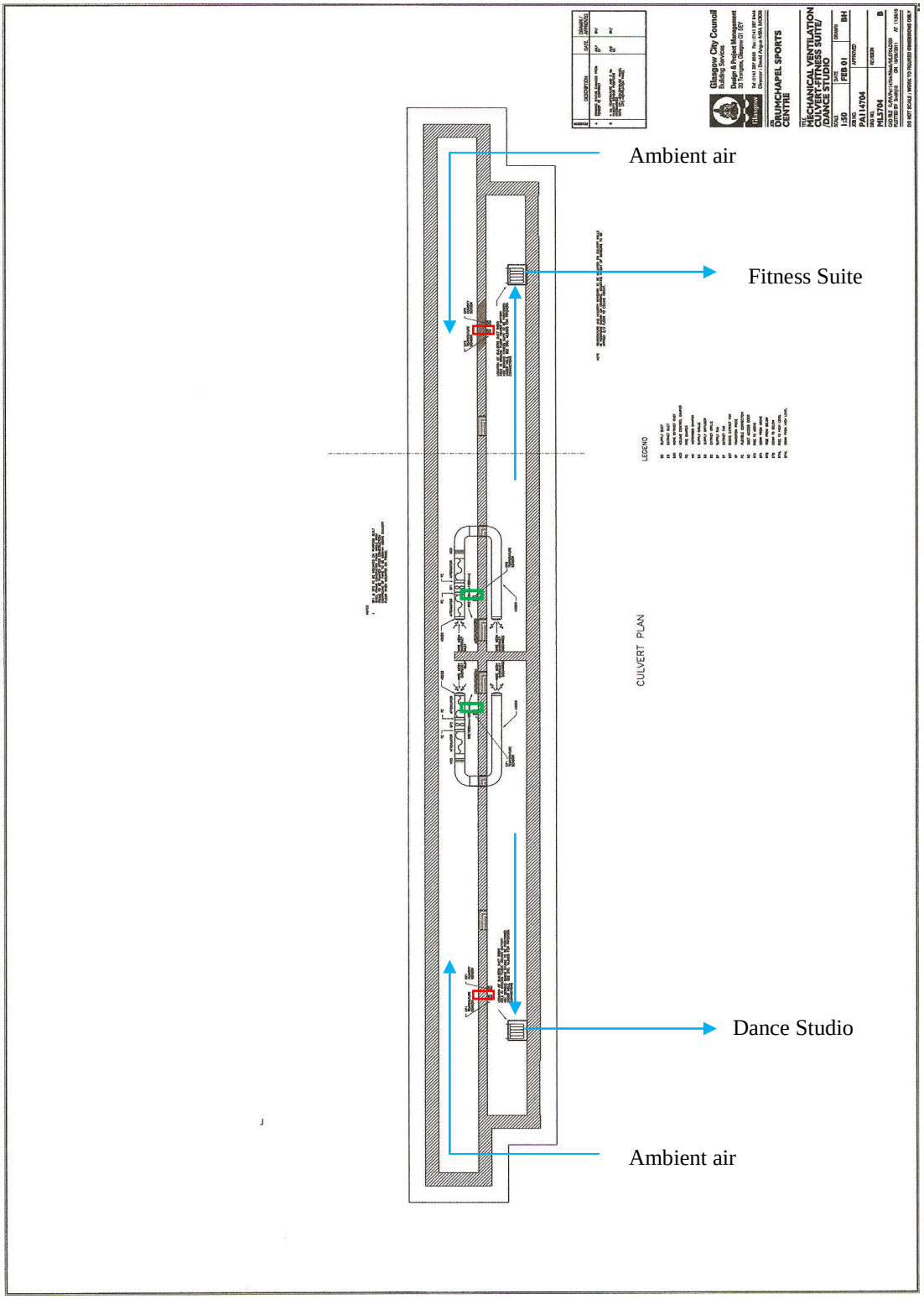

Figure 3.9: Air culvert schematic of Drumchapel Sports Centre (Glasgow City Council Building Services 2000).

Figure 3.10: Picture of Drumchapel air culvert under construction (Glasgow City Council Development and Regeneration Services 2001).

Figure 3.11: Picture of Drumchapel air culvert intake (Glasgow City Council Development and Regeneration Services 2001).

Table 3.6: Sample of an 8-day period monitored temperatures in °C of the air culvert supplying air to the fitness suite at Drumchapel Sports Centre, Glasgow, UK.

Time/ Temperature (°C)	Outside Air Temp.	Culvert Primary Temp.	Culvert Secondary Temp.	Fitness Supply Temp.	Fitness Space Temp.	Fitness Set-point Temp.
16/05/2011 23:30	11.5	7.5	13.9	16.3	18	16
16/05/2011 22:30	11.9	7.6	13.9	16.2	18.3	16
16/05/2011 21:30	12.2	7.6	13.7	15.6	18.7	16
16/05/2011 20:30	12.4	7.6	13.6	15.1	19.1	16
16/05/2011 19:30	12.7	7.7	13.6	15.1	19.2	16
16/05/2011 18:30	13.1	7.8	13.6	15.1	18.9	16
16/05/2011 17:30	13.3	7.8	13.6	15.1	18.7	16
16/05/2011 16:30	13.2	7.8	13.6	15.1	18.6	16
16/05/2011 15:30	13.7	8	13.6	15.2	18.5	16
16/05/2011 14:30	14.9	8.2	13.6	15.4	18.3	16
16/05/2011 13:30	15.7	8.2	13.6	15.4	17.9	16
16/05/2011 12:30	15.5	8	13.5	15.2	17.6	16
16/05/2011 11:30	14.4	7.7	13.2	14.9	17.2	16
16/05/2011 10:30	13.8	7.6	13.1	14.8	17	16
16/05/2011 09:30	13.5	7.4	13.1	14.7	17.1	16
16/05/2011 08:30	12.5	7.2	13.2	14.7	17.2	16
16/05/2011 07:30	11.6	7.1	13.3	15.1	17.3	16
16/05/2011 06:30	11.2	7.1	13.4	15.3	17.4	16
16/05/2011 05:30	11.1	7.1	13.4	15.3	17.4	16
16/05/2011 04:30	11.3	7.2	13.4	15.3	17.5	16
16/05/2011 03:30	11.6	7.3	13.4	15.4	17.5	16
16/05/2011 02:30	11.7	7.3	13.4	15.4	17.7	16
16/05/2011 01:30	11.9	7.4	13.4	15.5	17.7	16

As a result, convective heat transfer coefficients have to be assessed experimentally. This is not a straightforward task since the coefficient changes dynamically. Wachenfeldt (2003) constructed the graph of Figure 2.3 for a culvert with a large cross-sectional area. This shows that the measured, average convective heat transfer coefficient is about 10 times higher than those resulted from the use of fully developed turbulent flow correlations. Since the average convective heat transfer coefficient values are of interest here and the culvert in both locations share similar parameters, it was deemed acceptable to use the method of Wachenfeldt (2003). The fully developed turbulent flow convective heat transfer coefficient for

the Drumchapel Sports Centre culvert was thereby calculated at approximately 2W/m^2°K and therefore the non-fully developed turbulent coefficient would be about 20W/m^2°K. Now, referring to Figure 2.3, one can notice that the experimental coefficient sometimes could be more than 10 times the fully developed theoretical coefficient, but to be conservative it was suggested to increase the theoretical by only 10 folds.

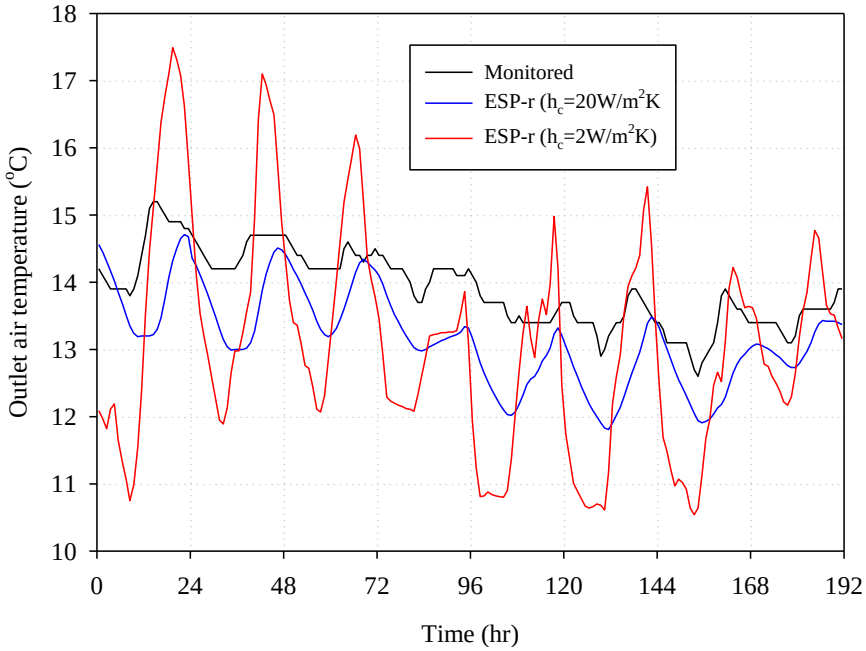

Figure 3.12: Effect of convective heat transfer coefficient on the Drumchapel Sports Centre culvert outlet air temperature.

$$T_g = 13 - 6.5e^{-0.41z}\cos\{2\pi/365[t - 343 - 24.1z]\} \qquad 3.11$$

Figure 3.12 depicts the difference between the monitored culvert secondary outlet air temperatures as listed in Table 3.6 and their equivalents in ESP-r for an 8 day period (May 9 – 16 2011) with the above convective heat transfer coefficients used by ESP-r. The culvert outlet air temperature profile produced by ESP-r was similar to those monitored when higher convective heat transfer coefficients were incorporated. But when the smaller values were used the profile followed that of the ambient air temperature and so higher convective heat transfer coefficient values were considered suitable.

In the transient solution as depicted from Figure 3.12 there is an agreement with the monitored result but with a time shift. This time shift is caused by several reasons because the coupling between earth and culvert is dynamic. For example, it could be due to the fact that the ESP-r transient model uses constant monthly ground temperatures whereas the physical culvert encounters instantaneous real ground temperatures and thus the time lag between ambient and ground temperatures is not only considered monthly but also daily and even hourly. Another reason could be that the assessment of the theoretical convective heat transfer coefficient is not matching well with the empirical set-up. The latter effect was studied by increasing the developing turbulent flow convective heat transfer coefficient from 10 times to 20 times the hydrodynamically and thermally developed case (from 20W/m^{2}K to 40W/m^{2}K). Figure 3.13 clearly shows that when convective heat transfer coefficient of the developing flow in the empirical culvert is doubled the time shift has dissipated a bit. To put this into perspective physically, velocity and temperature boundary layers are developing in the presence of heat transfer until entrance length of the culvert where they emerge.

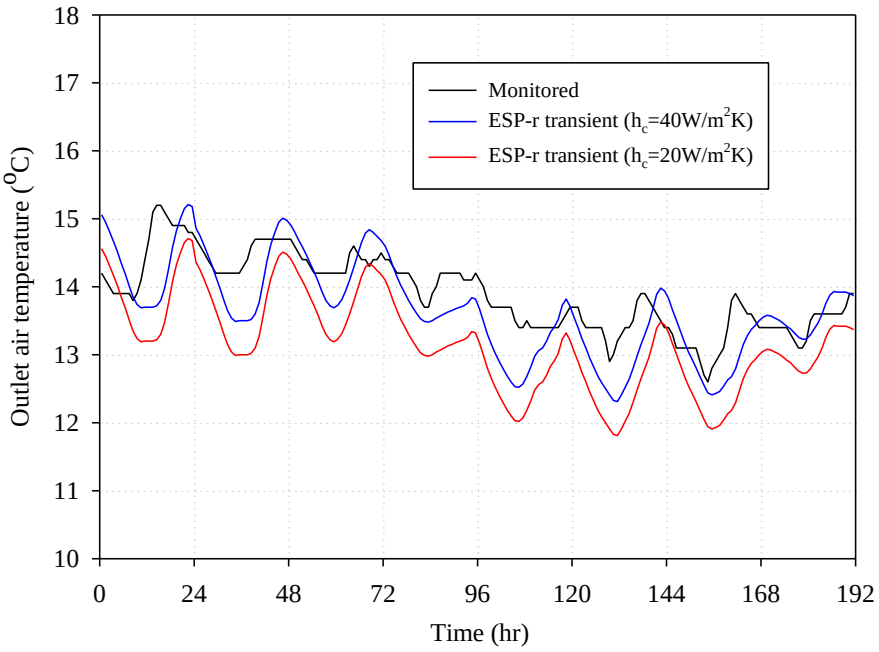

Figure 3.13: Time shift reduction due to convective heat transfer coefficient increase.

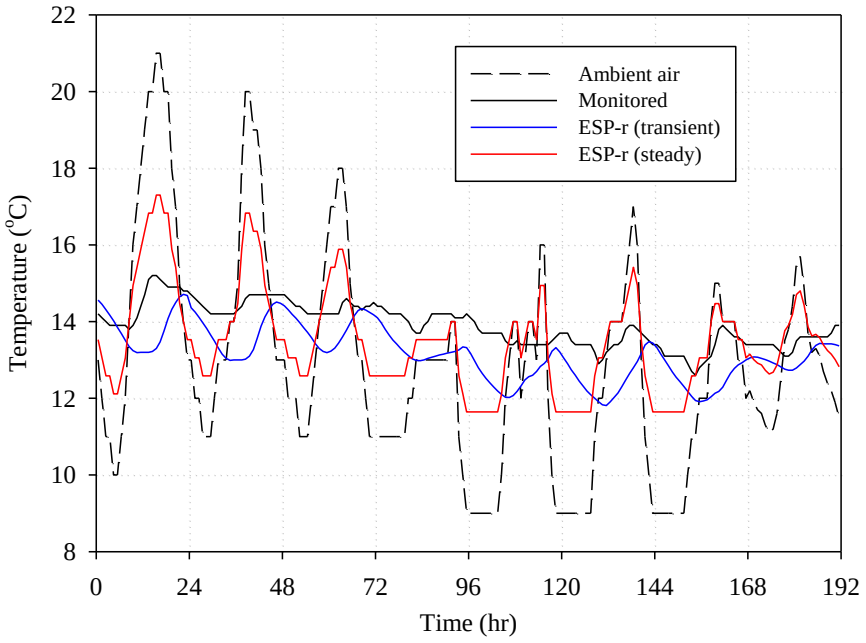

Figure 3.14: Culvert outlet air temperature at Drumchapel Sports Centre, May 9-16 2011.

Hence, the convective heat transfer coefficient is higher by far at the entrance than it is at the entrance length after which it stays constant in the fully developed region (Figure 3.15). During the developing region the coefficient is changing spontaneously which makes it difficult to be monitored or predicted and thus the scenario considered of multiplying the fully developed coefficient by 10 is considered comprehendible. Figure 3.14 shows that when the ESP-r solution was made steady-state, the culvert outlet air temperature profile followed the ambient temperature profile. The higher the diurnal temperature range (transient ambient temperatures), the more the steady-state solution follows the ambient air temperature profile and thus the use of transient culvert models would be essential in assessing culvert thermal performance when there is high alternation in outdoor temperatures. However, steady state culvert models can be beneficial when the diurnal temperature difference is small (steady ambient temperatures) when there is small change in outdoor temperatures. For instance, Figure 3.14 shows that on May 11 2011 the diurnal temperature range was 18-11°C whereas in May 16 it was 15.5-11°C. Figure 3.16 illustrates that on May 11 the ESP-r steady-state culvert outlet air temperatures were above or below the error band of ±8% whereas Figure 3.17 shows that when the

diurnal temperature range reduced from 7°C on May 11 to 4.5°C on May 16, the ESP-r steady-state solution is within a bounding error of ±8%. However, the ESP-r transient model temperatures were well within the 8% error band on May 11 and 16 as shown in Figure 3.16 and Figure 3.17.

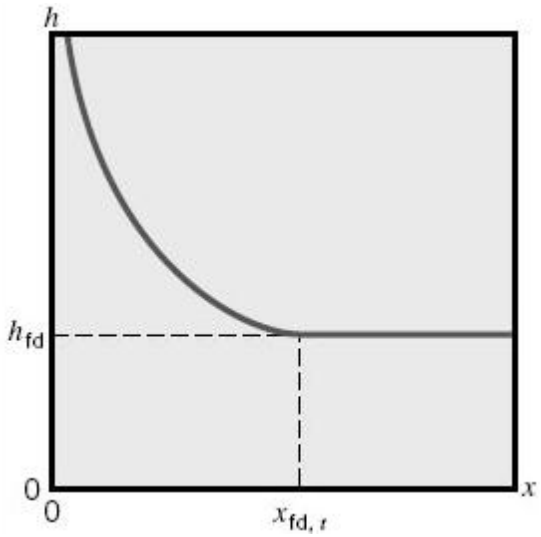

Figure 3.15: Convective heat transfer coefficient in developing and fully developed flow regions inside a duct (Cengel & Boles 2006).

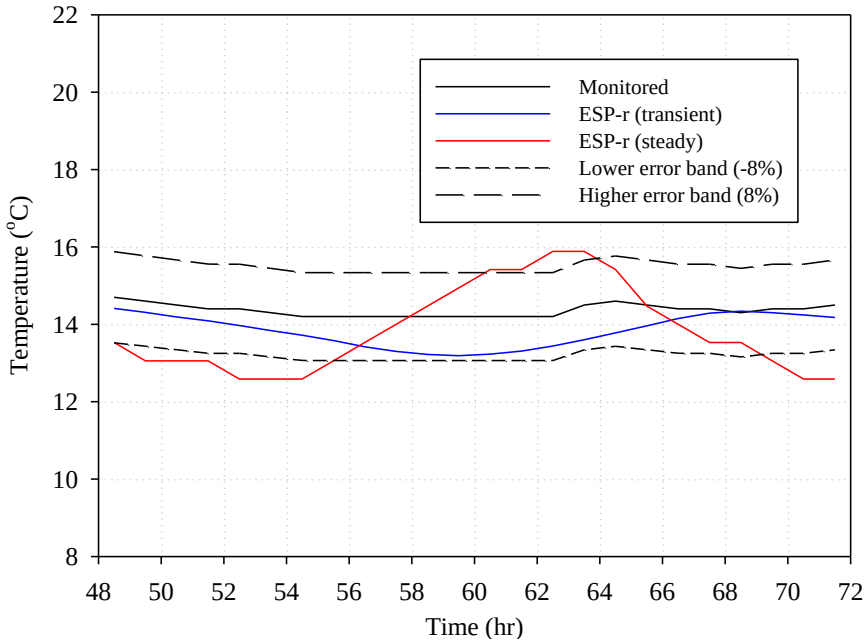

Figure 3.16: Culvert outlet air temperature at Drumchapel Sports Centre, May 11 2011.

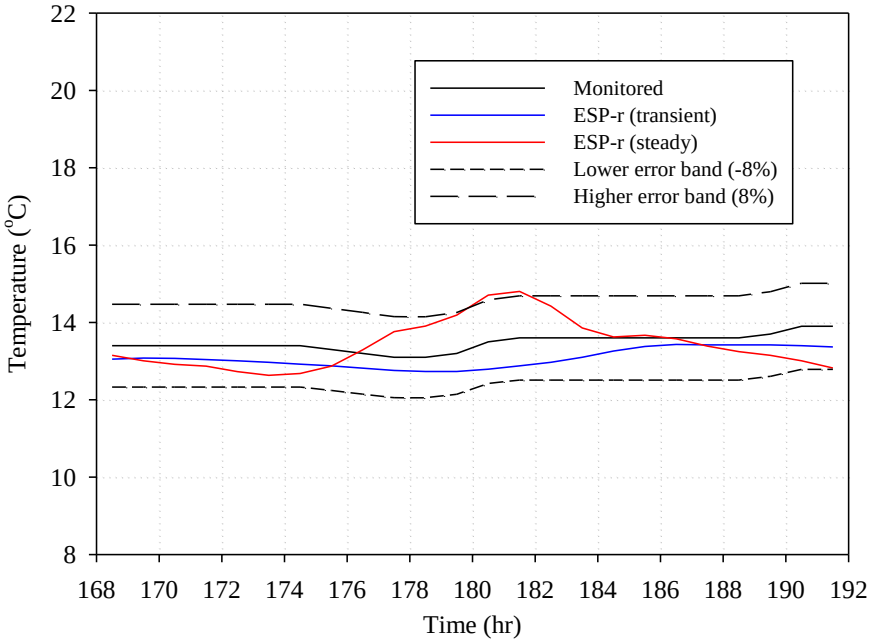

Figure 3.17: Culvert outlet air temperature at Drumchapel Sports Centre, May 16 2011.

3.3 Air culvert Sensitivity Analysis

A sensitivity analysis of the air culvert was performed to define a parametric priority list quantifying the importance of each culvert design parameter. The analysis is undergone based on results produced by theoretical simulation modelling tool not real data. Heating and cooling seasons were simulated with one parameter varied while the other parameters were held constant. The elements studied were:

1. Ambient temperature and relative humidity.
2. Soil temperature.
    a. Depth.
    b. Previous culvert operation.
    c. Earth treatment.
3. Heat exchange surface area.
    a. Length.
    b. Diameter.
4. Air flow rate.
5. Convective heat transfer coefficient.

3.3.1 Ambient Air Temperature and Relative Humidity

As shown in Table 3.7, the alteration of the hourly inlet air temperature has minimal effect on the culvert hourly outlet air temperature: a change of -10% to +36% (during seasonal days) in the former results in a ± 1% change in the latter. However, referring to equation 3.12, the culvert's hourly cooling or heating capacity is directly proportional to the inlet ambient air temperature. On the other hand, a hot/humid climate has been used rather than the hot/dry of Riyadh to study the impact of higher external relative humidity on culvert thermal performance. Figure 3.18 shows that for similar ambient air temperatures, but higher external relative humidity, culvert outlet air temperatures were significantly increased.

Table 3.7: Culvert outlet air temperature change as a result of maximum and minimum changes in ambient air temperature for seasonal days.

Properties/Season	Winter		Spring		Summer		Fall	
Ambient ΔT / T (%)	T_{oc}	$T_{amb.}$	T_{oc}	$T_{amb.}$	T_{oc}	$T_{amb.}$	T_{oc}	T_{amb}
Maximum	-1	36	-1	20	-1	10	0	17
Minimum	1	-9	0	-10	0	-4	1	-5

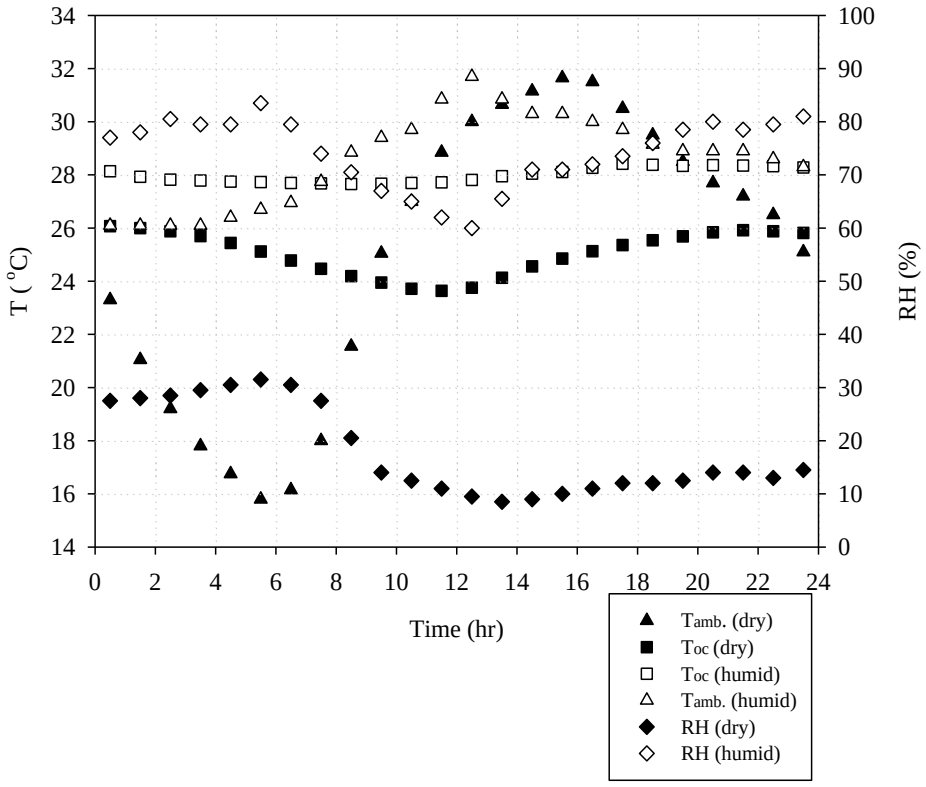

Figure 3.18: Influence of external relative humidity on culvert thermal performance.

$$\text{Culvert capacity} = \dot{m}_a c_p (T_{oc} - T_{amb}) \quad 3.12$$

For example, when the ambient air temperatures were 30.65°C and 30.85°C and the corresponding external relative humidity were 8.5% and 65.5%, the culvert outlet air temperatures were 24.13°C and 27.95°C for hot/dry and hot/humid climates respectively. This represents an air culvert outlet air temperature increase of 16% under a hot/humid climate.

3.3.2 Soil Temperature

The factors affecting soil temperature are incidence angle of solar radiation and surface reflectance/absorptance. In the sensitivity study, the effect of culvert depth, culvert operation and ground surface treatment on culvert thermal performance were the parameters studied. Culvert operation refers to shutting down the culvert in a certain season when its use is limited. Ground surface treatment involves changes to the surface cover or water sprinklers to reduce solar radiation take-up or to enhance heat loss by evaporation.

3.3.2.1 Depth

The solid line in Figure 3.19 illustrates how the culvert outlet air temperature decreases with increasing depth during summer; in winter, it increases with increasing depth as shown by the dashed line. The greater the depth, the more the ground temperature dominates the heat transfer exchange process and improves culvert thermal performance. At lower depth values the culvert's inlet temperature (ambient) dictates performance. Increasing the depth from 1m to 3m (200%) decreases and increases the culvert's outlet air temperature by about 8% in cooling and heating seasons respectively as shown in Figure 3.19.

3.3.2.2 Previous Culvert Operation

During late summer months the ground gets hot and the benefit of operating the air culvert reduces even at a depth of 3m. This situation can be taken advantage of by shutting down the culvert so that the ground does not receive an additional heat input. This will reduce the ground temperatures over the following months as shown in Table 3.8: the reduction is estimated by educated guess at 1°C during the first

month the culvert was operating after shutting down, with a 0.2°C incremental increase/month thereafter compared with ground temperatures in Table 3.2. The ground temperature profile in Table 3.8 is then inserted in the ESP-r culvert model instead of that in Table 3.2. Hence, the thermal performance of the culvert in the heating season is compromised since the ground temperature is lower. On the other hand, the culvert's thermal performance is enhanced in the early cooling season. In winter, the culvert outlet air temperature decreases by 2%, while in early summer it decreased by 1%.

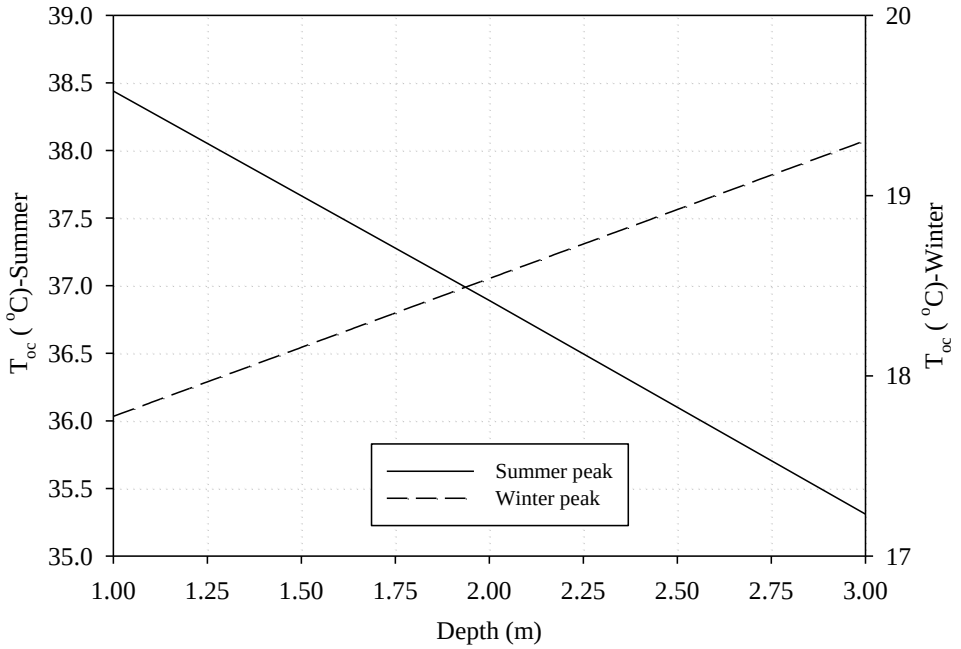

Figure 3.19: Effect of depth on culvert thermal performance.

Table 3.8: Monthly ground temperature profile of Riyadh with late summer culvert shutdown.

Jan.	Feb.	Mar.	Apr.	May	Jun.	Jul.	Aug.	Sep.	Oct.	Nov.	Dec.
25.2	23.0	21.7	21.8	23.2	25.4	28.2	30.6	off	off	off	28.0

3.3.2.3 Ground Surface treatment

Givoni (1994) conducted ground temperature measurements for a variety of earth treatment methods. He was able to reduce the surface ground temperature from 33°C to 24°C; the underground temperature at a depth of 3m was measured at 25.5°C. This impact of ground surface treatment is replicated for Riyadh in Table 3.9: the ground temperature at 3m depth as prescribed by Givoni (1994) under

similar ambient conditions for late summer months is 25.5°C. The ground temperature reduction in the first month (December) after completing earth treatment is at 4°C, with a 0.5°C incremental increase/month thereafter compared with ground temperatures in Table 3.2. The ground temperature profile in Table 3.9 is then inserted in the ESP-r culvert model instead of that in Table 3.2. As a result, culvert outlet air temperature was reduced by 8% and10% in heating and cooling seasons respectively. So, when earth treatment was undertaken, the culvert's thermal performance was reduced in winter, while in early and late summer it was enhanced. A ground temperature of 31.5 °C for the hot/dry climate studied was calculated by plugging the variables required into equation 3.13. This is the ground temperature of the hot/dry climate above which culvert cooling potential drops drastically as depicted from Figure 3.32 and therefore earth treatment is recommended. This ground temperature changes from climate to another and was extracted from a number of simulations based on trail and error.

$$T_{g\_set-point} = T_{ama} + \left(\frac{T_{hag} - T_{lag}}{2}\right) \quad 3.13$$

Table 3.9: Monthly ground temperature profile for Riyadh when ground surface treatment is introduced.

Jan.	Feb.	Mar.	Apr.	May	Jun.	Jul.	Aug.	Sep.	Oct.	Nov.	Dec.
22.5	20.6	19.6	20	21.7	24.4	27.7	30.6	25.5	25.5	25.5	25.0

3.3.3 Heat Exchange Surface Area

The culvert as represented in ESP-r is rectangular and its rectangular surface area is given by equation 3.14 whereas its hydraulic diameter is given by equation 3.15. Length, width and height of the culvert are space dimensions that when altered can impact significantly both the hydraulic diameter and the culvert surface area which would have an impact on culvert thermal performance.

$$A = 2(wH + Lw + LH) \quad 3.14$$

$$D_h = \frac{2wH}{(w + H)} \quad 3.15$$

3.3.3.1 Length

Note that, as listed in Table 3.10, the convective heat transfer coefficient before the entrance length was estimated at 10 times greater than that after the entrance length as discussed in section 3.2.2.2. This change between the developing and fully developed convective heat transfer coefficients is named transient, yet it should be emphasized that it is not literally transient because the coefficient used in modelling does not keep changing at every length before entrance length but it was assumed constant (10 times that after entrance length) to simplify the problem. In small cross-sectional culvert such as the one under study (D_h=0.23m and L=60m), the entrance length is small (5.5m) and thus only the air temperatures in first couple of culvert sections are impacted heavily when varying coefficients whereas the outlet air temperatures in latter culvert sections are not as shown in Figure 3.20. Obviously, using the proposed transient coefficient scheme in larger cross-sectional area culverts is even more substantial since entrance length is usually high. Figure 3.20 shows that during the cooling season the culvert outlet air temperature is decreased by about 5% and 7% under transient (using 10 times the fully developed correlation before entrance length and the fully developed correlation after entrance length) and constant (using fully developed correlation before and after entrance length) convective heat transfer coefficients schemes respectively when the culvert length is increased by 200% from 20m to 60m. For the heating season, the culvert outlet air temperature was increased by 47% and 51% under transient and constant convective heat transfer coefficients respectively for the same length increase.

Table 3.10: Convective heat transfer coefficient inside culvert.

L (m)	D (m)	$\dot{V}$ (m^3/s)	h_c (fully developed turbulent flow) (W/m^2K)	L_E (m)	h_c (before entrance length) (W/m^2K)
10	0.23	0.08	8.6	5.5	86
20	0.23	0.08	8.6	5.5	86
30	0.23	0.08	8.6	5.5	86
40	0.23	0.08	8.6	5.5	86
50	0.23	0.08	8.6	5.5	86
60	0.23	0.08	8.6	5.5	86

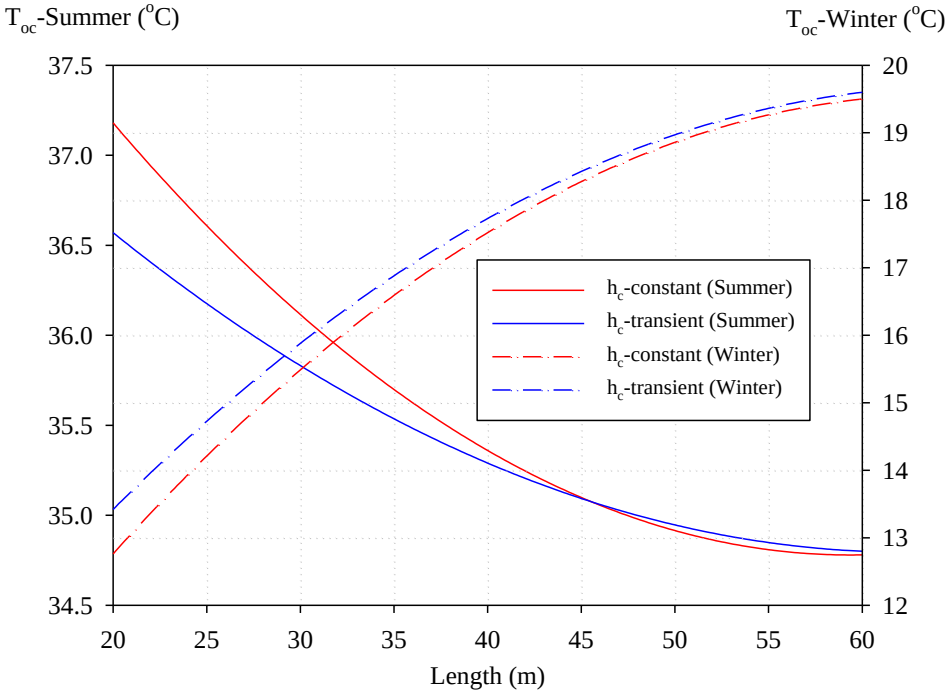

Figure 3.20: Impact of culvert length on thermal effectiveness at summer and winter peak times.

3.3.3.2 Diameter

For an accurate representation, the diameter change has to be accompanied by a change with the convective heat transfer coefficient as both are related in equation 3.10. Figure 3.21 depicts what happens inside the culvert in both cooling and heating seasons when its diameter increased by 200% from 0.23m to 0.67m (air speed decreased from 2m/s to 0.2m/s respectively because the volume flow rate is constant) – Table 3.11 shows the three related convective heat transfer coefficients. It is evident from Figure 3.21 that in low thermal load periods the culvert outlet air temperature is increased by 10% (when only diameter increased, it is 26%) and it is decreased by 8% (when only diameter increased, it is -9%) in high thermal load periods; both when the diameter is increased by 200% and the convective heat transfer coefficient modified accordingly.

Table 3.11: Simultaneous change of culvert diameter and convective heat coefficient.

D (m)	$\dot{V}$ (m^3/s)	V (m/s)	h_c (W/m^2K)
0.23	0.08	2.00	8.60
0.44	0.08	0.52	2.15
0.67	0.08	0.23	0.92

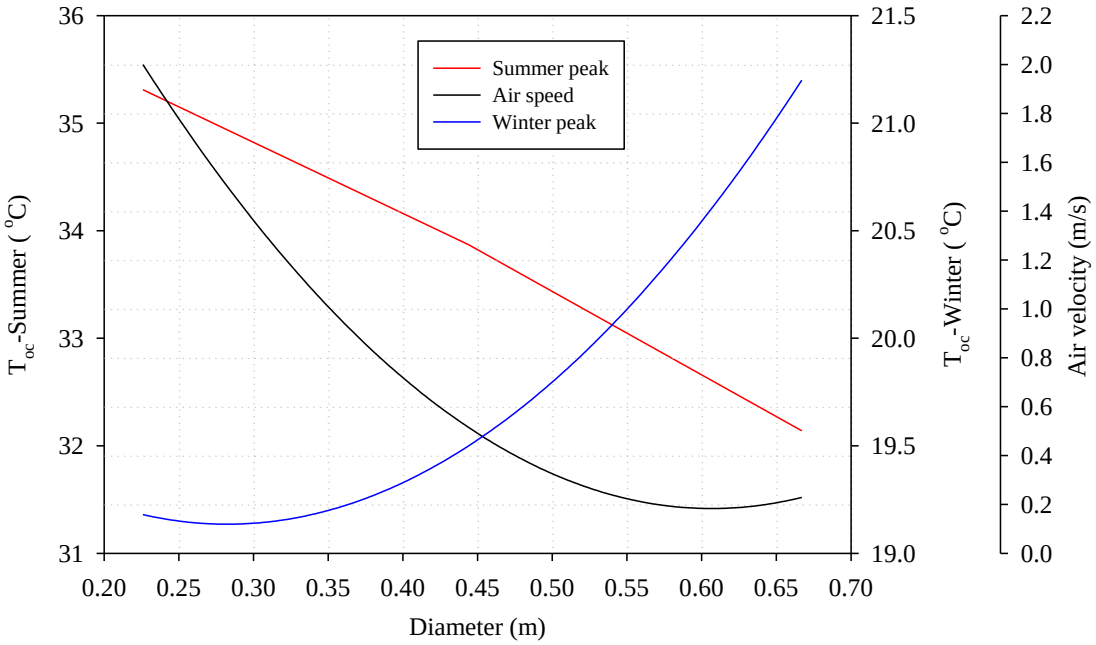

Figure 3.21: Effect of concurrent change of diameter and convective heat transfer coefficient on culvert thermal performance.

3.3.4 Volume Flow Rate

Table 3.12 lists the corresponding change in the convective heat transfer coefficient when volumetric flow rates are changed for the same diameter. Figure 3.22 shows that when the volume flow rate increases, the air velocity inside the culvert exceeds the nominal value recommended in CIBSE Guide B (2005) because of a higher pressure drop: the culvert diameter would therefore need to be altered as a function of the volume flow rate to maintain a constant air speed of 2m/s or less as listed in Table 3.13.

Table 3.12: Simultaneous change of flow rates and convective heat coefficients in culvert.

$\dot{V}$ (m^3/s)	D (m)	V (m/s)	h_c (W/m^2K)
0.08	0.23	2	8.60
0.16	0.23	4	17.4
0.24	0.23	6	26.3

Figure 3.23 depicts the results for a culvert where both volume flow rate and diameter are treated simultaneously to maintain the air speed at or below 2m/s. Figure 3.23 shows a 0% and -16% change in culvert outlet air temperature in summer and winter respectively when the volume flow rate is increased by 200% from 0.08 m^3/s to 0.24 m^3/s and accompanied by the corresponding diameter increase. On the other hand, when the volume flow rate was doubled with no corresponding diameter change, these percentages were +3% and -18% (Figure 3.22) for summer and winter peak times respectively. Figure 3.24 refers to the suitable diameter for the chosen volume air flow rate where the culvert pressure drop is kept low. A regression analysis was undertaken as shown in Figure 3.24 to determine the culvert diameter as a function of volume flow rate. It is important to state that Figure 3.24 was constructed under an air speed of 2 m/s so that an acceptable pressure drop in the culvert is possible when very large volume flow rates such as those in shopping malls or sports centres are required. However, when low volume flow rates are involved then the diameter found from Figure 3.24 can be increased substantially until site restrictions rise since the diameter increase under constant volume air flow rate would decrease the air speed and consequently the pressure drop.

Table 3.13: Simultaneous change of flow rates and diameters in culvert.

Variant	$\dot{V}$ (m^3/s)	D (m)	V (m/s)	h_c (W/m^2K)
1	0.08	0.23	2	8.59
2	0.16	0.32	2	8.68
3	0.24	0.39	2	8.72

- **Summary of Culvert Sensitivity Analysis.**
  - Length increase enhances culvert thermal performance. Convective heat transfer coefficient has to be monitored before and after entrance length.
  - Hydraulic diameter increase upgrades culvert thermal performance, but when experienced, this increase has to be accompanied with a change in convective heat transfer coefficient. However, air speed inside culvert is reduced because ventilation requirements keep constant.
  - When the volume flow rate in culvert is increased the hydraulic diameter has to be changed simultaneously with it keeping air speed inside culvert constant.

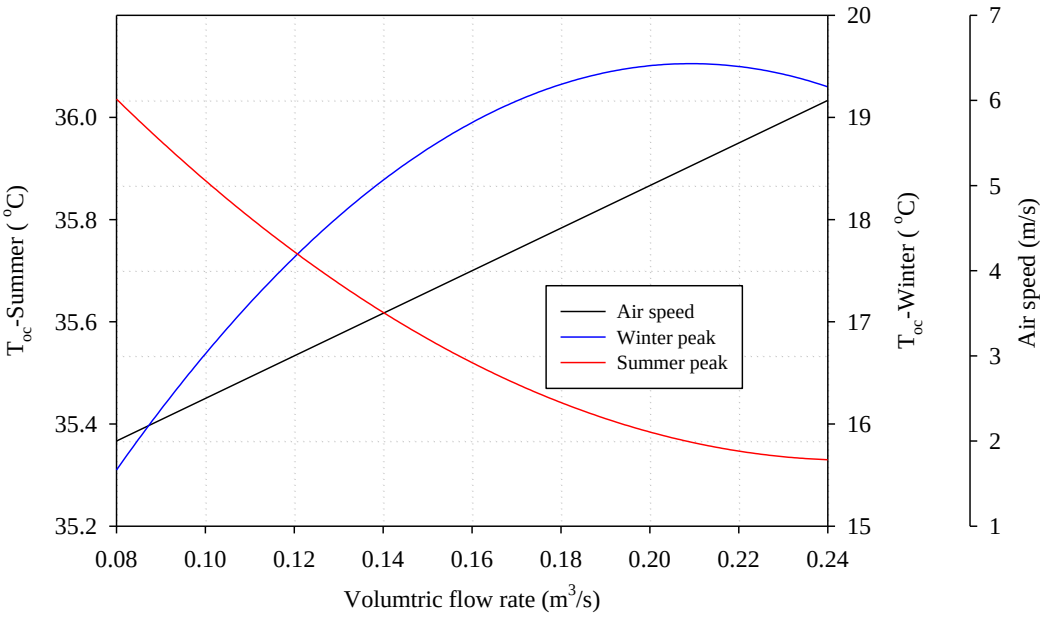

Figure 3.22: Effect of simultaneous change of volume flow rate and convective heat transfer coefficient on culvert outlet air temperature.

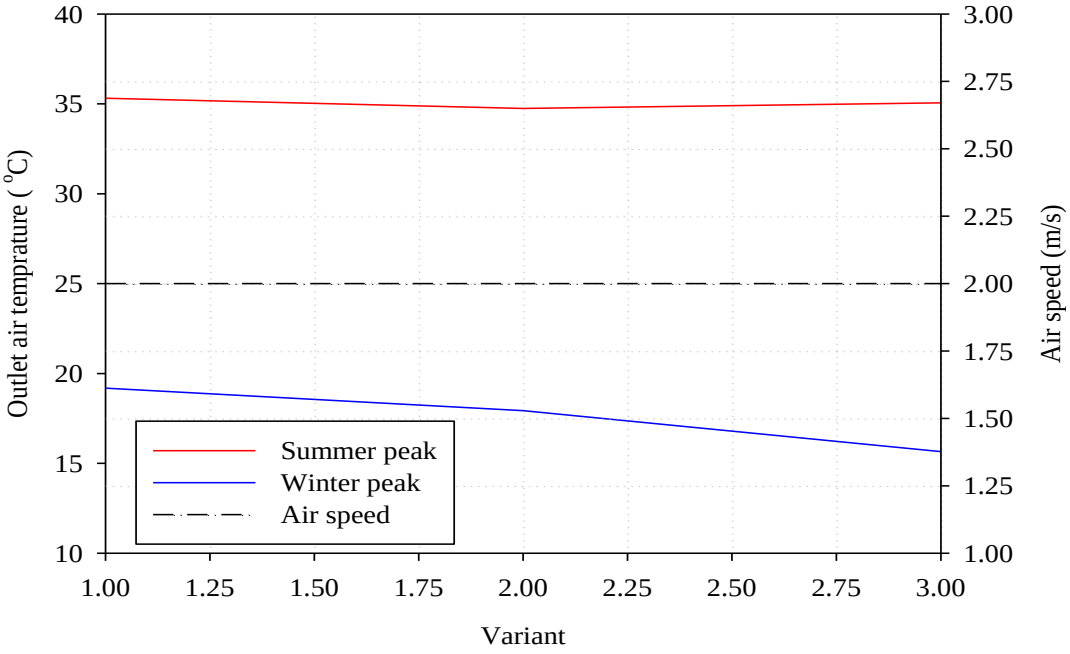

Figure 3.23: Effect of concurrent change of volumetric flow rate and diameter on culvert performance.

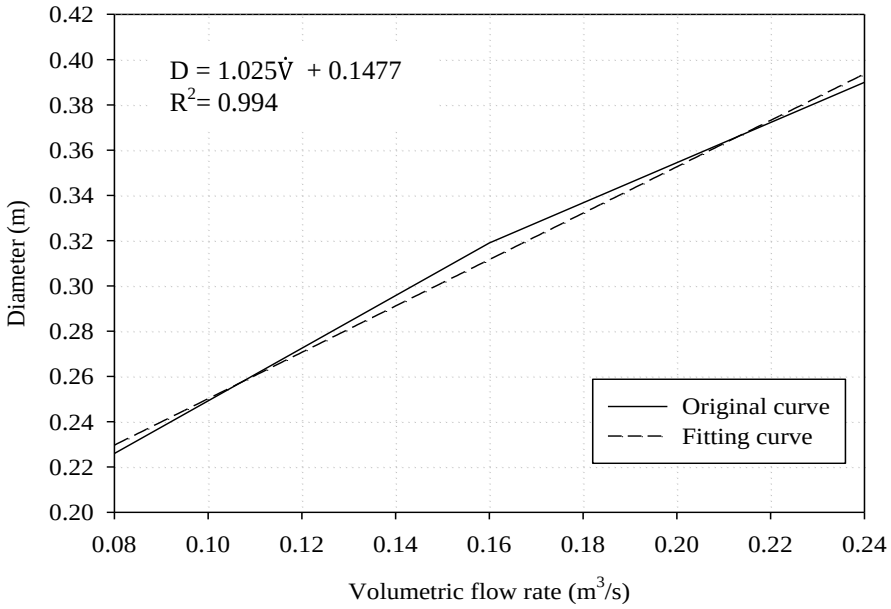

Figure 3.24: Regression analysis for the diameter required as a function of volume flow rate in the culvert.

3.4 Parametric Priority List for Heating/Cooling Seasons

The parameters examined in the sensitivity analysis have been evaluated and compared as shown in Figure 3.25. Culvert dimensions (diameter, length, depth) and volume flow rate were increased by 200%. Other parameters – ambient temperature and relative humidity, previous culvert use, and earth treatment – were studied in terms of their impact across time. The parameters that improve culvert performance in both cooling and heating seasons are listed in descending order in Table 3.14. For example, as displayed in Figure 3.25, both diameter and depth are capable of reducing the outlet air temperature in the cooling season by 8% while the contribution of diameter is 2% greater than depth in heating season; diameter should therefore be prioritised over depth as a design parameter to be adjusted to improve performance. The parameter selected from Table 3.12 priority list should be the one that can best reduce culvert outlet air temperature in cooling season without adverse impact in the heating season.

Table 3.14: Parametric priority list to upgrade culvert thermal performance.

Rank	Parameter (action)	Constraints or Consequences
1	Hydraulic diameter (increase)	Site restrictions.
2	Depth (increase)	Drilling costs.
3	Length (increase)	Pressure drop increase in the system.
4	Earth treatment (late summer)	Winter thermal performance degradation.

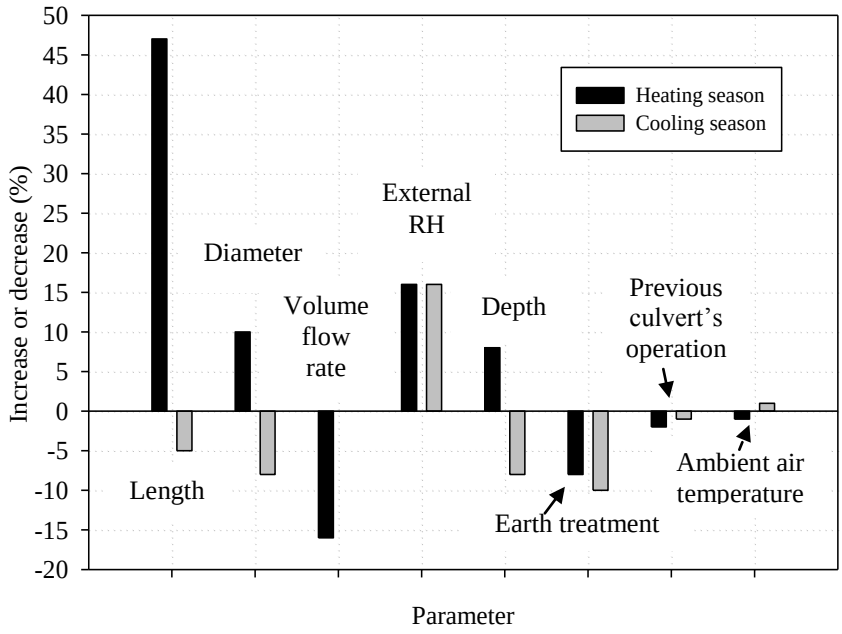

Figure 3.25: Culvert parametric study chart identifying percentage of change in culvert outlet air temperature for heating and cooling seasons.

3.5 Upgrading Thermal Efficiency of Air Culvert

The air culvert was simulated for the four seasons of the year to quantify its thermal effectiveness in each season. The objective was to maximise performance under the different weather regimes. Thermal effectiveness (ε) and Coefficient of Performance (COP) are two indicators used in the present context to define culvert thermal performance. COP is the ratio of culvert cooling energy to fan energy

consumption, while ε represents how close the culvert outlet air temperature approaches the ground temperature.

3.5.1 Culvert Thermal Effectiveness

- **Winter Season**

The dashed line in Figure 3.26 shows that during winter season the culvert can satisfy the heat load required to ensure the wellbeing of occupants without auxiliary heating: the outlet air temperature is around 17°C when the ambient temperature is at its minimum. The temperature difference between culvert outlet air temperature (17.5°C) and ambient temperature (4.85°C) at the winter peak time (5:30) is 12.65°C. About 70% of this temperature difference has been achieved by culvert section 3, as illustrated in Figure 3.31, whereas only 10% of this temperature difference was contributed by the addition of section 6. The winter culvert ε at a ground temperature of 26°C was calculated from equation 3.16 to be 0.59. However, when the culvert hydraulic diameter is increased from 0.23m to 0.67m, its outlet air temperature increases to 22.5°C and ε improved to 0.83.

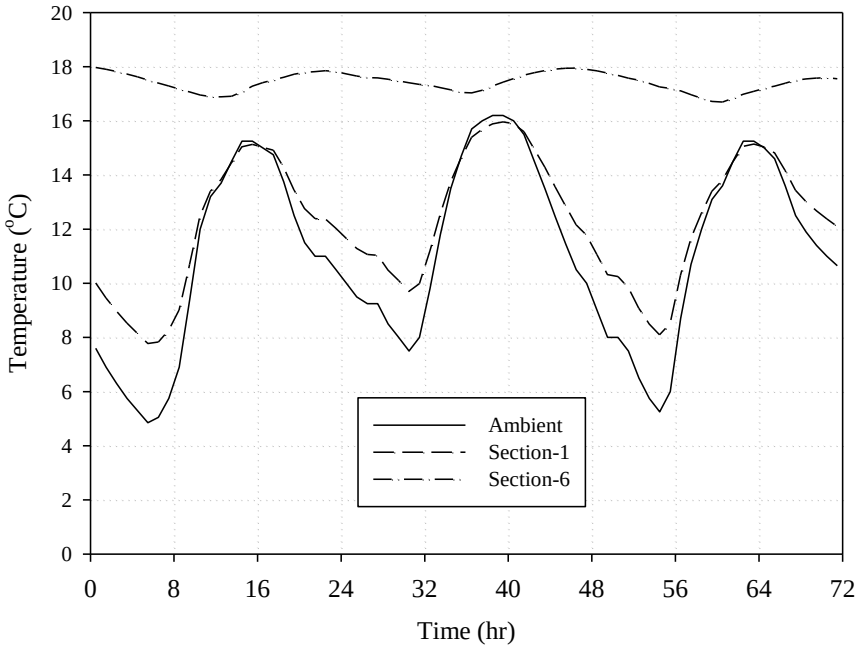

Figure 3.26: Ambient and culvert section temperatures for the period January 1-3.

$$\varepsilon = \frac{(T_{amb} - T_{oc})}{(T_{amb} - T_g)} \qquad 3.16$$

By increasing the culvert hydraulic diameter, the building spaces will need no heating although the culvert fan must operate continuously since the culvert outlet air temperature is always higher than the inlet ambient air temperature; the issue of flow control is discussed in chapter 4.

- **Spring Season**

The dashed line in Figure 3.27 shows that the culvert during the spring season can passively provide cooling for ambient air temperatures less than 27°C without an auxiliary cooling system. Figure 3.31 confirms that 90% of the temperature difference between the culvert outlet and ambient air is provided by 4 culvert sections. The culvert thermal performance in spring can be contrasted with that of autumn. Even though the seasons share the same weather conditions, they differ vastly in their ground temperature as shown in Table 3.2, which favours Spring. The Spring culvert temperature efficiency (ε) at a ground temperature of 22°C is 0.6, but when the larger hydraulic diameter of 0.67m is adopted the culvert outlet temperature decreases to 23°C and the temperature efficiency rises to 0.89. Figure 3.27 illustrates that the culvert fan should be turned off in the early morning when the ambient temperature is less than the culvert outlet temperature.

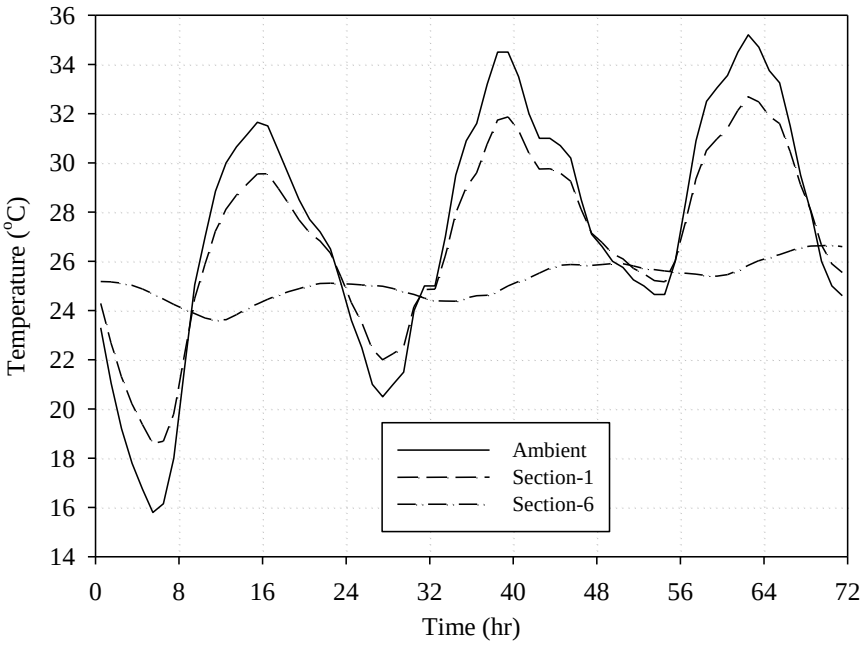

Figure 3.27: Ambient and culvert section temperatures for the period April 1-3.

In cases where a culvert of small cross-sectional area can not provide passive cooling, natural ventilation or mechanical cooling should be used; with a larger hydraulic diameter, the culvert can provide passive cooling unaided. The control approach is fully elaborated in chapter 4.

- **Summer Season**

Figure 3.28 shows that the culvert outlet temperature exceeds the required indoor temperature and therefore the culvert cannot provide passive cooling during summer. A hybrid cooling approach is therefore required. The outlet air temperature (Figure 3.28) is about 36°C with corresponding temperature efficiency at a ground temperature of 31°C of 0.67. When a larger hydraulic diameter is used, the outlet air temperature reduced to 33°C and the temperature efficiency increases to 0.84. When the ambient temperature is less than the culvert outlet air temperature, the active cooling system should be provided with ambient air; otherwise it should be supplied by air exiting the culvert. The control of such a hybrid cooling system is the subject of chapter 4. Figure 3.31 indicates that around 75% of the temperature difference between culvert outlet (section 6) and ambient air is achieved at section 3. For the selected parameters, most of the passive cooling is achieved by half the culvert's length.

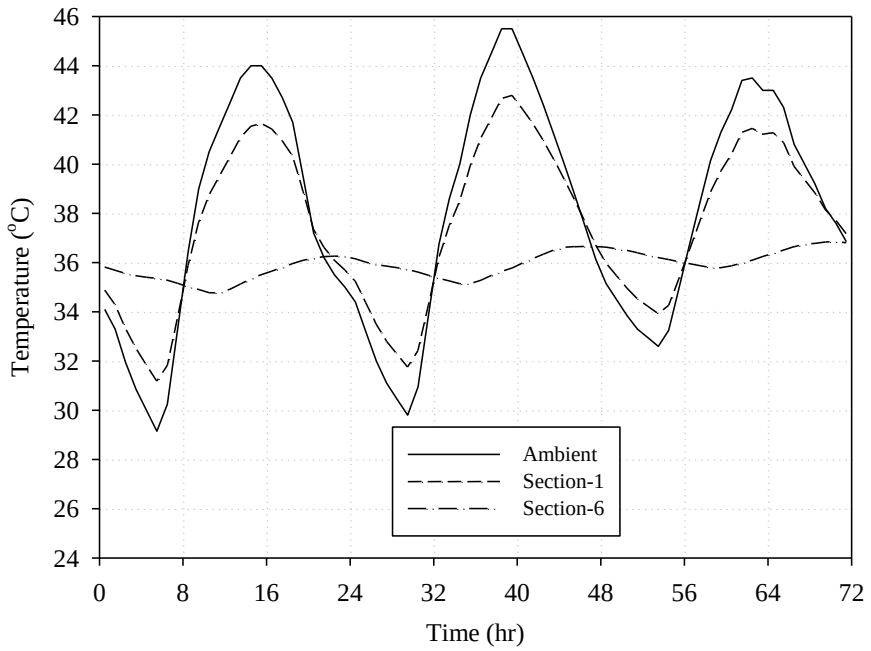

Figure 3.28: Ambient and culvert section temperatures for the period August 5-7.

- **Autumn Season**

The ground temperatures at a depth of 3m in Riyadh peak during the autumn season as shown in Table 3.2. The temperature at this depth is lagging the ambient temperature by a season due to the thermal inertia of the soil – thus, if it is autumn aboveground then it is summer-like underground. Further, the monthly mean ambient temperature starts decreasing after the peak summer time, while the monthly ground temperature is increasing as shown in Figure 3.30. This scenario produces a negligible temperature difference between the inlet and outlet of the culvert. That is why the culvert cooling potential is low during the autumn season as evident from Figure 3.29 where the air temperature at section 6 is approximately 28°C (compared to 26°C in Figure 3.27). To worsen the situation, when a larger hydraulic diameter is used, the culvert outlet air temperature increases to 29.5°C for a ground temperature of 31°C. In this case, earth treatment can be implemented to lower the sub-surface temperature (at depth 0m) from 32-33°C to 24°C as concluded by Givoni (1994), who stated that at 3m below the surface, the temperature is 1.5°C more than the surface temperature.

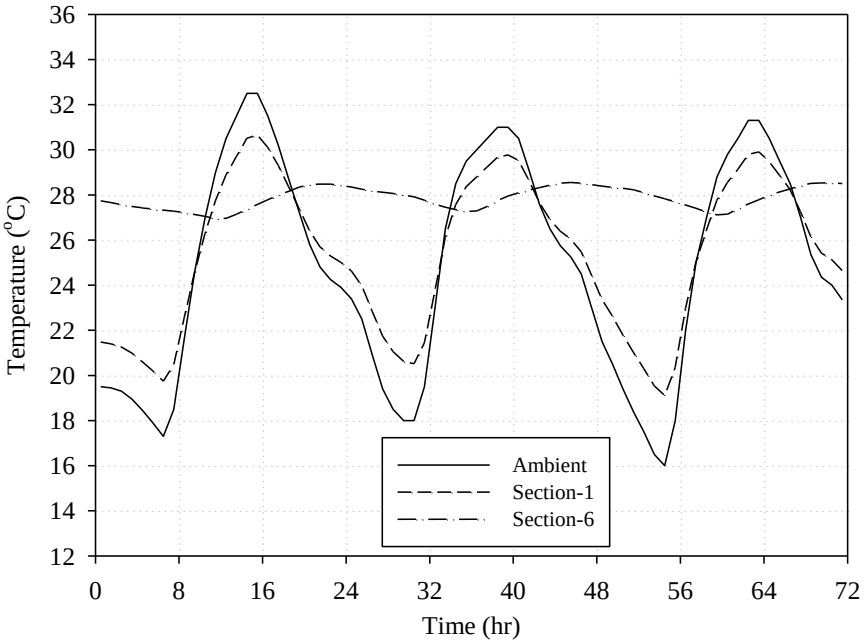

Figure 3.29: Ambient and culvert section temperatures for the period November 1–3.

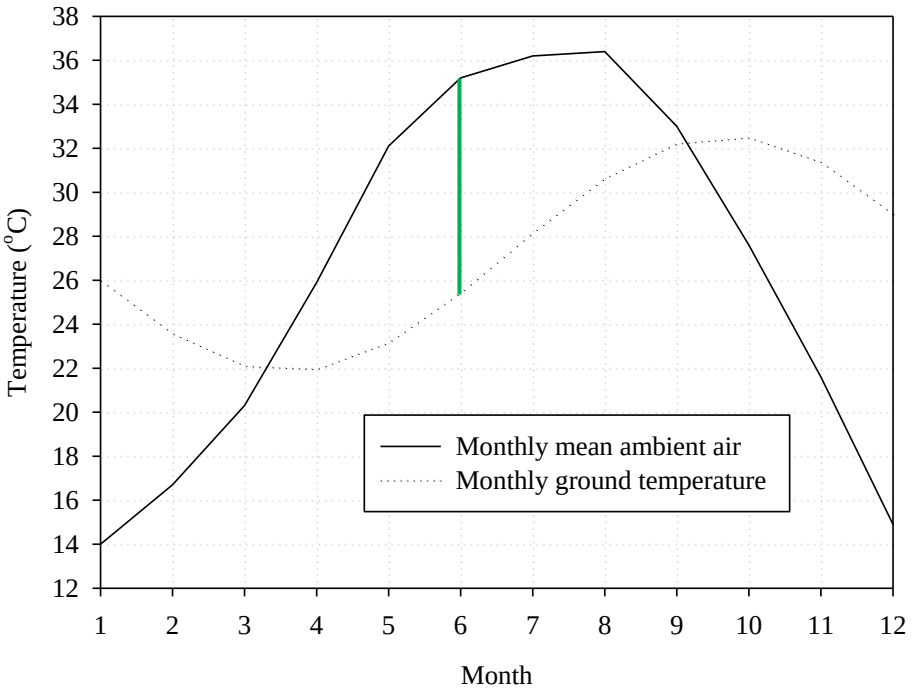

Figure 3.30: Monthly mean ambient air and ground temperatures in hot/dry climate.

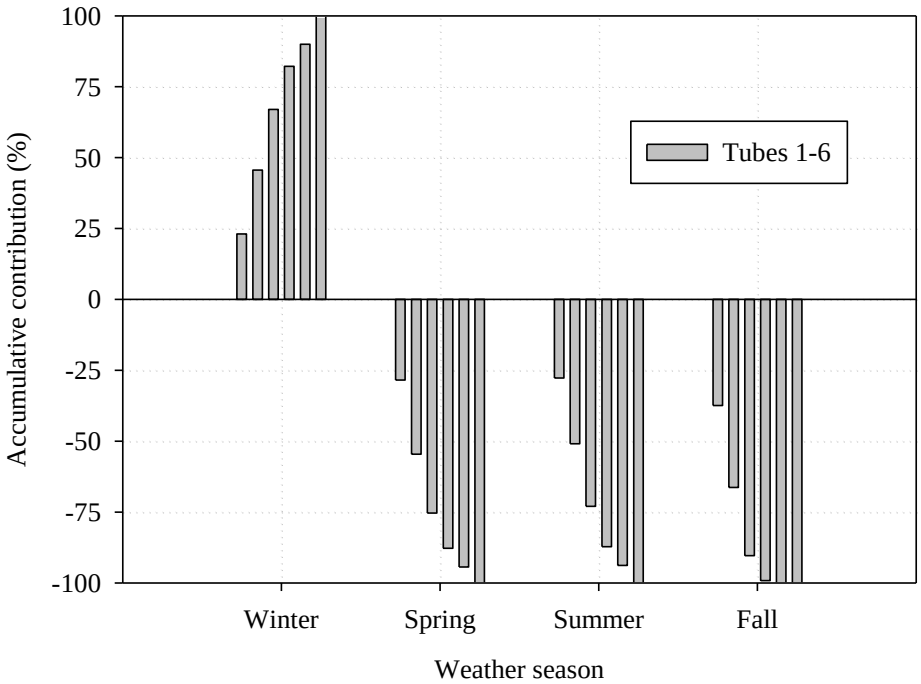

Figure 3.31: The contribution of culvert sections (1-6) to (T_{oc}-T_{amb}) for the four seasons at peak times.

When a large cross-sectional culvert was earth treated the outlet air at section 6 was close to that of the ground at 25.5°C. Referring to Figure 3.30, the thermal effectiveness of the culvert during the Summer, Spring and Autumn (cooling seasons) is at its highest (the green line showing that the ΔT between ambient and ground is at its highest in June), mid and lowest values respectively when earth treatment is not implemented. When earth treatment is implemented, the autumn cooling potential equates to that for Spring.

3.5.2 Culvert Coefficient of Performance

Figure 3.32 shows ambient air and ground temperatures along with hourly culvert cooling and heating COPs for 8 selected days (first day of each month in the cooling season starting from April to November so that a sample of all cooling season months is represented). It is clear that the maximum hourly cooling COP of the air culvert increased from April until a peak in June when the temperature difference between the ambient and ground temperatures was the highest (green double arrow) for the cooling season; from June the culvert cooling potential starts to descend until a ground temperature of 31.5°C is reached at which point the culvert maximum heating potential (peak hourly heating COP) surpasses that of the peak hourly cooling COP for the day (blue oval); more on this ground temperature set-point will be seen in chapter 4. It is important to explain why the COP value is so high; as mentioned in the culvert parametric priority list section, it is important to increase the culvert hydraulic diameter as much as possible for two reasons:

1. Enhancing the culvert thermal performance by reducing the outlet air temperature in the cooling season.
2. Installing a smaller capacity fan due to the larger diameter incorporated.

Besides, it is not strange to have high COP for culvert; for example Pfafferott (2003) claimed a cooling COP of 380 for one of the culverts studied. Culvert cooling COP was calculated as shown in equation 3.17 where culvert cooling power consumption was calculated by equation 3.12 and the fan power by equation 3.18. Here Δp is the pressure difference across the fan from inlet to outlet and $\dot{V}$ and η refer respectively to the volumetric air flow rate and fan efficiency.

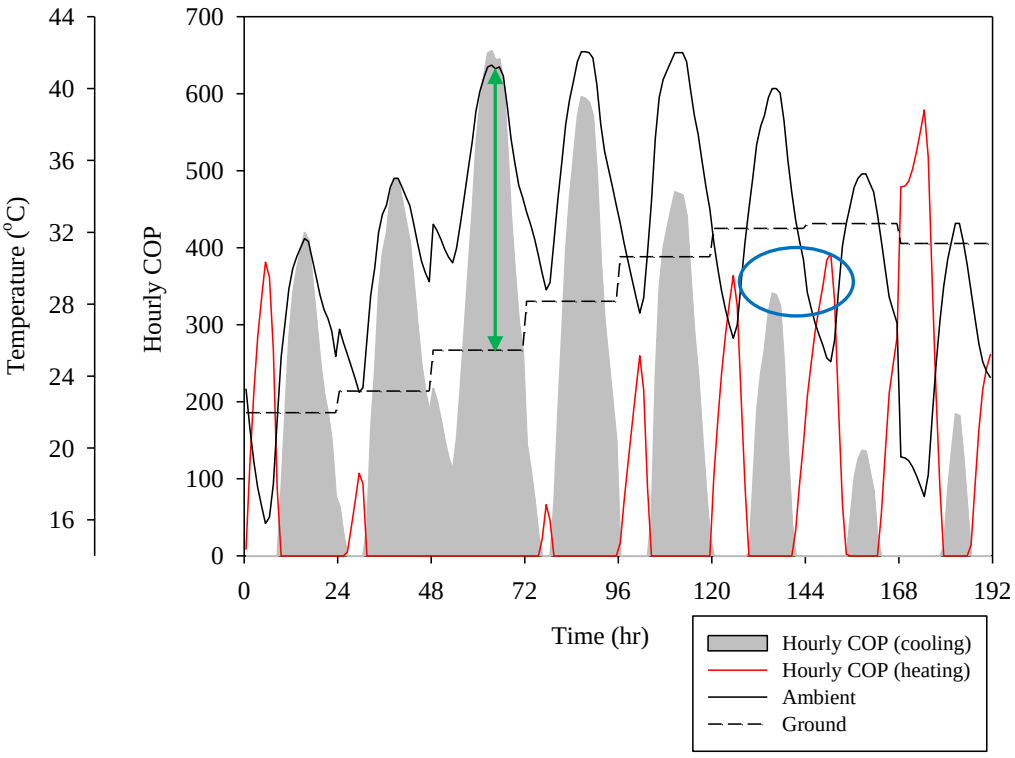

Figure 3.32: Culvert hourly COP for 8 selective days in the cooling season.

The total pressure difference from culvert inlet to outlet is approximately 17 Pa as depicted in Figure 3.33 (the parameters of culvert are those detailed in Table 3.2 and Table 3.4). Culvert annual cooling COP for different control models are listed in Table 3.15. Obviously, the lowest COP in Table 3.15 is significantly larger than that offered by a conventional mechanical air chiller. Referring to the same table, and relative to the no control variant, the annual cooling COP is doubled when the On/Off control variant is used. On/Off control refers to operating the culvert fan only when the culvert outlet air temperature is lower than the ambient. In comparison with the air flow control variant (allowing 100% or 50% volume flow rate), the annual cooling COP is tripled when the On/Off variant is used; culvert air flow control is explained in section 3.7.2.1. When the fan air flow rate is controlled, culvert cooling capacity is about 50% lower than when no air flow control is used. However, it will be established in chapter 4 that the active cooling system energy consumption and peak cooling capacity is less when the culvert air flow rate control is engaged compared to the no flow control case –a contradiction! Actually, both arguments are true because indoor air temperatures over 27°C (maximum comfort

indoor dry-bulb temperature) are experienced during high ambient air temperature conditions and thus active cooling is required. The higher culvert cooling capacity which is obtained at 100% fan load is useful in transitional seasons but not when ambient air temperatures are higher than a certain threshold (30°C) (this threshold is justified in chapter 4). Because since culvert air flow control is able to reduce the AHU inlet air temperature by 1°C (sometimes 2°C as shown in Figure 3.34), it can reduce both active cooling energy and peak cooling power as will be seen in next chapter.

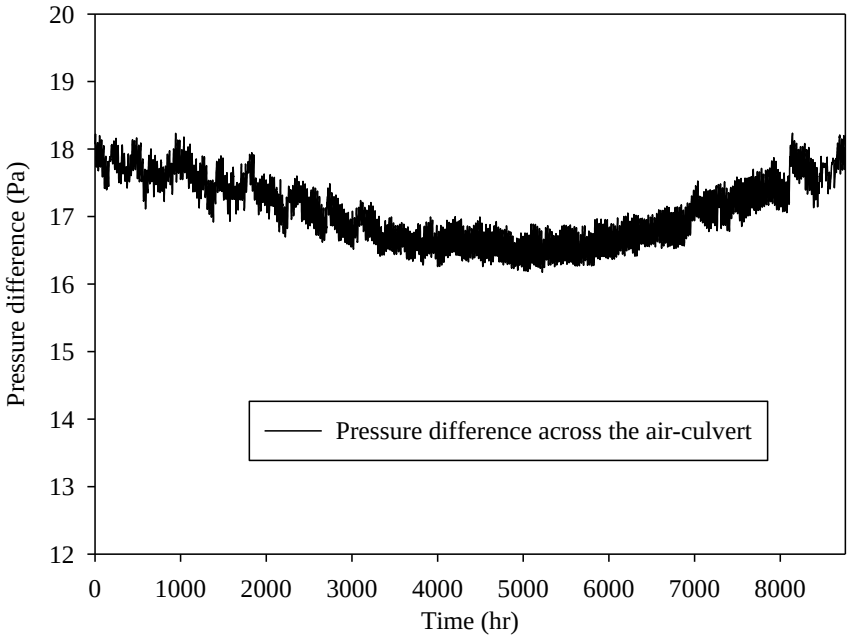

Figure 3.33: Air culvert fan pressure difference.

$$\text{COP} = \frac{\text{Culvert cooling energy}}{\text{Fan energy}} = \frac{(\text{equation } \mathbf{3.12})(\text{time of culvert operation})}{(\text{equation } \mathbf{3.18})\ (\text{time of culvert operation})} \quad 3.17$$

$$\text{Fan power consumption } = \frac{\Delta p \dot{V}}{\eta} \quad 3.18$$

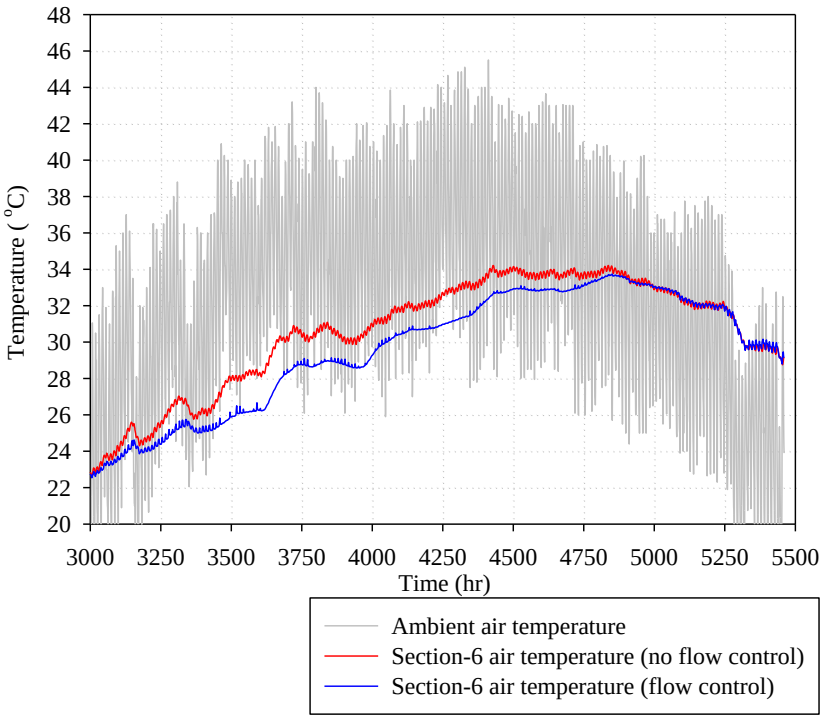

Figure 3.34: Effect of air flow control on culvert outlet air temperature.

Table 3.15: Annual cooling COP of the air culvert cooling system.

Course of action on air culvert cooling system/Property	Culvert annual cooling energy (kWh)	Fan annual energy consumption (kWh)	Annual cooling COP
(No control)	-3117	30.1	104
(On/Off control)	-4301	18.7	230
(Air flow control)	-1566	18.9	83
(Air flow control + On/Off)	-2788	10.9	256

3.6 Building Model in ESP-r

The objective here is to quantify the impact of culvert thermal performance on residential building energy use and comfort conditions. Retrofit of buildings is not common in the GCC region due to the high standards of living as discussed in chapter 1 and new buildings are the norm, so the building to be studied is considered new. The building's geometry and construction, as suited for a hot/dry climate, are listed in detail in Appendix B. A hot/arid climate requires the use of heavyweight materials to prevent overheating. A Villa comprising living, eating and sleeping areas was constructed in ESP-r (Figure 3.35). The rooms (living, eating and sleeping) all

account for 120m^2 total floor area. The constructions used for each room are external wall, internal wall, ground floor, roof, door and window. Every construction type consists of list of materials with thickness, density, thermal conductivity and specific heat capacity; they are all detailed in Appendix B with external wall materials only listed in Table 3.16 as a sample. Occupational details corresponding to the average number of people residing in Kuwaiti homes (5 persons) were assumed as listed in Appendix B.

Table 3.16: Thermohpysical properties for a sample construction.

Construction	Material	l (mm)	k (W/mK)	ρ (kg/m^3)	c_p (J/kg.K)
External wall	Sand-lime block	90	1.3	1918	795
	Insulation	50	0.032	30	1120
	Cement block	200	1.64	2011	910
	Cement plaster	20	1	2085	840

3.6.1 Model Calibration

Due to comparatively large windows used, the predicted sensible cooling energy consumption using ESP-r was 218kWh/m^2/yr (Table 3.17). Without the inclusion of the latent cooling load, this is near to the average residential annual cooling energy consumption in GCC states, which is 250kWh/m^2/yr; the A/C system in section 4.2.1 is validated against that average. Table 3.17 also illustrates that the peak summer load is 82W/m^2, which is 17% more than the maximum desired value of 70W/m^2 as set by the Kuwaiti energy code of practice. Table 3.17 suggests that 92% of the annual HVAC energy used in residential buildings in hot/dry climates is associated with the cooling system, with only 8% of the energy used for heating.

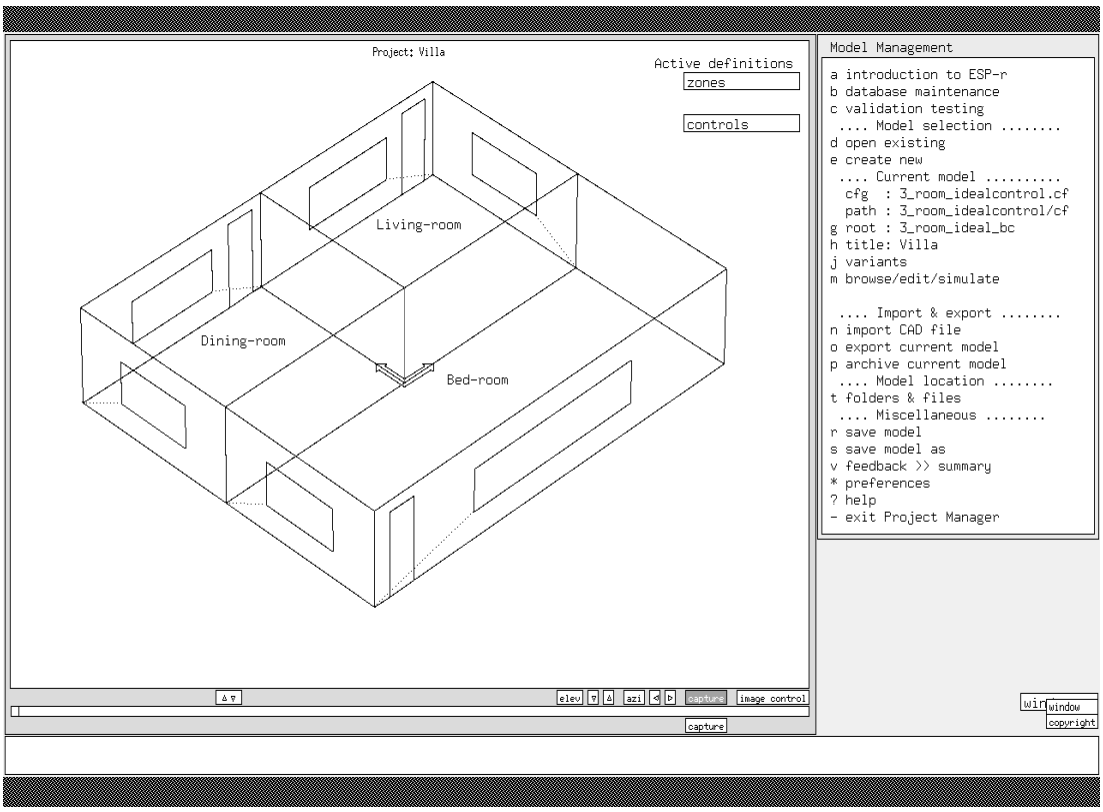

Figure 3.35: 3 zone Villa as represented in ESP-r.

Table 3.17: ESP-r predicted HVAC sensible cooling energy and power usage for the Villa in a hot/dry climate.

Season (set-point)/ Parameter	Energy (kWh)	Area (m^2)	Energy ($kWh/m^2/yr$)	Peak Power (kW)	Power (W/m^2)	Energy (%)
Cooling (25 °C)	26130	120	217.8	9.81	81.8	91.9
Heating (20 °C)	2561	120	21.3	4.19	34.9	8.1

3.7 Culvert Coupling to Building

The culvert model has been coupled to the Villa model as shown in Appendix B. Ambient air is extracted by a blower into culvert inlet and transferred from one culvert section to another until it enters the 3 Villa zones via grilles; one grille for each building zone. This was done as shown in Appendix B by coupling the thermal Villa and culvert sections zones to the corresponding air flow nodes. The scale of culvert depends on the ventilation required for the house; the more ventilation needed indoors the larger the hydraulic diameter would be. This study is concerned with one house, but hypothetically speaking if culvert is to ventilate more houses then a larger cross-sectional culvert is required. If there are too many houses to be

ventilated by culvert then parallel of equal hydraulic diameters should be aligned. Different model variants were tested to find the best one that can sustain comfortable indoor air temperatures to avoid active cooling incorporation by changing individual characteristics between variants; those characteristics are:

- Shading element.
- Ground surface treatment.
- Occupancy ventilation control (only the occupied zone receives culvert air).
- Culvert air flow control (when 50% or 100% of air flow is used in culvert).

Table 3.18: Variant models of culvert-building coupling.

Variant/Factors	Shading element	Ground surface treatment	Occupancy ventilation control	Culvert air flow control
1	No	No	No	No
2 (slash flow By 50%)	No	No	No	No
2 (flow control)	No	No	No	Yes
3	No	No	Yes	No
4	Yes	No	No	Yes
5	No	Yes	No	Yes
6	Yes	Yes	No	Yes

A base case model (variant 1) as listed in Table 3.18 has been formed comprising the Villa stated earlier but with no energy efficiency measure (shading) applied to the building or ground surface treatment. In this base model no control is applied to the culvert air flow rates. And, no occupancy ventilation control is exercised; this implies all building zones receive constant ventilation. To achieve this, the air velocity inside the culvert is set at 2m/s or less. The volume flow rate inside the culvert in variant 1 model was $0.24m^3/s$ or $0.08m^3/s$ for each zone in the Villa as prescribed in the air culvert design. The culvert hydraulic diameter (using Figure 3.24) for this air flow rate is 0.39m. Table 3.18 summarizes the different variant models. Hereafter, the living zone will be used for comparison purposes since it is mostly occupied during the day unless otherwise stated. The variant models are compared with the free floating and natural ventilation modes of operation; free floating mode represents when the indoor temperature is allowed to float freely in an uncontrolled manner. Natural ventilation is exercised by opening windows when certain indoor and outdoor weather conditions prevail; these conditions are explained when the control strategy is laid out in chapter 4.

3.7.1 Variant model 1

As mentioned in the previous section, the hydraulic diameter for variant 1 is increased from 0.23m (used in air culvert design) to 0.39m (Figure 3.24) to accommodate the air flow rate increase required to ventilate all 3 zones regardless of occupancy. However, Figure 3.24 was constructed based on a culvert air velocity of 2m/s so that the culvert hydraulic diameter could be quantified under acceptable pressure drop when very high ventilation rates are required. When lower flow rates are required, such as is the case here, this would result in a small culvert hydraulic diameter (0.39 m), which can be increased within limits imposed by site constraints. The new hydraulic diameter was quadrupled from 0.23m to 1m, which reduces the pressure drop and enhances the thermal performance. Some variant models use different hydraulic diameter values, requiring the convective heat transfer coefficient to be changed accordingly. Table 3.19 lists the convective heat transfer coefficient and other parameters for each of the six culvert sections and all variant models. The referred table indicates that if the length is less than the entrance length $h_{c\text{-}before}$ is used but if higher then $h_{c\text{-}after}$ is used.

Table 3.19: Convective heat transfer coefficients for variant models.

Variant	$\dot{V}$ (m^3/s)	D (m)	V (m/s)	L_E (m)	h_{c_before} (W/m^2K)	h_{c_after} (W/m^2K)
1	0.24	1	0.31	23	12.9	1.29
2 (slash flow by half)	0.12	1	0.15	20	6.1	0.61
2 (flow control), 4, 5, 6 & 7	0.24	1	0.31	23	12.9	1.29
	0.12	1	0.15	20	6.1	0.61
3	0.08	1	0.1	19	3.9	0.39

Table 3.21, Table 3.22 and Table 3.23 indicate that when the air culvert and/or natural ventilation is introduced to the Villa the living room air temperatures in the transition seasons and summer are less than when the free floating mode is imposed. That is because during the free floating mode, only thermal mass is playing the cooling device role. Despite the fact that Spring and Autumn have comparable above-ground weather conditions, the underground conditions differ vastly causing degradation of the culvert thermal performance during late Summer. For variant 1, Table 3.21 and Table 3.23 show that when the culvert is used in the Autumn season,

the living room air temperature is 2-3°C higher than that in Spring for approximately the same ambient air temperature; this issue is discussed in variant 5. Referring to Table 3.21, it is obvious that natural ventilation during early morning hours in Spring can maintain the living room air temperature within a comfortable air temperature range of 20-25°C as required by ANSI/ASHRAE Standard 55 (2004). When natural ventilation is not sufficient, it is shown in variant 1 that the living room air temperature is never below 25°C in Spring. Usually people residing in hot climates can accommodate an elevated temperature (Olesen 2008) allowing an increase in the maximum indoor air temperature to 27°C; variant 1 in Spring shows indoor air temperatures below 27°C for 71% of the time. It is important to mention that natural ventilation efficiency is directly related to wind speed and direction in addition to ambient air temperature and humidity. On April 1, the air speed in the early hours was 2.1-2.6m/s and its direction was 280°-360°, which means that only windows facing North and/or West can benefit from the higher air speed at low ambient air temperature. However, on November 1, the air speed was 0m/s during the early morning where natural ventilation was not able to maintain the living room air temperature within the comfortable range even when the ambient air temperatures is low (Table 3.23). The culvert thermal performance in Autumn is compromised and the living room air temperature is above 27°C for 100% of the time.

3.7.2 Variant model 2

3.7.2.1 Flow rate slash by 50%

Variant 2 is the same as Variant 1 except the air flow rate was halved; that was done to examine flow rate reduction effect on culvert performance. The results of Table 3.21 and Table 3.23 show that in Spring and Autumn, the living room and bed room air temperatures are about 1°C above those corresponding to Variant 1, whereas in Winter and Summer, Variant 2 is more efficient than Variant 1 as illustrated in Table 3.22.

3.7.2.2 Culvert air flow control

As a consequence of variant 2 (half flow rate), the volumetric air flow rate in the culvert should be controlled as shown in Table 3.20. When the ambient air

temperature is below 15°C or above 30°C, the culvert fan operates at a 50% capacity with each building zone receiving 0.04 m^3/s, which is the ventilation rate required for 5 persons (CIBSE Guide B 2005). When the ambient condition is in the range 15-30°C, the culvert fan operates at 100% load. Figure 3.36 shows how the fan operates when the air flow rate is switched between full and half capacity based on the ambient air temperature. Chapter 4 describes how the culvert air flow rate may be controlled to produce a higher cooling capacity in the transitional seasons and a lower air flow rate in Summer to reduce the supplied air temperature. The rationale for the selection of 15°C and 30°C will be considered when the control strategy for hybrid cooling system in hot/dry climate is laid-out in the next chapter.

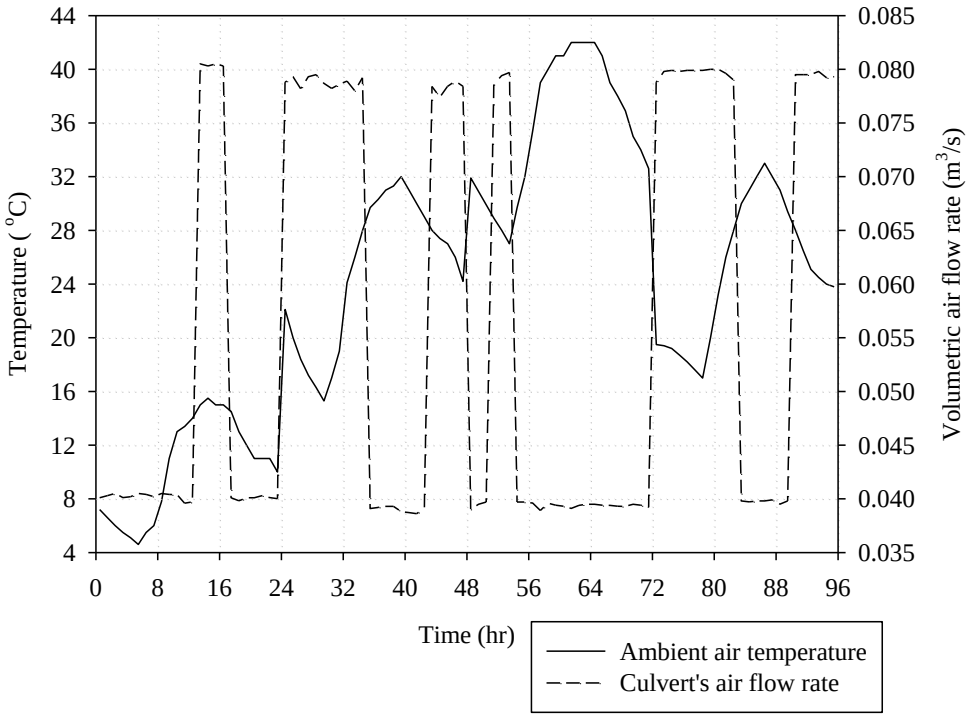

Figure 3.36: Volumetric air flow rate control for different seasons.

Table 3.20: Control loop components of Variant 2 (culvert air flow rate control).

Sensor	Actuator	Control Law	Data	Occupancy
Ambient Temperature	Fan air flow rate	Range based for low/default/medium/high	(15 22 30) (0.5 1 0.5)	Not included

Table 3.21: Core villa indoor air temperatures in °C of different variant models on April 1.

Time (hr)	$T_{amb.}$	Liv*_ FF**	Liv_ NV***	Liv_ V1	Liv_ V2	Liv_ V3	Liv_ V4	Liv_ V5	Liv_ V6	Liv_ V7	Bed_ V1	Bed_ V2	Bed_ V3	Bed_ V4
00h30	23.3	29.46	25.37	26.58	27.38	27.16	25.61	25.8	24.7	24.58	26.73	27.25	27.92	25.4
01h30	21.05	28.32	24.11	25.94	26.56	27.22	24.96	25.27	24.07	23.42	26.8	27.36	27.32	25.54
02h30	19.2	27.75	23.03	25.91	26.33	27.06	24.77	25.17	24.01	21.9	26.78	27.35	27.17	25.54
03h30	17.8	27.86	24.02	25.87	26.31	26.97	24.8	25.12	23.99	22.36	26.73	27.28	27.19	25.51
04h30	16.75	27.67	26.02	25.74	26.18	26.89	24.71	25	23.89	23.42	26.71	27.24	27.11	25.5
05h30	15.8	27.5	26.13	25.71	26.12	26.81	24.68	24.96	23.87	23.45	26.67	27.2	27.06	25.47
06h30	16.15	27.5	25.95	25.67	26.1	26.81	24.63	24.93	23.81	23.42	26.64	27.17	27.03	25.46
07h30	18	27.75	24.62	25.87	26.3	27.06	24.63	25.11	23.82	22.54	26.7	27.24	27.07	25.48
08h30	21.55	28.31	24.28	26.23	26.72	27.6	24.7	25.47	23.87	22.81	26.87	27.46	27.24	25.58
09h30	25.05	28.92	26.88	26.56	27.1	27.48	24.79	25.81	23.96	24.16	27.06	27.67	27.79	25.65
10h30	27	29.76	27.89	26.88	27.5	27.14	25.09	26.12	24.26	23.87	27.22	27.84	28.68	25.66
11h30	28.85	30.33	28.4	27.13	27.88	27.43	25.51	26.35	24.62	24.12	27.44	28.1	29.14	25.71
12h30	30	30.15	28.81	27.14	27.95	27.44	25.64	26.35	24.71	24.51	27.63	28.35	29.21	25.81
13h30	30.65	30.25	28.47	27.17	27.99	27.43	25.66	26.4	24.77	24.5	27.81	28.55	29.45	26
14h30	31.15	30.22	28.44	27.06	27.81	27.36	25.49	26.29	24.63	24.42	27.97	28.71	29.67	26.27
15h30	31.65	30.2	28.5	27.07	27.75	27.33	25.46	26.3	24.62	24.35	28.01	28.75	29.73	26.39
16h30	31.5	30.65	28.94	27.37	28.16	27.62	25.86	26.58	24.99	24.83	27.93	28.63	29.68	26.29
17h30	30.5	30.78	29.19	27.5	28.4	27.72	26.13	26.7	25.21	25.08	27.76	28.4	29.53	26.14
18h30	29.5	30.89	29.34	27.62	28.57	27.8	26.33	26.79	25.43	25.3	27.6	28.2	29.37	26
19h30	28.5	30.91	29.43	27.63	28.61	27.79	26.4	26.79	25.5	25.35	27.49	28.09	29.27	25.93
20h30	27.7	30.37	28.93	27.17	28.06	27.37	26.01	26.39	25.07	24.86	27.45	28.04	29.24	25.94
21h30	27.2	30.4	28.97	27.1	27.88	27.31	25.94	26.34	25.02	24.78	27.43	28.02	29.22	25.98
22h30	26.5	31.12	29.77	27.72	28.71	27.86	26.62	26.89	25.68	25.48	27.41	27.99	29.21	26.01
23h30	25.1	31.05	28.33	27.88	28.99	27.92	26.83	26.95	25.86	25.41	27.39	27.96	29.18	26.02

*Liv refers to living room.

**FF stands for free-floating.

***NV stands for natural ventilation.

Table 3.22: Core villa indoor air temperatures in °C of different variant models on August 1.

Time (hr)	$T_{amb.}$	Liv_ FF	Liv_ V1	Liv_ V2	Liv_ V3	Liv_ V4	Liv_ V5	Liv_ V6	Liv_ V7	Bed_ V1	Bed_ V2	Bed_ V3	Bed_ V4
00h30	32.5	38.63	35.08	35.17	34.85	34.73	34.81	34.48	34.53	34.27	34.2	34.58	34.17
01h30	31.4	37.56	34.35	34.27	34.71	34.04	34.08	33.79	33.84	34.36	34.31	34.13	34.27
02h30	30.4	37.01	34.11	33.93	34.46	33.81	33.86	33.56	33.61	34.33	34.28	33.99	34.25
03h30	29.4	37.02	34.07	33.92	34.37	33.81	33.82	33.56	33.62	34.25	34.19	33.97	34.19
04h30	28.45	36.79	33.92	33.76	34.25	33.69	33.67	33.44	33.49	34.19	34.13	33.87	34.15
05h30	27.5	36.59	33.84	33.65	34.12	33.63	33.58	33.37	33.42	34.12	34.06	33.8	34.09
06h30	28.35	36.6	33.83	33.65	34.13	33.55	33.57	33.3	33.35	34.07	34.01	33.75	34.05
07h30	30.85	36.95	34.04	33.88	34.43	33.55	33.78	33.3	33.35	34.09	34.05	33.77	34.05
08h30	33.7	37.49	34.35	34.25	34.93	33.6	34.1	33.34	33.4	34.19	34.18	33.87	34.11
09h30	37.2	38.02	34.58	34.53	34.82	33.66	34.33	33.4	33.48	34.24	34.24	34.22	34.11
10h30	39.5	38.62	34.88	34.91	34.46	33.95	34.62	33.69	33.78	34.22	34.21	34.72	34.05
11h30	40.5	39	35.17	35.31	34.66	34.33	34.9	34.07	34.17	34.29	34.3	34.9	34.06
12h30	41	38.9	35.15	35.31	34.67	34.38	34.88	34.13	34.25	34.37	34.4	34.9	34.11
13h30	41.5	38.93	35.11	35.28	34.61	34.38	34.85	34.14	34.21	34.45	34.49	35.04	34.22
14h30	42	38.76	34.9	35.04	34.42	34.2	34.62	33.95	33.98	34.6	34.65	35.23	34.43
15h30	42	38.67	34.8	34.9	34.31	34.14	34.51	33.87	33.91	34.73	34.79	35.38	34.55
16h30	42	39.11	35.17	35.34	34.68	34.49	34.91	34.24	34.27	34.78	34.85	35.46	34.52
17h30	41.5	39.39	35.47	35.7	34.94	34.75	35.21	34.52	34.53	34.76	34.82	35.45	34.48

18h30	40	39.51	35.62	35.84	35.1	34.95	35.38	34.71	34.73	34.62	34.67	35.34	34.39
19h30	38.5	39.42	35.55	35.77	35.02	34.99	35.3	34.75	34.78	34.42	34.43	35.13	34.18
20h30	37.45	38.78	35.03	35.18	34.42	34.57	34.74	34.32	34.36	34.29	34.27	34.99	34.07
21h30	35.95	38.72	34.9	35.02	34.29	34.53	34.59	34.25	34.3	34.26	34.23	34.94	34.09
22h30	34.5	39.35	35.5	35.7	34.9	35.09	35.23	34.83	34.87	34.22	34.18	34.89	34.08
23h30	33.3	39.22	35.61	35.82	35.01	35.15	35.35	34.92	34.95	34.16	34.11	34.81	34.04

Table 3.23: Core villa indoor air temperatures in °C of different variant models on November 1.

Time (hr)	$T_{amb.}$	Liv_ FF	Liv_ NV	Liv_ V1	Liv_ V2	Liv_ V3	Liv_ V4	Liv_ V5	Liv_ V6	Liv_ V7	Bed_ V1	Bed_ V2	Bed_ V3	Bed_ V4
00h30	19.5	31.43	25.48	29.83	30.76	30.82	29.47	28.21	27.79	22.63	30.4	31.26	31.51	29.4
01h30	19.45	30.4	27.57	29.16	30.03	29.97	28.86	27.49	27.1	22.66	30.43	31.31	31.5	29.46
02h30	19.3	29.98	27.95	28.93	29.76	29.58	28.65	27.36	26.9	22.56	30.36	31.22	31.41	29.42
03h30	18.95	29.96	27.74	28.9	29.71	29.53	28.63	27.32	26.88	22.33	30.25	31.09	31.29	29.35
04h30	18.45	29.77	27.91	28.75	29.53	29.33	28.5	27.15	26.76	22	30.16	30.99	31.2	29.29
05h30	17.9	29.61	27.69	28.67	29.45	29.2	28.44	27.08	26.69	22.5	30.05	30.87	31.08	29.22
06h30	17.3	29.45	27.69	28.56	29.34	29.07	28.35	26.97	26.6	23.7	29.95	30.77	30.98	29.15
07h30	18.5	29.51	27.79	28.6	29.38	29.1	28.3	27	26.54	23.28	29.96	30.77	30.98	29.12
08h30	21.6	29.92	28.16	28.82	29.65	29.39	28.31	27.22	26.55	23.01	30.21	31.03	31.22	29.19
09h30	24.6	30.43	28.65	29.1	29.96	29.96	28.38	27.48	26.6	23.89	30.56	31.39	31.6	29.26
10h30	27	31.16	29.24	29.48	30.39	30.57	28.69	27.84	26.91	24.29	30.87	31.71	31.98	29.28
11h30	29	31.75	29.69	29.78	30.72	30.8	29.04	28.17	27.32	25.12	31.15	32.01	32.32	29.34
12h30	30.5	31.7	29.7	29.75	30.69	30.77	29.05	28.18	27.4	25.44	31.35	32.24	32.55	29.43
13h30	31.5	31.75	29.77	29.76	30.71	30.82	29.07	28.18	27.4	25.3	31.52	32.42	32.75	29.59
14h30	32.5	31.6	29.59	29.57	30.51	30.63	28.91	27.94	27.2	25.25	31.61	32.53	32.87	29.76
15h30	32.5	31.47	29.49	29.49	30.4	30.57	28.87	27.81	27.12	25.25	31.51	32.43	32.78	29.75
16h30	31.5	31.81	29.92	29.76	30.71	30.81	29.18	28.13	27.47	25.62	31.26	32.18	32.52	29.61

17h30	30.2	31.96	30.17	29.88	30.85	30.92	29.34	28.32	27.72	25.8	30.93	31.86	32.18	29.43
18h30	28.7	32.07	30.36	30.02	30.99	31.05	29.52	28.5	27.9	25.95	30.62	31.55	31.85	29.25
19h30	27.25	32.07	30.45	30.05	31.01	31.06	29.57	28.54	27.95	26.03	30.44	31.35	31.63	29.16
20h30	25.8	31.47	29.92	29.63	30.54	30.66	29.19	28.05	27.53	25.67	30.36	31.24	31.51	29.18
21h30	24.8	31.42	29.9	29.62	30.5	30.63	29.2	27.93	27.46	25.22	30.29	31.15	31.41	29.18
22h30	24.25	32.13	30.67	30.15	31.09	31.11	29.72	28.58	28.05	25.09	30.22	31.06	31.31	29.15
23h30	23.9	32.09	30.73	30.13	31.09	31.12	29.74	28.72	28.17	25.54	30.15	30.97	31.21	29.13

3.7.3 Variant model 3

The volumetric flow rate in Variant 3 is divided between the living room and bed room since they are occupied for more than 90% of the time. Table 3.24 lists the control loop components for this Variant where, for example, (0 1 1) means that the fan is on at full fraction when the ambient air temperature is 0°C or more whereas (0 1 0) means that the fan is off when the ambient air temperature is 0°C or more; Figure 3.37 depicts the result for this occupancy ventilation variant model. The results of Table 3.21 and Table 3.23 show that Variant 3 can help reduce the Variant 1 internal air temperatures only during occupancy since the air flow rate is zero during non-occupied periods.

Table 3.24: Control loops for Variant model 3.

Room	Occupancy	Sensor	Actuator	Control Law	Data
Bed	00:00-9:00 9:00-00:00	Ambient air temperature	Fan air flow rate	On/Off	(0 1 1) (0 1 0)

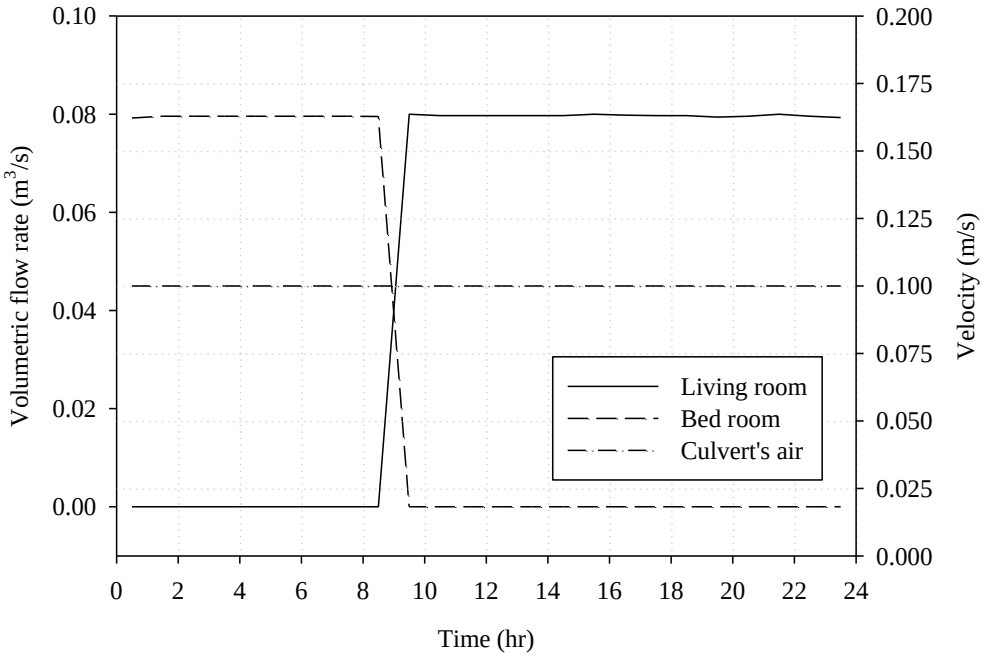

Figure 3.37: Flow rate distribution for Variant 3.

3.7.4 Variant model 4

Variant 2 (flow control) model as a result is the variant that best can reduce indoor temperatures, thus, from Variant 4 and on the characteristics are entangled with it. Window blind control and external shading devices were examined to select

one that is effective in the given case. External shading was modelled in ESP-r by defining surrounding and façade obstructions. Blind control was modelled explicitly in ESP-r by introducing an additional transparent layer to the window which is only activated when the incident solar radiation exceeds 100W/m^2. Table 3.25 demonstrates that external shading is more efficient than blind control and thus it is the shading method used as the preferred building energy efficiency measure. The discrepancy, however, in the indoor air temperature reductions is due to the different window orientations of the Villa zones receiving the solar radiation. Figure 3.38 shows how the sun traverses the sky between seasons. Table 3.21 and Table 3.23 show that the living room air temperatures in Variant 4 in Spring and Autumn are 38% and 0% of the time below 25°C respectively and are 100% and 0% of the time below 27°C.

Table 3.25: Indoor air temperature reductions (°C) at peak cooling load time for different seasons and different shading techniques.

Season/ Room (property)	Living		Dinning		Bed	
	Blind control	External shading	Blind control	External shading	Blind control	External shading
Spring	0.50	1.52	0.32	1.34	0.16	1.00
Summer	0.67	1.91	0.72	2.04	0.23	1.51
Fall	0.67	1.85	0.54	1.69	0.16	2.64

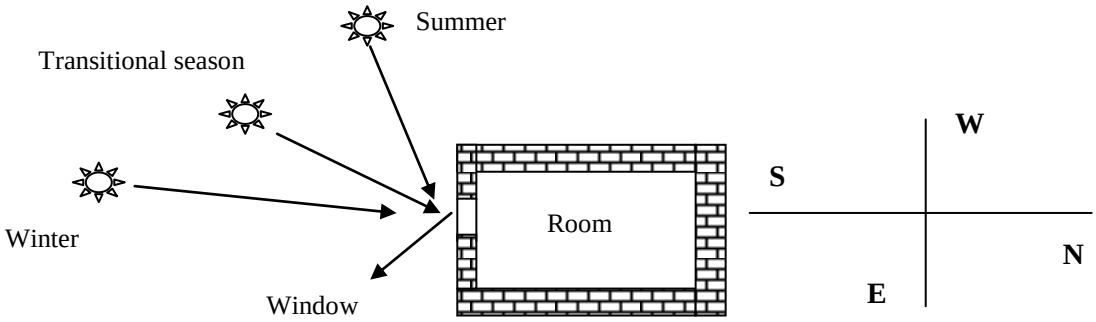

Figure 3.38: Sun position and window insolation.

3.7.5 Variant model 5

As considered in the previous sensitivity analysis, water sprinkling and ground evaporation reduce ground temperatures. This treatment was applied to Variant 2 (flow control) to produce Variant 5. The ground temperature profile under ground surface treatment (Table 3.8) was entered in the ESP-r model. Table 3.23

shows that, in the Autumn, the Variant 5 living room air temperature is more than 2°C lower than in Variant 1, whereas, in Spring, the reduction is about 1 °C (Table 3.21) and, in Summer, it is 0.5°C (Table 3.22). Thus, earth treatment is best utilized during Autumn and Spring since culvert performance is downgraded significantly without it. Secondly, Variant 5 is able to provide a living room air temperature of 25°C or less in Spring for 8% of the time and a temperature of 27°C or less for 100% of the time; however, in Autumn, it was able to provide 27°C or less for only 4% of the time. It should be noted that whether ground surface treatment is energy efficient measure or not needs to be examined. The energy required to spray water could outweigh the energy savings that can be achieved, thus ground surface treatment is terminated here and its impact on cooling energy consumption will not be evaluated in the next chapter.

3.7.6 Variant model 6

Shading, earth treatment and culvert air flow control were added to Variant 1 to comprise Variant 6. As shown by the results of Table 3.21 and Table 3.23, Variant 6 was able to provide a living room air temperature of 25°C or less for 71% and 0% of the time in Spring and Autumn respectively. It provided a living room air temperature of 27°C or less for 100% and 38% of the time in Spring and Autumn.

3.7.7 Variant model 7

Natural ventilation was added to Variant 6 to produce Variant 7, resulting in a living room air temperature of 25°C or less for 79% and 46% of the time in Spring and Autumn respectively (Table 3.21 and Table 3.23). A living room air temperature of 27°C or less was observed for 100% of the time in both Spring and Autumn.

3.8 Standalone Culvert Scenario

The aim in using a culvert is to maximise free cooling in order to reduce the auxiliary cooling required from a downsized air conditioning plant. Cooling and heating power requirements of the Variant models were quantified in Figure 3.39 against an indoor thermal comfort criteria given by ANSI/ASHRAE Standard 55 (2004) where the indoor dry-bulb air temperature range throughout the year should be 20-25°C. It can be seen from Figure 3.39 that Variant 2 would be the best design

if heating requirements minimization was the desired result but that this Variant comes with a higher cooling requirement. Where occupants can be expected to tolerate a higher indoor air temperature, say up to 27°C, Variant 7 performed best, with living room air temperatures above 27°C for 48% of the time; that is, a 27% improvement relative to the free floating mode case. However, Variant 7 also resulted in the highest percentage of time (22%) when the indoor temperature was below 20°C, thus increasing the living room heating load. But, because shading and natural ventilation should not be permitted in winter, Variant 5 was deemed suitable. This Variant kept the living room air temperature below 20°C for 9% of the time, which marginally higher than the corresponding figure for the free floating mode. This result may be improved to 1.4% if the air temperature can be reduced to 18°C (i.e. people are content to wear warmer clothes). Figure 3.40 shows how much people were dissatisfied with a living room air temperature of 18-20°C when clothing preferences are changed from 'light'to'heavy' thus maintaining the PPD below 20% at all times. The worst Variant in terms of producing indoor air temperature higher than 27°C (after the free floating case), was Variant 2 (half flow rate) as depicted in Figure 3.39. Variant 2 (flow control) provides indoor air temperatures in the range 20-27°C more than Variant 2 (half flow). The summer season officially runs from April until November but the need for cooling devices starts one month earlier and ends one month later. ANSI/ASHRAE Standard 55 (2004) recommends an indoor air temperature for summer in the range 23-25°C. Table 3.26 shows that from March 1 to December 1, when free floating mode is used, the living room requires active cooling for 96.5% of the time during the cooling season, whereas, when natural acclimatization (willingness of people to sustain couple of extra degrees in warm climates) is considered, active cooling is needed only for 88.6% of the time. Referring to Table 3.26 Variant 1 reduces the time where active cooling was required by 7% compared to the free floating mode case when natural acclimatization was not considered, whereas, when natural acclimatization is included, the reduction is 4.1%. Variant 2, with fan flow rate control, has almost identical indoor air temperatures to those found in Variant 1 although Variant 1 offers the advantage of a lower pressure drop and fan power consumption. For example, the air velocity in Variant 1 was 0.31m/s whereas in

Variant 2 with flow control it cycled between 0.15m/s and 0.31m/s. Fan relations, equations 3.19 and 3.20, suggest that when the air speed is increased the pressure and power consumption increases to the power of 2 and 3 respectively. Variant 2 with flow control reduces the air pressure by 76.6% and fan power consumption by 88.7%. Table 3.26 shows that when shading was added in Variant 4 the time where active cooling was needed is reduced by 7.9% compared to the free floating mode case, while the reduction when natural acclimatization is considered is 8.8%. When earth treatment is added in Variant 5 the time where active cooling is needed is reduced by 9% compared to the free floating mode case, while with natural adaptation the reduction was 10.9%. The reduction without natural adaptation was 12.2% and 26.1% for Variants 6 and 7 respectively compared to free floating, while the reduction in the time needed for active cooling for Variant 6 and 7 when natural acclimatization is considered was 17.7% and 25.9% respectively (compared to the free floating mode case).

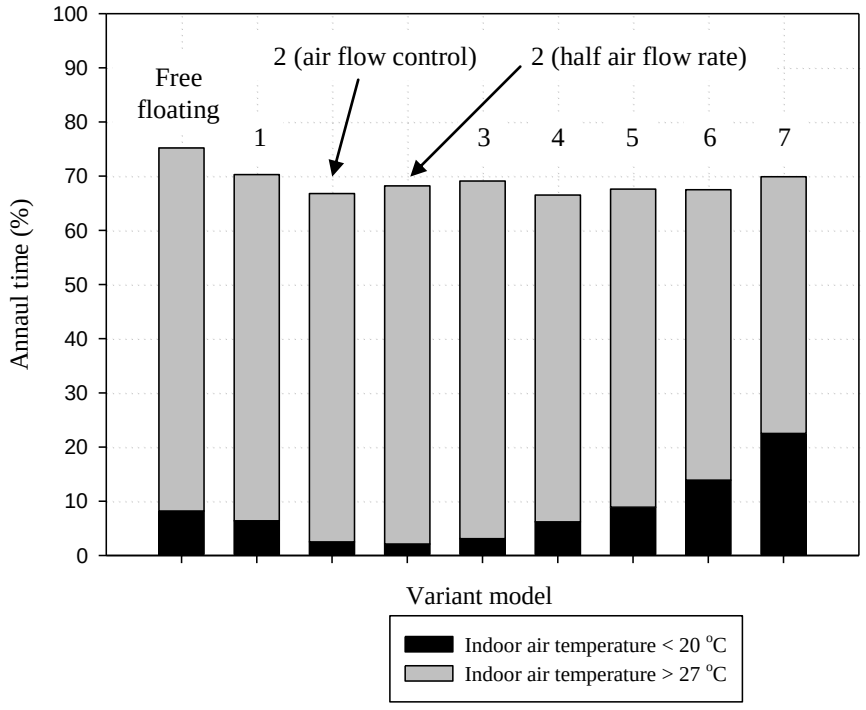

Figure 3.39: Annual time for heating and cooling requirements in living room for different Variant models.

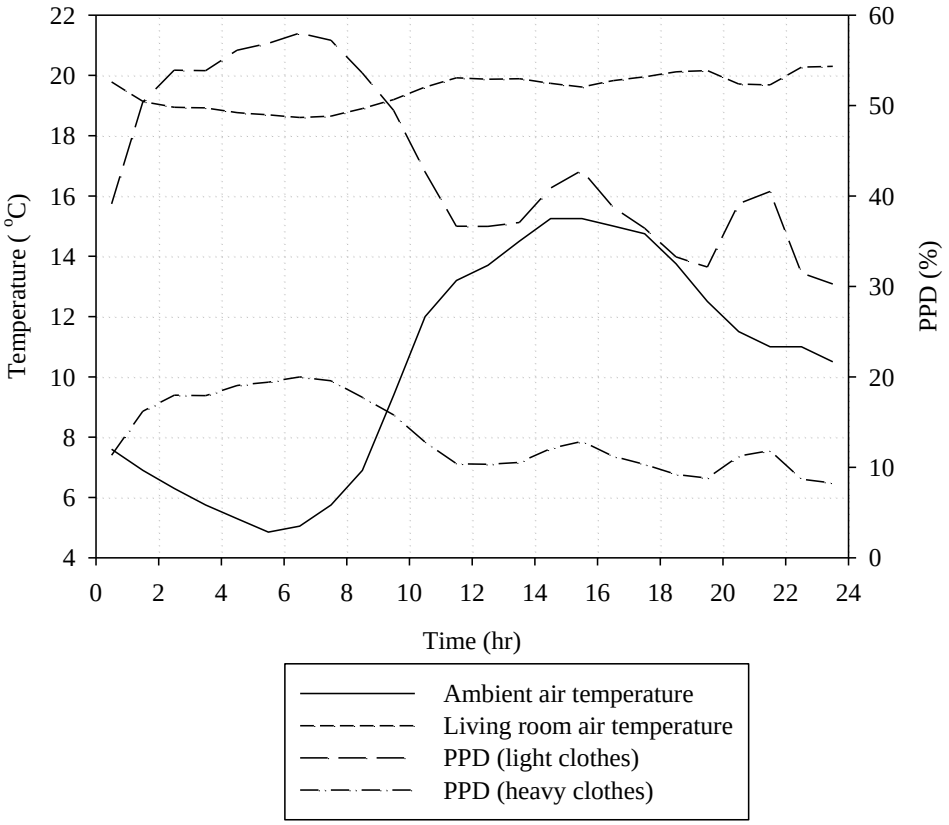

Figure 3.40: PPD at 18-20°C living room air temperature.

Table 3.26: Duration of active cooling in living room for different Variant models for the cooling season (1/3-1/12).

Variant/Criterion	Hours above 25°C (%)	Hours above 27°C (%)
Free floating	6391 (96.5)	5867 (88.6)
1	5926 (89.5)	5597 (84.5)
2 (half flow rate)	6103 (92.1)	5791 (87.4)
2 (flow control)	5940 (89.7)	5634 (85.1)
3	6049 (91.3)	5778 (87.2)
4	5871 (88.6)	5283 (79.8)
5	5799 (87.5)	5145 (77.7)
6	5581 (84.3)	4699 (70.9)
7	4661 (70.4)	4155 (62.7)

Table 3.26 shows that when natural acclimatization is considered in Variant 7, active cooling is required for only 62.7% of the cooling season whereas in free floating it was 88.6%. It is concluded that even when the culvert is well designed and supported by energy efficiency measure (Shading), ground surface treatment and air flow control there is still a requirement for mechanical cooling. The introduction of

an active cooling component to work alongside the air culvert and how this hybrid system can be controlled is the subject of the next chapter.

$$\frac{p_2}{p_1} = \left(\frac{V_2}{V_1}\right)^2 \qquad 3.19$$

$$\frac{P_2}{P_1} = \left(\frac{V_2}{V_1}\right)^3 \qquad 3.20$$

3.9 Concluding Remarks

A modified ground temperature profile for hot/dry climate was extracted and verified against real data for the cooling season. That profile was entered in an ESP-r air culvert model; the culvert model was validated empirically and by inter-comparison. A sensitivity analysis was undertaken from which a parametric priority list was produced. Culvert thermal performance was investigated on two fronts; thermal effectiveness and coefficient of performance. A 3 zone Villa representing a residential unit in a hot/arid climate was constructed in ESP-r and verified. The culvert was coupled to the Villa upon which several variant models were undergone to foresee how much the Villa can sustain comfortable indoor conditions utilizing passive cooling measures before introducing active cooling system.

Chapter 4 : Hybrid Cooling System

This chapter addresses the hybrid cooling system comprising active cooling plant and air culvert. It studies how the culvert can improve the A/C system performance and it considers how the two systems may best be coordinated. An overall control strategy is developed, justified and presented.

4.1 CAV A/C System Model in ESP-r

Active cooling devices are required if, after the application of building energy efficiency measures and a culvert-based air supply, the indoor air temperatures are still higher than ANSI/ASHRAE Standard 55 (2004) comfort threshold. Since the cooling requirement of residential buildings in hot climates is relatively constant, a CAV A/C system can provide temperature control more efficiently with less complexity than other A/C types (as justified in chapter 2). Further, CAV all-air A/C and culvert systems are compatible because both utilize air as the cooling exchange medium. A single-zone CAV all-air A/C system as shown in Figure 4.1 was established as an ESP-r active cooling model. Appendix C details the active cooling plant definition including components and connections (Table 4.1) comprising this model.

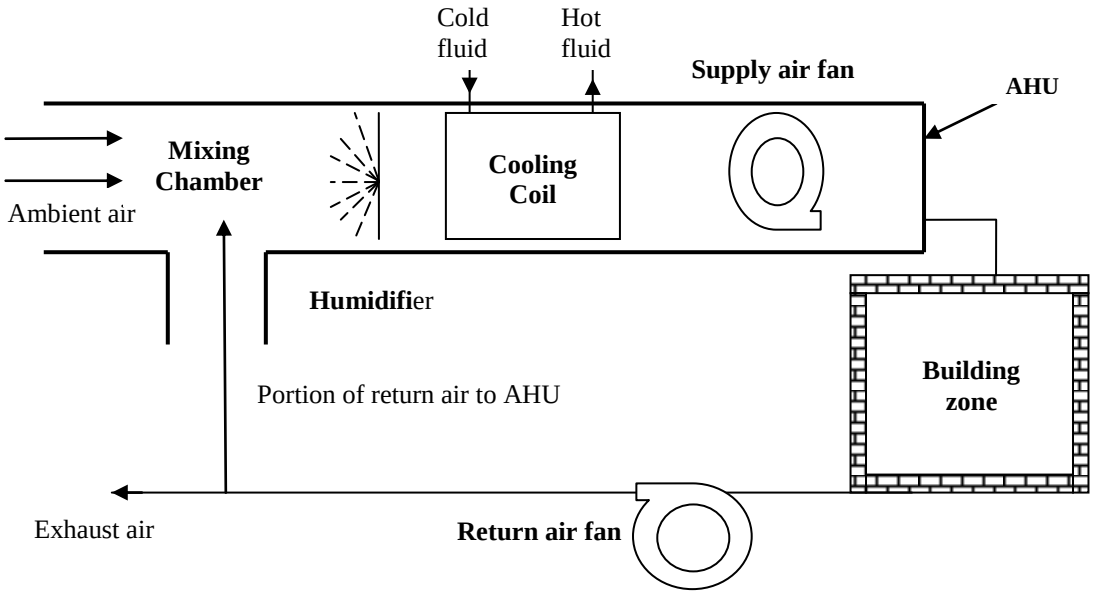

Figure 4.1: Single-zone CAV all-air A/C system Schematic.

Table 4.1: ESP-r single-zone CAV A/C (components and connections).

Connection No	Supply component	Receiving component
1	Ambient air	Duct-1
2	Duct-1	Mixing-box
3	Return-fan	Mixing-box
4	Mixing-box	Humidifier
5	Humidifier	Duct-2
6	Duct-2	Cooling-coil
7	Cooling-coil	Duct-3
8	Duct-3	Supply-fan
9	Supply-fan	Supply-duct 1
10	Supply-fan	Supply-duct 2
11	Supply-fan	Supply-duct 3
12	Living room	Return-duct 1
13	Dinning room	Return-duct 2
14	Bed room	Return-duct 3
15	Return-duct 1	Converge-1
16	Return-duct 2	Converge-1
17	Return-duct 3	Converge-2
18	Converge-1	Converge-2
19	Converge-2	Return-fan

$$\dot{V}_{CAV} = \frac{\text{Peak Sensible Cooling Capacity}}{\rho c_p \left(T_{mixing-box} - T_{cooling-coil}\right)} \quad 4.1$$

$$T_{mixing-box} = [\%\ \text{of outside air}\ (T_{amb} - T_{in})] + T_{in} \quad 4.2$$

$$\dot{m} = \dot{V}\rho\Delta\omega \quad 4.3$$

Supply and return fan air flow rates were assigned values based on peak summer time conditions using equation 4.1. Table 3.17 shows a peak space sensible cooling load of 9.8kW for an indoor air temperature set-point of 25°C and an ambient air temperature of 46°C. Using relation 4.2 for a 10% outside air intake into the AHU, the temperature at the mixing box would be 27°C. An off cooling coil air temperature of 13°C(55°F) is usually recommended, ± 3°C is given here for the air temperature coming off the cooling coil to be in the range 10°C-16°C. The cooling coil temperature calculated in equation 4.1 is at the low end of the cooling coil temperature (10°C). Thus, the supply/return fan flow volume flow rate is 0.48m^3/s (circled green in Appendix C). Now, the question is why the supply and return fan flow rates are computed steadily not dynamically since the A/C model is to be simulated transiently in ESP-r? Well, it is possible to get flow rates dynamically by changing the fan flow rate for several times until certain parameters such as cooling coil off air temperature and mixing box temperature are verified against standard values, however, this consumes more time and even yet the model gets vulnerable to errors due to the high number of simulations that should be conducted. Besides, the objective is not to study the impact of quantifying fan flow rate dynamically but the dynamic coupling between building thermal sub-systems (Villa, Culvert and A/C plant) is the target. The humidity ratio for indoor conditions (25°C and 50% RH) and outdoor conditions (46°C and 8% RH) are 0.01kg/kg and 0.004kg/kg respectively (Figure 4.5). Thus, using relation 4.3, the humidifier rate is 0.0035kg/s (circled red in Appendix C).

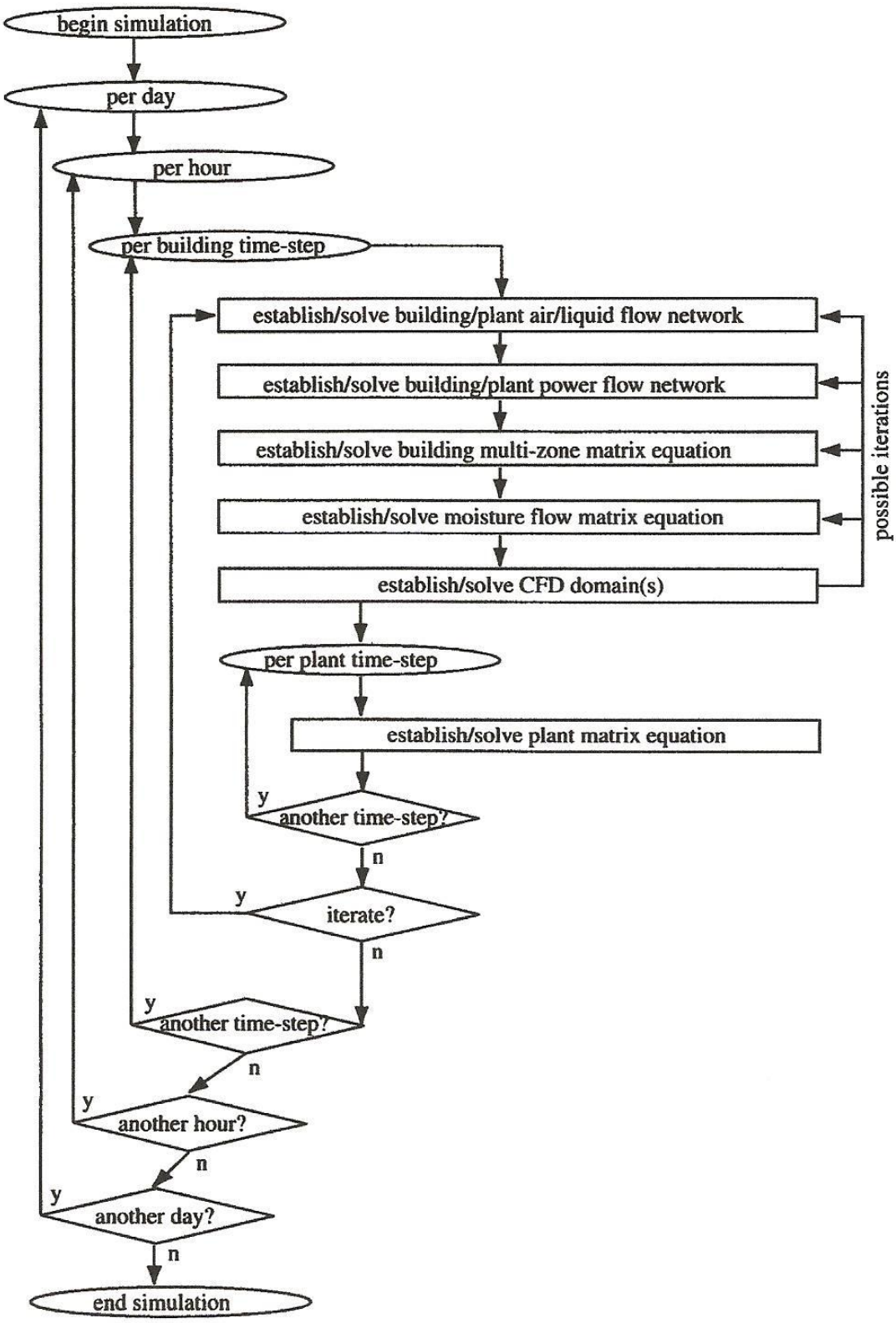

Figure 4.2: Co-operative simulation process in ESP-r (Clarke 2001).

The simulation process in ESP-r is illustrated in Figure 4.2 where different domains equation-sets corresponding to the building, HVAC system and culvert are iteratatively solved at time steps that depend on the underlying time constants. The first task therefore is to select appropriate time steps for each domain; this was done by undertaking a parametric analysis. The number of building time-step per hour as listed in Table 4.2 was set at 1, 5, 10 and 60 while keeping the number of plant time-steps per building time-step constant at 60. Then, the value for the building time-step which allowed the peak cooling load to be calculated with acceptable accuracy and with the lowest computational effort was selected. It is evident from Table 4.2 that the time-stepping scheme required to accurately estimate the peak cooling load with least computational effort is 10 building-side time steps per hour and 60 plant time steps per building time step. Then, different plant time-steps of 1, 5, 10 and 60 per the building time-step selected were imposed. The result corresponding to an acceptable peak cooling capacity for the lowest computational effort was selected. The simulation run-time was reduced from 55.7 seconds to 4.9 seconds when the plant time-step per building time-step was decreased from 60 to 5 at a building time-step per hour of 10, without unacceptably reducing the accuracy of the peak cooling capacity assessment. Thus, 10 and 5 were used in Villa/HVAC simulation for building time-step/hour and plant time-step per building time-step.

Table 4.2: Building time-step/hour and plant time-step/building time-step selection for the simulation of A/C plant and building coupling.

Run/ Item	Building time-step/hour	Plant time-step/Building time-step	Peak cooling load (W)	Per day simulation CPU time (s)
1	1	60	-10,000	5.36
2	5	60	-9,236	25.78
3	10	60	-8,454	55.65
4	60	60	-8,467	389.4
5	10	1	-9,673	1.61
6	10	5	-8,533	4.92
7	10	10	-8,529	10.11

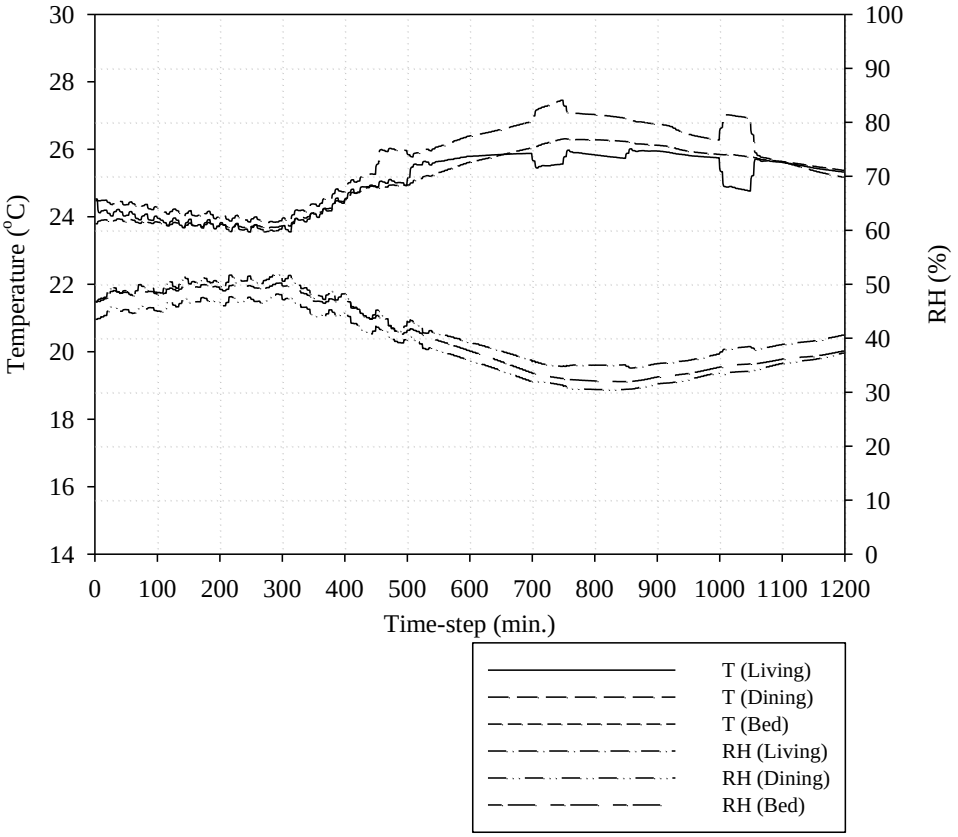

Figure 4.3: ESP-r predicted indoor conditions on a Summer peak day with CAV A/C system.

As shown in Table 3.17, the peak space sensible cooling load is 9.8kW to provide an indoor air temperature of 25°C but when the A/C plant was simulated in ESP-r the peak coil cooling load was 8.5kW (Table 4.2) for an air temperature above 25°C in the 3 zones of the model. Figure 4.3 summarizes the indoor operating conditions during a peak summer day in the 3 zones: the air temperature varies between 24-27°C and the relative humidity between 30-50%. The indoor relative humidity is as required by ANSI/ASHRAE Standard 55 (2004), and the indoor air temperatures are within range when natural acclimatization in hot climate is considered.

4.1.1 ESP-r A/C Model versus Psychometric Chart Cooling Load

The single-zone CAV A/C model represented in ESP-r was compared against the cooling load calculated using the psychometric chart to appreciate the use of energy transient tool in assessing building cooling requirements. Figure 4.4

illustrates that at peak times the off cooling coil air temperature and the air temperature at the mixing box exit are 12°C and 32°C respectively. Referring to the same figure, the relative humidity for the corresponding AHU components are 100% and 33% respectively. Cooling and dehumidification processes are plotted on the psychometric chart shown in Figure 4.5. Sensible cooling starts from T_{db} (32°C) and RH (33%) moving through the green line until it reaches the dew-point temperature at the saturation line where latent cooling commences (the blue line) until the off cooling coil air temperature of 12°C is reached. Using Figure 4.5, the enthalpy at mixing box and cooling coil exits are 57kJ/kg and 32kJ/kg respectively. By approximation, the cooling coil load (sensible and latent) of 14.4kW is calculated using relation 4.4: this is a 70% increase over that predicted by ESP-r!

$$Q_{S+L} = \rho \dot{V} \Delta h \qquad 4.4$$

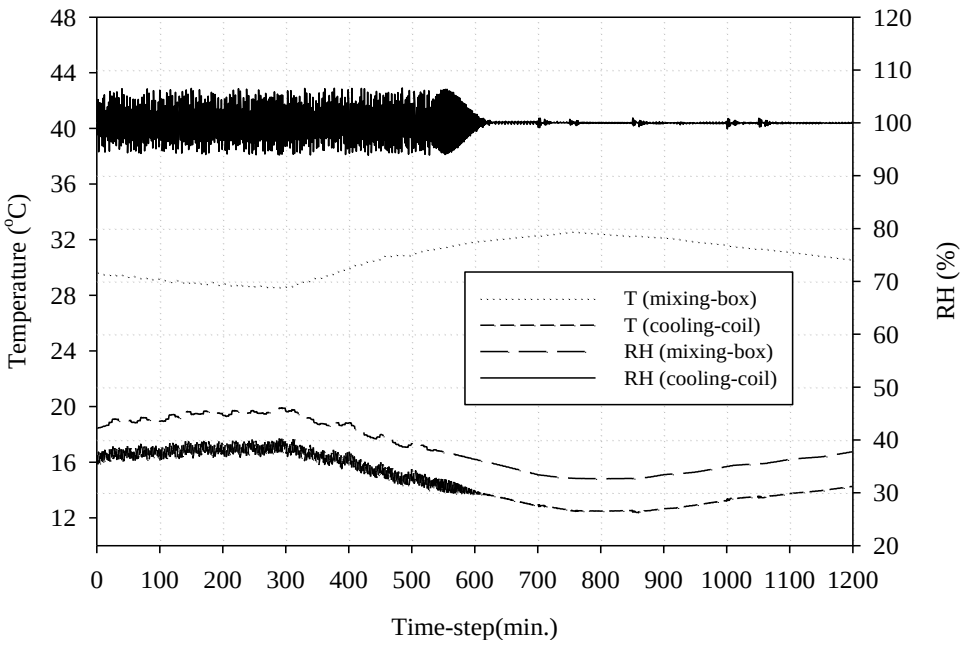

Figure 4.4: ESP-r predicted parameters of the cooling coil and mixing box of the single-zone CAV AHU on a summer peak day.

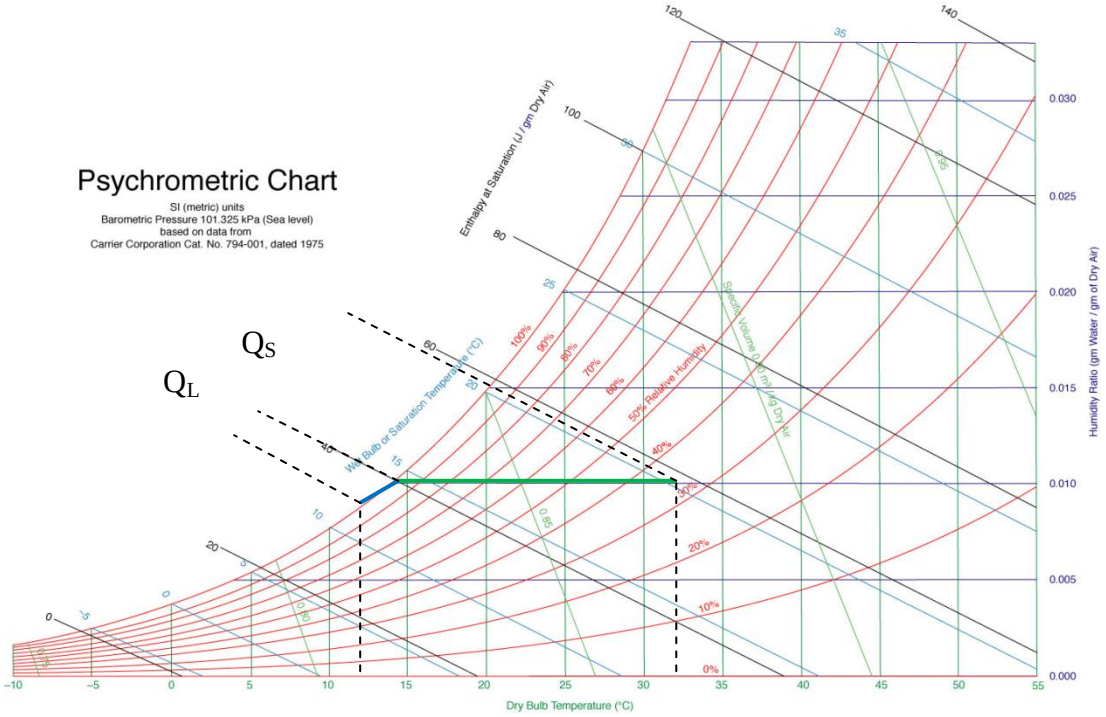

Figure 4.5: Sensible and latent cooling load as shown in the psychometric chart provided by Carrier Corporation.

4.1.2 A/C Short Cycling

It is not practical to maintain an exact 25°C indoor air temperature using an A/C plant to avoid A/C short cycling. Table 4.3 lists the cooling coil control element where a 4°C throttling range was imposed to allow the cooling capacity to float from minimum (0kW) to maximum (10kW) to provide an indoor set-point temperature of 25°C; this means as long as the indoor air temperature is 25°C±2°C the A/C system is on with cooling capacity varying. The impact of imposing different throttling ranges around the temperature controller set-point is examined. Referring to Figure 4.6, using a small throttling range near zero stabilizes the indoor air temperature near the set-point temperature more than when a large one is used but that is at the expense of A/C short cycling causing the system operating efficiency to downgrade. It is better for the A/C system to run long cycles than shorter ones at the maximum cooling load, and therefore it is important that the system is appropriately sized since optimum efficiency is achieved at continuous running. This issue can be resolved by using two or more A/C units of similar cooling capacity so that one A/C unit operates at partial load with additional A/C units activated as the peak cooling load is approached; multi-chiller control is discussed in later sections. Figure 4.6 shows that

for a 4°C throttling range, the A/C system is running continuously with gradual indoor air temperature increase or decrease so that the Villa occupier does not feel a sudden temperature change; the problem here is energy waste because the electricity consumption corresponds to the peak cooling load condition.

Table 4.3: Cooling coil control loop elements.

Sensor	Actuator	Control Law	Data
Return air dry-bulb temperature.	Cooling coil flux.	PID flux control.	(-1 10000 0 25 4)

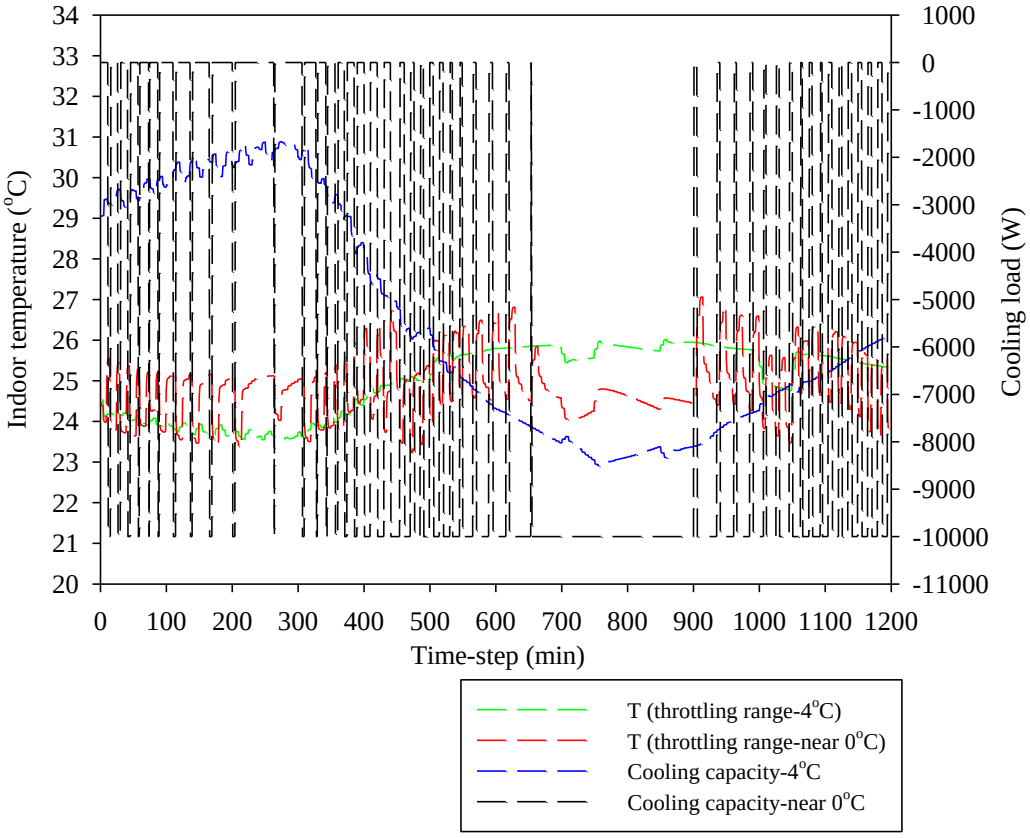

Figure 4.6: ESP-r predicted cooling coil performance and indoor condition for different throttling ranges.

4.2 CAV A/C System Coupling with Villa/Culvert

The culvert was coupled to the A/C plant such that the plant receives air from the culvert in place of outside air. This coupling physically is illustrated by Mathur et al. (2012) such that air from culvert is supplied to the condenser coils of the air

conditioner using well insulated wooden boxes provided on the outer casing of the air conditioner. It is important to state that the A/C system fan flow rate has to be reduced according to how much the sensible cooling load is reduced due to Villa/Culvert coupling. The culvert is able to reduce the space peak sensible cooling load by ~36% (Table 4.4) at an indoor set-point temperature of 25°C and thus the fan volume flow rate used in the A/C plant according to equation 4.1 has to be reduced from 0.48 m^3/s to 0.31m^3/s. Figure 4.7 indicates that the culvert can be used to downsize the A/C system cooling capacity throughout the year. It also confirms, as discussed in chapter 3, that the culvert performance retreats in late Summer. It also indicates that further hybrid cooling system improvements are possible – for example, by spraying the ground surface in late Summer to cause evaporative cooling. It also suggests that using shading and natural ventilation in the transitional seasons can improve the hybrid system's cooling potential further. Figure 4.8 shows that the active cooling capacity has been reduced by ~38% at the Summer peak condition when the culvert was coupled with the CAV A/C system. In the early morning, the A/C cooling load needed to offset the heat gain is lower than that of the hybrid cooling system and *vice versa* from late morning until midnight. Culvert fan power consumption versus culvert cooling capacity should be evaluated. Figure 4.9 shows the corresponding indoor air temperature and relative humidity within the Villa zones. It can be seen that the culvert increases the indoor relative humidity to the range 55-70% except in the morning in the bed room where it exceeds 70%. However, at this time the culvert input is not beneficial and it is best to deactivate its contribution to the hybrid cooling system. The indoor air temperatures in all 3 zones are maintained within 24-27°C. Thus, the hybrid cooling system can maintain acceptable indoor conditions as long as it is subjected to an effective control strategy that adjusts key parameters designed to minimise the use of the active cooling component.

Table 4.4: Culvert effect on Villa sensible cooling load at summer peak time.

Time/Sensible cooling load (kW)	Without culvert use	With culvert use
Summer peak time	9.81	6.27

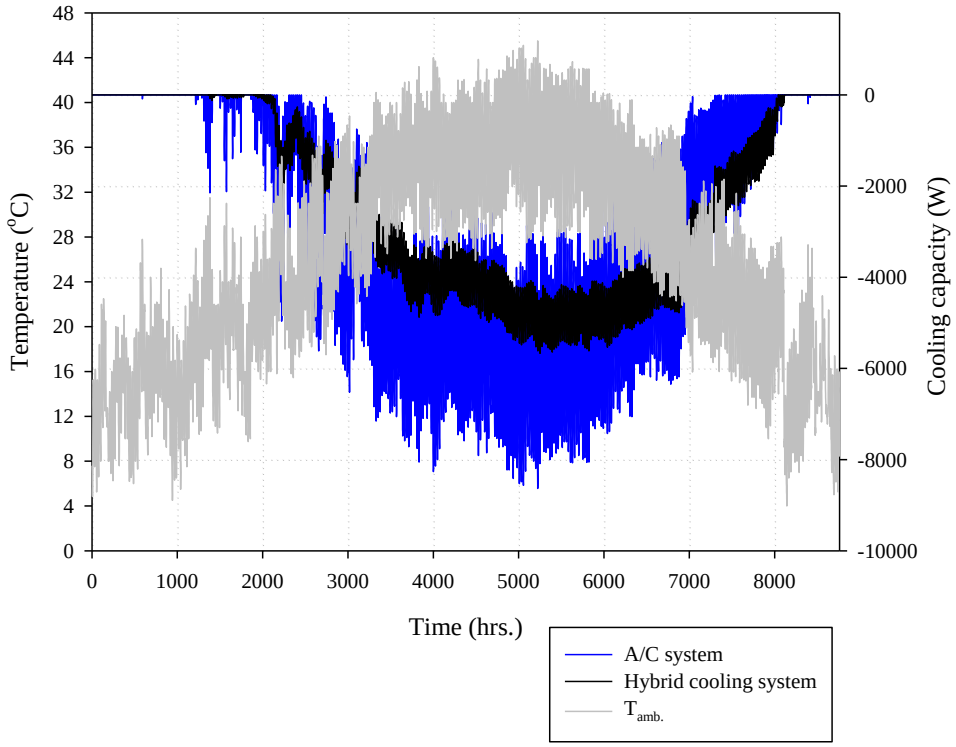

Figure 4.7: A/C cooling load with and without the culvert for the cooling season.

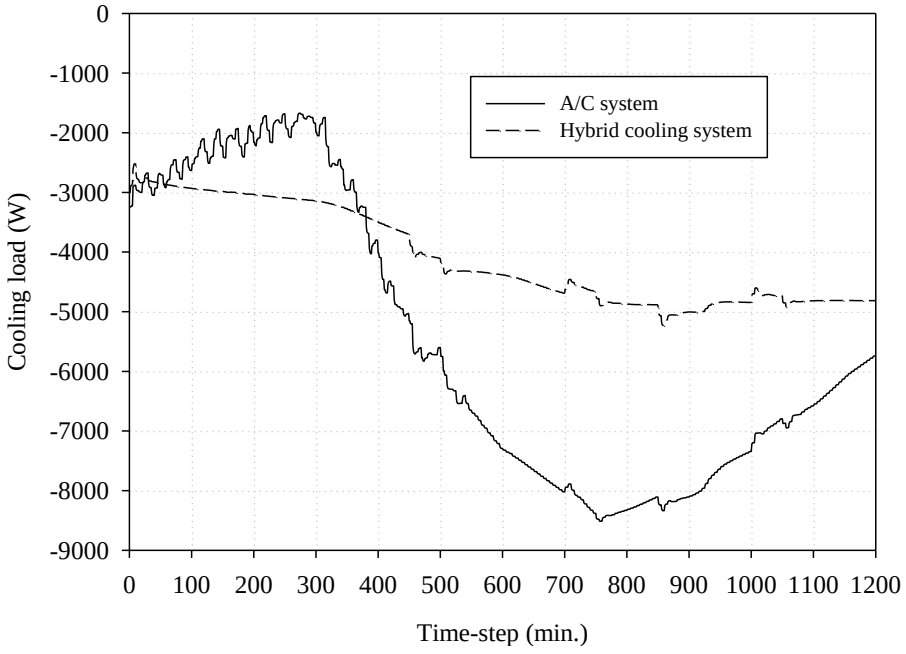

Figure 4.8: Peak cooling loads for A/C plant and hybrid cooling system.

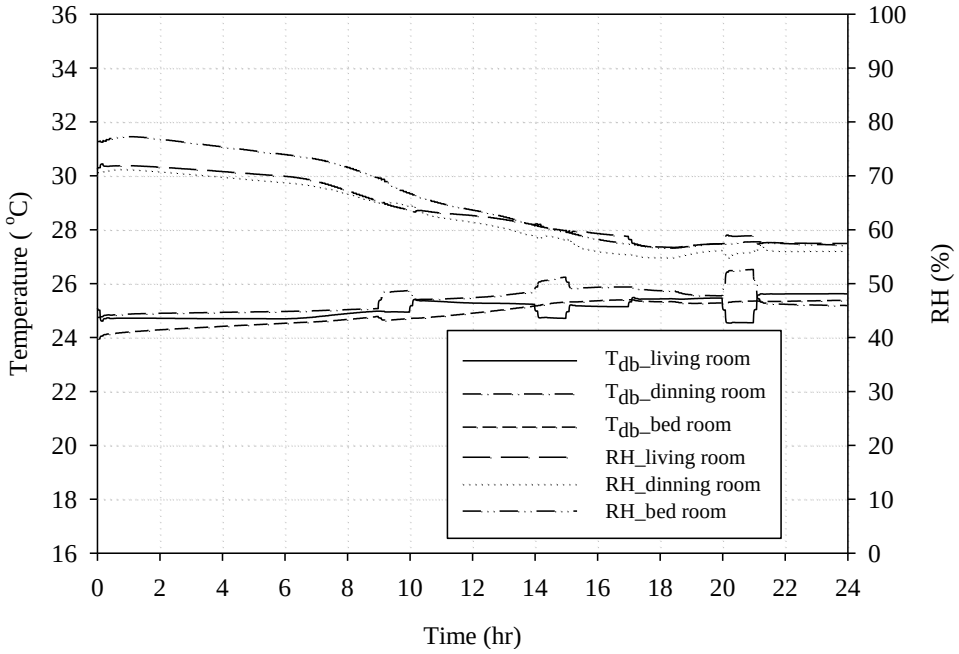

Figure 4.9: Indoor conditions for the Villa with the hybrid cooling system at peak Summer time.

4.2.1 Culvert Effect on A/C System Performance

By integrating the load predictions over the cooling season equation 4.5 may be used to obtain the COP. The CAVA/C system monthly cooling energy consumption, along with the monthly number of hours required for the compressor to operate, is tabulated in Table 4.5. This table indicates that the culvert was able to reduce annual A/C system cooling energy consumption by 13% compared with the A/C cooling energy consumption before culvert use - note that in late Summer (September to November) which is part of the cooling season, the inclusion of the culvert is wasteful; a point that needs to be addressed in future study to examine if ground surface treatment should be used by assessing how much energy savings can be achieved. Referring to the same table, June is the best month for the culvert cooling contribution, whereas November is the worst month. As shown in Figure 3.30 June is the best month for culvert thermal performance because the temperature difference between ambient and ground temperatures is at its highest so that the cooling potential is at its annual maximum. An A/C cooling energy consumption of 251.2 kWh/m^2/yr (CAV total monthly cooling energy consumption/Villa floor area) is calculated from Table 4.5 before the culvert incorporation; a value that agrees well

with the GCC residential average cooling energy consumption of 250 kWh/m^2/yr. The culvert's effect on CAV A/C system performance is presented next.

$$\text{COP} = \frac{\text{Energy Output}}{\text{Energy Input}} \qquad 4.5$$

Table 4.5: CAV A/C system energy consumption before and after culvert inclusion.

Month/ Property	Energy Consumption without culvert use (kWh)	Compressor operation required (hr.)	Energy Consumption with culvert use (kWh)	Compressor operation required (hr.)
Mar.	-297	240	-66	150
Apr.	-1972	630	-1405	744
May	-4051	768	-2716	768
Jun.	-5019	744	-3701	744
Jul.	-5476	768	-4313	768
Aug.	-5560	768	-4785	768
Sep.	-4310	744	-4338	744
Oct.	-2770	768	-3453	768
Nov.	-688	380	-1402	744
Total	-30143	5810	-26179	6198

4.2.1.1 CAV A/C System COP Prior to Culvert Use

The maximum ambient air temperature when the culvert is not in use is 46°C (114.8°F) and for 25°C and 50% RH the wet-bulb temperature indoors from the psychometric chart is 18°C (64.4°F). So from Table A.1, the power consumed by the compressor at those close parameters (115°F for outdoor T_{db}) and (63°F for indoor T_{wb}) is 2.23kW (red circle). Thus, the compressor energy input using Table 4.5 is -12956kWh and by using relation 4.5 the CAV A/C system COP before culvert inclusion is 2.33.

4.2.1.2 CAV A/C system COP after culvert use

When the culvert is coupled to the CAV A/C system, the maximum ambient air temperature is ~33°C (91°F) as shown in Figure 4.7. From Table A.1, the power consumed by the compressor at (90°F as outdoor T_{db}) and (63°F as indoor T_{wb}) is 1.69kW (blue circle). Thus, the compressor energy input using Table 4.5 is -10475kWh and by using relation 4.5 the CAV A/C system COP after culvert inclusion is 2.5. That is the culvert increases the CAV A/C system COP by 7%.

4.3 Control Strategy of the Hybrid Cooling System

The control algorithm for the hybrid cooling system for buildings in hot/dry climates is elaborated in this section and this is then generalised for any climate context in chapter 5. Several variant models were simulated for different parts of the cooling season. The build-up of the control strategy was based on selecting temperature boundaries (ambient, indoor, culvert and ground) of the variant model that eliminates or minimizes the space cooling load among others at a certain point of time during the cooling season without endangering ventilation and thermal comfort requirements. Some of those variant models were already discussed in the previous chapter such as (Villa + Culvert) and some are new such as (Villa + A/C system); however those variant models presented in chapter 3 were approached to examine the sustainability of comfortable indoor temperature passively whereas the variant models here evaluate cooling capacities and thus annual cooling energy consumption required for the Villa. The variant models were as follow.

- Villa in free floating mode.
- Villa + natural ventilation.
- Villa + free cooling.
- Villa + culvert.
- Villa + A/C system.
- Villa + A/C system + culvert.

The first issue in the controller is to specify indoor set-point temperatures that trigger certain terms and conditions to be considered. The specific algorithm, as shown in Figure 4.10, starts by sensing if the indoor dry-bulb temperature is larger

than 27°C (Summer season); a value that corresponds to the upper limit for acceptable comfort because it corresponds to a PPD of less than 20% with suitable indoor air speeds and clothing levels (Table 4.6).

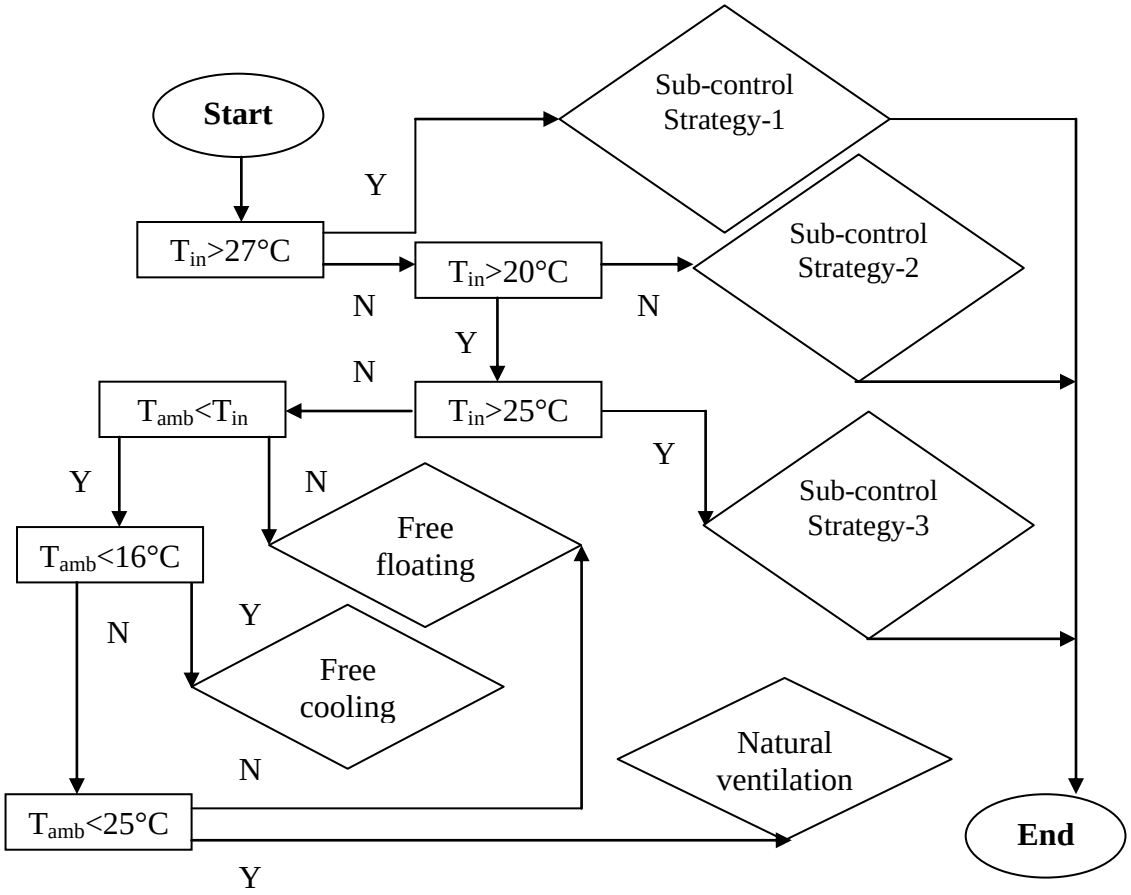

Figure 4.10: Control strategy for hybrid cooling system in a hot climate.

Nevertheless, thermal comfort can ideally be defined by the resultant[3] temperature not PPD so that thermal comfort is assessed transiently not based on steady state. The suggested resultant temperature in the Summer is between 24°C and 26° and in the Winter it is recommended to be between 21°C and 23°C (ANSI/ASHRAE Standard 55 2004). Figure 4.11 shows that the resultant temperature inside the living room for example is a bit more than the upper comfort threshold by ~0.5°C for the indoor dry-bulb temperature to be 27°C. This was deemed suitable for hot/dry climate when natural acclimatization is considered since people living in hot climate can sustain extra degrees above comfort threshold (Olesen 2008). However, it is permissible for different climate type or even when

[3] Resultant temperatures refer to the average of dry-bulb and mean radiant temperatures.

hot/dry climate occupants feel discomfort as a result of resultant temperature increase to decrease the indoor set-point dry-bulb temperature without affecting the sequence of the controller.

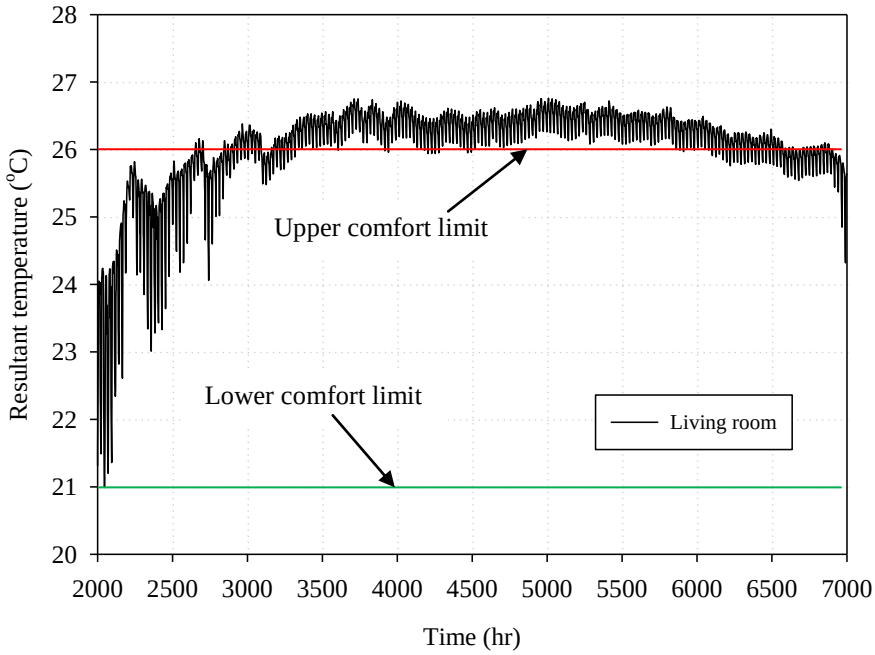

Figure 4.11: Living room resultant temperature during summer time of the control strategy for hybrid cooling system.

Table 4.6: ESP-r predicted PPD corresponding to different indoor air temperatures at 0.6Clo (clothing level), 90W/m^2 (activity level) and 0.2m/s (indoor air speed).

T_{in} (°C)	25.63	25.31	25.06	24.97	26.29	26.94	27.23
PPD (%)	14.46	10.37	8.63	8.42	15.36	22.56	28.58

When the dry-bulb temperature is above 27°C, sub-control strategy 1 is invoked (Figure 4.12). The algorithm checks if the ambient air temperature is higher than 30°C (a value justified in the next paragraph); if yes then 50% flow rate is allowed, if not 100% flow is exercised. It is explained in chapter 3 that if 25% of the 5 persons living in the house are smokers then the ventilation requirement is 0.08m^3/s (100% flow rate) while if there are no smokers, this value may be halved according to CIBSE Guide B (2005). As explained in section 3.3.4, the culvert outlet air temperature increases and decreases in Summer and Winter respectively when the culvert air volume flow rate is increased. Thus, culvert volume flow rate control is vital and, if applied properly, will lead to significant reductions in the annual cooling energy and peak cooling load.

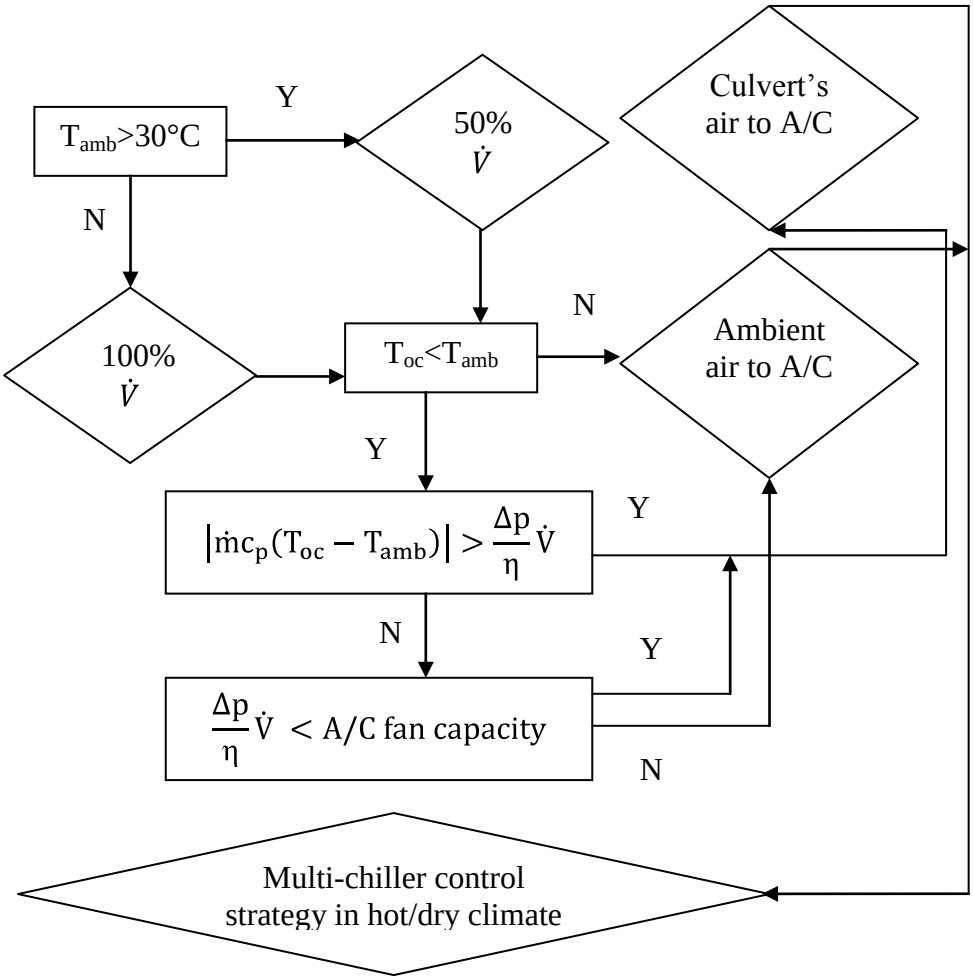

Figure 4.12: Sub-control strategy 1 in a hot/dry climate.

Selection of 30°C as an ambient temperature, where a change over from 100% flow rate to 50% is imposed when that temperature is passed, was based on the following factors:

1. peak cooling power reduction potential;
2. annual cooling energy consumption minimization; and
3. meeting air ventilation requirements.

Table 4.7 shows different sensed ambient temperatures above which the culvert fan in the hybrid cooling system operates at 50% capacity. Both the annual cooling energy and peak cooling power for the hybrid cooling system at different sensed ambient temperatures were compared to those resulting from an A/C plant when used alone. A/C system energy simulation is a complex matter in terms of accuracy and computation speed and thus for this change over test the A/C system

was replaced with a basic control On/Off control system. However, after this flow rate change over test is done the A/C system is resumed again in the hybrid cooling system. This was done by sensing ambient dry-bulb temperature and actuating the culvert fan flow rate.

Table 4.7: Culvert air flow rate control effect on Villa cooling energy and peak load for the period from March1 to December 1 at an indoor air temperature of 27°C.

Cooling system /Parameter	Cooling energy consumption ($kWh/m^2/a$)	Peak cooling load (W/m^2)	Reduction compared to Basic control On/Off (%)	
			Energy	Peak load
Basic control On/Off	166	72	0	0
Basic control+ air culvert (no flow control)	131	41	21	43
Basic control + air culvert (sensed $T_{amb.}$ > 48 °C)	131	41	21	43
Basic control + air culvert (sensed $T_{amb.}$ > 40 °C)	124	33	25	54
Basic control + air culvert (sensed $T_{amb.}$> 34 °C)	114	32	31	56
Basic control + air culvert (sensed $T_{amb.}$ > 32 °C)	111	32	33	56
Basic control + air culvert (sensed $T_{amb.}$> 30 °C)	108	32	35	56
Basic control + air culvert (sensed $T_{amb.}$ > 28 °C)	107	32	36	56

As shown in Table 4.7, when the sensed ambient air temperature is higher than 48°C no culvert air flow control was exercised because the maximum ambient temperature is 46°C. When the sensed ambient air temperature is higher than 40°C, the peak cooling power reduction of the hybrid cooling system compared to that at 48°C has increased from 43% to 54%. It may be seen from Table 4.7 that the annual cooling energy consumption reduction of the hybrid cooling system at 40°C versus that at 48°C increases from 21% to 25%. Table 4.7 also shows that by reducing the sensed ambient temperature from 40°C to 28°C, the peak cooling power reduction (first criteria) is minimal from 54% to 56% whereas the annual energy consumption reduction (second criteria) changes from 25% to 36% (lowest). Obviously, there was no point of reducing sensed ambient temperature to less than 28°C because both peak cooling power and annual cooling energy consumption would no be reduced at all. However, 28°C as sensed ambient temperature was replaced by 30°C as a result of

the third criterion above since the required level of ventilation will be available more often but at the expense of a lower annual cooling energy saving (36% to 35%). Again, when 50% flow rate is used in culvert to provide ventilation requirements the Villa occupiers must not smoke during ambient temperatures that are higher than 30°C.

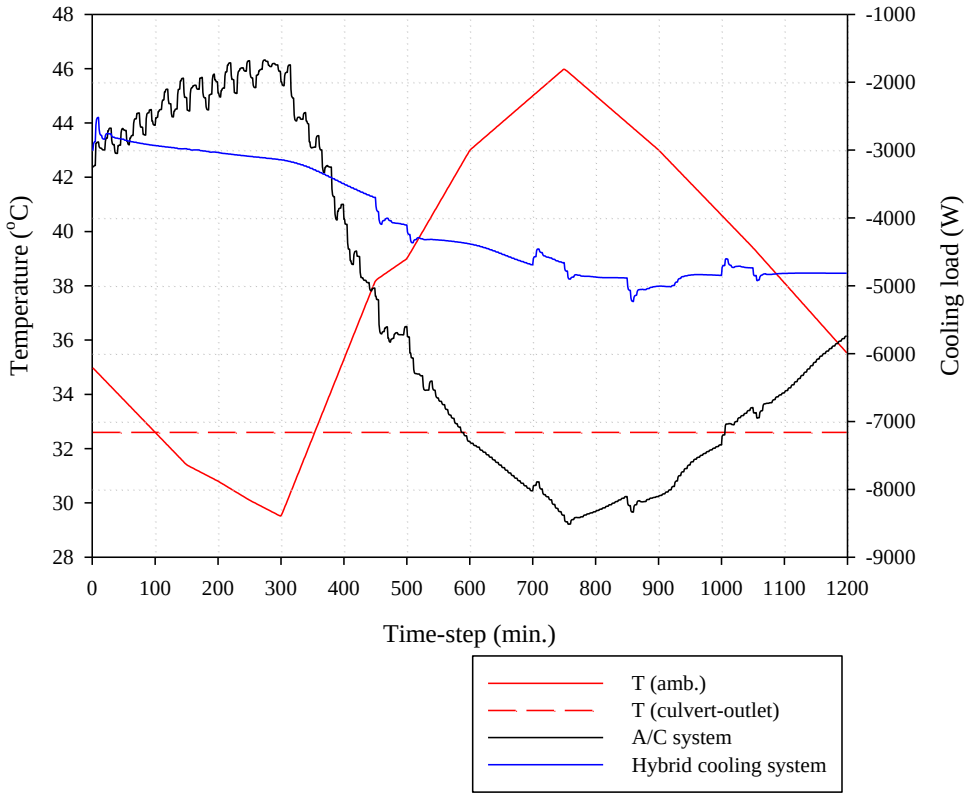

Figure 4.13: Ambient and culvert outlet air temperature intersection when hybrid cooling system is used.

Continuing with sub-control strategy 1, if the ambient air temperature is higher than 30°C then 50% of the culvert fan capacity is used; else the full capacity is activated. The control set-up then examines if the culvert outlet air temperature is less than the ambient air temperature. If the answer is no, the ambient air is supplied to the AHU, if yes then the algorithm determines if the culvert cooling capacity is higher than the fan power consumption. If this answer is no then the ambient air is supplied to the AHU, if the answer is yes then the AHU will be supplied by culvert air. That point is clearly shown in Figure 4.13 where the air temperature at the culvert outlet is less than the ambient air temperature and, thus the culvert air should be supplied to the AHU as shown from late morning until midnight. However,

referring to the same figure, when the ambient temperature is less than the culvert outlet air temperature, as seen in early morning, then the AHU is supplied by ambient air. The purpose of the culvert is to provide cool air to the Villa or AHU. The culvert fan capacity for Villa is too small that can be recovered by any increase of culvert outlet air temperature over the ambient temperature. To illustrate this point, for a volume flow rate of $0.08m^3/s$ for each Villa zone, a pressure difference across the culvert of 17 Pa (Figure 3.33) and a fan efficiency of 70%, the culvert fan power is 0.00583kW (equation 3.18). Equating the culvert cooling capacity using equation 3.12 with the resulting culvert fan power yields a T_{oc}-T_{amb} of 0.02°C; this small temperature difference increases with increasing zone ventilation rates, which is the case in commercial facilities (Figure 2.4) where T_{oc}-T_{amb} must be 2°C to switch on culvert fan. In that case when the culvert cooling capacity is smaller than the culvert fan capacity then the final test would be to examine if the culvert fan load is smaller than the A/C fan load. If yes then air is supplied to the AHU by the culvert, but if not then ambient air is supplied (Figure 4.12). In this model as discussed earlier, the temperature difference between ambient and culvert outlet air required to switch the culvert fan on is small (0.02°C) and thus this condition may not be encountered as if the system was to be used in commercial facilities where culvert fan load is noticeable. Sub-control strategy 1 ends by transferring to the multi-chiller controller for hot/dry climate to determine how much active cooling capacity is required for different culvert cooling contributions.

- **Multi-Chiller Control Strategy for Hot/Dry Climate**

The multi-chiller control strategy for hot/dry climate as included in sub-control strategy 1 (Figure 4.12) is elaborated in Figure 4.20; such modularization reduces plant short cycling. Ground condition is a key parameter in the assessment of multi-chiller controller since there are times when culvert air is supplied directly to the AHU. The culvert thermal performance will determine the active cooling fraction required to offset the building's cooling load. Figure 4.14 presents the cooling load required by the active cooling system after considering culvert cooling contribution. It shows that 75%-100% of peak cooling load is experienced in the afternoon in a typical summer day. The same figure indicates that 25%-50% of peak cooling load is

usually encountered in a typical spring afternoon, however, in autumn; 50%-75% of the peak cooling load is often seen in the afternoon.

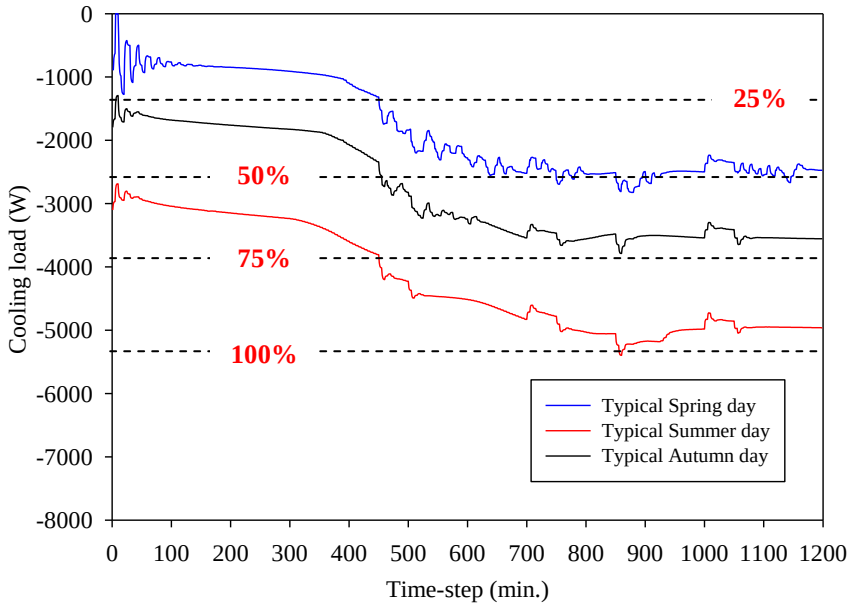

Figure 4.14: Selection justification of 4 A/C units for multi-chiller controller.

Thus, the A/C system was divided into 4 A/C units of equal cooling capacities after considering the maximum cooling contribution for summer peak day. It is important to emphasize that the proportionality was for the A/C cooling load not for the flow rate; this means that air is either supplied by the ambient or the culvert at any point in time with no proportional percentage between ambient and culvert air. The objective of multi-chiller control set-up was to specify when one or more A/C units should operate considering culvert cooling contribution. For example, there are times when the building requires only 25% of the full cooling load; if only 1 large A/C unit is available then short cycling will be experienced (as opposed to only 1 of 4 smaller A/C units operating). In order to generalise the multi-chiller control algorithm as will be seen in the next chapter, the ground operating conditions are included since they vary markedly between climate regions. The multi-chiller control strategy therefore depends on both the ambient and ground temperatures. Clearly, while the ambient air temperature maybe the same between regions, the ground condition may vary. The operating conditions involved in the multi-chiller control scheme are as follows.

1. Ambient air temperature.

2. Ground temperature.
3. Annual lowest ground temperature.
4. Annual mean ambient air temperature.
5. Annual highest ground temperature.

The validation of the global multi-chiller control strategy in different climates is the subject of chapter 5; here only multi-chiller controller in a hot/dry climate is considered. The multi-chiller control strategy for the hybrid cooling system in a hot/dry climate, as shown in Figure 4.20, was formulated from plots such as those presented in Figure 4.15, Figure 4.16, Figure 4.17, Figure 4.18 and Figure 4.19. It is important to relate the 'if statements' in Figure 4.20 to the former figures as well as to the results generated in Table 4.8 in order to determine the percentage of active cooling that should operate at any time. The variables in Table 4.8 are defined, from left to right, as:

1. Ambient air temperature (°C).
2. Culvert outlet air temperature (°C).
3. A/C cooling capacity (kW).
4. Culvert cooling capacity (kW) (Equation 3.12).
5. Total hybrid cooling system cooling load (kW).
6. Culvert cooling contribution to the hybrid cooling system (%) (Equation 4.6).
7. A/C cooling contribution to the hybrid cooling system (%) (Equation 4.7).
8. Old modularized A/C cooling before culvert inclusion (%) (Equation 4.8).
9. New modularized A/C cooling required after considering culvert cooling contribution (%) (Equation 4.9).
10. Multi-chiller control strategy recommendation (%).

$$\text{Culvert cooling contribution} = \left(\frac{\text{Culvert cooling load}}{\text{Total cooling load}}\right) \text{x}100(\%) \qquad 4.6$$

$$\text{A/C cooling contribution} = (100\% - \text{culvert cooling contribution (\%)}) \qquad 4.7$$

$$\text{Old modulrized A/C} = \left(\frac{\text{Old A/C cooling load}}{\text{Old peak A/C cooling load}}\right) \text{x (A/C cooling contribution)} \qquad 4.8$$

$$\text{New modulrized A/C} = \left(\frac{\text{Old modulrized A/C \%}}{\text{Old peak A/C \%}}\right) \text{x}100(\%) \qquad 4.9$$

The last column (column 10) was included in Table 4.8 as a gauge for multi-chiller control strategy validity with a cooling load match rate of 96% with that produced by ESP-r hybrid cooling system model. Figure 4.14 and Table 4.8 show that the active cooling load, after considering the culvert contribution at peak summer time, was (~5.2kW) and, therefore, the multi-chiller can be modularized into 4 segments (column 8): 0-25% (0kW-1.3kW), 25-50% (1.3kW – 2.6kW), 50-75% (2.6kW – 3.9kW) and 75-100% (3.9kW – 5.2kW). While such a small cooling load does not need to be modularized, this study is general and thus larger A/C plants, when encountered, can follow the same guidelines. In hot/dry climate, no cooling load can be used to do the segmentation mentioned above other than the peak load because there the reduction in peak A/C cooling load due to culvert cooling contribution is maximum; this is not the case in hot/humid climate for example as will be seen in the next chapter. The multi-chiller control strategy is validated using the following procedure.

- Since there are 4 A/C ranges- 0%-25%, 25%-50%, 50%-75% and 75%-100%.
- Say that the predicted A/C (%) from multi-chiller control strategy is 50% (Column 10) from Table 4.8.
- And, if the simulated A/C (%) (Column 9 from Table 4.8) was 35% then a 1 is given.
- And, if the simulated A/C (%) (Column 9 from Table 4.8) is 23% then 1 is given because a 10% error from 25% was met otherwise 0 is given.
- Yet, if the simulated A/C % is 55% then 1 is given because a 10% error from 50% was met otherwise 0 is given.
- The 1's and 0's are summed up to give the successful time steps shown in Table 4.8. The result is then divided by the total time steps to produce the cooling load match rate percentage.

Table 4.8: Sample of the synchronization of the multi-chiller control strategy for hot/dry climate.

Time (hr)	T_{amb} (°C)	T_{oc} (°C)	A/C (kW)	Culvert (kW)	Total (kW)	Culvert cooling contribution (%)	A/C (%)	Old Modularized A/C (%)	New Modularized A/C (%) (ESP-r)	Control strategy recommendation
0.5	23.30	23.46	-0.09	0.05	-0.04	0	100	1	1	0
1.5	21.05	23.49	0	0.71	0.71	0	0	0	0	0
2.5	19.20	23.51	0	1.25	1.25	0	0	0	0	0
3.5	17.80	23.52	0	1.66	1.66	0	0	0	0	0
4.5	16.75	23.51	0	1.96	1.96	0	0	0	0	0
5.5	15.80	23.48	0	2.22	2.22	0	0	0	0	0
6.5	16.15	23.43	0	2.11	2.11	0	0	0	0	0
7.5	18.00	23.38	0	1.56	1.56	0	0	0	0	0
8.5	21.55	23.32	0	0.51	0.51	0	0	0	0	0
9.5	25.05	23.26	-0.19	-0.52	-0.71	73	27	1	1	25
10.5	27.00	23.19	-0.69	-1.10	-1.79	62	38	3	4	25
11.5	28.85	23.14	-1.36	-1.65	-3.01	55	45	7	10	25
12.5	30.00	23.11	-1.77	-1.99	-3.76	53	47	10	14	25
13.5	30.65	23.12	-2.08	-2.18	-4.26	51	49	12	17	25
14.5	31.15	23.15	-2.33	-2.32	-4.65	50	50	14	19	25
15.5	31.65	23.19	-2.52	-2.45	-4.97	49	51	15	21	25
16.5	31.50	23.23	-2.46	-2.39	-4.85	49	51	14	20	25
17.5	30.50	23.28	-2.11	-2.09	-4.20	50	50	12	17	25
18.5	29.50	23.33	-1.76	-1.79	-3.55	50	50	10	14	25
19.5	28.50	23.38	-1.39	-1.48	-2.87	52	48	8	11	25
20.5	27.70	23.43	-1.11	-1.24	-2.35	53	47	6	9	25

21.5	27.20	23.48	-0.94	-1.08	-2.02	53	47	5	7	25
22.5	26.50	23.51	-0.74	-0.87	-1.61	54	46	4	6	25
23.5	25.10	23.54	-0.44	-0.45	-0.89	51	49	3	4	25
24.5	26.60	25.3	-1.36	-0.38	-1.74	22	78	12	17	25
25.5	25.85	25.31	-0.94	-0.16	-1.10	14	86	9	13	25
26.5	25.20	25.3	-0.71	0.03	-0.68	0	100	8	12	25
27.5	24.55	25.29	-0.52	0.21	-0.31	0	100	6	8	25
28.5	23.85	25.28	-0.36	0.41	0.05	0	100	4	6	0
29.5	23.10	25.26	-0.27	0.63	0.36	0	100	3	4	0
30.5	23.35	25.24	-0.29	0.55	0.26	0	100	3	5	0
31.5	26.00	25.21	-0.98	-0.23	-1.21	19	81	9	13	25
32.5	28.50	25.18	-1.8	-0.96	-2.76	35	65	14	19	25
33.5	30.00	25.14	-2.47	-1.41	-3.88	36	64	18	26	50
34.5	32.00	25.1	-3.25	-2.00	-5.25	38	62	23	33	50
35.5	33.00	25.07	-3.63	-2.30	-5.93	39	61	26	36	50
36.5	33.50	25.07	-3.85	-2.44	-6.29	39	61	27	38	50
37.5	34.50	25.1	-4.25	-2.72	-6.97	39	61	30	42	50
38.5	35.00	25.12	-4.49	-2.86	-7.35	39	61	32	45	50
39.5	35.00	25.16	-4.59	-2.85	-7.44	38	62	33	46	50
40.5	34.50	25.2	-4.52	-2.69	-7.21	37	63	33	46	50
41.5	34.00	25.24	-4.43	-2.54	-6.97	36	64	33	46	50
42.5	33.50	25.29	-4.22	-2.38	-6.60	36	64	31	44	50
43.5	32.50	25.33	-3.74	-2.08	-5.82	36	64	28	39	50
44.5	31.40	25.38	-3.29	-1.74	-5.03	35	65	25	35	50
45.5	30.40	25.41	-2.93	-1.44	-4.37	33	67	23	32	50
46.5	29.75	25.44	-2.71	-1.25	-3.96	32	68	21	30	50

47.5	29.25	25.47	-2.53	-1.09	-3.62	30	70	20	29	50
48.5	32.45	28.07	-3.8	-1.27	-5.07	25	75	33	46	50
49.5	32.10	28.06	-3.49	-1.17	-4.66	25	75	30	43	50
50.5	31.60	28.06	-3.28	-1.02	-4.30	24	76	29	41	50
51.5	31.05	28.05	-3.07	-0.87	-3.94	22	78	28	39	50
52.5	30.60	28.05	-2.89	-0.74	-3.63	20	80	27	38	50
53.5	30.30	28.05	-2.76	-0.65	-3.41	19	81	26	36	50
54.5	31.10	28.04	-3.01	-0.89	-3.90	23	77	27	38	50
55.5	32.50	28.03	-3.55	-1.29	-4.84	27	73	30	42	50
56.5	34.00	28.01	-4.17	-1.73	-5.90	29	71	34	48	50
57.5	35.50	28	-4.82	-2.17	-6.99	31	69	38	54	50
58.5	37.00	27.98	-5.44	-2.61	-8.05	32	68	43	60	50
59.5	38.75	27.98	-5.99	-3.12	-9.11	34	66	46	64	75
60.5	39.85	27.99	-6.35	-3.43	-9.78	35	65	48	67	75
61.5	40.60	28.01	-6.7	-3.64	-10.34	35	65	50	71	75
62.5	41.20	28.05	-7.01	-3.81	-10.82	35	65	53	74	75
63.5	41.30	28.09	-7.18	-3.82	-11.00	35	65	54	76	75
64.5	41.10	28.14	-7.24	-3.75	-10.99	34	66	55	78	75
65.5	41.20	28.2	-7.32	-3.76	-11.08	34	66	56	79	75
66.5	40.70	28.26	-7.11	-3.60	-10.71	34	66	55	77	75
67.5	39.00	28.32	-6.4	-3.09	-9.49	33	67	50	70	75
68.5	37.20	28.38	-5.71	-2.55	-8.26	31	69	46	64	50
69.5	35.80	28.43	-5.21	-2.13	-7.34	29	71	43	60	50
70.5	34.60	28.48	-4.81	-1.77	-6.58	27	73	41	57	50
71.5	33.90	28.53	-4.57	-1.55	-6.12	25	75	39	56	50
72.5	33.1	30.17	-4.03	-0.85	-4.88	17	83	39	54	75

73.5	32.45	30.17	-3.63	-0.66	-4.29	15	85	36	50	50
74.5	31.65	30.17	-3.34	-0.43	-3.77	11	89	34	48	50
75.5	30.7	30.16	-3.01	-0.16	-3.17	5	95	33	47	50
76.5	29.7	30.15	-2.68	0.13	-2.55	0	100	31	44	75
77.5	28.8	30.14	-2.38	0.39	-1.99	0	100	28	39	50
78.5	29.2	30.13	-2.48	0.27	-2.21	0	100	29	40	50
79.5	31.5	30.11	-3.25	-0.40	-3.65	11	89	33	47	50
80.5	33.85	30.08	-4.12	-1.09	-5.21	21	79	38	53	75
81.5	35.85	30.05	-4.94	-1.68	-6.62	25	75	43	60	50
82.5	38	30.01	-5.75	-2.31	-8.06	29	71	47	67	50
83.5	39.4	29.98	-6.21	-2.73	-8.94	31	69	50	70	75
84.5	40.4	29.98	-6.53	-3.02	-9.55	32	68	52	73	75
85.5	41.5	30	-6.95	-3.33	-10.28	32	68	54	77	75
86.5	42.05	30.04	-7.22	-3.48	-10.70	32	68	56	79	75
87.5	42.05	30.08	-7.34	-3.46	-10.80	32	68	58	81	75
88.5	42	30.13	-7.46	-3.44	-10.90	32	68	59	83	75
89.5	41.7	30.18	-7.43	-3.33	-10.76	31	69	59	84	75
90.5	40.2	30.24	-6.92	-2.88	-9.80	29	71	57	80	75
91.5	38	30.3	-6.04	-2.23	-8.27	27	73	51	72	50
92.5	36.5	30.36	-5.43	-1.78	-7.21	25	75	47	67	75
93.5	35.5	30.41	-5.04	-1.47	-6.51	23	77	45	64	75
94.5	34.5	30.45	-4.73	-1.17	-5.90	20	80	44	62	75
95.5	33.5	30.49	-4.38	-0.87	-5.25	17	83	42	60	75
96.5	34.4	32.84	-4.06	-0.45	-4.51	0	100	47	66	75
97.5	33.2	32.83	-4.64	-0.11	-4.75	0	100	54	76	75
98.5	32	32.82	-4.08	0.24	-3.84	0	100	47	67	75

99.5	31.1	32.8	-3.65	0.49	-3.16	0	100	42	60	75
100.5	30.45	32.77	-3.34	0.67	-2.67	0	100	39	54	75
101.5	29.8	32.73	-3.09	0.85	-2.24	0	100	36	50	75
102.5	30.95	32.69	-2.85	0.50	-2.35	0	100	33	46	75
103.5	33.85	32.65	-3.19	-0.35	-3.54	0	100	37	52	75
104.5	36.75	32.6	-4.11	-1.20	-5.31	23	77	37	52	75
105.5	38.6	32.55	-5.15	-1.75	-6.90	25	75	44	63	75
106.5	40	32.49	-5.96	-2.17	-8.13	27	73	51	71	100
107.5	42	32.44	-6.59	-2.77	-9.36	30	70	54	76	75
108.5	43.5	32.43	-7.25	-3.20	-10.45	31	69	58	82	100
109.5	44.5	32.44	-7.74	-3.49	-11.23	31	69	62	87	100
110.5	45.5	32.48	-8.15	-3.77	-11.92	32	68	65	91	100
111.5	45.5	32.52	-8.53	-3.76	-12.29	31	69	69	97	100
112.5	**44.5**	**32.56**	**-8.64**	**-3.46**	**-12.10**	**29**	**71**	**71**	**101**	**100**
113.5	43.5	32.6	-8.43	-3.15	-11.58	27	73	71	100	100
114.5	42.4	32.64	-8.2	-2.82	-11.02	26	74	71	99	100
115.5	41.2	32.69	-7.81	-2.46	-10.27	24	76	69	97	100
116.5	40	32.73	-7.25	-2.10	-9.35	22	78	65	92	100
117.5	38.75	32.77	-6.72	-1.73	-8.45	20	80	62	87	100
118.5	37.45	32.81	-6.27	-1.34	-7.61	18	82	60	84	75
119.5	36.15	32.83	-5.86	-0.96	-6.82	14	86	58	82	75
120.5	31.45	33.52	-5.43	0.60	-4.83	0	100	63	89	75
121.5	30	33.52	-3.06	1.02	-2.04	0	100	35	50	75
122.5	28.75	33.51	-2.63	1.38	-1.25	0	100	30	43	50
123.5	27.7	33.49	-2.26	1.68	-0.58	0	100	26	37	50
124.5	26.85	33.46	-1.95	1.91	-0.04	0	100	23	32	50

125.5	26.1	33.43	-1.67	2.12	0.45	0	100	19	27	50
126.5	26.85	33.39	-1.86	1.89	0.03	0	100	22	30	50
127.5	29.15	33.34	-2.59	1.21	-1.38	0	100	30	42	50
128.5	31.45	33.28	-3.43	0.53	-2.90	0	100	40	56	75
129.5	33.3	33.23	-4.27	-0.02	-4.29	0	100	49	69	75
130.5	35	33.17	-5.04	-0.53	-5.57	10	90	53	74	75
131.5	36.9	33.12	-5.72	-1.09	-6.81	16	84	56	78	75
132.5	37.9	33.11	-6.07	-1.39	-7.46	19	81	57	81	75
133.5	38.5	33.11	-6.35	-1.56	-7.91	20	80	59	83	75
134.5	39.5	33.12	-6.7	-1.85	-8.55	22	78	61	86	100
135.5	40	33.13	-6.91	-1.99	-8.90	22	78	62	87	100
136.5	40	33.17	-6.94	-1.98	-8.92	22	78	63	88	100
137.5	39.75	33.2	-6.86	-1.90	-8.76	22	78	62	88	100
138.5	38.25	33.23	-6.35	-1.45	-7.80	19	81	60	84	75
139.5	36	33.27	-5.51	-0.79	-6.30	13	87	56	79	75
140.5	34.2	33.32	-4.81	-0.25	-5.06	5	95	53	74	75
141.5	32.7	33.35	-4.27	0.19	-4.08	0	100	49	70	75
142.5	31.5	33.39	-3.87	0.55	-3.32	0	100	45	63	75
143.5	30.5	33.41	-3.52	0.84	-2.68	0	100	41	57	75
144.5	28.65	32.82	-2.46	1.21	-1.25	0	100	28	40	50
145.5	27.75	32.81	-1.97	1.46	-0.51	0	100	23	32	50
146.5	26.95	32.81	-1.68	1.70	0.02	0	100	19	27	50
147.5	26.3	32.79	-1.44	1.88	0.44	0	100	17	23	50
148.5	25.7	32.77	-1.22	2.05	0.83	0	100	14	20	25
149.5	25	32.74	-0.97	2.24	1.27	0	100	11	16	25
150.5	24.8	32.7	-0.88	2.29	1.41	0	100	10	14	25

151.5	26	32.67	-1.27	1.93	0.66	0	100	15	21	25
152.5	28.75	32.63	-2.25	1.12	-1.13	0	100	26	37	50
153.5	31.25	32.59	-3.32	0.39	-2.93	0	100	38	54	50
154.5	32.5	32.54	-4.01	0.01	-4.00	0	100	47	66	75
155.5	33.5	32.5	-4.44	-0.29	-4.73	6	94	48	68	75
156.5	34.5	32.47	-4.83	-0.59	-5.42	11	89	50	70	75
157.5	35	32.47	-5.11	-0.73	-5.84	13	87	52	73	75
158.5	35.25	32.49	-5.27	-0.80	-6.07	13	87	53	75	75
159.5	35.25	32.51	-5.28	-0.79	-6.07	13	87	53	75	75
160.5	34.75	32.53	-5.06	-0.64	-5.70	11	89	52	73	75
161.5	34.25	32.55	-4.77	-0.49	-5.26	9	91	50	70	75
162.5	33	32.58	-4.25	-0.12	-4.37	3	97	48	67	75
163.5	31.5	32.61	-3.65	0.32	-3.33	0	100	42	60	75
164.5	29.9	32.63	-3.1	0.79	-2.31	0	100	36	51	75
165.5	28.4	32.65	-2.57	1.23	-1.34	0	100	30	42	50
166.5	27.65	32.66	-2.3	1.45	-0.85	0	100	27	37	50
167.5	26.95	32.66	-2.05	1.65	-0.40	0	100	24	33	50
									Successful time-steps	161
									Total time-steps	168
									Cooling load match rate (%)	96

Cooling inside the building was not required when the ambient air temperature was below 24.1°C; this is calculated using relation 4.10 and clearly supported in Figure 4.15 and Figure 4.19 where 0% A/C is used; but if the ambient air temperature is higher than 24.1°C then the control routine examines if it is less than or equal to 26.2°C (relation 4.11). If yes, the controller then determines if the culvert cooling contribution is larger than 75% and, if yes, 0% A/C is employed (Figure 4.15); if no, then 1 A/C unit is despatched (Figure 4.17).

$$T_{amb\_set-point\_1} = (T_{lag} + T_{ama})/2 \qquad 4.10$$

$$T_{amb\_set-point\_2} = T_{ama} \qquad 4.11$$

$$T_{amb\_set-point\_4} = T_{hag} \qquad 4.12$$

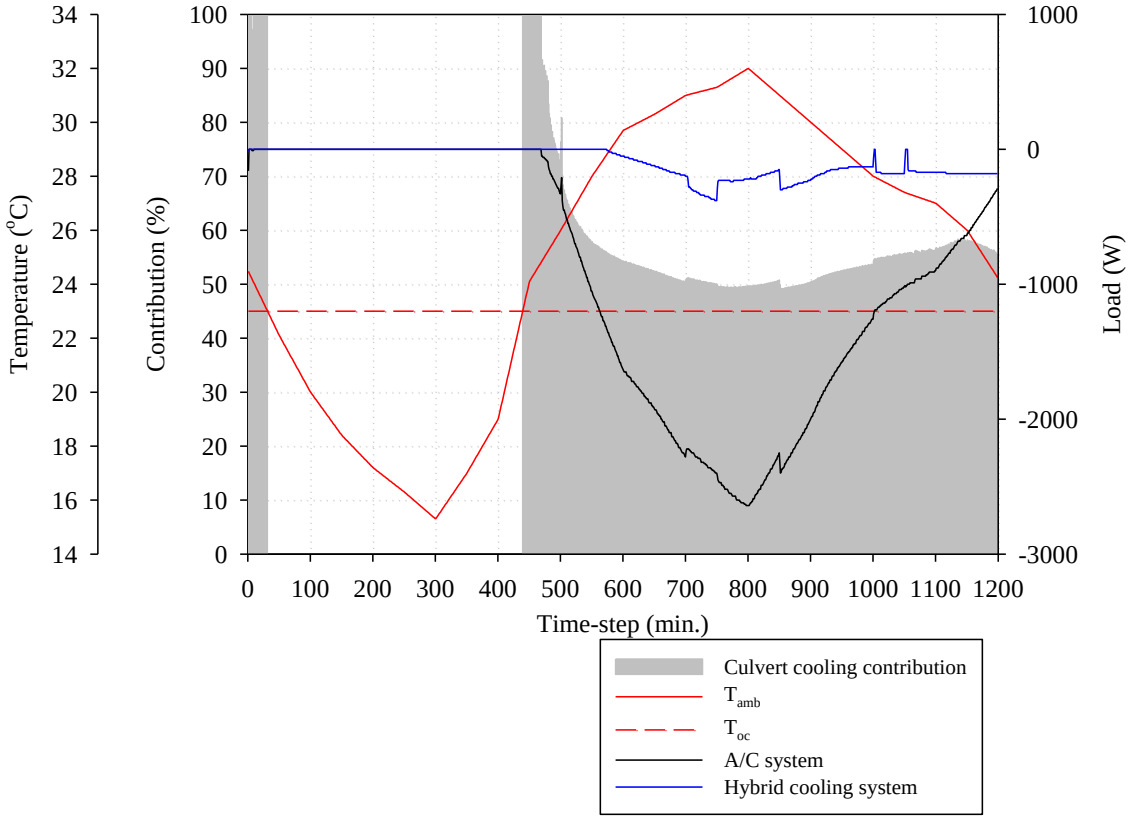

Figure 4.15: Sample of 0% and 25% multi-chiller selection rationale.

However, if the ambient air temperature is higher than 26.2°C then the controller checks whether the ambient air temperature is less than or equal to 29.3°C, a value determined from relation 4.13. If the answer is yes then the controller

determines if the culvert's cooling contribution is greater than 0% and if so then 25% A/C is used (Figure 4.15), but if there is no culvert cooling contribution then 50% A/C is required (Figure 4.16 and Figure 4.18). Now, if the ambient temperature is higher than 29.3°C, the controller examines if it is less than or equal to 32.5°C (relation 4.12). If yes, is the culvert cooling contribution higher than 50% then 25% A/C is used (Figure 4.15 and Figure 4.17) but if the contribution is between 0% and 50% then 50% A/C is used (Figure 4.18 and Figure 4.19), but if the contribution is 0% then 75% A/C is used (Figure 4.16). The multi-chiller control strategy displayed in Figure 4.20 is readily traceable and so only the conditions are explained, not the actions as depicted on the related flow charts. Thereafter, if the ambient air temperature is higher than 32.5°C, the multi-chiller control strategy establishes if the ambient air temperature is less than or equal to 34°C; a value determined from relation 4.14. If yes, then when the culvert cooling contribution is higher than 25% only 50% A/C is used (Figure 4.17 and Figure 4.18) but if the contribution is between 0% and 25% then 75% A/C is used (Figure 4.16, Figure 4.18, and Figure 4.19), but if the contribution is 0% then 100% A/C is used (Figure 4.16). Finally, if the ambient air temperature is higher than 34°C, the control establishes whether it is less than or equal to 38.8°C; a value determined from relation 4.15. Relations 3.13, 4.10, 4.11, 4.12, 4.13, 4.14 and 4.15 were not mathematically modelled but were modified and put in context based on simulated results that were validated for different climates as will be seen in chapter 5. If the ambient air temperature is less than 38.8°C and the culvert cooling contribution is higher than 25% then 3 A/C units operate (Figure 4.18) but if not then 4 A/C units operate (Figure 4.16 and Figure 4.18). However, if the ambient temperature is higher than 38.8°C and the culvert cooling contribution greater than 50% then 75% A/C is used while when contribution is lower than or equal to 50%, 100% A/C is used (Figure 4.18).

$$T_{\text{amb\_set-point\_3}} = \left(\frac{T_{\text{hag}} + T_{ama}}{2}\right) \quad 4.13$$

$$T_{\text{amb\_set-point\_5}} = T_{\text{hag}} + \left(\frac{T_{\text{hag}} - T_{ama}}{4}\right) \quad 4.14$$

$$T_{\text{amb\_set-point\_6}} = \left(2T_{\text{hag}} - T_{ama}\right) \quad 4.15$$

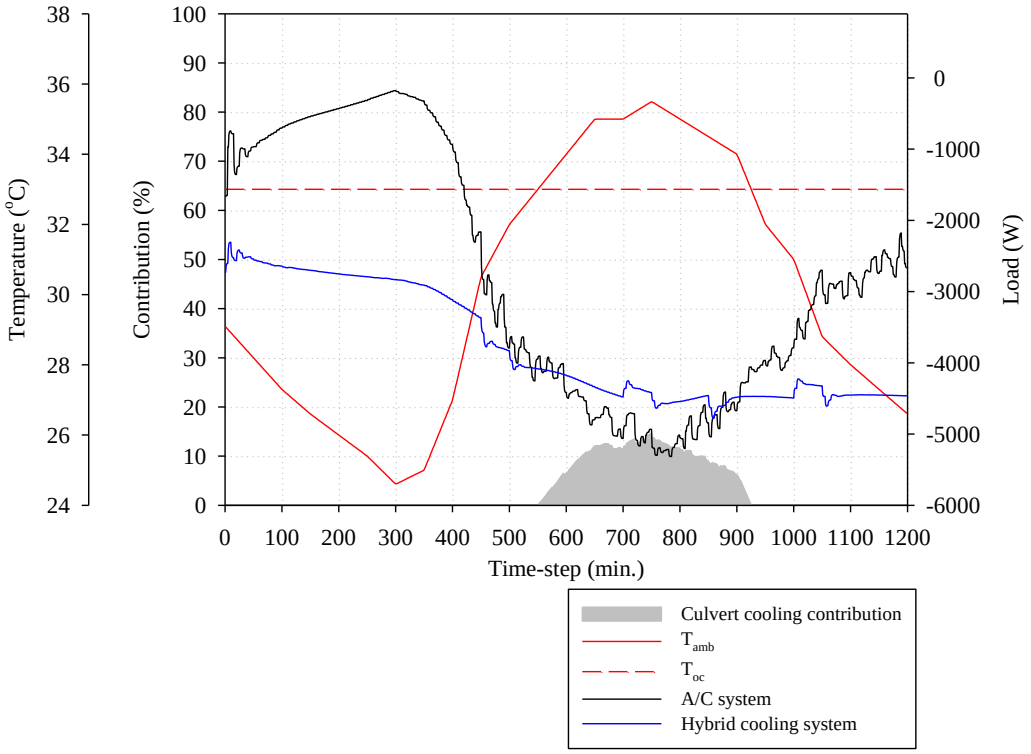

Figure 4.16: Illustration of 50%, 75% and 100% multi-chiller.

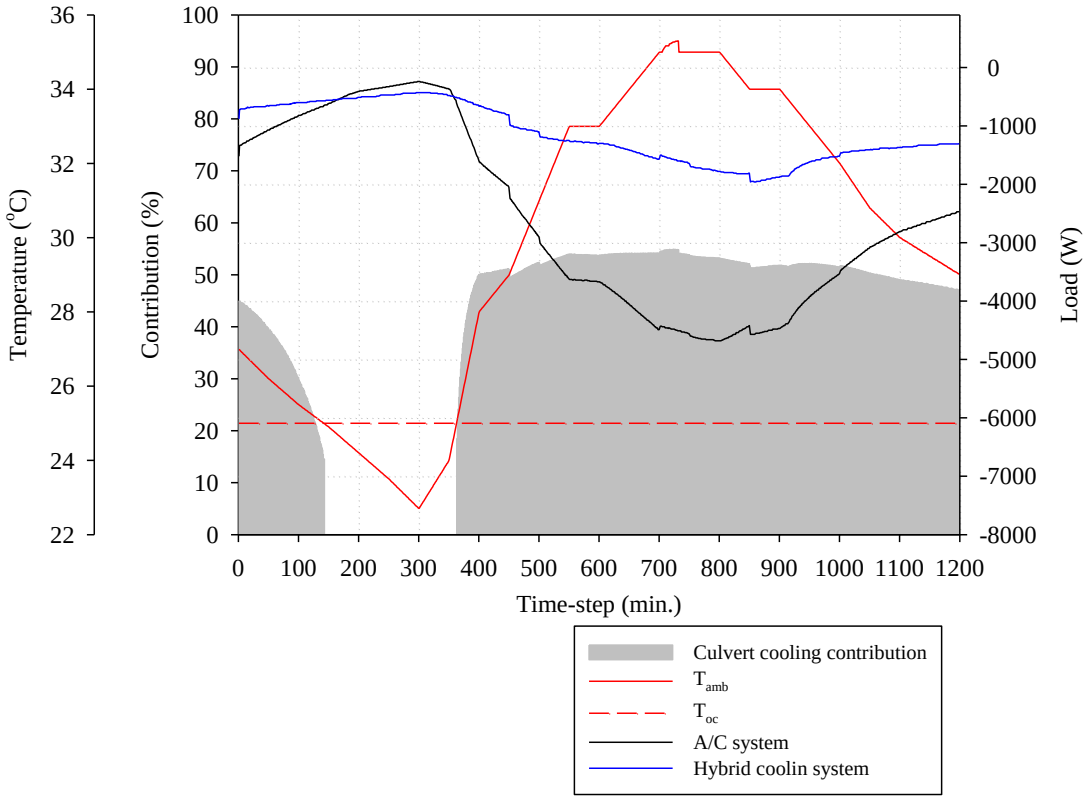

Figure 4.17: Example of 25% and 50% multi-chiller.

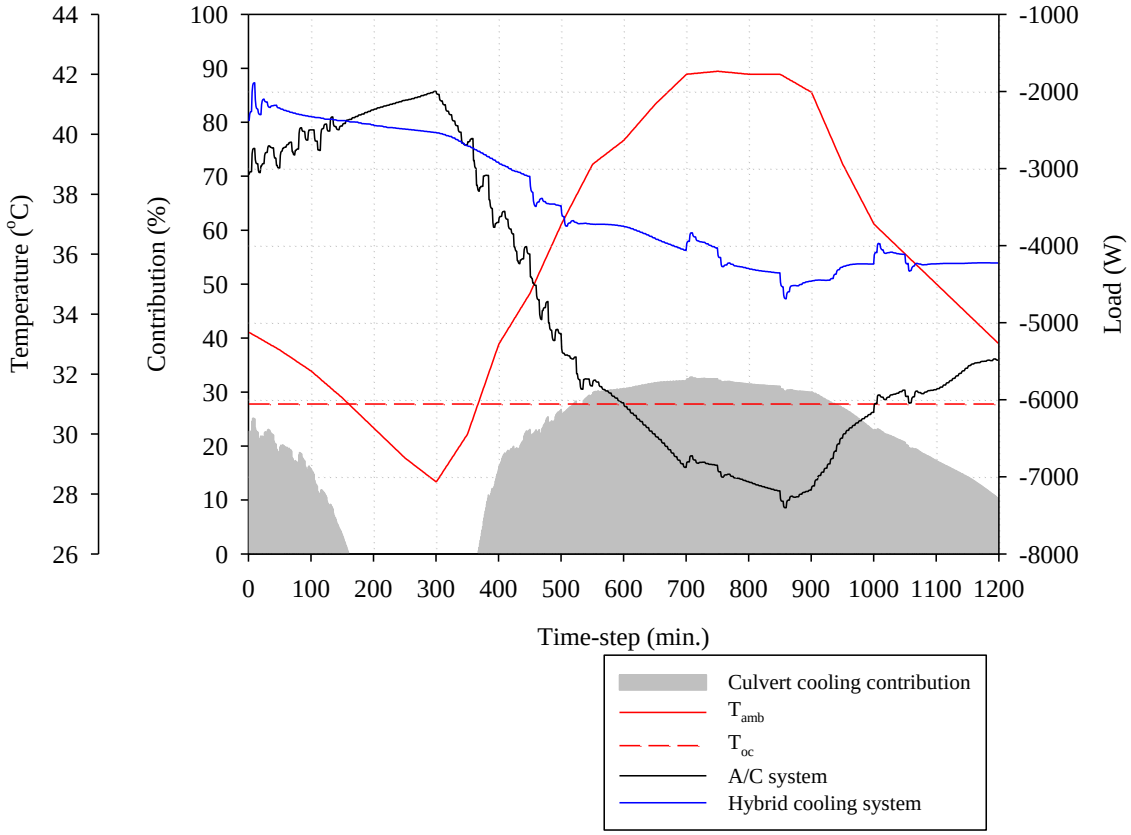

Figure 4.18: Representation of 50%, 75% and 100% multi-chiller.

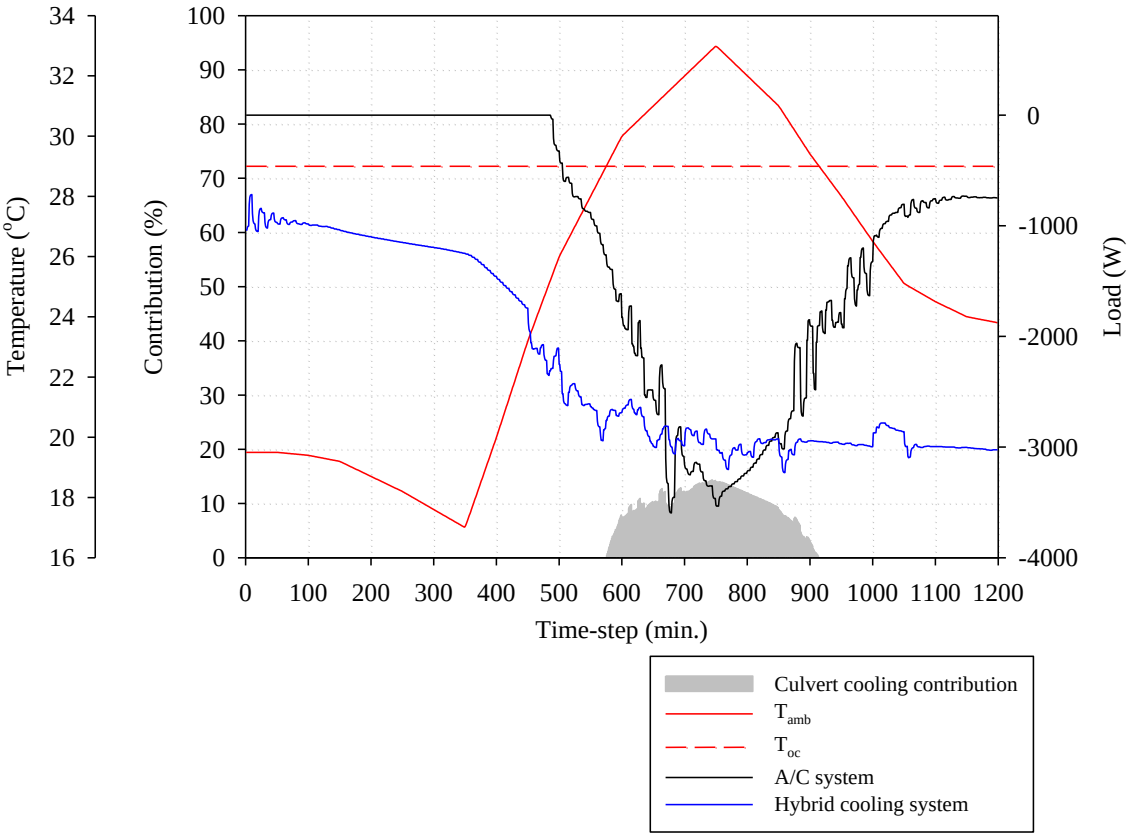

Figure 4.19: The 0%, 50% and 75% multi-chiller justification.

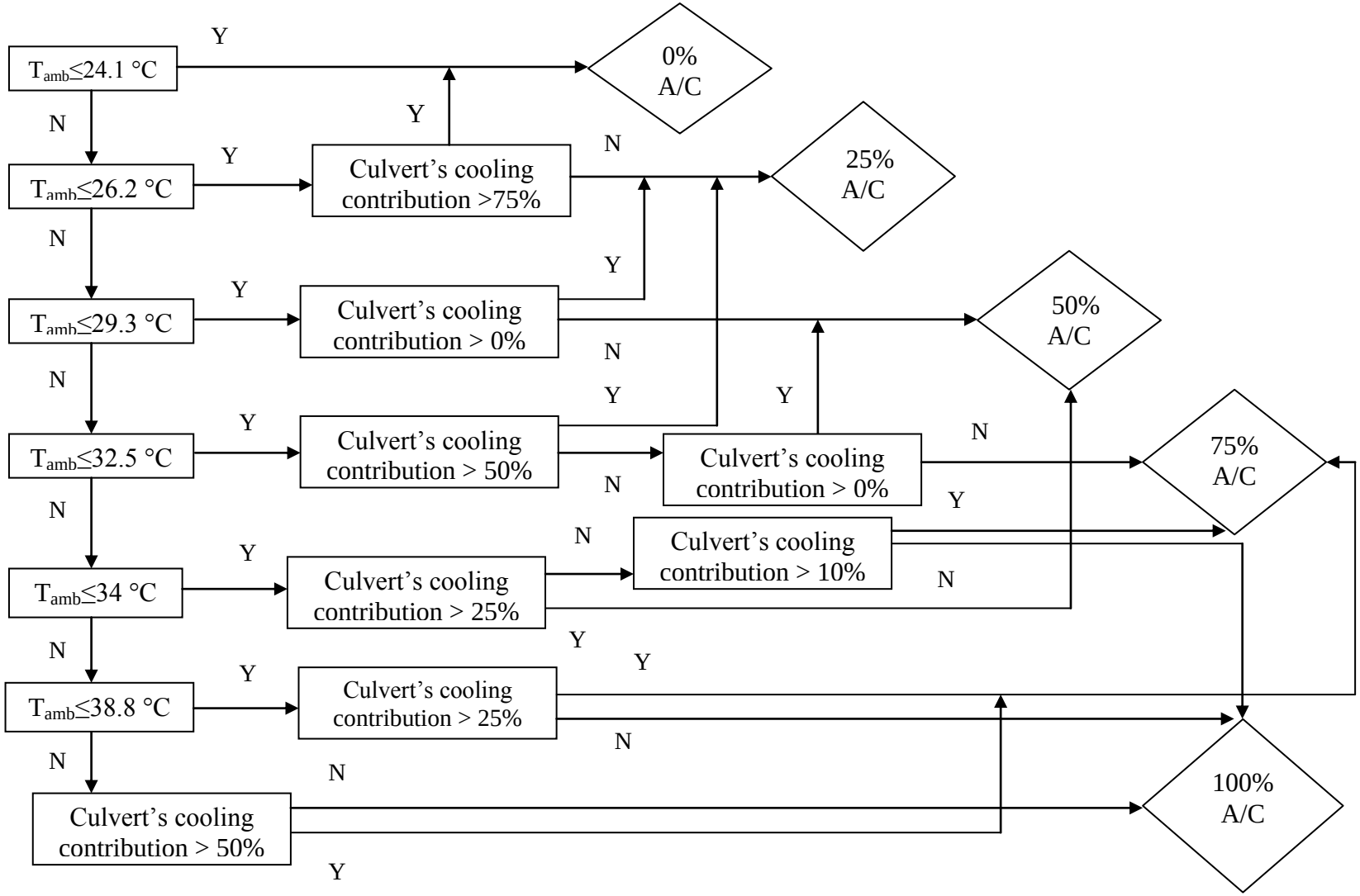

Figure 4.20: Multi-chiller control strategy for a hot/dry climate.

This concludes the multi-chiller control strategy used in the hybrid cooling system controller that is suitable only for a hot/dry climate because the ambient set-point temperatures, above which certain modularized A/C cooling load is engaged, are different than those used for hot/humid climate for example. Now, going back to the main control strategy for the hybrid cooling system in hot climate (Figure 4.10), if the indoor temperature is below 27°C then the control routine checks to ascertain if the temperature is higher than 20°C, which is the minimum comfortable temperature as listed by ANSI/ASHRAE Standard 55 (2004). If the answer is no, sub-control strategy 2 is invoked, if yes, then a test is applied to determine whether the indoor dry-bulb temperature is greater than some optimum value, here chosen as 25°C corresponding to a PPD of less than 10% as indicated in Table 4.6. This indoor dry-bulb temperature (25°C) results in a resultant temperature being in the range (24.5-25.5°C); Al-Ajmi & Loveday (2010) concluded in a study about occupant's thermal comfort during Summer in Kuwait that the indoor optimum comfort resultant temperature would be 25.2°C based on Actual Mean Vote. So, if the answer is yes, sub-control strategy 3 is invoked; if not then the ambient air temperature is examined to determine if it is less than the indoor air temperature. If not, the building zone is allowed to free float, if yes, the controller checks if the ambient air is less than 16°C; a value chosen as it corresponds to the temperature of the A/C chiller supply air at which no mechanical refrigeration is required. Free cooling is engaged when the answer is positive while, if negative, the controller tests if the ambient air temperature is less than 25°C and, if yes, activates natural ventilation, else allows the building to free float. To explain how the free cooling and natural ventilation cases may be interchanged consider Table 4.9 which shows that free cooling is efficient at the times when the ambient air temperature is below 16°C with the indoor air temperature being around the optimum comfort level of 25°C. When natural ventilation is utilized, the indoor temperature follows the ambient air temperature, which leads to low indoor air temperatures in the morning. However, when both free cooling and natural ventilation are controlled, the indoor air temperature in the morning is above the minimum comfort threshold of 20°C thus benefiting from free cooling. From noon until midnight the temperatures are similar to those when natural ventilation is used alone throughout the day without control. Both free cooling and

natural ventilation are emulated in the hybrid cooling system model supplemented in Appendix B. Free cooling was simulated as a free floating mode but at ambient temperature from 10-16°C. Natural ventilation was simulated by constructing an air flow network such that windows open when ambient temperature is higher than 16°C and lower than 25°C.

Table 4.9: Effect of free cooling (FC) and natural ventilation (NV) on living room air temperature on a Spring day.

Time	T_{amb} (°C)	T(°C)_FC	T(°C)_ NV	T(°C)_ Control FC & NV
01h30	18.85	26.33	21.79	23.29
03h30	15.50	25.80	21.67	22.56
05h30	14.90	25.46	19.24	21.18
07h30	15.50	25.45	19.28	23.57
09h30	16.50	25.94	19.9	22.09
11h30	20.20	27.36	23.17	25.01
13h30	23.50	27.56	24.28	24.75
15h30	25.80	27.35	24.35	24.68
17h30	25.40	27.96	24.98	25.3
19h30	23.50	28.08	24.01	24.31
21h30	21.50	27.47	22.91	23.17

The sub-control strategies 2 and 3 are now detailed.

- **Sub-Control Strategy-2:**

As shown in Figure 4.10 activation occurs when the indoor air temperature is less than 20°C (Winter season). The control routine, as depicted in Figure 4.21, checks if the ambient air temperature is less than 15°C (a value justified on the same basis as the 30°C selection for sub-control strategy 1 but here on the basis of annual heating energy and peak heating power. Table 4.10 shows that the impact of the air culvert on both the annual heating energy consumption and the peak heating power is large regardless of culvert air flow controlled status. When the sensed ambient temperature is 5°C below that at which the culvert fan operates at 50% capacity, the heating energy and peak power profiles are identical to those generated when there is no air flow control. When the sensed ambient temperature increases to 20°C (Table 4.10), the reduction in the annual heating energy and peak heating power is 89.5% to 97.2% and 96.9% to 100% respectively. Yet, if 20°C is selected then the period when full air ventilation is possible is reduced, whereas at 15°C with the period where full

air ventilation is possible increases so that only 0.8% of the annual heating energy consumption reduction is lost.

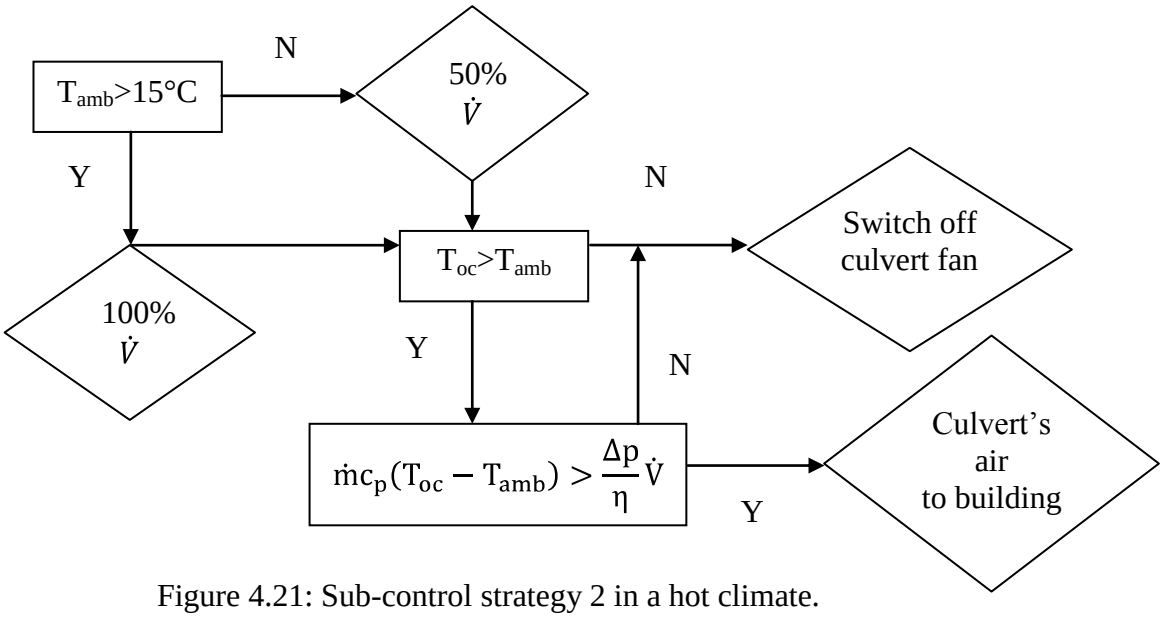

Figure 4.21: Sub-control strategy 2 in a hot climate.

Table 4.10: Culvert flow control effect on Villa annual heating energy and peak heating power from December 1 to March 1 at an indoor air temperature of 20°C.

Heating system /Parameter	Heating energy consumption (kWh/m^2/a)	Peak heating power consumption (W/m^2)	Reduction compared to heat pump system (%)	
			Energy	Peak power
Heat pump system	21.3	34.9	0	0
Heat pump + air-culvert (No flow control)	2.25	1.08	89.4	96.9
Heat pump + air-culvert (sensed $T_{amb.}$ < 5 °C)	2.23	1.08	89.5	96.9
Heat pump + air-culvert (sensed $T_{amb.}$< 10 °C)	1.39	0	93.5	100
Heat pump + air-culvert (sensed $T_{amb.}$ < 15 °C)	0.77	0	96.4	100
Heat pump + air-culvert (sensed $T_{amb.}$ < 20 °C)	0.6	0	97.2	100

It is important to mention that the selection of the sensed ambient temperature for the culvert fan air flow control in winter in a hot climate is less important than that in summer since the full culvert fan capacity is able to provide almost all the heating required. This situation is reversed in a cold climate where low ambient air temperatures throughout much of the year are the norm. What matters during high ambient air temperatures in a hot climate is to reduce the cooling energy

consumption and peak cooling power at the expense of reducing air ventilation requirements but to some acceptable threshold; this threshold already has been discussed early on in section 4.3. With low ambient air temperatures in a hot climate, the priority is to provide air ventilation requirements before attempting to reduce heating energy consumption and peak heating power, which are likely to be low anyway. During high ambient air temperatures in a cold climate, the priority is for air ventilation followed by cooling energy consumption and peak cooling power reductions, whereas during low ambient air temperatures, heating energy consumption and peak heating power reductions should be prioritised before air ventilation needs are met. Hence, the control strategy then examines if the ambient air temperature is higher than 15°C; if yes then the fan operates at 100% capacity but, if not, it operates at 50% capacity. The next check determines if the culvert outlet air temperature is larger than the ambient air temperature. If no then the air supply is switched from culvert to ambient; if yes then the control algorithm determines if the culvert heating power capacity is larger than the culvert fan power capacity. If no then the culvert air is again by-passed to ambient; if yes then culvert air is supplied directly to the building.

- **Sub-Control Strategy-3:**

This control strategy (Figure 4.22) is applicable in the transitional seasons when the indoor air temperature is between 25°C and 27°C as shown in Figure 4.10. The control routine checks if the ambient air temperature is higher than the indoor air temperature. If the answer is yes then a check is performed to establish how much air flow will be allowed, 50% or 100% (based on whether the ambient air temperature is higher than 30°C). If the culvert outlet air temperature is less than the ambient air temperature then the algorithm examines the cooling power against the fan power: if the former is greater than the culvert air is supplied to the building; if not then culvert fan is switched off. When the ambient air temperature is lower than the indoor air temperature then the fan is operated at 100% and the control strategy then examines the culvert outlet air temperature to establish if it is less than the ambient air temperature. If not, culvert fan is switched off but if yes then a test is made to determine whether the cooling power is higher than the fan power. If yes then the culvert supplies the building zone, but if not, culvert fan is switched off. This

concludes the control strategy for the hybrid cooling system for buildings in a hot/dry climate. The next chapter deals with the implementation of the control strategy and its generalization to accommodate any climate.

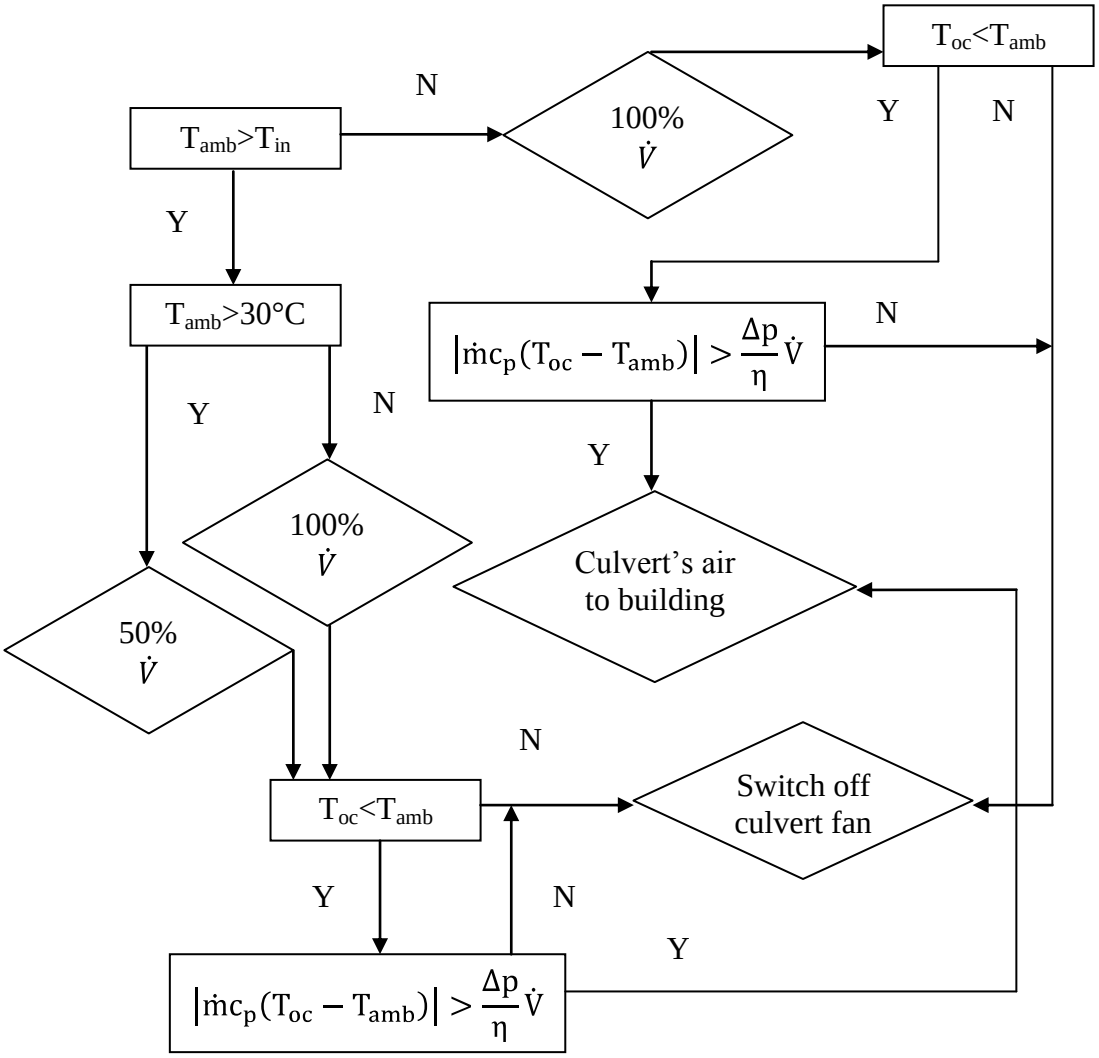

Figure 4.22: Sub-control strategy 3 in a hot climate.

4.4 Concluding Remarks

This chapter discussed the following points.

- Implementation of the single-zone CAV all-air A/C system in ESP-r.
- Coupling between the 3 building thermal sub-systems; Villa, Culvert and A/C plant using ESP-r.
- The extraction of the control strategy for the hybrid cooling system where multi-chiller control is playing a major part in it but only for hot/dry climate.

Chapter 5 : General Control Strategy for Air-culvert Air-conditioning Hybrid Cooling System

This chapter presents the control strategy simulated in ESP-r for hot/dry climate. The regional control algorithm laid out in chapter 4 for a hot/dry climate is generalised for all climates. The robustness of this generalised control strategy is examined after applying it on moderate, cool, and hot/humid climates.

5.1 Implementation of the Control Strategy in ESP-r

The objective of this thesis is to develop a control strategy for the hybrid cooling system. This strategy was devised by simulating the system performance under different weather conditions while systematically varying principal operating parameters. As discussed in chapter 4, sensible cooling represents the major component of the total A/C cooling load in a hot/dry climate while a culvert provides mostly sensible cooling. In such climate, culvert can rarely provide latent cooling because this requires culvert air dew point temperature to reach that at saturation**.** The difference in humidity ratios between culvert air flow and culvert superficial layer is usually negative and condensation does not occur (Hollmuller & Lachal 2005) and accordingly the culvert can only provide sensible cooling whereas in hot/humid climate some latent cooling can be provided but on the expense of lowering sensible cooling capacity. Since the A/C system and culvert cooling loads in hot/dry climate are mainly sensible, the control strategy therefore is implemented in ESP-r using an idealised indoor set-point temperature scheme (basic On/Off control) instead of the CAV A/C system as employed: this reduction in complexity facilitated the combinatorial quantification of the energy consumption for different design variants and control set-ups. The basic On/Off control tackles the major component of the AHU total cooling coil load - the space sensible cooling load; however, it does not quantify the cooling loads of A/C fan and duct air leakage which are usually far less than the space sensible cooling load. It can accurately quantify the space sensible cooling load required to offset the space heat load. It is

shown in Figure 5.1 how the space sensible cooling load is represented in ESP-r just as it occurs dynamically in real A/C systems considering heat storage in the building's thermal mass. So, the idealised indoor set-point temperature scheme can represent the A/C system in a hot/dry climate to a better degree. Table 5.1 lists the basic control parameters with maximum (3kW) and minimum (0kW) heating capacity, maximum (6kW) and minimum (0kW) cooling capacity, as activated when the heating and cooling indoor temperature set-points are 20°C and 27°C respectively.

Table 5.1: Optimized control of indoor air temperature set-points.

Sensor	Actuator	Control Law	Data
T_{db} in each room.	Flux applied to each zone's air point.	Basic controller for heating/cooling.	(3000 0 6000 0 20 27)

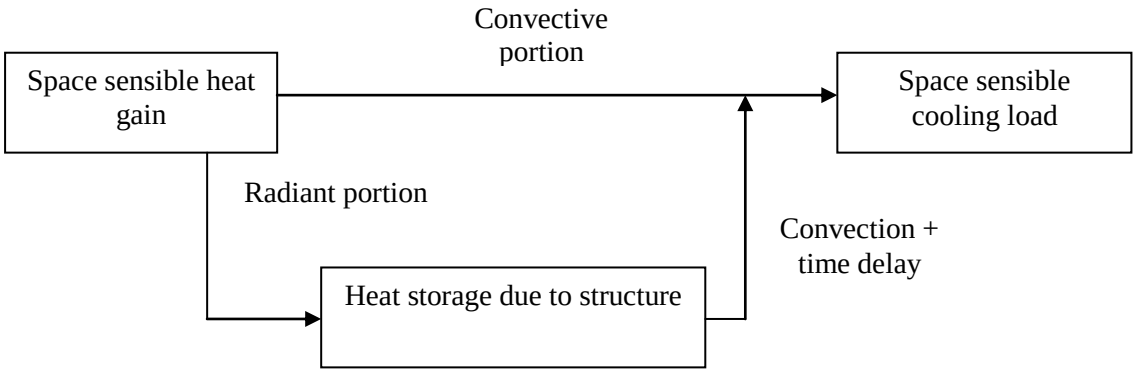

Figure 5.1: Space sensible cooling load constituents.

This basic control operates as the active cooling system that activates when the Villa indoor air temperature exceeds 27°C. Now, the culvert is coupled to the 3 zone Villa for the hybrid cooling system to complete. Table 3.26 indicates that the time required (annually) for active cooling is reduced drastically when the following measures are applied: shading (Villa), natural ventilation (Villa), acclimatization (people), fan flow rate control (Culvert) and earth treatment (Culvert). The Villa shading was controlled on a seasonal basis – applied the cooling seasons (Spring, Summer and Autumn) and retracted during the heating season (Winter). Chapter 4 discussed the indoor and outdoor operating conditions, under which the windows are

opened or closed, as well as Culvert flow rate control. Modularizing the A/C system has no effect on the culvert cooling potential or thermal effectiveness but was pursued only to capitalize on savings due to the elimination of A/C system short cycling. As a result, multi-chiller control was not included in the ESP-r control strategy model. Instead, space sensible cooling loads were compared to the peak space sensible cooling load to establish how many active sensible cooling units are required. The control strategy was applied to a model with 3 constituent parts:

1. 3-room Villa.
2. Air culvert.
3. A/C system (with optimized temperature set-point control).

Appendix B includes the control strategy of the hybrid sensible cooling system as constructed in ESP-r. While the strategy in chapter 4 has many if statements, these are implemented in the ESP-r model based on their approximate time of occurrence. For example, when the ambient air temperature in the morning during the cooling season is less than the culvert outlet air temperature, say from 03:00 until 07:00, the culvert fan is switched off. Thus, the control strategy was divided into 3 control loops as listed in Appendix B where each loop is divided into day types. Each day type is valid for a period of time after which another day type takes over and so on until the entire year is covered.

An example of how the control strategy built in Appendix B is given here for clarification purposes. Box 1 shows the actuation of 6kW cooling capacity when the dry-bulb temperature in the living room control loop exceeds 27°C during the day type specified. Box 2 shows the free cooling mechanism that happens when the living room is running on free floating mode and the ambient temperature is below 16°C which occurs for sometime during the specified day type. As explained above, different day types are specified as stated in Appendix B for the 3 control loos; 1 for each Villa zone. Before free cooling commences natural ventilation should have been exercised first as shown in box 3. That box illustrates that ambient temperatures are sensed and if above 16°C and below 25°C window in a living room on the north side opens by actuating the air flow rate percentage. Windows on all sides open when these conditions are met as prescribed in Appendix B.

Day type 3 is valid Sat-16-Apr to Sat-15-Oct, 1988 with 1 period.
Per|Start|Sensing |Actuating | Control law | Data
1 0.00 db temp > flux basic control 0.0 0.0 6000.0 0.0 0.0 27.0 0.0
Basic control: max heating capacity 0.0W min heating capacity 0.0W max cooling capacity 6000.0W min cooling capacity 0.0W. Heating set point 0.00C cooling set point 27.00C.

Day type 4 is valid Sun-16-Oct to Thu-01-Dec, 1988 with 1 period.
Per|Start|Sensing |Actuating | Control law | Data
1 0.00 db temp > flux free floating

The sensor for function 1 senses ambient dry bulb temperature.
The actuator for function 1 is flow connection: 13 north - Living-room via Grill.
There have been 1 day types defined.
Day type 1 is valid Fri-01-Jan to Sat-31-Dec, 1988 with 1 period.
Per|Start|Sensing |Actuating | Control law | Data
1 0.00 outside ambient > flo low/default/mid/hi 16.0 21.0 25.0 0.0 1.0 0.0
Range set points: low 16.00 mid 21.00 high 25.00 actuation ranges: low (< low sp) 0.00 mid (>mid sp) 1.00 high (>high sp) 0.00.

The switch on/off of culvert fan both in terms of time and flow percentage is listed briefly in the box 4. For example, every Villa zone is given a control function that senses ambient temperature and actuates the connection between the Villa zone and an external point via a fan. Day type periods were divided based on generally when the ambient temperature is lower than the culvert outlet air and thus the culvert fan is switched off; this time was approximately estimated by looking at when often this intersection between the two temperatures occurs. In case where ambient temperature is sensed to be higher than culvert outlet temperature the culvert fan flow rate is actuated varying percentages as prescribed.

The sensor for function 7 senses ambient dry bulb temperature.
The actuator for function 7 is flow connection: 10 Living-room - External_pt via Fan. There have been 9 day types defined.

Day type 1 is valid Fri-01-Jan to Tue-01-Mar, 1988 with 1 period.
Per|Start|Sensing |Actuating | Control law | Data
1 0.00 outside ambient > flo low/default/mid/hi 15.0 22.0 30.0 0.5 1.0 0.5
Range set points: low 15.00 mid 22.00 high 30.00 actuation ranges: low (< low sp) 0.50 mid (>mid sp) 1.00 high (>high sp) 0.50.

Day type 2 is valid Wed-02-Mar to Fri-01-Apr, 1988 with 2 periods.
Per|Start|Sensing |Actuating | Control law | Data
1 0.00 outside ambient > flo on / off 0.0 1.0 0.0
On/off set point 0.00 direct action ON fraction 0.000.
2 9.00 outside ambient > flo low/default/mid/hi 15.0 22.0 30.0 0.5 1.0 0.5
Range set points: low 15.00 mid 22.00 high 30.00 actuation ranges: low (< low sp) 0.50 mid (>mid sp) 1.00 high (>high sp) 0.50.

Day type 3 is valid Sat-02-Apr to Sun-01-May, 1988 with 3 periods.
Per|Start|Sensing |Actuating | Control law | Data
1 0.00 outside ambient > flo low/default/mid/hi 15.0 22.0 30.0 0.5 1.0 0.5
Range set points: low 15.00 mid 22.00 high 30.00 actuation ranges: low (< low sp) 0.50 mid (>mid sp) 1.00 high (>high sp) 0.50.
2 2.00 outside ambient > flo on / off 0.0 1.0 0.0
on/off set point 0.00 direct action ON fraction 0.000.
3 6.00 outside ambient > flo low/default/mid/hi 15.0 22.0 30.0 0.5 1.0 0.5
Range set points: low 15.00 mid 22.00 high 30.00 actuation ranges: low (< low sp) 0.50 mid (>mid sp) 1.00 high (>high sp) 0.50.

Day type 4 is valid Mon-02-May to Fri-01-Jul, 1988 with 1 period.
Per|Start|Sensing |Actuating | Control law | Data
1 0.00 outside ambient > flo low/default/mid/hi 15.0 22.0 30.0 0.5 1.0 0.5
Range set points: low 15.00 mid 22.00 high 30.00 actuation ranges: low (< low sp) 0.50 mid (>mid sp) 1.00 high (>high sp) 0.50.

5.1.1 Hot/dry Climate

Figure 5.2 displays the annual cooling energy consumption and peak cooling load savings corresponding to different control approaches exploited in a hot/dry climate. The air culvert with no window shading or control applied was able to reduce the annual cooling energy and peak cooling load by 21% and 42% respectively compared with the case when the culvert was not coupled. When culvert air flow control was imposed, the annual cooling energy consumption reduction

almost doubled while the reduction in the peak cooling load surpassed 55%. The control strategy enabled a reduction in annual cooling energy consumption in excess of 50%, that is, about 46% greater than when flow control is used alone and 143% greater than when there is no flow control at all. The control strategy did not add a lot to the peak cooling load reduction compared to the flow control case since natural ventilation and free cooling do not apply there. Shading as a building efficiency measure resulted in a 5% reduction in both the cooling energy and peak cooling load compared to those resulting when only the control strategy operated alone.

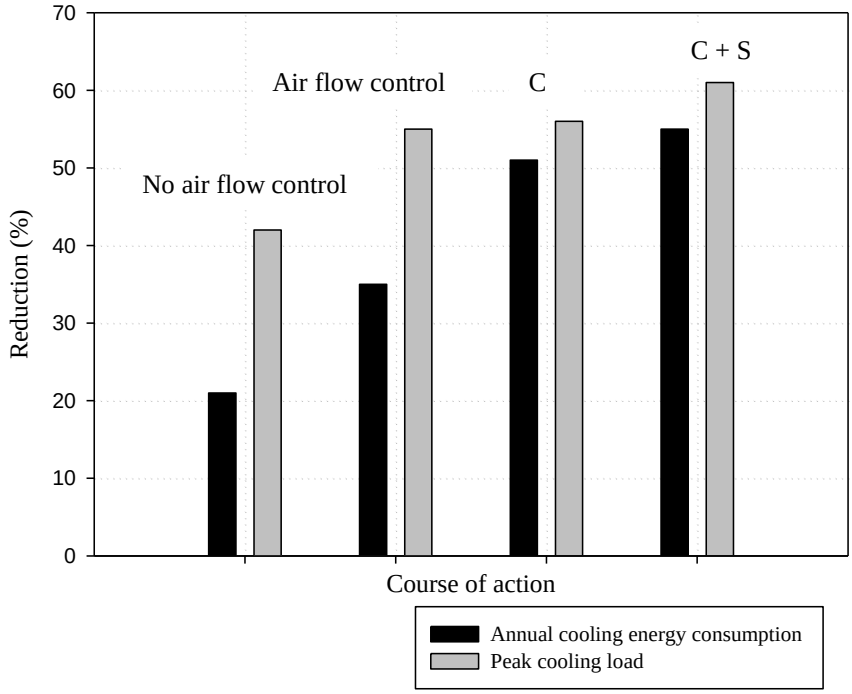

C: control strategy

S: shading

Figure 5.2: Reduction in the annual cooling energy consumption and peak cooling load due to culvert inclusion in the hybrid cooling system compared to using A/C system only for different set-ups.

As far as the multi-chiller control strategy for hot/dry climate is concerned, Table 4.8 shows that the control strategy shown in Figure 4.20 is able to predict the hourly modularized A/C cooling load over 7 selected days from April to October; one typical month's day of the cooling season were selected to represent different A/C cooling load and culvert cooling contributions. Referring to Table 4.8, the

modularized space sensible cooling load predicted by the control strategy (column 10) matches that produced by the ESP-r Villa/culvert model when basic On/Off control is employed (column 9) for 96% of the time. This percentage was calculated by giving a value of 1 to every simulation time-step when conditions are met (as explained in chapter 4) and assigning 0 when conditions are not met. The scores are then added and the result divided by the number of simulation time-steps to obtain the cooling load match percentage.

5.2 Generalization of Control Strategy

Chapter 4 introduced the hybrid cooling system control strategy for a hot climate as shown in Figure 4.10; a strategy tailored to the needs of people who can accommodate extra couple of degrees. The multi-chiller controller (Figure 4.20) is appropriate only for hot/dry climate and is not applicable for any other climate type. It has been stated in the previous chapter that such multi-chiller controller suits only hot/dry climate because the ambient set-point temperatures described by equations 4.10, 4.11, 4.12, 4.13, 4.14 and 4.15 suit only that climate set, but when the climate profile is changed then those ambient set-point temperatures change accordingly using the same equations mentioned. Thus, a general control strategy will be constructed to suit all climate types: hot/dry, hot/humid, moderate and cool. The strategy will possess general variables that may be altered when the climate type is changed.

5.2.1 Global Control Strategy

The general control strategy for the hybrid cooling system for any climate is shown in Figure 5.3. The following three caveats are applicable.

- A cost analysis would be required to establish precisely when active cooling must be activated to help the air culvert provide the required cooling. For simplicity, an educated guess it was made that active cooling should be introduced when the culvert provides cooling for less than 75% of the cooling season. If the culvert can provide more than 75% then the rest of the cooling load can be offset by other energy efficiency measures.

- To reduce short cycling, the A/C system was modularized into 4 units each accounting for 25% of the total cooling capacity. The required number of units must operate for at least 2 hours to insure continuous operation otherwise no other units may be added or subtracted. This condition was extracted backwards after checking the synchronization of the A/C modularization control strategy shown in Table 4.8, Table B.1 and Table B.2, where a sudden change from one modularized percentage to another occurs only for a single time-step. Even though this did not occur frequently it was important to add this condition to tune the control strategy.
- In order to reduce A/C system energy consumption drastically in hot/dry climate the indoor dry-bulb air temperature set-point was higher than the optimum comfort threshold of 25°C by 2°C and thus a comfort index such as the resultant temperature during Summer season was ~26.5° (Figure 4.11) (the maximum threshold is 26°C). Clearly, this is acceptable if occupants are adapted to stand couple extra degrees but if not then discomfort is experienced. Thus, in the general control strategy general indoor temperature variables were included so that they change based on occupant's preferences.

The maximum, minimum and optimum indoor dry-bulb temperature values change between climate types. People in cold climates tend to be accustomed to lower indoor temperatures, whereas those residing in a hot climate can tolerate higher temperatures (Olesen 2008). The free floating, free cooling and natural ventilation conditions stand true for all climate types, whereas the multi-chiller controller differs with the climate. Starting with the general control strategy (Figure 5.3), when the indoor dry-bulb temperature is greater than the maximum comfort value then sub-control strategy 1 (Figure 5.4) is activated. The next checkpoint in sub-control strategy 1 is the percentage of the culvert volume flow rate: in a hot/dry climate the ambient temperature beyond which the culvert fan capacity is halved is 30°C (i.e. an optimum indoor temperature of 25°C+5°C). Thus, in sub-control strategy 1 the ambient temperature is tested against the sum of the optimum indoor temperature for the specific climate and 5°C to implement the culvert flow control; this 5°C was theoretically predicted (section 4.3) as a gauge for the hot/dry climate and assumed the same for any other climate, but the only difference would be the

preference for optimum indoor temperature of the climate under test. If the condition is true then 50% fan load is engaged but if it is not then 100% fan load is exercised.

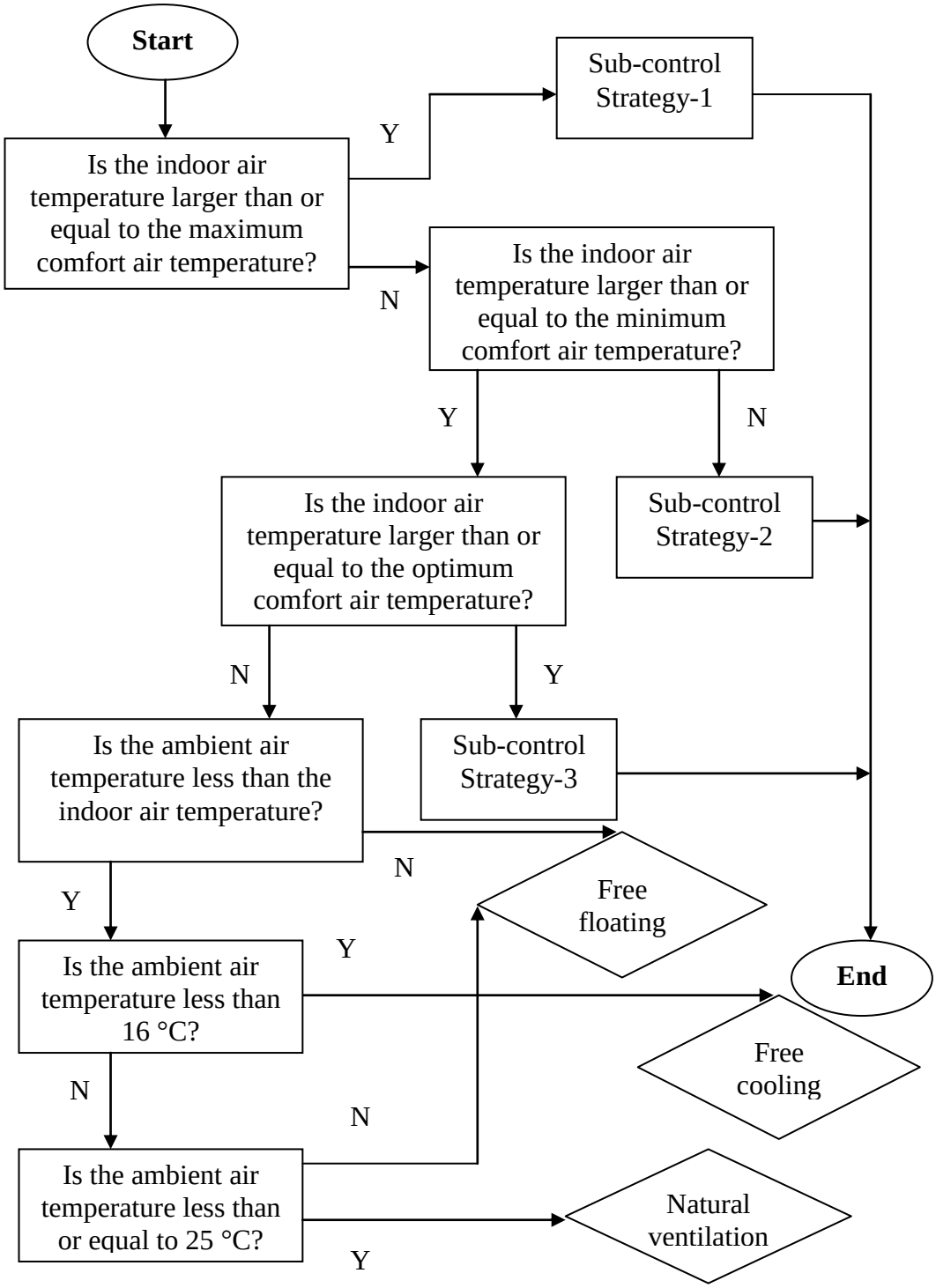

Figure 5.3: Generalised control strategy for the hybrid cooling system.

The next question in general sub-control strategy 1 is if the culvert outlet air temperature is less than the ambient; if the answer is no then ambient air supplies the

AHU and this directs the control routine to the generalised multi-chiller controller as depicted in Figure 5.6. If the answer is yes then a check is made on the culvert fan power: if the culvert cooling capacity is larger then air is supplied to the AHU by the culvert but, if smaller, then the last check would be if the culvert fan power consumption is less than the A/C fan power; if yes the AHU receives culvert air but if not then the AHU receives the ambient air directly. Control is then passed to the generalised multi-chiller control strategy as shown in Figure 5.6.

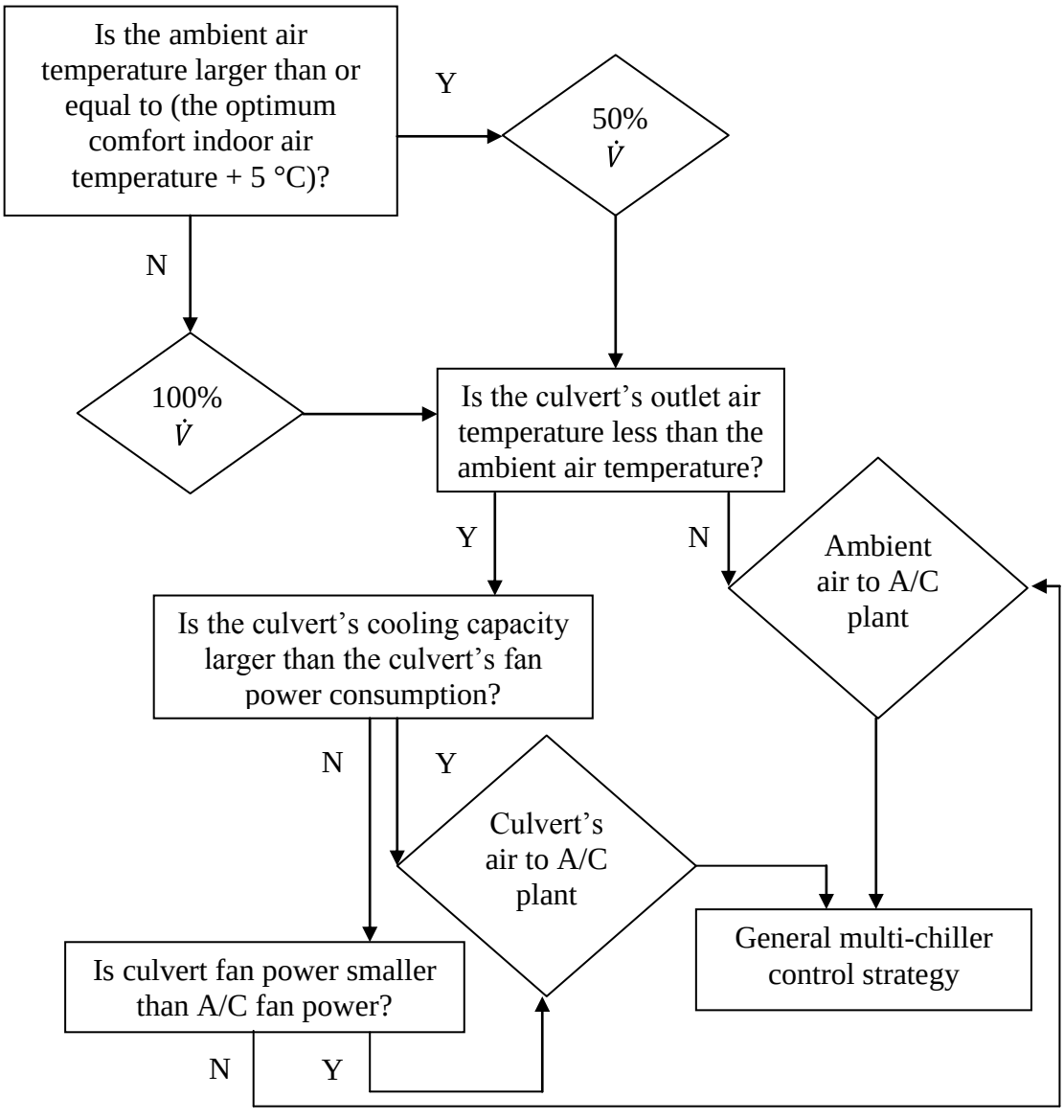

Figure 5.4: General sub-control strategy 1.

The ambient set-point temperatures (set-points that trigger the use of different modularized A/C percentage) calculated by relations 4.10, 4.11, 4.12, 4.13, 4.14 and

4.15 are reflected in Figure 5.6 and Figure 5.7. These relations increase the ambient air temperature ranges as functions of the ground temperatures that differ with climate. As mentioned in chapter 4 these relations were established from simulations for different climates. Figure 5.5 shows how ambient set-point temperatures act as support and resistance points for the ambient temperatures selected for 7 days; one day for each cooling season month. The same figure depicts how cooling load changes from one range to another when those ambient set-point ranges are crossed. For example, when the ambient temperature is below 24°C 0% A/C is required and if it is higher than 38.8°C then most probably 100% A/C is required depending on culvert cooling contribution. Culvert cooling contribution has to be known for other ambient set-point temperature ranges and their corresponding A/C cooling load has to be specified; this was not included in Figure 5.5 to avoid complexity, yet the same idea is applied.

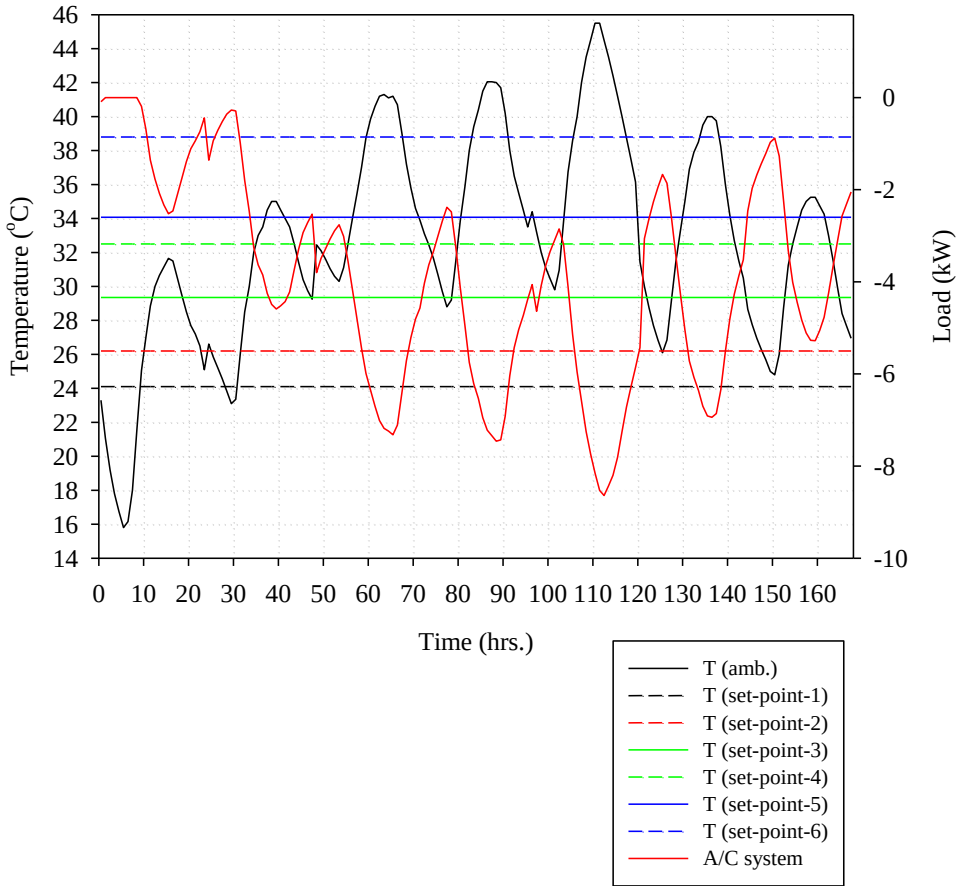

Figure 5.5: Ambient set-point temperatures used in the multi-chiller control strategy in hot/dry climate.

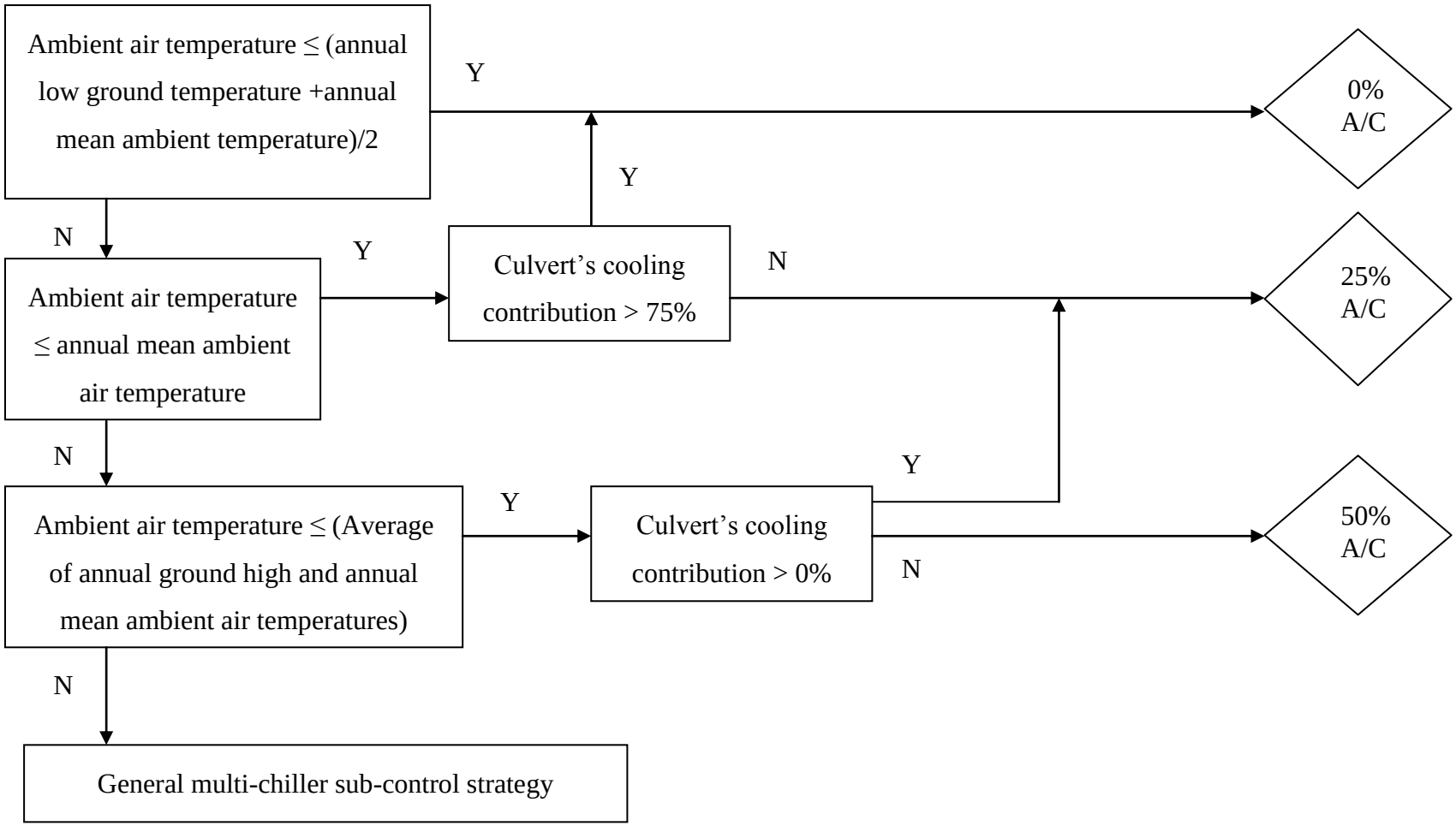

Figure 5.6: General multi-chiller controller.

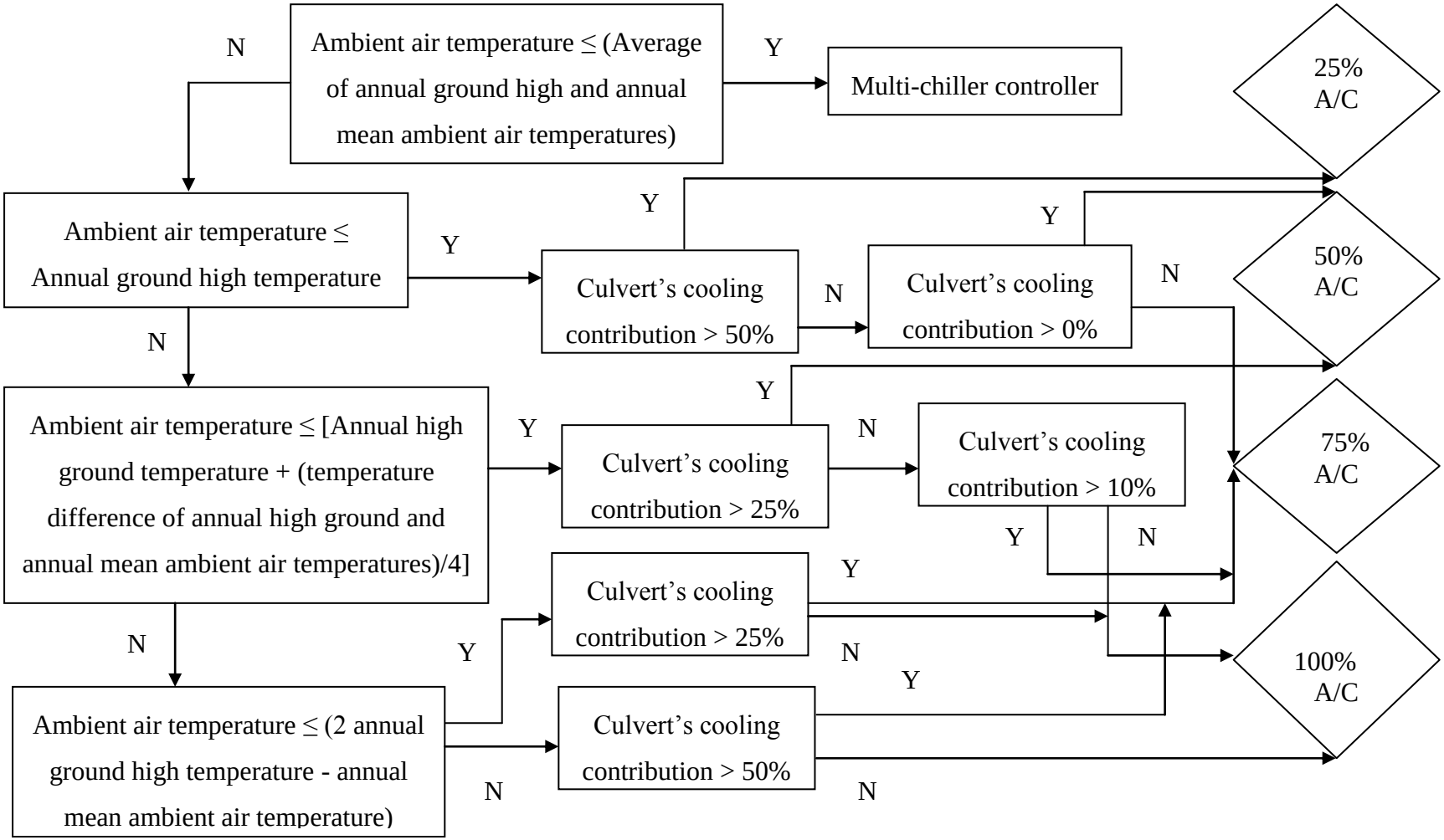

Figure 5.7: General multi-chiller sub-control strategy.

The modularized A/C versus culvert cooling contribution for all ambient set-point temperature ranges was discussed in chapter 4 for a hot/arid climate for selected days. Moreover, the multi-chiller control strategy displayed in Figure 5.6 and the multi-chiller sub-control strategy shown in Figure 5.7 are explained by text instead of symbols to make it easy to follow. The multi-chiller for a hot/dry climate has already been explained in chapter 4 and thus there is no intention here to detail how the general multi-chiller should be worked out as the charts (Figure 5.6 and Figure 5.7) are easily scrutinised. Now, when the indoor temperature is lower than the maximum comfort value (Figure 5.3) then the question would be 'is the indoor temperature larger than the minimum required for comfort?' If the answer is no then general sub-control strategy 2 (Figure 5.8) is activated. In sub-control strategy 2, the culvert flow control test is done such that if the ambient temperature is larger than the difference between the minimum comfort indoor temperature for a specific climate and 5°C then 50% culvert fan load is operated but if not then 100% load is exercised; this 5°C was theoretically predicted (section 4.3) as a gauge for the hot/dry climate and assumed the same for any other climate, but the only difference would be the preference for the minimum comfortable indoor temperature of the climate under test. Sub-control strategy 2 is explained by words and in general variables so that it is applicable for different climates; it can be readily followed (Figure 5.8) as that used for hot/dry climate in chapter 4. But, if the indoor temperature is larger than the minimum comfort temperature (Figure 5.3) then the check is if the indoor temperature is larger than the optimum comfort temperature. So, when the indoor temperature is between maximum and optimum values then general sub-control strategy 3 (Figure 5.9) is employed. Again, the strategy is explained in words and generalised so that it can be applied when climates are varied. Chapter 4 explained how the strategy works for a hot/dry climate. If the indoor temperature is between the minimum and optimum comfort indoor temperatures then the question as shown in Figure 5.3 is posed: 'is the ambient air temperature less than the indoor temperature?'. If no then the Villa is placed in free float mode but, if yes, then the supplemental question is asked: 'is the ambient air temperature less than 16°C. If yes then the Villa is cooled freely, if not the ambient

temperature is examined for less than 25°C. If yes then the Villa is naturally ventilated, if no then the free floating mode persists.

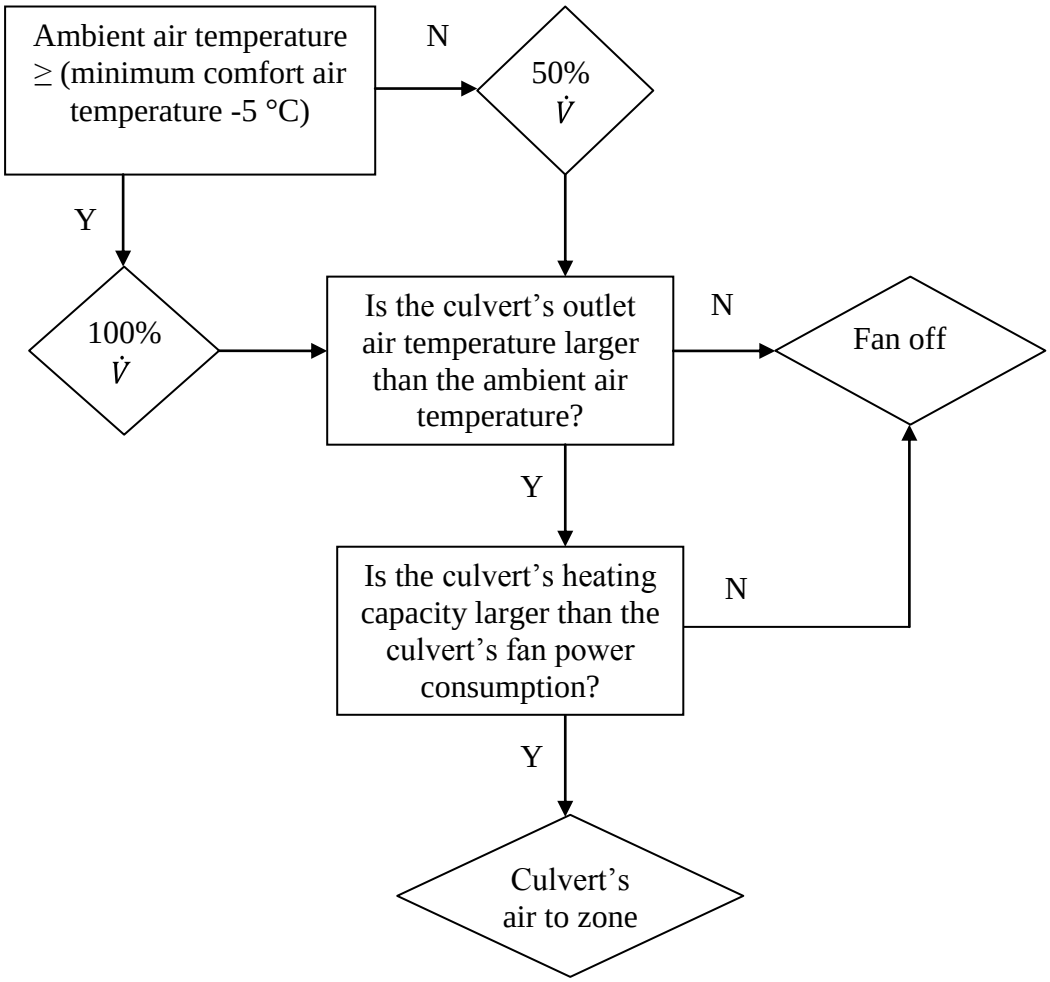

Figure 5.8: General sub-control strategy 2.

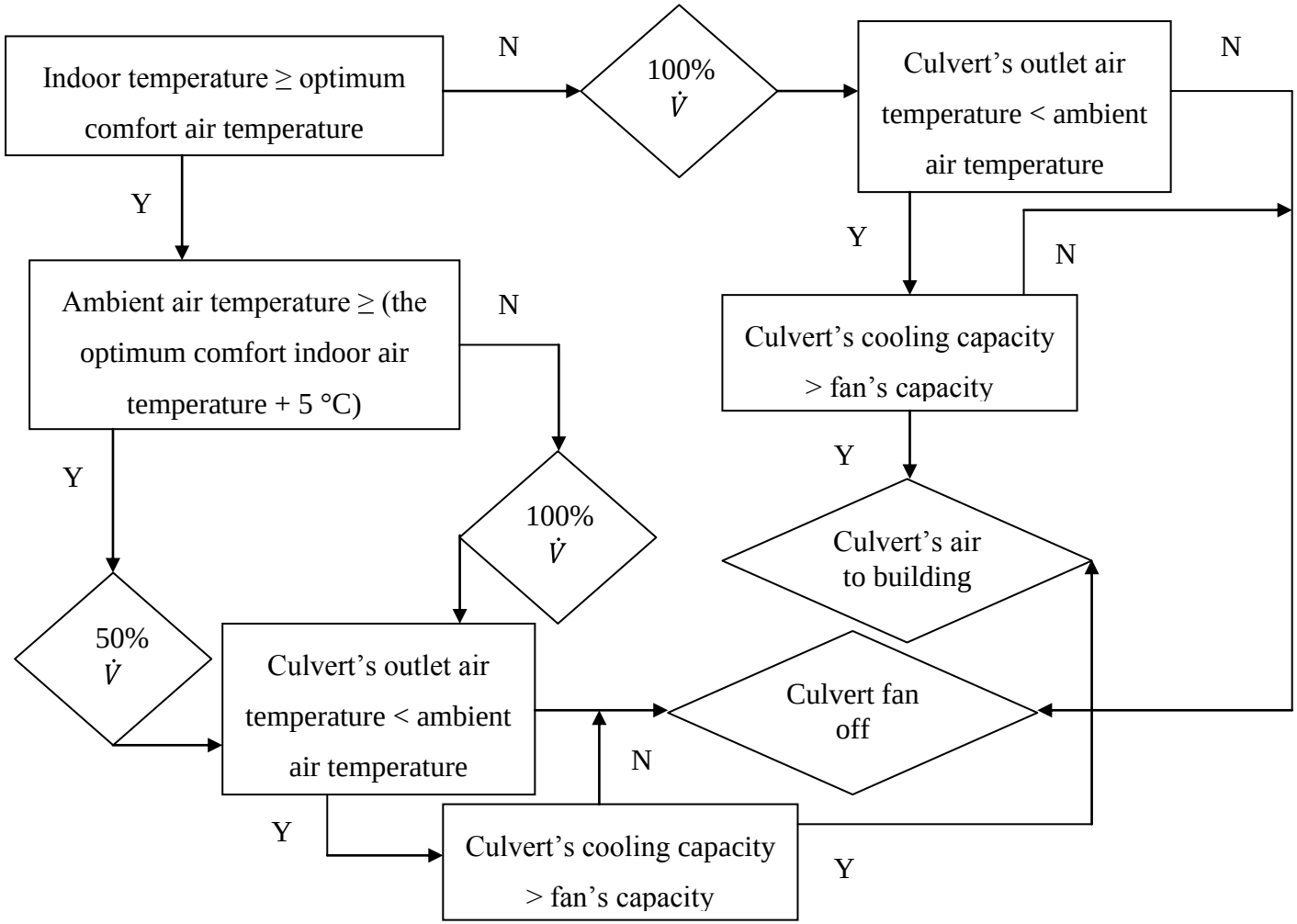

Figure 5.9: General sub-control strategy 3.

5.3 General Control Strategy Validation

The multi-chiller control strategy is a major component of the control algorithm as tested for a hot/dry climate in section 5.1.1. However, the applicability of such a controller in other climate types has yet to be explored. Thus, the following sections relates to tests applied for the following climate types:

- Hot/humid.
- Moderate.
- Cool.

Again, the main part of the general control strategy is the multi-chiller controller, which couples the active cooling system to that of air culvert system based on culvert cooling contribution, while altering several parameters that change with the climate type. In addition to these parameters only the indoor dry-bulb temperatures (maximum, minimum and optimum) are changed as a function of the climate type (hot or cool); these temperatures may be fixed for all climates if natural acclimatization is not considered. The verification of the multi-chiller controller algorithm gives authority to the general control strategy for the hybrid cooling system.

5.3.1 Hot/Humid Climate

The hot/humid climate corresponds to latitude of 25.8°N with an annual mean ambient relative humidity of 72.3%. The first check in the general control strategy ensures that the building indoor temperatures should be greater than the maximum requirement during more than 25% of the cooling season, otherwise it is not activated because then there is no need for active cooling and the culvert and energy efficiency measures can provide the required cooling. For the hot/humid climate chosen, the indoor temperatures inside the Villa were higher than 27°C for 91% of the cooling season; 27°C was selected as the maximum comfortable indoor dry-bulb temperature similar to hot/dry climate. The building sensible cooling demand and culvert cooling capacity were computed for 7 selected days, one day for each month from April to October; again, those days were selected to appraise how the building sensible cooling load and culvert cooling contribution differ from one typical

month's day to another. The building and culvert components were identical to those used in chapter 4. Table 5.2 lists the monthly ground temperatures as extracted from equation 5.1. It is emphasized that the soil thermal diffusivity is a decisive element in calculating the soil temperatures. When the soil water content increases, its thermal diffusivity increases, which reduces the soil temperature. This parameter changes with depth from one location to another and, since there is no way to calculate it accurately, it must be measured. Thus, for the hot/humid climate file used in this study, the soil thermal diffusivity was assumed by increasing it by 20% to 0.11 m^2/day from that used for the hot/dry climate file.

$$T_g = 24 + 12e^{-0.28z}\cos\left\{\frac{2\pi}{365}[t - 3 - 16.3z]\right\} \qquad 5.1$$

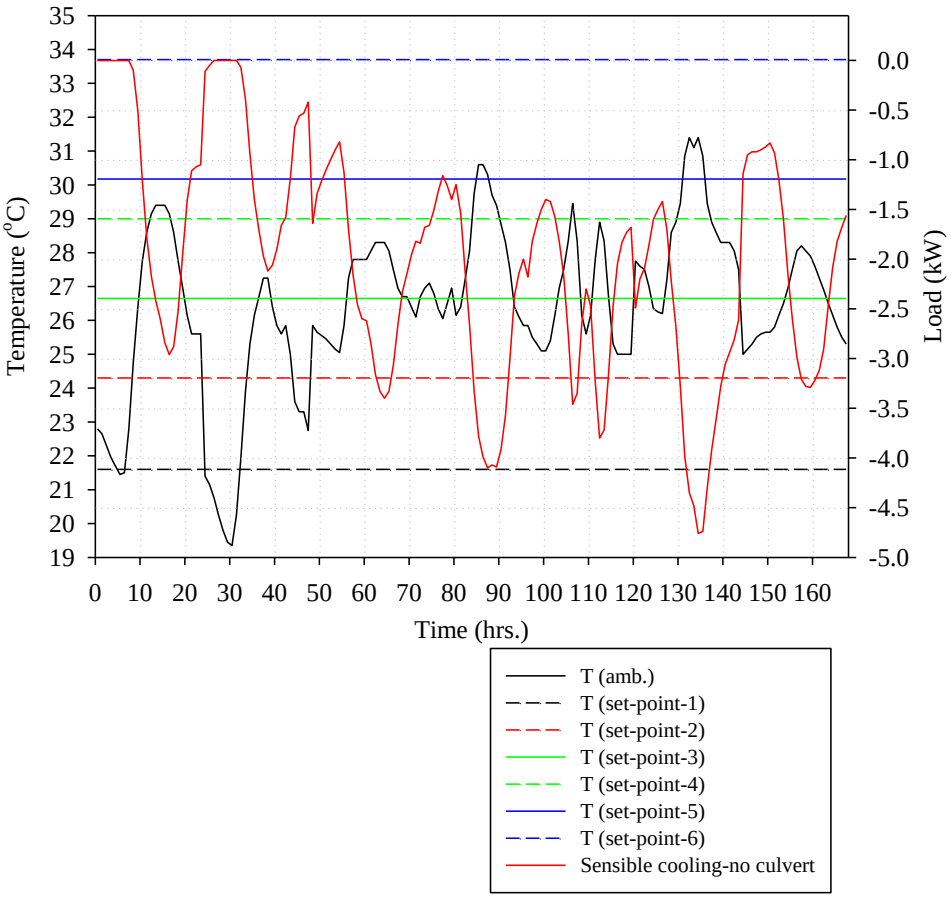

Figure 5.10: Ambient set-point temperatures used in the multi-chiller control strategy in a hot/humid climate.

Table 5.2: Monthly ground temperature profile in °C for a hot/humid climate at 3 m depth.

Jan.	Feb.	Mar.	Apr.	May	Jun.	Jul.	Aug.	Sep.	Oct.	Nov.	Dec.
19.9	18.9	19.3	20.9	23.3	25.9	28	29.1	28.8	27.3	24.9	22.1

Referring to Table 5.2, the ground temperatures used in the A/C modularization algorithm were the annual low (18.9°C) and annual high (29.1°C) values. The corresponding annual mean ambient air temperature was 24.3°C. Figure 5.10 presents how ambient set-point temperatures behave as support and resistance points for the ambient temperatures in a hot/humid climate. The ambient temperature set-points were discussed in chapter 4 for hot/dry climate that constitute how multi-chiller controller is approached such that when a set-point is reached the modularized A/C cooling load is figured out knowing the culvert cooling contribution beforehand. Figure 5.10 reveals that not all ambient set-points are utilized as the sixth set-point has not been passed. That is acceptable since the 100% A/C capacity can be experienced in the fifth set-point as shown in Figure 5.7. Figure 5.11 illustrates the impact of culvert cooling on Villa sensible cooling load reduction. It is emphasized that the multi-chiller control strategy stands true for a hot/dry climate for both sensible and latent cooling and it was made general for the culvert's effect on the building's sensible cooling when used in other climates. The peak sensible cooling load for the Villa in a hot/humid climate is ~4.75kW with a 13% culvert cooling contribution (Table B.1); hence the new sensible peak cooling load, after considering the culvert impact, is ~4.1kW. So, the peak sensible cooling load is ~4.1kW from which the modularized cooling loads of 25%, 50% and 75% are calculated. Referring to Figure 5.11, at 6 A.M the ambient temperature is ~26°C with a 0% culvert cooling contribution and, from Figure 5.10, this ambient temperature is between the second and third ambient set-points, ~24.5°C and ~26.5°C respectively. Thus, from Figure 5.6 between these set-points where the culvert contribution is 0%, the modularized sensible cooling required is 50% with ambient air being supplied to the AHU. Examining Figure 5.11 again, at noon the ambient temperature is ~29°C with 20% culvert cooling contribution and from Figure 5.10 this ambient temperature is between the fourth and fifth ambient set-points, ~29°C and ~30°C respectively. Thus, from Figure 5.7 between these set-points where culvert contribution is 20%,

the modularized sensible cooling required is 75% with air being supplied to the AHU by the culvert. Again, at 2 P.M the ambient temperature is ~30.5°C, with 20% culvert cooling contribution (Figure 5.11), and from Figure 5.10 this ambient temperature is between the fifth and sixth ambient set-points, ~30°C and ~34°C respectively. Thus, from Figure 5.7 between these set-points where culvert contribution is 20%, the modularized sensible cooling required is 100%, with air being supplied to the AHU by the culvert. It is obvious that the general multi-chiller control strategy can accurately quantify the modularized sensible cooling load for the hot/humid climate.

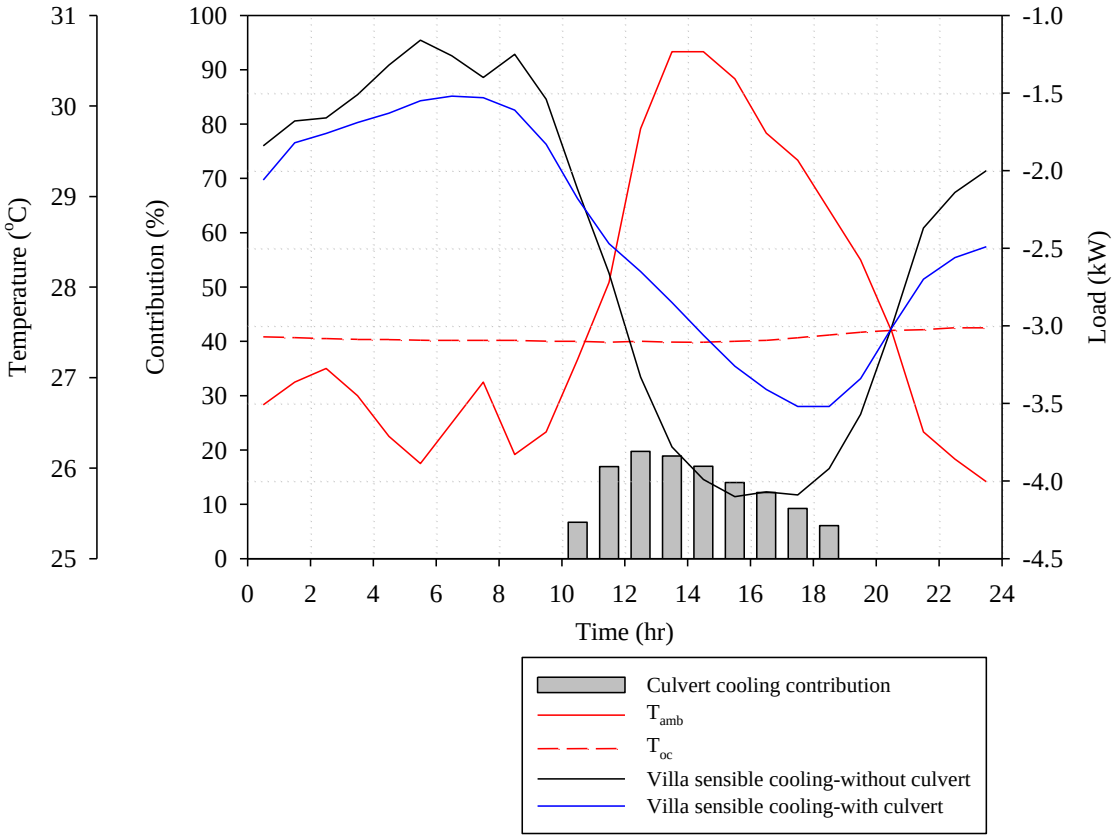

Figure 5.11: Sensible cooling modularization when culvert cooling contribution is considered for a selected day in a hot/humid climate.

Table B.1 lists the hourly modularized A/C sensible cooling load percentage for the 7 selected days from April to October. The generalised control strategy was able to predict how many cooling units should operate for 87% of the 168 total simulation time-steps compared to 96% when the general control strategy was used in a hot/dry climate.

5.3.2 Temperate Climate

The moderate climate selected for the multi-chiller analysis is located at latitude 38.2°N with a maximum and minimum ambient temperatures of 34°C and 4.8°C respectively and an annual mean value of 18.8°C. In such a climate, the indoor temperature inside the Villa is higher than 25°C for 96% of the cooling season. In chapter 3, where Glasgow (cool climate) ground temperatures were calculated, the assumed soil thermal diffusivity was 0.05 m^2/day. Meanwhile the annual mean ambient relative humidity of the present temperate climate is similar to that in the cool climate (~74%), the annual mean ambient air temperature is greater by ~8°C. The thermal diffusivity (relation 5.2) was therefore increased by 20% to 0.07 m^2/day –since both climates have similar water content, the volumetric heat capacity was assumed to be the same and the thermal conductivity higher: "*Thermal conductivity of materials is temperature dependent. In general, materials become more conductive to heat as the average temperature increases*"(Callister 2003). The ground temperature model given by equation 5.3 was produced for this location while ground temperatures at 3 m depth were extracted from Table 5.3.

$$\alpha = {}^{k}/_{\rho c_p} \qquad 5.2$$

$$T_g = 21.5 + 10.8e^{-0.35z}\cos\left\{\frac{2\pi}{365}[t - 33 - 20.4z]\right\} \qquad 5.3$$

Table 5.3: Monthly ground temperature profile in °C for temperate climate at 3 m depth.

Jan.	Feb.	Mar.	Apr.	May	Jun.	Jul.	Aug.	Sep.	Oct.	Nov.	Dec.
20.7	19	18	17.9	18.7	20.3	22.1	23.9	25	25.2	24.4	22.8

Figure 5.12 shows how the culvert can reduce the Villa sensible cooling load. The peak sensible cooling load for the Villa in a moderate climate is ~6kW with a 26% culvert cooling contribution (Table B.2), leading to ~4.4kW as a new peak sensible cooling capacity. However, the same table gives another sensible cooling load (5.25kW) with a lower culvert cooling contribution (8%), leading to a 4.8kW as a new peak sensible cooling load. Hence, the new sensible peak cooling load selected after considering the culvert impact is the latter one.

Referring to Figure 5.12, at 8 A.M the ambient temperature is ~24.5°C with a 0% culvert cooling contribution and from Figure 5.13 this ambient temperature is between the third and fourth ambient set-points, ~22°C and ~25°C respectively. Thus, from Figure 5.7 between these set-points where culvert contribution is 0%, the modularized sensible cooling required is 75% with ambient air being supplied to the AHU. At noon the ambient temperature is ~26.5°C with 6% culvert cooling contribution (Figure 5.12) and from Figure 5.13 this ambient temperature is between the fourth and fifth ambient set-points, ~25°C and ~27°C respectively. Thus, from Figure 5.7 between these set-points, where the culvert contribution is 6%, the modularized sensible cooling required is 100% with air being supplied to the AHU by the culvert. Again, at 4 P.M the ambient temperature is ~27.2°C with an 8% culvert cooling contribution (Figure 5.12) and from Figure 5.13 this ambient temperature is between the fifth and sixth ambient set-points, ~27°C and ~32°C respectively.

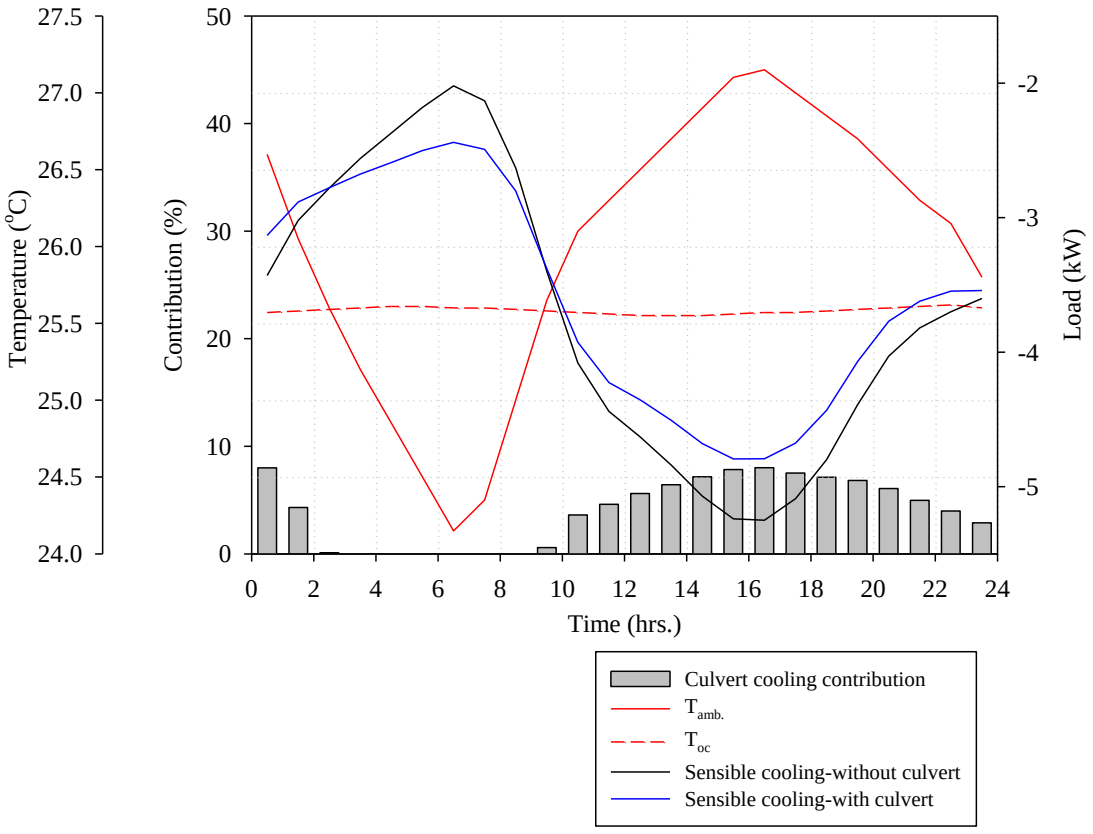

Figure 5.12: Sensible cooling modularization when culvert cooling contribution is considered for a selected day in a moderate climate.

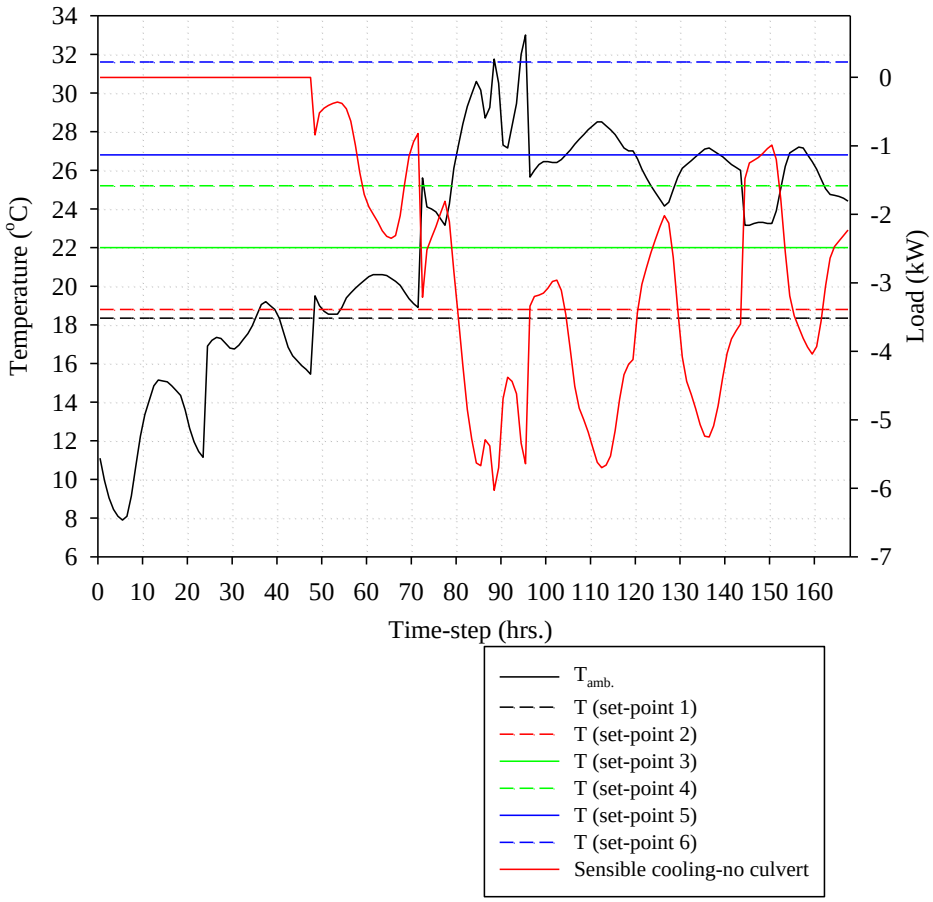

Figure 5.13: Ambient set-point temperatures used in the multi-chiller control strategy in a moderate climate.

Thus, from Figure 5.7 between these set-points where culvert contribution is 8% the modularized sensible cooling required is 100% with air being supplied to the AHU by the culvert. Table B.2 lists the hourly A/C modularized percentage as recommended by the multi-chiller strategy for 7 selected days from April to October (temperate climate). The multi-chiller general control strategy was able to match the simulated sensible cooling requirement for 88% of the 168 simulation time steps.

5.3.3 Cool Climate

The cool climate chosen is that used in the empirical verification of the culvert model. In this case, the indoor temperatures inside the Villa is higher than 25°C for 6% of the cooling season and so there is no need to include active cooling system in such a climate since the cooling load can be satisfied by the culvert and energy efficiency measures such as shading and natural ventilation.

5.3.4 Control Strategy: Constraints, and Consequences

One constraint of the control strategy would be fan power consumption when large ventilation requirements exist. As stated earlier the culvert fan power in the residential sector is small compared to its commercial counterpart and therefore is not a constraint in a Villa. However, if a non-renewable energy supply source is utilized then CO_2 emissions for each kWh accumulate even though they are small. For example, the annual fan energy consumption for the present control strategy is 10.9 kWh as listed in Table 3.15 and since for each kWh 0.19 kg CO_2 is emitted, the fan gives rise to a 2.07 kg CO_2 emission. When flow control is used, the CO_2 emissions are reduced by more than half compared to the no flow case. Hypothetically speaking, if a renewable energy supply is employed, such as PV components or small wind turbines, then other issues may arise such as:

1. Renewable component energy storage.
2. High ambient temperature and its negative impact on the PV cell efficiency.
3. Placement of wind turbines in the urban micro-climate.

The main constraint is the total cost of the hybrid cooling system. This includes fixed cost (overhead cost) and variable cost (operating or running cost) elements. The combination of active/passive cooling components should be viable. The use of an A/C system in hot and moderate climates is desirable because the air culvert can not offset the entire cooling load required. However, in a cold climate, culverts can provide a substantial portion of the required cooling if designed and controlled efficiently. Thus, the general control strategy that is presented in chapter 5 includes a conditional term so that active cooling is not included in the mix if the culvert contributes more than 75% of the required cooling energy. This control strategy has consequences such as:

- IAQ issues arise in this control strategy when the air flow rate is reduced from 100% to 50% since less fresh air increases indoor CO_2 levels above the threshold of 1000 ppm as illustrated in Figure 5.14. Thus, a CO_2 contaminants definition was added to the ESP-r hybrid cooling system model as listed in Appendix C to give an indication of IAQ.

- Indoor thermal comfort can be jeopardized when natural acclimatization is considered in selecting acceptable indoor dry-bulb temperature that triggers other conditions. In hot/dry climate control strategy, when the maximum indoor dry-bulb temperature was 27°C the indoor resultant temperature was higher than the maximum comfort threshold by a bit (Figure 4.11). Again, it was explained that the general control strategy accommodate for that so that the dry-bulb temperatures (maximum, optimum and minimum) are selected by preference.

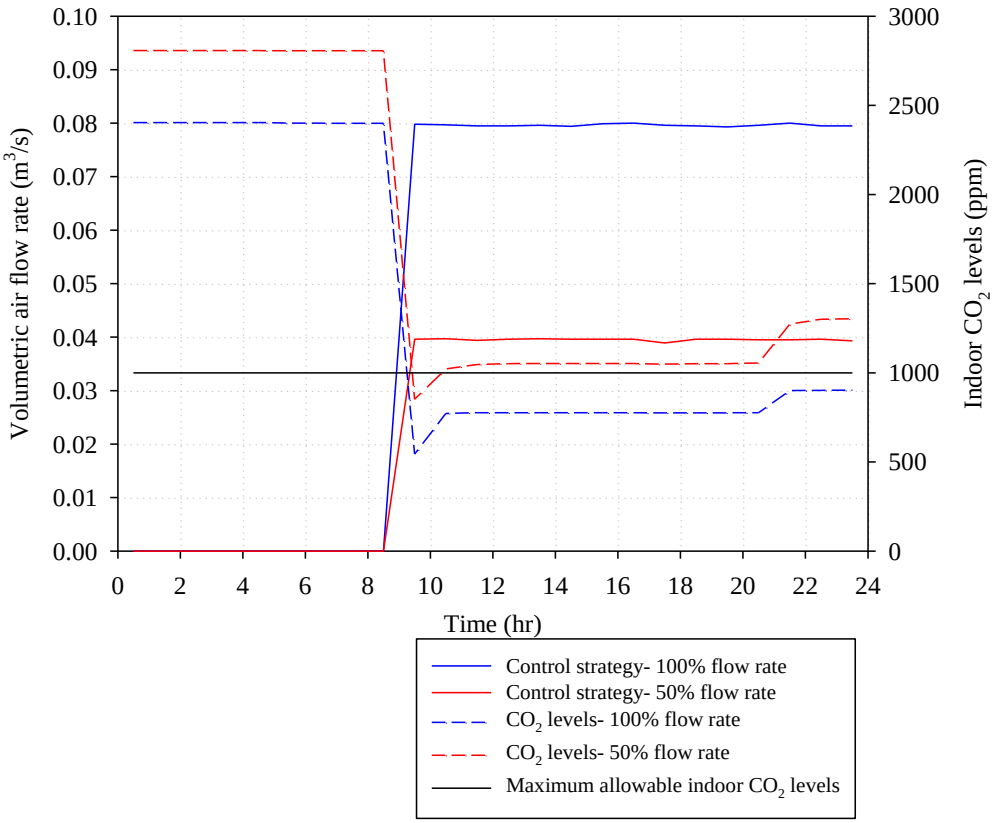

Figure 5.14: Villa living room CO_2 levels for different culvert flow rates.

5.4 General Guidelines for Culvert Applicability

Entangled issues related to culvert suitability are discussed such as.

- Geometry and ground surface treatment.

Increasing the hydraulic diameter as discussed in section 3.4 is the first priority to maximize culvert thermal performance. However, large hydraulic diameter when used in hot/dry climate as concluded in section 3.5.1 would

undermine culvert thermal performance even more than when small hydraulic diameter is used during late Summer time requiring the need for ground surface treatment. Nevertheless, in hot/humid climate, ground surface treatment is not beneficial since the degradation in culvert thermal performance is not due to the high ground temperatures but to the condensation of air inside culvert; moreover, the ground set-point temperature (a temperature above which ground surface treatment is recommended) calculated by equation 3.13 is not reached. Another culvert geometrical parameter is length; it was emphasized in section 3.2.2.1 that when small hydraulic diameter is used the optimum length that should be used to upgrade both culvert thermal and hydraulic performance is 40m, but when large hydraulic diameter encountered then 50-60m would be the optimum length regardless of the climate type.

- HVAC/culvert coupling.

The fractional portions of both the A/C system and the culvert system are discussed in detail in the general multi-chiller control strategy that can be used for the hybrid cooling system in any climate. As a result, the following comments are made.

  - In hot/dry climate, a hybrid cooling system of A/C and culvert is used. The culvert is beneficial throughout the year except in Autumn season and the peak A/C cooling load is the highest compared to other climate types.
  - In hot/humid climate, a hybrid cooling system of A/C and culvert is used. The culvert is less beneficial throughout the year than it is in hot/dry climate and the peak A/C cooling load is comparable to that in moderate climate.
  - In moderate climate, a hybrid cooling system of A/C and culvert is used. The culvert is beneficial throughout the year and the peak A/C cooling load is comparable to that in hot/humid climate.
  - In cool climate, no hybrid cooling system is used but only culvert for cooling.

5.5 Concluding remarks

The control strategy for the hybrid cooling system for hot/dry climate was implemented in ESP-r. The regional version of the control strategy was then generalized to all climates in terms of principal parameters relating to indoor, ambient and ground temperature conditions. This chapter also exhibited the validation of the multi-chiller controller in different climates; hot/humid, moderate and cool.

Chapter 6 : Conclusions & Future Work

This chapter summarises the conclusions of the thesis and presents recommendations for future work.

6.1 Conclusions

Cooling energy demand in residential buildings is high in developing countries with a hot/arid climate. Cooling requirements in hot climates in general is mainly provided by active cooling plant, which has shortcomings as discussed in chapter 1. The main problem is the running cost associated with rising cooling energy consumption and the capital cost associated with rising peak cooling capacity; the objective of this thesis was to reduce both quantities. This goal was achieved by pursuing the synergy between an active cooling system and an earth-coupled air culvert. There are several issues related to culvert design and the ones targeted in this thesis are centred on the following 3 elements.

- *The quantification of air culvert thermal efficacy.*

ESP-r was used to appraise air culvert thermal performance. As explained in chapter 2 ESP-r considers all heat exchange processes and how they interact in a dynamic manner.

  - A ground temperature model was developed and validated against measured data sourced from the literature.
  - That ground temperature profile for a hot/dry climate was entered in the ESP-r culvert model to enable inter-model comparison.
  - An empirical validation was exercised for a culvert in a Sports Centre in Glasgow.
  - It was concluded (chapter 3) from a sensitivity analysis that the culvert hydraulic diameter is the most significant parameter that can be used to improve culvert thermal efficacy. Depth increase was the second most significant parameter, followed by length and earth treatment.

- A regression analysis was performed to establish a curve representing culvert diameter as a function of volumetric air flow rate at which the pressure drop in the system is low. If the required air flow rate is small then the resulting diameter can be increased until site restrictions are encountered.
- It was concluded from chapter 3 that both heat transfer and air flow mechanisms behave differently and are difficult to quantify when large cross-section areas are employed. It was also found that with large diameter culverts, the air flow is not fully developed and the convective heat transfer coefficient correlations for fully developed turbulent flow, as often used for small diameter culverts, would be misleading. When the culvert length is less than the entrance length, the convective heat transfer coefficients were assumed to be 10 times greater than the values corresponding to fully developed turbulent flow, otherwise the correlations for fully developed turbulent flow were used. In this sense, the convective heat transfer coefficients were handled in a dynamic manner in order to more accurately emulate the reality.
- Culvert temperature effectiveness and COP improved as stated in chapter 3; the former by increasing the culvert diameter and the latter by culvert On/Off control and air flow control simultaneously.

- *The elaboration of an integrated system design method that accounts for the transient interaction between the culvert and A/C system.*

As stated in chapter 1 and reiterated in chapter 2, the finite volume approach of ESP-r facilitates the representation of more than one technical domain in an integrated manner.

- It was concluded from chapter 3 that the culvert is able to provide passive cooling of the Villa for about 15% of the cooling season in hot/dry climate. This percentage increases to 38% when shading, natural ventilation and earth treatment are added.
- ESP-r handles the coupling between the system components: 3 zone Villa, air culvert and CAV A/C plant.
- Chapter 4 discussed how the building and plant simulation time-steps were selected to represent the coupling accurately.

- The culvert, with no air flow control and when coupled to the A/C plant, was able to reduce the annual cooling energy and peak cooling power of the active cooling system by 13% and 38% respectively for an indoor temperature of 25°C. Further, the A/C system COP improved by 7%.
- When air flow control is exercised, the culvert COP decreases to 83 from 104 when there was no flow control; however, the annual sensible cooling energy and peak sensible cooling power reductions were drastically enhanced from 21% to 35% and from 42% to 55% respectively at 27°C indoor temperature. When air flow is controlled, the fan power is reduced, which should have increased the culvert COP but did not; it decreased. The reason for this is that the culvert cooling capacity decreased because of the lower air flow rate, which reduced the culvert outlet air temperature, leading to cooling energy and power reductions in the A/C plant when needed the most in the Summer season.
- A control strategy for the hybrid cooling system in a hot/dry climate was constructed and implemented in ESP-r. This was able to reduce both the annual cooling energy and peak cooling power by 51% and 56% respectively.

- *The requirement for hybrid system control when deployed within different climates.*

Another problem linked with culverts is that the control strategies differ from one climate type to another. The present work is intended to serve as a means to overcome this issue by constructing a general control strategy that can be used for any climate type.

- Normally, only indoor and ambient air temperatures are considered in the control algorithms; but the generalised controller also included the ground condition.
- There are no fixed temperatures in this control system. The climate type, hot or cold, will dictate the indoor temperature set-points while the ambient set-points are generated on the basis of the ground operating conditions that vary with the climate type.

- The multi-chiller strategy is a main part of the generalised controller. This modularization will result in energy savings in the long run due to the elimination of A/C system short cycling and energy consumption reduction.
- It is worth stating once again that the culvert can supply sensible cooling more than latent cooling and thus the modularization controller addresses the sensible cooling only. Therefore, the multi-chiller control strategy was implemented in different climate types -hot/dry, hot/humid, moderate and cool - using basic On/Off control instead of directly controlling the individual components of the CAV A/C system.
- Selection of modularized sensible cooling load against culvert sensible cooling contributions were addressed and justified based on ambient set-point temperatures as functions of ground temperatures.
- Simulations were performed for 7 days, selected from April through October, and an hourly sensible cooling load percentage was determined and compared against that found by the modularized general control strategy.
- Over 168 simulation time steps a 96% cooling load match rate was achieved for a hot/dry climate compared to 87% for a hot/humid climate and 88% for a moderate climate. The strategy was not applied for a cool climate because there is then no need for active cooling.

The conclusion was that the general control strategy is able to quantify how much modularized sensible cooling load is required when coupled to an air culvert in any climate thus bridging a knowledge gap that existed at the commencement of this research.

6.2 Future Work

The present work can be improved by adding elements that were not possible throughout the course of this research due to time and resource constraints. Some recommendations for future work follow.

- The control strategy was approximately implemented in the ESP-r hybrid cooling system model by dividing the year into day types where each day type was divided into hourly periods to represent when the fan switches on or off. A future work would be to digitise the general control strategy so that inputs are given and

the outputs would dictate which hybrid cooling system should operate. ESP-r's time rewind control facility could also be used to enable a 'look-ahead' facility as part of an exploratory forecasting algorithm.

- A major issue is how to handle large cross sectional area culverts and quantify the thermal efficiency. The convective heat flux is a large portion of the heat transfer exchange in large culverts. An air flow network in ESP-r can represent small culverts to high accuracy since fully developed turbulent flow develops shortly after the culvert entrance (using convective heat transfer coefficients corresponding to fully developed turbulent flow is suitable). However, when large culverts employed quantifying the convective heat transfer coefficients becomes problematic and can only be done experimentally due to entrance length and buoyancy effects. Such experiments are difficult to run for changed conditions (such as culvert dimensions and ground conditions). Thus, it is more appropriate to predict convective heat transfer coefficients theoretically. In ESP-r, it is possible to conflate thermal and flow (CFD) domains, where the former produces boundary conditions for the latter and the latter calculates the convective heat transfer coefficients that are inserted in the energy balance matrix equation to produce more realistic results. This approach is recommended for large cross-sectional air culverts so that the convective heat fluxes are accurately modelled.
- Most of the methods used to calculate the culvert outlet air temperature are sophisticated and not suitable for a novice. A need rises to develop a procedure for calculating the transient culvert outlet air temperature through regression analysis based on dynamic energy simulation results. This would give rise to a dynamic but simple model based on look-up table data for different culvert designs and ambient operating conditions. In this way the designer can readily compare alternative design approaches.
- Culvert's thermal performance in late summer is less advantageous when compared to other cooling season periods. Earth treatment and domestic hot water (DHW) system efficiency improvement are the two actions recommended to improve the culvert's performance at that time of year. The impact of earth treatment on HVAC energy consumption savings is to be studied in the future as

mentioned in chapter 3; also the DHW energy efficiency measure could be presented. Assuming a hot water supply temperature of 50°C, it can be observed that when the ground temperature is 31.4°C and ambient air temperature is 17.3°C the culvert's outlet air temperature is 29°C. Thus, instead of heating water from 17.3°C to 50°C it will only be heated from 29°C to 50°C (assuming that the DHW flow rate equals that of the culvert fan and neglecting differences between c_p and ρ for air and water), a temperature rise of 72% instead of 189% resulting in power saving calculated from equation 6.1. A mathematical relationship is required between the different DHW and culvert flow rates to represent the significance of this energy saving in practice where thermo-physical properties are different. Such a relationship is not evaluated here and is left for future investigation.

$$q = \dot{w} c_p \rho \Delta T \qquad 6.1$$

where,

q: DHW capacity (W)

$\dot{w}$: water volumetric flow rate (m^3/s)

ΔT: difference between ambient and hot water supply temperatures (°C)

Reference List

Aasem, E.O. (1993) 'Practical simulation of buildings and air-conditioning systems in the transient domain', *PhD thesis*, University of Strathclyde, Glasgow, UK.

AboulNaga, M.M. & Elsheshtawy, Y.H. (2001) 'Environmental sustainability assessment of buildings in hot climates: the case of the UAE', *Renewable Energy*, 24 (3/4), pp553-563.

Adnot, J. (1999) 'Energy Efficiency of Room Air-Conditioners (EERAC)', *Study for the Directorate General for Energy (DG XVII) of the Commission of the European Communities*, Luxembourg.

Agrawal, P.C. (1988) 'A review of passive systems for natural heating and cooling of buildings', *Healthy Buildings 88 Conference Proceedings*: Stokholm, Sweden, pp585-602.

Akridge, J. (1982) 'Investigation of passive cooling techniques for hot-humid climates', *Research report*, College of Architecture, Georgia Institute of Technology, Atlanta, Georgia.

Akridge, T. & Benton, C. (1981) 'Performance studies of a thermal envelope house' *Phase II cooling performance*, Southern Solar Energy Center, Atlanta, Georgia.

Al-Ajmi, F., Hanby, V.I. & Loveday, D.L. (2002) 'Thermal performance of the sub-soil environment in dry desert climate', *ASHRAE Transactions*, Vol. 108, Part 2.

Al-Ajmi, F. & Loveday, D. (2010) 'Indoor thermal conditions and thermal comfort in air-conditioned domestic buildings in the dry-desert climate of Kuwait', *Building and Environement*, 45, pp704-710.

Ameen, A. (2006) '*Refrigeration and Air Conditioning'*, Prentice-Hall of India: New Delhi, India.

Ananthanarayanan, P.N. (2005) '*Basic Refrigeration and Air Conditioning (2nd edition)*', Tata Mc-Graw-Hill Publising Company Limited.

ANSI/ASHRAE Standard 55. (2004) 'Thermal Environmental Conditions for Human Occupancy', *ASHRAE Inc.*: Atlanta, GA, USA.

ANSI/ASHRAE Standard 62.1. (2007) 'Ventilation and Acceptable Indoor Air Quality', *ASHRAE* Inc.: Atlanta, GA, USA.

Argiriou, A., Tzaferis, A., Liparakis, D., Santamouris, M. & . (1992) 'Analysis of the accuracy and sensitivity of eight models to predict the performance of earth-to-air heat exchangers', *Energy and Buildings*, 18 (1), pp35-43.

ASHRAE Handbook. (2004) 'Systems and Equipment Volume', *ASHRAE Inc.*: Atlanta, GA, USA.

Athienitis, A.K. & Santamouris, M. (2002) '*Thermal Analysis and Design of Passive Solar Buildings*', James & James (Science Publishers) Ltd: London, UK.

Badescu, V. (2007) 'Simple and accurate model for the ground heat exchanger of a passive house', *Renewable Energy*, 32 (5), pp845-855.

Beausoleil-Morrison, I. (2000) 'The adaptive coupling of heat and air flow modlling within dynamic whole-building simulation', *PhD thesis*, University of Strathclyde, Glasgow, UK.

Beggs, C. (2009) '*Energy Management, Supply and Conservation (2nd edition)*', Butterworth-Heinemann: Oxford, UK.

BizEE Software. (2011) 'Software developed based on temperature data from Weather Underground', http://www.degreedays.net/.

Bojic, M., Trifunovic, N., Papadakis, G. & Kyritsis, S. (1997) 'Numerical simulation, technical and economic evaluation of air-to-earth heat exchanger coupled to a building', *Energy*, 22 (12), pp1151-1158.

Boulard, T., Razafinjohany, E. & Baille, A. (1989) 'Heat and water vapour transfer in agricultural greenhouse with an underground heat storage system, parts 1 & 2', *Agricultural and Forest Meteorology*, 45, pp175-194.

BP. (2007) BP Statistical Review of World Energy.

Callister, W. (2003) '*Materials Science and Engineering - An Introduction*', John Wiley & Sons, INC: New York, USA.

Cengel, Y.A. & Boles, M.A. (2006) '*Thermodynamics An Engineering Approach (5th edition)*', McGraw-Hill: New York, USA.

Chen, B., Wang, T., Maloney, J. & Newman, M. (1983) 'Measured and predicted cooling performance of earth contact cooling tubes', *Proc. ASES Annual Meet*: Minneapolis, MN, USA.

CIBSE Guide B. (2005) '*Heating, Ventilation, air conditioning, and refrigeration*', London, UK.

Clarke, J.A. (1977) 'Environmental Systems Performance', *PhD thesis*, University of Strathclyde, Glasgow, UK.

Clarke, J.A. (2001) '*Energy Simulation in Building Design (2nd edition)*', Butterworth Heinemann: Oxford, UK.

De Paepe, M. (2002) 'Three dimensional time accurate unstructured finite volume technique for modelling ground-coupled heat exchangers', *Proceedings of HEFAT2002*, Satara Kamp, Kruger National Park, South Africa.

De Paepe, M. & Janssens, A. (2003) 'Thermo-hydraulic design of earth-air heat exchangers', *Energy and Buildings*, 35 (4), pp389-397.

Dhaliwal, A. & Goswami, D. (1984) 'Heat transfer analysis environment control using an underground air tunnel', *ASME Solar Energy Div.*: Las Vegas, USA, pp505-510.

Elmer, D. & Schiller, G. (1981) 'A preliminary examination of the dehumidification potential of earth-air heat exchangers', *Proc. 1st Nat. Passive Cooling Conf.*, Miami, FL, pp161-165.

Francis, C. (1981) 'Earth cooling tubes-case studies of three Midwest installations', *Proceedings of the international passive cooling conference*: Miami, Florida, pp171-175.

Gauthier, C., Lacroix, M. & Bernier, H. (1997) 'Numerical simulation of soil heat exchanger-storage systems for greenhouses', *Solar Energy*, 60 (6), pp333-346.

Ghosal, M.K. & Tiwari, G.N. (2006) 'Modelling and parametric studies for thermal performance of an earth to air heat exchanger integrated with a greenhouse', *Energy Conversion and Management*, 47 (13-14), pp1779-1798.

Giardina, J.J. (1995) 'Evaluation of ground coupled heat pumps for the state of Wisconson', *Masters of science*, university of Wisconson-Madison.

Givoni, B. (1994) '*Passive and Low Energy Cooling of Buildings*', John Wiley & Sons, Inc.: New York, USA.

Glasgow City Council Building Services. (2000) 'Drumchapel Sports Centre', Glasgow, UK.

Glasgow City Council Development and Regeneration Services. (2001) 'Drumchapel Sports Centre', Glasgow, UK.

Gnielinski, V. (1976) 'New Equations for Heat and Mass Transfer in Turbulent Pipe and Channel Flow', *Int.Chem.Eng.*, 16, pp359.

Goswami, D.Y. & Ileslamlou, S. (1990) 'Performance analysis of a closed-loop climate control system using underground air tunnel', *Journal of Solar Energy Engineering*, 112, pp76-81.

Grazzini , G. (1993) 'Irreversible Refrigerators with isothermal heat exchangers', *International Journal of Refrigeration*, 16 (2), pp101-106.

Grondzik, W. (2007) '*Air-Conditioning System Design Manual (2nd edition)*', Butterworth-Heinemann: Oxford, UK.

Gygli, W. & Fort, K. (1994) Trnsys-model type 60 for hypocaust thermal storage and floor heating.

Hand, J.W. (1998) 'Removing barriers to the use of simulation in the building design professions', *PhD thesis*, University of Strathclyde, Glasgow, UK.

Harris, D.J. & Elliot, C.J. (1997) 'Energy Accounting for Recycled Building Components, *Proc. 2nd Int. Conf. on Buildings and the Environment*: CIB TG8 (Paris), France.

Hensen, J.L.M. (1991) 'On the thermal interaction of building structure and heating and ventilating systems', *PhD thesis*, Eindhoven University of Technology, Eindhoven, Netherlands.

Hollmuller, P. (2003) 'Analytical characterisation of amplitude-dampening and phase-shifting in air/soil heat-exchangers', *International Journal of Heat and Mass Transfer*, 46 (22), pp4303-4317.

Hollmuller, P. & Lachal, B. (2001) 'Cooling and preheating with buried pipe systems: monitoring, simulation and economic aspects', *Energy and Buildings*, 33 (5), pp509-518.

Hollmuller, P. & Lachal, B. (2005) 'Buried pipe systems with sensible and latent heat exchange: Validation of numerical simulation against analytical solution and long-term monitoring', *Ninth International IBPSA Conference*: Montreal, Canada.

Huber, A. & Remund, S. (1996) 'Wiederstands-Kapazitaten-Model WKM_Lte: Program for the simulation of air-earth heat exchangers', Huber Energietechnik: Zurich, Switzeland.

IEA. (2008) Home/Statistics/Indicators. http://www.iea.org/stats/index.asp.

IEA. (2009) 'Annex 44 Integrating Environmentally Responsive Elements in Buildings', *IEA Research*, Paris, France.

Jenkins, D.P. (2009) 'The Importance of Office Internal Heat Gains in Reducing Cooling Loads in a Changing Climate', *International Journal of Low-Carbon Technologies*, 4 (3), pp134-140.

Jiménez, C.C., Tejedor, M., Díaz, F. & Rodríguez, C.M. (2005) Effectiveness of sand mulch in soil and water conservation in an arid region, Lanzarote, Canary Islands, Spain', *Journal os soil and water conservation*, 60 (1), pp63-66.

Kasuda, T. & Archenbach, P.R. (1965) 'Earth Temperature amd Thermal Diffusivity at Selected Stations in the United States', *ASHRAE Transactions*, Vol. 71, Part 1.

Kelly, N.J. (1998) 'Towards a design environment for building-integrated energy systems: the integration of electrical power flow modelling with building simulation', *PhD thesis*, University of Strathclyde, Glasgow, UK.

Kumara, R., Rameshb, S. & Kaushika, S.C. (2003) 'Performance evaluation and energy conservation potential of earth-air-tunnel system coupled with non-air-conditioned building', *Building and Environment*, 38, pp807-813.

Levit, H.J., Gaspar, R. & Piacentini, R.D. (1989) 'Simulation of greenhouse microclimate produced by earth tube heat exchangers', *Agricultural and Forest Meteorology*, 47 (1), pp31-47.

Loveday, D.L., Al-Ajmi, F. & Hanby, V.I. (2006) 'The cooling potential of earth-air heat exchangers for domestic buildings in a desert climate', *Building and Environment*, 41 (3), pp235-244.

MacQueen, J. (1997) 'The modelling and simulation of energy management control systems', *PhD thesis*, University of Strathclyde, Glasgow, UK.

Mathur, J., Misra, R., Bansal, V., Agarwal, G. & Aseri, T. (2012) 'Thermal performance investigation of hybrid earth air tunnel heat exchanger', *Energy and Buildings*.

Mihalakakou, G., Santamouris, M. & Asimakopoulos, D. (1995) 'Parametric prediction of the buried pipes cooling potential for passive cooling applications', *Solar Energy*, 55, pp163-173.

Mihalakakou, G., Santamouris, M. & Asimakopoulos, D. (1994) 'Modelling the thermal performance of earth-to-air heat exchangers', *Solar Energy*, 53 (3), pp301-305.

Nakhi, A.E. (1995) 'Adaptive construction modelling within whole building dynamic simulation', *PhD thesis*, University of Strathclyde, Glasgow, UK.

Negrao, C.O.R. (1995) 'Conflation of computational fluid dynamics and building thermal simulation', *PhD thesis*, University of Strathclyde, Glasgow, UK.

NERC. (2010) 'BGS Report No: GR_200370', *British Geological Survey*- Natural Environment Research Council, Swindon, UK.

Olesen, B. (2008) 'International standards for the indoor enviroment. Where are we and do they apply worldwide?', *Technical report*, Technical University of Denmark, International Centre for Indoor Environment and Energy: Lyngby, Denmark.

Peel, M.C., Finlayson, B.L. & Mcmahon, T.A. (2007) 'Updated world map of the Koppen-Geiger climate classification', *Hydrology and Earth System Sciences*, 4, pp439-473.

Petukhov, B.S., Irvine, T.F. & Hartnett, J.P. (1970) '*Advances in Heat Transfer (6th edition)*', Academic Press: New York, USA.

Pfafferott, J. (2003) 'Evaluation of earth-to-air heat exchangers with a standardised method to calculate energy efficiency', *Energy and Buildings*, 35 (10), pp971-983.

Rodriguez, E.A., Cjudo, J.M. & Alvarez, S. (1988) 'Earth-tube systems performance', *Proc. CIB Meeting, Air Quality and Air Conditioning*, Paris, France.

Santamouris, M. & Asimakopoulos, D. (1996) '*Passive Cooling of Buildings*', James & James (Science Publishers) Ltd: London, UK.

Santamouris, M. & Lefas, C.C. (1986) 'Thermal analysis and computer control of hybrid greenhouses with subsurface heat storage', *Energy in Agriculture*, 5 (2), pp161-173.

Sawhney, R., Buddhi, D. & Thanu, N. (1999) 'An experimental study of summer performance of a recirculation type underground air pipe air conditioning system', *Building and Environment*, 34, pp189-196.

Schiller, G. (1982) 'Earth tubes for passive cooling, The development of a transient numerical model for predicting the performance of earth/air heat exchangers', *Project Report for MS degree*, MIT, Mechanical Engineering.

Seroa da Motta, A.L.T. & Younf, A.N. (1985) 'The predicted performance of buried pipe cooling system for hot humid climates', *Proc. of Solar Engineering Conf.*, TN, USA.

Serres, L., Trombe, A. & Conilh, J.H. (1997) 'Study of coupled energy saving systems sensitivity factor analysis', *Building and Environment*, 32 (2), pp137-148.

Shingari, B. (1995) 'Earth tube heat exchanger', *Poultry International*, 34 (14), pp92-97.

Sodha, M.S., Goyal, I., Bansal, K. & Kumar, A. (1984) 'Temperature Distribution in an Earth-Air Tunnel System'

Sodha, M.S., Sharma, A., Singh, S. & Bansal, K. (1985) 'Evaluation of an earth-air tunnel system for cooling/heating of a hospital complex', *Building and Environment*, 20 (2), pp115-122.

Thiers, S. & Peuportier, B. (2008) 'Thermal and environmental assessment of a passive building equipped with an earth-to-air heat exchanger in France', *Solar Energy*, 82 (9), pp820-831.

Tiwari, G.N., Lugani, N. & Singh, A.K. (1993) 'Design parameters of a non-air-conditioned cinema hall for thermal comfort under arid-zone climatic conditions', *Energy and Buildings*, 19 (4), pp249-261.

Tjelflaat, P.O. (2002) 'Media School: Case study report in principles of hybrid ventilation (Ed. Heiselberg) hybrid ventilation centre', Aalborg University: Aalborg, Norway.

Tombazis, A., Argiriou, A. & Santamouris, M. (1990) 'Performance Evaluation of Passive and Hybrid Cooling Components for a Hotel Complex', *International Journal of Solar Energy*, 9 (1), pp1-12.

UN Population Division. (2001) 'World Population Prospects: The 2000 Revision', United Nations: New York.

Wachenfeldt, B.J. (2003) 'Natural Ventilation in Buildings Detailed Prediction of Energy Performance', *PhD Thesis*, Norwegian University of Science and Technology, Trondheim, Norway.

Wang, S.K., Lavan, Z. & Norton, P. (2000) *'Air Conditioning and Refrigeration Engineering'*, CRC Press: New York, USA.

Watkins, R., Palmer, J., Kolokotroni, M. & Littlefair, P. (2002) 'The London Heat Island: Results from summertime monitoring', *Building Services Engineering Research and Technology*, 23 (2), pp97-106.

WBCSD. (2004) 'Facts and Trends to 2050 - Energy and Climate Change', *World Energy Congress*, Sydney, Australia.

White, F.M. (1987) '*Fluid Mechanics*', McGraw-Hill Book Company.

Winkelmann, F. & Clarke, J.A. (1986) 'Implementation of Time-step Control in ESP', *Technical note*, Lawrence Berkley Laboratory, USA.

Winkler, J. (2009) 'Development of a Component Based Simulation Tool for the State and Transient Analysis of Vapour Compression Systems', *PhD thesis*, University of Maryland, College Park , USA.

Wu, J. & Nofziger, D.L. (1999) 'Incorporating temperature effects on pesticide degradation into a management model', *J.Environ.Qual*, 28, pp92-100.

Appendix A : A/C System Factory Specifications

Table A.1: A/C chiller specifications manufactured by Trane Company.

WCZ060F100—A AT 1100 CFM
(CAPACITIES ARE NET IN BTUH/1000-INDOOR FAN HEAT DEDUCTED)

O.D. D.B.	I.D. W.B.	TOTAL CAP.	SENS. CAP. AT ENTERING D.B. TEMP. 72	74	76	78	80	COMPR. KW	APP.DEW PT.
85	59	28.4	23.6	25.5	27.4	28.7*	29.4*	1.56	46.7
	63	30.4	19.7	21.7	23.6	25.5	27.5	1.58	50.7
	67	32.6	15.5	17.4	19.4	21.3	23.3	1.61	54.9
	71	34.8	11.2	13.1	15.1	17.0	18.9	1.63	59.2
90	59	27.2	23.0	25.0	26.9	27.7*	28.4*	1.66	47.3
	63	29.2	19.2	21.2	23.1	25.0	27.0	1.69	51.2
	67	31.3	15.0	17.0	18.9	20.8	22.8	1.72	55.4
	71	33.5	10.7	12.6	14.6	16.5	18.5	1.75	59.7
95	59	25.9	22.5	24.5	26.1*	26.8*	27.4*	1.77	47.9
	63	27.9	18.7	20.7	22.6	24.5	26.5	1.80	51.8
	67	30.0	14.5	16.5	18.4	20.3	22.3	1.83	56.0
	71	32.1	10.2	12.2	14.1	16.1	18.0	1.86	60.3
100	59	24.7	22.0	23.9	25.1*	25.8*	26.4*	1.87	48.5
	63	26.6	18.2	20.1	22.1	24.0	26.0	1.90	52.4
	67	28.7	14.0	16.0	17.9	19.9	21.8	1.94	56.6
	71	30.7	9.8	11.7	13.6	15.6	17.5	1.98	60.8
105	59	23.5	21.5	23.5*	4.1*	24.8*	25.4*	1.97	49.1
	63	25.4	17.7	19.6	21.6	23.5	25.4*	2.01	53.0
	67	27.4	13.5	15.5	17.4	19.4	21.3	2.05	57.1
	71	29.4	9.3	11.2	13.2	15.1	17.1	2.09	61.4
115	59	21.1	20.4	21.6*	22.2*	22.8*	23.5*	2.18	50.3
	63	22.9	16.7	18.6	20.6	22.5	23.5*	2.23	54.1
	67	24.8	12.6	14.5	16.5	18.4	20.3	2.28	58.3
	71	26.7	8.4	10.3	12.2	14.2	16.1	2.33	62.5

CORRECTION FACTORS - OTHER AIRFLOWS
(multiply or add as indicated)

AIRFLOW	975	1250
TOTAL CAP.	X0.99	X1.01
SENS. CAP.	X0.95	X1.06
COMPR. KW	X1.00	X1.00
A.D.P.	-1.2	+1.1

VALUES AT ARI RATING CONDITIONS

TOTAL NET CAPACITY = 30000 BTUH
AIRFLOW = 1100 CFM
APP. DEW PT. = 56.0 DEG. F
COMPRESSOR POWER = 1830 WATTS
I.D. FAN POWER = 140 WATTS
O.D. FAN POWER = 340 WATTS
E.E.R. = 13.00 BTUH/WATT

*** DRY COIL CONDITION (TOTAL CAPACITY = SENSIBLE CAPACITY)**
TOTAL CAPACITY, COMP. KW AND APP. DEW PT. ARE VALID ONLY FOR WET COIL
ALL TEMPERATURES IN DEGREES F.

Appendix B : Implementation of A/C and Culvert Hybrid Cooling System Controller in ESP-r

Synopsis

```
This is a synopsis of the implementation of the hybrid sensible
cooling control strategy defined in cntr-str.cfg generated on Mon
Oct 10 22:02:24 2011. The model is located at latitude 24.70 with a
longitude difference of 1.80 from the local time meridian. The year
used in simulations is 1988. The site exposure is typical city
centre and the ground reflectance is 0.20.

The climate used is: RIYADH - SAU and is held in:
/usr/esru/esp-r/climate/Hot_climate and uses hour centred solar
data.

There are currently  2 user defined ground temperature profiles.
Ground temperatures Jan-Dec:
26.0  23.6  22.1  22.0  22.2  25.4  28.2  30.6  32.5  32.2  31.4
29.0
Ground temperatures Jan-Dec:
14.0  17.0  20.0  26.0  26.0  26.0  26.0  26.0  26.0  26.0  22.0
15.0

Databases associated with the model:
 pressure distributions : pressc.db1
 materials              : /usr/esru/esp-r/databases/constr.db1
 constructions          : /usr/esru/esp-r/databases/multicon.db1
 plant components       : plantc.db1
 event profiles         : /usr/esru/esp-r/databases/profiles.db2.a
 optical properties     : optics.db2

 ____________________________________________________________


Zones control includes  3 functions.

The sensor for function  1 senses dry bulb temperature in Living-
room. The actuator for function  1 is the air point in Living-room.
There have been  5 day types defined.

Day type  1 is valid Fri-01-Jan to Tue-01-Mar, 1988 with  1 periods.
Per|Start|Sensing  |Actuating  | Control law       | Data
1  0.00 db temp   > flux      basic control       3000.0 0.0 0.0 0.0
20.0 100.0 0.0
basic control: max heating capacity 3000.0W min heating capacity
0.0W max cooling capacity 0.0W min cooling capacity 0.0W. Heating
setpoint 20.00C cooling setpoint 100.00C.

Day type  2 is valid Wed-02-Mar to Fri-15-Apr, 1988 with  1 periods.
Per|Start|Sensing  |Actuating  | Control law       | Data
1  0.00 db temp   > flux      free floating
```

Day type 3 is valid Sat-16-Apr to Sat-15-Oct, 1988 with 1 periods.
Per|Start|Sensing |Actuating | Control law | Data
1 0.00 db temp > flux basic control 0.0 0.0 6000.0 0.0 20.0 27.0 0.0
basic control: max heating capacity 0.0W min heating capacity 0.0W max cooling capacity 6000.0W min cooling capacity 0.0W. Heating setpoint 20.00C cooling setpoint 27.00C.

Day type 4 is valid Sun-16-Oct to Thu-01-Dec, 1988 with 1 periods.
Per|Start|Sensing |Actuating | Control law | Data
1 0.00 db temp > flux free floating

Day type 5 is valid Fri-02-Dec to Sat-31-Dec, 1988 with 1 periods.
Per|Start|Sensing |Actuating | Control law | Data
1 0.00 db temp > flux basic control 3000.0 0.0 0.0 0.0 20.0 100.0 0.0
basic control: max heating capacity 3000.0W min heating capacity 0.0W max cooling capacity 0.0W min cooling capacity 0.0W. Heating setpoint 20.00C cooling setpoint 100.00C.

The sensor for function 2 senses dry bulb temperature in Dining-room. The actuator for function 2 is the air point in Dining-room. There have been 5 day types defined.

Day type 1 is valid Fri-01-Jan to Tue-01-Mar, 1988 with 1 periods.
Per|Start|Sensing |Actuating | Control law | Data
1 0.00 db temp > flux basic control 3000.0 0.0 0.0 0.0 20.0 100.0 0.0
basic control: max heating capacity 3000.0W min heating capacity 0.0W max cooling capacity 0.0W min cooling capacity 0.0W. Heating setpoint 20.00C cooling setpoint 100.00C.

Day type 2 is valid Wed-02-Mar to Fri-15-Apr, 1988 with 1 periods.
Per|Start|Sensing |Actuating | Control law | Data
1 0.00 db temp > flux free floating

Day type 3 is valid Sat-16-Apr to Sat-15-Oct, 1988 with 1 periods.
Per|Start|Sensing |Actuating | Control law | Data
1 0.00 db temp > flux basic control 0.0 0.0 6000.0 0.0 20.0 27.0 0.0
basic control: max heating capacity 0.0W min heating capacity 0.0W max cooling capacity 6000.0W min cooling capacity 0.0W. Heating setpoint 20.00C cooling setpoint 27.00C.

Day type 4 is valid Sun-16-Oct to Thu-01-Dec, 1988 with 1 periods.
Per|Start|Sensing |Actuating | Control law | Data
1 0.00 db temp > flux free floating

Day type 5 is valid Fri-02-Dec to Sat-31-Dec, 1988 with 1 periods.
Per|Start|Sensing |Actuating | Control law | Data
1 0.00 db temp > flux basic control 3000.0 0.0 0.0 0.0 20.0 100.0 0.0
basic control: max heating capacity 3000.0W min heating capacity 0.0W max cooling capacity 0.0W min cooling capacity 0.0W. Heating setpoint 20.00C cooling setpoint 100.00C.

The sensor for function 3 senses dry bulb temperature in Bed-room.

The actuator for function 3 is the air point in Bed-room. There have been 5 day types defined.

Day type 1 is valid Fri-01-Jan to Tue-01-Mar, 1988 with 1 periods.
Per|Start|Sensing |Actuating | Control law | Data
1 0.00 db temp > flux basic control 3000.0 0.0 0.0 0.0 20.0 100.0 0.0
basic control: max heating capacity 3000.0W min heating capacity 0.0W max cooling capacity 0.0W min cooling capacity 0.0W. Heating setpoint 20.00C cooling setpoint 100.00C.

Day type 2 is valid Wed-02-Mar to Fri-15-Apr, 1988 with 1 periods.
Per|Start|Sensing |Actuating | Control law | Data
1 0.00 db temp > flux free floating

Day type 3 is valid Sat-16-Apr to Sat-15-Oct, 1988 with 1 periods.
Per|Start|Sensing |Actuating | Control law | Data
1 0.00 db temp > flux basic control 0.0 0.0 6000.0 0.0 20.0 27.0 0.0
basic control: max heating capacity 0.0W min heating capacity 0.0W max cooling capacity 6000.0W min cooling capacity 0.0W. Heating setpoint 20.00C cooling setpoint 27.00C.

Day type 4 is valid Sun-16-Oct to Thu-01-Dec, 1988 with 1 periods.
Per|Start|Sensing |Actuating | Control law | Data
1 0.00 db temp > flux free floating

Day type 5 is valid Fri-02-Dec to Sat-31-Dec, 1988 with 1 periods.
Per|Start|Sensing |Actuating | Control law | Data
1 0.00 db temp > flux basic control 3000.0 0.0 0.0 0.0 20.0 100.0 0.0
basic control: max heating capacity 3000.0W min heating capacity 0.0W max cooling capacity 0.0W min cooling capacity 0.0W. Heating setpoint 20.00C cooling setpoint 100.00C.

 Zone to contol loop linkages:
 zone (1) Living-room << control 1
 zone (2) Dining-room << control 2
 zone (3) Bed-room << control 3
 zone (4) tube-1 << control 0
 zone (5) tube-2 << control 0
 zone (6) tube-3 << control 0
 zone (7) tube-4 << control 0
 zone (8) tube-5 << control 0
 zone (9) tube-6 << control 0

Flow control includes 9 loops.

The sensor for function 1 senses ambient dry bulb temperature.
The actuator for function 1 is flow connection: 13 north - Living-room via Grill. There have been 1 day types defined.

Day type 1 is valid Fri-01-Jan to Sat-31-Dec, 1988 with 1 periods.
Per|Start|Sensing |Actuating | Control law | Data
1 0.00 outside ambient > flo low/default/mid/hi 16.0 21.0 25.0 0.0 1.0 0.0
range setpoints: low 16.00 mid 21.00 high 25.00 actuation ranges: low (< low sp) 0.00 mid (>mid sp) 1.00 high (>high sp) 0.00.

```
The sensor for function  2 senses ambient dry bulb temperature.
The actuator for function  2 is flow connection:  14 east - Living-
room via Grill. There have been  1 day types defined.

Day type  1 is valid Fri-01-Jan to Sat-31-Dec, 1988 with  1 periods.
Per|Start|Sensing  |Actuating  | Control law       | Data
1  0.00 outside ambient > flo low/default/mid/hi  16.0 21.0 25.0 0.0
1.0 0.0
range setpoints: low 16.00 mid 21.00 high 25.00 actuation ranges:
low (< low sp) 0.00 mid (>mid sp) 1.00 high (>high sp) 0.00.

The sensor for function  3 senses ambient dry bulb temperature.
The actuator for function  3 is flow connection:  16 north - Dining-
room via Grill. There have been  1 day types defined.

Day type  1 is valid Fri-01-Jan to Sat-31-Dec, 1988 with  1 periods.
Per|Start|Sensing  |Actuating  | Control law       | Data
1  0.00 outside ambient > flo low/default/mid/hi  16.0 21.0 25.0 0.0
1.0 0.0
range setpoints: low 16.00 mid 21.00 high 25.00 actuation ranges:
low (< low sp) 0.00 mid (>mid sp) 1.00 high (>high sp) 0.00.

The sensor for function  4 senses ambient dry bulb temperature.
The actuator for function  4 is flow connection:  17 west - Dining-
room via Grill. There have been  1 day types defined.

Day type  1 is valid Fri-01-Jan to Sat-31-Dec, 1988 with  1 periods.
Per|Start|Sensing  |Actuating  | Control law       | Data
1  0.00 outside ambient > flo low/default/mid/hi  16.0 21.0 25.0 0.0
1.0 0.0
range setpoints: low 16.00 mid 21.00 high 25.00 actuation ranges:
low (< low sp) 0.00 mid (>mid sp) 1.00 high (>high sp) 0.00.

The sensor for function  5 senses ambient dry bulb temperature.
The actuator for function  5 is flow connection:  19 west - Bed-room
via Grill. There have been  1 day types defined.

Day type  1 is valid Fri-01-Jan to Sat-31-Dec, 1988 with  1 periods.
Per|Start|Sensing  |Actuating  | Control law       | Data
1  0.00 outside ambient > flo low/default/mid/hi  16.0 21.0 25.0 0.0
1.0 0.0
range setpoints: low 16.00 mid 21.00 high 25.00 actuation ranges:
low (< low sp) 0.00 mid (>mid sp) 1.00 high (>high sp) 0.00.

The sensor for function  6 senses ambient dry bulb temperature.
The actuator for function  6 is flow connection:  20 south - Bed-
room via Grill. There have been  1 day types defined.

Day type  1 is valid Fri-01-Jan to Sat-31-Dec, 1988 with  1 periods.
Per|Start|Sensing  |Actuating  | Control law       | Data
1  0.00 outside ambient > flo low/default/mid/hi  16.0 21.0 25.0 0.0
1.0 0.0
range setpoints: low 16.00 mid 21.00 high 25.00 actuation ranges:
low (< low sp) 0.00 mid (>mid sp) 1.00 high (>high sp) 0.00.

The sensor for function  7 senses ambient dry bulb temperature.
The actuator for function  7 is flow connection:  10 Living-room -
External_pt via Fan. There have been  9 day types defined.
Day type  1 is valid Fri-01-Jan to Tue-01-Mar, 1988 with  1 periods.
```

```
Per|Start|Sensing  |Actuating  | Control law       | Data
1  0.00 outside ambient > flo low/default/mid/hi  15.0 22.0 30.0 0.5
1.0 0.5
range setpoints: low 15.00 mid 22.00 high 30.00 actuation ranges:
low (< low sp) 0.50 mid (>mid sp) 1.00 high (>high sp) 0.50.

Day type  2 is valid Wed-02-Mar to Fri-01-Apr, 1988 with  2 periods.
Per|Start|Sensing  |Actuating  | Control law       | Data
1  0.00 outside ambient > flo on / off            0.0 1.0 0.0
on/off setpoint 0.00 direct action ON fraction 0.000.
2  9.00 outside ambient > flo low/default/mid/hi  15.0 22.0 30.0 0.5
1.0 0.5
range setpoints: low 15.00 mid 22.00 high 30.00 actuation ranges:
low (< low sp) 0.50 mid (>mid sp) 1.00 high (>high sp) 0.50.

Day type  3 is valid Sat-02-Apr to Sun-01-May, 1988 with  3 periods.
Per|Start|Sensing  |Actuating  | Control law       | Data
1  0.00 outside ambient > flo low/default/mid/hi  15.0 22.0 30.0 0.5
1.0 0.5
range setpoints: low 15.00 mid 22.00 high 30.00 actuation ranges:
low (< low sp) 0.50 mid (>mid sp) 1.00 high (>high sp) 0.50.
2  2.00 outside ambient > flo on / off            0.0 1.0 0.0
on/off setpoint 0.00 direct action ON fraction 0.000.
3  6.00 outside ambient > flo low/default/mid/hi  15.0 22.0 30.0 0.5
1.0 0.5
range setpoints: low 15.00 mid 22.00 high 30.00 actuation ranges:
low (< low sp) 0.50 mid (>mid sp) 1.00 high (>high sp) 0.50.

Day type  4 is valid Mon-02-May to Fri-01-Jul, 1988 with  1 periods.
Per|Start|Sensing  |Actuating  | Control law       | Data
1  0.00 outside ambient > flo low/default/mid/hi  15.0 22.0 30.0 0.5
1.0 0.5
range setpoints: low 15.00 mid 22.00 high 30.00 actuation ranges:
low (< low sp) 0.50 mid (>mid sp) 1.00 high (>high sp) 0.50.

Day type  5 is valid Sat-02-Jul to Thu-01-Sep, 1988 with  2 periods.
Per|Start|Sensing  |Actuating  | Control law       | Data
1  0.00 outside ambient > flo on / off            0.0 1.0 0.0
on/off setpoint 0.00 direct action ON fraction 0.000.
2  8.00 outside ambient > flo low/default/mid/hi  15.0 22.0 30.0 0.5
1.0 0.5
range setpoints: low 15.00 mid 22.00 high 30.00 actuation ranges:
low (< low sp) 0.50 mid (>mid sp) 1.00 high (>high sp) 0.50.

Day type  6 is valid Fri-02-Sep to Sat-01-Oct, 1988 with  3 periods.
Per|Start|Sensing  |Actuating  | Control law       | Data
1  0.00 outside ambient > flo on / off            0.0 1.0 0.0
on/off setpoint 0.00 direct action ON fraction 0.000.
2  8.00 outside ambient > flo low/default/mid/hi  15.0 22.0 30.0 0.5
1.0 0.5
range setpoints: low 15.00 mid 22.00 high 30.00 actuation ranges:
low (< low sp) 0.50 mid (>mid sp) 1.00 high (>high sp) 0.50.
3 22.00 outside ambient > flo on / off            0.0 1.0 0.0
on/off setpoint 0.00 direct action ON fraction 0.000.



Day type  7 is valid Sun-02-Oct to Tue-01-Nov, 1988 with  3 periods.
```

```
Per|Start|Sensing  |Actuating  | Control law       | Data
1  0.00 outside ambient > flo on / off            0.0 1.0 0.0
on/off setpoint 0.00 direct action ON fraction 0.000.
2 10.00 outside ambient > flo low/default/mid/hi  15.0 22.0 30.0 0.5
1.0 0.5
range setpoints: low 15.00 mid 22.00 high 30.00 actuation ranges:
low (< low sp) 0.50 mid (>mid sp) 1.00 high (>high sp) 0.50.
3 18.00 outside ambient > flo on / off            0.0 1.0 0.0
on/off setpoint 0.00 direct action ON fraction 0.000.

Day type  8 is valid Wed-02-Nov to Thu-01-Dec, 1988 with  3 periods.
Per|Start|Sensing  |Actuating  | Control law       | Data
1  0.00 outside ambient > flo on / off            0.0 1.0 0.0
on/off setpoint 0.00 direct action ON fraction 0.000.
2 12.00 outside ambient > flo low/default/mid/hi  15.0 22.0 30.0 0.5
1.0 0.5
range setpoints: low 15.00 mid 22.00 high 30.00 actuation ranges:
low (< low sp) 0.50 mid (>mid sp) 1.00 high (>high sp) 0.50.
3 16.00 outside ambient > flo on / off            0.0 1.0 0.0
on/off setpoint 0.00 direct action ON fraction 0.000.

Day type  9 is valid Fri-02-Dec to Sat-31-Dec, 1988 with  1 periods.
Per|Start|Sensing  |Actuating  | Control law       | Data
1  0.00 outside ambient > flo low/default/mid/hi  15.0 22.0 30.0 0.5
1.0 0.5
range setpoints: low 15.00 mid 22.00 high 30.00 actuation ranges:
low (< low sp) 0.50 mid (>mid sp) 1.00 high (>high sp) 0.50.

The sensor for function  8 senses ambient dry bulb temperature.
The actuator for function  8 is flow connection:  11 Dining-room -
External_pt via Fan. There have been  9 day types defined.

Day type  1 is valid Fri-01-Jan to Tue-01-Mar, 1988 with  1 periods.
Per|Start|Sensing  |Actuating  | Control law       | Data
1  0.00 outside ambient > flo low/default/mid/hi  15.0 22.0 30.0 0.5
1.0 0.5
range setpoints: low 15.00 mid 22.00 high 30.00 actuation ranges:
low (< low sp) 0.50 mid (>mid sp) 1.00 high (>high sp) 0.50.

Day type  2 is valid Wed-02-Mar to Fri-01-Apr, 1988 with  2 periods.
Per|Start|Sensing  |Actuating  | Control law       | Data
1  0.00 outside ambient > flo on / off            0.0 1.0 0.0
on/off setpoint 0.00 direct action ON fraction 0.000.
2  9.00 outside ambient > flo low/default/mid/hi  15.0 22.0 30.0 0.5
1.0 0.5
range setpoints: low 15.00 mid 22.00 high 30.00 actuation ranges:
low (< low sp) 0.50 mid (>mid sp) 1.00 high (>high sp) 0.50.

Day type  3 is valid Sat-02-Apr to Sun-01-May, 1988 with  3 periods.
Per|Start|Sensing  |Actuating  | Control law       | Data
1  0.00 outside ambient > flo low/default/mid/hi  15.0 22.0 30.0 0.5
1.0 0.5
range setpoints: low 15.00 mid 22.00 high 30.00 actuation ranges:
low (< low sp) 0.50mid (>mid sp) 1.00 high (>high sp) 0.50.
2  2.00 outside ambient > flo on / off            0.0 1.0 0.0
on/off setpoint 0.00 direct action ON fraction 0.000.
3  6.00 outside ambient > flo low/default/mid/hi  15.0 22.0 30.0 0.5
1.0 0.5
```

```
range setpoints: low 15.00 mid 22.00 high 30.00 actuation ranges:
low (< low sp) 0.50 mid (>mid sp) 1.00 high (>high sp) 0.50.

Day type  4 is valid Mon-02-May to Fri-01-Jul, 1988 with  1 periods.
Per|Start|Sensing  |Actuating  | Control law       | Data
1  0.00 outside ambient > flo low/default/mid/hi  15.0 22.0 30.0 0.5
1.0 0.5
range setpoints: low 15.00 mid 22.00 high 30.00 actuation ranges:
low (< low sp) 0.50 mid (>mid sp) 1.00 high (>high sp) 0.50.

Day type  5 is valid Sat-02-Jul to Thu-01-Sep, 1988 with  2 periods.
Per|Start|Sensing  |Actuating  | Control law       | Data
1  0.00 outside ambient > flo on / off            0.0 1.0 0.0
on/off setpoint 0.00 direct action ON fraction 0.000.
2  8.00 outside ambient > flo low/default/mid/hi  15.0 22.0 30.0 0.5
1.0 0.5
range setpoints: low 15.00 mid 22.00 high 30.00 actuation ranges:
low (< low sp) 0.50 mid (>mid sp) 1.00 high (>high sp) 0.50.

Day type  6 is valid Fri-02-Sep to Sat-01-Oct, 1988 with  3 periods.
Per|Start|Sensing  |Actuating  | Control law       | Data
1  0.00 outside ambient > flo on / off            0.0 1.0 0.0
on/off setpoint 0.00 direct action ON fraction 0.000.
2  8.00 outside ambient > flo low/default/mid/hi  15.0 22.0 30.0 0.5
1.0 0.5
range setpoints: low 15.00 mid 22.00 high 30.00 actuation ranges:
low (< low sp) 0.50 mid (>mid sp) 1.00 high (>high sp) 0.50.
3 22.00 outside ambient > flo on / off            0.0 1.0 0.0
on/off setpoint 0.00 direct action ON fraction 0.000.

Day type  7 is valid Sun-02-Oct to Tue-01-Nov, 1988 with  3 periods.
Per|Start|Sensing  |Actuating  | Control law       | Data
1  0.00 outside ambient > flo on / off            0.0 1.0 0.0
on/off setpoint 0.00 direct action ON fraction 0.000.
2 10.00 outside ambient > flo low/default/mid/hi  15.0 22.0 30.0 0.5
1.0 0.5
range setpoints: low 15.00 mid 22.00 high 30.00 actuation ranges:
low (< low sp) 0.50 mid (>mid sp) 1.00 high (>high sp) 0.50.
3 18.00 outside ambient > flo on / off            0.0 1.0 0.0
on/off setpoint 0.00 direct action ON fraction 0.000.

Day type  8 is valid Wed-02-Nov to Thu-01-Dec, 1988 with  3 periods.
Per|Start|Sensing  |Actuating  | Control law       | Data
1  0.00 outside ambient > flo on / off            0.0 1.0 0.0
on/off setpoint 0.00 direct action ON fraction 0.000.
2 12.00 outside ambient > flo low/default/mid/hi  15.0 22.0 30.0 0.5
1.0 0.5
range setpoints: low 15.00 mid 22.00 high 30.00 actuation ranges:
low (< low sp) 0.50 mid (>mid sp) 1.00 high (>high sp) 0.50.
3 16.00 outside ambient > flo on / off            0.0 1.0 0.0
on/off setpoint 0.00 direct action ON fraction 0.000.

Day type  9 is valid Fri-02-Dec to Sat-31-Dec, 1988 with  1 periods.
Per|Start|Sensing  |Actuating  | Control law       | Data
1  0.00 outside ambient > flo low/default/mid/hi  15.0 22.0 30.0 0.5
1.0 0.5
range setpoints: low 15.00 mid 22.00 high 30.00 actuation ranges:
low (< low sp) 0.50 mid (>mid sp) 1.00 high (>high sp) 0.50.
```

```
The sensor for function  9 senses ambient dry bulb temperature.
The actuator for function  9 is flow connection:  12 Bed-room -
External_pt via Fan. There have been  9 day types defined.

Day type  1 is valid Fri-01-Jan to Tue-01-Mar, 1988 with  1 periods.
Per|Start|Sensing  |Actuating  | Control law       | Data
1  0.00 outside ambient > flo low/default/mid/hi  15.0 22.0 30.0 0.5
1.0 0.5
range setpoints: low 15.00 mid 22.00 high 30.00 actuation ranges:
low (< low sp) 0.50 mid (>mid sp) 1.00 high (>high sp) 0.50.

Day type  2 is valid Wed-02-Mar to Fri-01-Apr, 1988 with  2 periods.
Per|Start|Sensing  |Actuating  | Control law       | Data
1  0.00 outside ambient > flo on / off            0.0 1.0 0.0
on/off setpoint 0.00 direct action ON fraction 0.000.
2  9.00 outside ambient > flo low/default/mid/hi  15.0 22.0 30.0 0.5
1.0 0.5
range setpoints: low 15.00 mid 22.00 high 30.00 actuation ranges:
low (< low sp) 0.50 mid (>mid sp) 1.00 high (>high sp) 0.50.

Day type  3 is valid Sat-02-Apr to Sun-01-May, 1988 with  3 periods.
Per|Start|Sensing  |Actuating  | Control law       | Data
1  0.00 outside ambient > flo low/default/mid/hi  15.0 22.0 30.0 0.5
1.0 0.5
range setpoints: low 15.00 mid 22.00 high 30.00 actuation ranges:
low (< low sp) 0.50 mid (>mid sp) 1.00 high (>high sp) 0.50.
2  2.00 outside ambient > flo on / off            0.0 1.0 0.0
on/off setpoint 0.00 direct action ON fraction 0.000.
3  6.00 outside ambient > flo low/default/mid/hi  15.0 22.0 30.0 0.5
1.0 0.5
range setpoints: low 15.00 mid 22.00 high 30.00 actuation ranges:
low (< low sp) 0.50 mid (>mid sp) 1.00 high (>high sp) 0.50.

Day type  4 is valid Mon-02-May to Fri-01-Jul, 1988 with  1 periods.
Per|Start|Sensing  |Actuating  | Control law       | Data
1  0.00 outside ambient > flo low/default/mid/hi  15.0 22.0 30.0 0.5
1.0 0.5
range setpoints: low 15.00 mid 22.00 high 30.00 actuation ranges:
low (< low sp) 0.50 mid (>mid sp) 1.00 high (>high sp) 0.50.

Day type  5 is valid Sat-02-Jul to Thu-01-Sep, 1988 with  2 periods.
Per|Start|Sensing  |Actuating  | Control law       | Data
1  0.00 outside ambient > flo on / off            0.0 1.0 0.0
on/off setpoint 0.00 direct action ON fraction 0.000.
2  8.00 outside ambient > flo low/default/mid/hi  15.0 22.0 30.0 0.5
1.0 0.5
range setpoints: low 15.00 mid 22.00 high 30.00 actuation ranges:
low (< low sp) 0.50 mid (>mid sp) 1.00 high (>high sp) 0.50.

Day type  6 is valid Fri-02-Sep to Sat-01-Oct, 1988 with  3 periods.
Per|Start|Sensing  |Actuating  | Control law       | Data
1  0.00 outside ambient > flo on / off            0.0 1.0 0.0
on/off setpoint 0.00 direct action ON fraction 0.000.
2  8.00 outside ambient > flo low/default/mid/hi  15.0 22.0 30.0 0.5
1.0 0.5
range setpoints: low 15.00 mid 22.00 high 30.00 actuation ranges:
low (< low sp) 0.50 mid (>mid sp) 1.00 high (>high sp) 0.50.
3 22.00 outside ambient > flo on / off            0.0 1.0 0.0
on/off setpoint 0.00 direct action ON fraction 0.000.
```

```
Day type  7 is valid Sun-02-Oct to Tue-01-Nov, 1988 with  3 periods.
Per|Start|Sensing  |Actuating  | Control law       | Data
1  0.00 outside ambient > flo on / off            0.0 1.0 0.0
on/off setpoint 0.00 direct action ON fraction 0.000.
2 10.00 outside ambient > flo low/default/mid/hi  15.0 22.0 30.0 0.5
1.0 0.5
range setpoints: low 15.00 mid 22.00 high 30.00 actuation ranges:
low (< low sp) 0.50 mid (>mid sp) 1.00 high (>high sp) 0.50.
3 18.00 outside ambient > flo on / off            0.0 1.0 0.0
on/off setpoint 0.00 direct action ON fraction 0.000.

Day type  8 is valid Wed-02-Nov to Thu-01-Dec, 1988 with  3 periods.
Per|Start|Sensing  |Actuating  | Control law       | Data
1  0.00 outside ambient > flo on / off            0.0 1.0 0.0
on/off setpoint 0.00 direct action ON fraction 0.000.
2 12.00 outside ambient > flo low/default/mid/hi  15.0 22.0 30.0 0.5
1.0 0.5
range setpoints: low 15.00 mid 22.00 high 30.00 actuation ranges:
low (< low sp) 0.50 mid (>mid sp) 1.00 high (>high sp) 0.50.
3 16.00 outside ambient > flo on / off            0.0 1.0 0.0
on/off setpoint 0.00 direct action ON fraction 0.000.

Day type  9 is valid Fri-02-Dec to Sat-31-Dec, 1988 with  1 periods.
Per|Start|Sensing  |Actuating  | Control law       | Data
1  0.00 outside ambient > flo low/default/mid/hi  15.0 22.0 30.0 0.5
1.0 0.5
range setpoints: low 15.00 mid 22.00 high 30.00 actuation ranges:
low (< low sp) 0.50 mid (>mid sp) 1.00 high (>high sp) 0.50.
```

```
The model includes an air flow network.

 Flow network description.

15 nodes,   4 components,  21 connections;     wind reduction =
1.000
# Node      Fluid   Node Type           Height Temperature    Data_1
Data_2
1 Living-room  air   internal & unknown    1.2000   20.000     (-)
0.000  vol   72.001
2 Dining-room  air   internal & unknown    1.2000   20.000     (-)
0.000  vol   72.001
3 Bed-room     air   internal & unknown    1.2000   20.000     (-)
0.000  vol  144.000
4 tube-1       air   internal & unknown   -1.5000   20.000     (-)
0.000  vol    1.815
5 tube-2       air   internal & unknown   -1.5000   20.000     (-)
0.000  vol    1.950
6 tube-3       air   internal & unknown   -1.5000   20.000     (-)
0.000  vol    2.550
7 tube-4       air   internal & unknown   -1.5000   20.000     (-)
0.000  vol    2.325
8 tube-5       air   internal & unknown   -1.5000   20.000     (-)
0.000  vol    1.298
9 tube-6       air   internal & unknown   -1.5000   20.000     (-)
0.000  vol    2.325
10 ground_inlet air   boundary & wind ind   0.0000   0.0000     coef
9.000  azim   0.000
```

```
11 External_pt  air   boundary & wind ind   2.4000   0.0000     coef
4.000  azim   0.000
12 north        air   boundary & wind ind   1.2000   0.0000     coef
9.000  azim   0.000
13 east         air   boundary & wind ind   1.2000   0.0000     coef
9.000  azim  90.000
14 west         air   boundary & wind ind   1.2000   0.0000     coef
9.000  azim 270.000
15 south        air   boundary & wind ind   1.2000   0.0000     coef
9.000  azim 180.000

Component    Type C+ L+ Description

Fan            30  2  0 Constant vol. flow rate component   m =
rho.a
 Fluid  1.0 flow rate (m^3/s)  0.80000E-01

Tube          210  6  0 General flow conduit component      m =
rho.f(D,A,L,k,SCi)
   Fluid, hydr diam, x-sect, conduit ln, roughness, loss fac.
  1.0    1.000    0.790   10.000    0.010    0.500

Grill         110  2  0 Specific air flow opening           m =
rho.f(A,dP)
 Fluid  1.0 opening area (m) 10.000

crack         120  3  0 Specific air flow crack             m =
rho.f(W,L,dP)
 Fluid  1.0 crack width (m)  0.0100 crack length (m)  3.000

# +Node         dHght   -Node          dHght   Component       Z @+
Z @-
1 tube-1        0.000   tube-2         0.000   Tube           -1.500
-1.500
2 tube-2        0.000   tube-3         0.000   Tube           -1.500
-1.500
3 tube-3        0.000   tube-4         0.000   Tube           -1.500
-1.500
4 tube-4        0.000   tube-5         0.000   Tube           -1.500
-1.500
5 tube-5        0.000   tube-6         0.000   Tube           -1.500
-1.500
6 ground_inlet -0.750   tube-1         0.750   Tube           -0.750
-0.750
7 tube-6        1.350   Living-room   -1.350   Grill          -0.150
-0.150
8 tube-6        1.350   Dining-room   -1.350   Grill          -0.150
-0.150
9 tube-6        1.350   Bed-room      -1.350   Grill          -0.150
-0.150
10 Living-room   0.600   External_pt   -0.600   Fan             1.800
1.800
11 Dining-room   0.600   External_pt   -0.600   Fan             1.800
1.800
12 Bed-room      0.600   External_pt   -0.600   Fan             1.800
1.800
13 north         0.000   Living-room    0.000   Grill           1.200
1.200
```

```
14 east          0.000   Living-room   0.000   Grill          1.200
1.200
15 Living-room   0.000   east          0.000   crack          1.200
1.200
16 north         0.000   Dining-room   0.000   Grill          1.200
1.200
17 west          0.000   Dining-room   0.000   Grill          1.200
1.200
18 Dining-room   0.000   west          0.000   crack          1.200
1.200
19 west          0.000   Bed-room      0.000   Grill          1.200
1.200
20 south         0.000   Bed-room      0.000   Grill          1.200
1.200
21 Bed-room      0.000   south         0.000   crack          1.200
1.200

thermal zone to air flow node mapping:
thermal zone -> air flow node
Living-room  -> Living-room
Dining-room  -> Dining-room
Bed-room     -> Bed-room
tube-1       -> tube-1
tube-2       -> tube-2
tube-3       -> tube-3
tube-4       -> tube-4
tube-5       -> tube-5
tube-6       -> tube-6
```

```
ID Zone         Volume|          Surface
   Name         m^3   | No. Opaque  Transp  ~Floor
 1 Living-room    72.0   9   107.5     5.3    30.0  zone-1 describes
a
 2 Dining-room    72.0   9   107.5     5.3    30.0  zone-2 describes
a
 3 Bed-room      144.0  10   193.4     8.2    60.0  zone-3 describes
a
 4 tube-1          9.7   8    52.1     0.0     6.1  tube-1 describes
a
 5 tube-2         10.4  14    56.2     0.0     6.5  tube-2 describes
a
 6 tube-3         13.6  12    73.0     0.0     8.5  tube-3 describes
a
 7 tube-4         12.4  10    66.7     0.0     7.8  tube-4 describes
a
 8 tube-5          6.9  10    37.6     0.0     4.3  tube-5 describes
a
 9 tube-6         12.4  10    66.7     0.0     7.8  tube-6 describes
a
   all           353.   92    761.     19.    161.
```

```
Zone Living-room ( 1) is composed of 9 surfaces and 20 vertices.
It encloses a volume of 72.0m^3 of space, with a total surface
area of 113.m^2 & approx floor area of 30.0m^2. There is 56.400m2 of
exposed surface area, 26.400m2 of which is vertical. Outside walls
are 70.400 % of floor area & avg U of 0.737 & UA of 15.575
```

Flat roof is 100.00 % of floor area & avg U of 0.463 & UA of 13.897
Glazing is 17.600 % of floor & 20.000 % facade with avg U of 2.811 & UA of 14.840

A summary of the surfaces in Living-room(1) follows:

Sur	Area	Azim	Elev	surface	geometry	construction	environment	
	m^2	deg	deg	name	type	loca	name	other side
1	14.4	180.	0.	Wall-1	OPAQUE	VERT	intern_wall	||< Wall-8:Bed-room
2	9.60	90.	0.	Wall-2	OPAQUE	VERT	extern_wall	||< external
3	9.84	0.	0.	Wall-3	OPAQUE	VERT	extern_wall	||< external
4	30.0	0.	90.	Top-5	OPAQUE	CEIL	roof	||< external
5	30.0	0.	-90.	Base-6	OPAQUE	FLOR	grnd_floor	||< user def grnd profile 2
6	1.68	0.	0.	d	OPAQUE	VERT	door	||< external
7	12.0	270.	0.	Wall-5	OPAQUE	VERT	intern_wall	||< Wall-1:Dining-room
8	2.40	90.	0.	w	DCF767	VERT	dbl_glz	||< external
9	2.88	360.	0.	w1	DCF767	VERT	dbl_glz	||< external

Ventilation & infiltration is assessed via network analysis
and the associated network node is: Living-room

Number of weekdays, Saturday and Sunday casual gains= 16

Day	Gain No.	Type labl	Period Hours	Sensible Magn.(W)	Latent Magn. (W)	Radiant Frac	Convec Frac
Wkd	1	OccuptW	0 - 10	0.0	0.0	0.50	0.50
Wkd	2	OccuptW	10 - 14	240.0	120.0	0.50	0.50
Wkd	3	OccuptW	14 - 15	0.0	0.0	0.50	0.50
Wkd	4	OccuptW	15 - 20	240.0	120.0	0.50	0.50
Wkd	5	OccuptW	20 - 21	0.0	0.0	0.50	0.50
Wkd	6	OccuptW	21 - 24	350.0	175.0	0.50	0.50
Wkd	7	LightsW	0 - 17	0.0	0.0	0.50	0.50
Wkd	8	LightsW	17 - 20	300.0	0.0	0.50	0.50
Wkd	9	LightsW	20 - 21	0.0	0.0	0.50	0.50
Wkd	10	LightsW	21 - 24	300.0	0.0	0.50	0.50
Wkd	11	EquiptW	0 - 10	0.0	0.0	0.40	0.60
Wkd	12	EquiptW	10 - 14	200.0	100.0	0.50	0.50
Wkd	13	EquiptW	14 - 15	0.0	0.0	0.50	0.50
Wkd	14	EquiptW	15 - 20	200.0	100.0	0.50	0.50
Wkd	15	EquiptW	20 - 21	0.0	0.0	0.50	0.50
Wkd	16	EquiptW	21 - 24	200.0	100.0	0.50	0.50

Zone Dining-room (2) is composed of 9 surfaces and 20 vertices. It encloses a volume of 72.0m^3 of space, with a total surface area of 113.m^2 & approx floor area of 30.0m^2. There is 56.400m2 of exposed surface area, 26.400m2 of which is vertical. Outside walls are 70.400 % of floor area & avg U of 0.737 & UA of 15.575. Flat roof is 100.00 % of floor area & avg U of 0.463 & UA of 13.897

Glazing is 17.600 % of floor & 20.000 % facade with avg U of 2.811 & UA of 14.840

A summary of the surfaces in Dining-room(2) follows:

Sur	Area m^2	Azim deg	Elev deg	surface name	geometry type	loca	construction name	environment other side
1	12.0	90.	0.	Wall-1	OPAQUE	VERT	intern_wall	||< Wall-5:Living-room
2	9.84	0.	0.	Wall-2	OPAQUE	VERT	extern_wall	||< external
3	9.60	270.	0.	Wall-3	OPAQUE	VERT	extern_wall	||< external
4	14.4	180.	0.	Wall-4	OPAQUE	VERT	intern_wall	||< Wall-4:Bed-room
5	30.0	0.	90.	Top-5	OPAQUE	CEIL	roof	||< external
6	30.0	0.	-90.	Base-6	OPAQUE	FLOR	grnd_floor	||< user def grnd profile 2
7	1.68	0.	0.	d	OPAQUE	VERT	door	||< external
8	2.88	360.	0.	w	DCF767	VERT	dbl_glz	||< external
9	2.40	270.	0.	w1	DCF767	VERT	dbl_glz	||< external

Ventilation & infiltration is assessed via network analysis
and the associated network node is: Dining-room

Number of weekdays, Saturday and Sunday casual gains= 13

Day	Gain No.	Type labl	Period Hours	Sensible Magn.(W)	Latent Magn. (W)	Radiant Frac	Convec Frac
Wkd	1	OccuptW	0 - 9	0.0	0.0	0.50	0.50
Wkd	2	OccuptW	9 - 10	350.0	175.0	0.50	0.50
Wkd	3	OccuptW	10 - 14	70.0	30.0	0.50	0.50
Wkd	4	OccuptW	14 - 15	350.0	175.0	0.50	0.50
Wkd	5	OccuptW	15 - 20	0.0	0.0	0.50	0.50
Wkd	6	OccuptW	20 - 21	350.0	175.0	0.50	0.50
Wkd	7	OccuptW	21 - 24	0.0	0.0	0.50	0.50
Wkd	8	LightsW	0 - 20	0.0	0.0	0.50	0.50
Wkd	9	LightsW	20 - 21	300.0	0.0	0.50	0.50
Wkd	10	LightsW	21 - 24	0.0	0.0	0.50	0.50
Wkd	11	EquiptW	0 - 9	0.0	0.0	0.50	0.50
Wkd	12	EquiptW	9 - 21	200.0	100.0	0.50	0.50
Wkd	13	EquiptW	21 - 24	0.0	0.0	0.50	0.50

Zone Bed-room (3) is composed of 10 surfaces and 22 vertices. It encloses a volume of 144.m^3 of space, with a total surface area of 202.m^2 & approx floor area of 60.0m^2. There is 112.80m2 of exposed surface area, 52.800m2 of which is vertical. Outside walls are 74.400 % of floor area & avg U of 0.620 & UA of 27.679. Flat roof is 100.00 % of floor area & avg U of 0.463 & UA of 27.794. Glazing is 13.600 % of floor & 15.455 % facade with avg U of 2.811 & UA of 22.935.

A summary of the surfaces in Bed-room(3) follows:

Sur	Area	Azim	Elev	surface name	geometry type	construction loca	construction name	environment other side
	m^2	deg	deg					
1	9.60	270.	0.	Wall-1	OPAQUE VERT	extern_wall	||<	external
2	21.4	180.	0.	Wall-2	OPAQUE VERT	extern_wall	||<	external
3	12.0	90.	0.	Wall-3	OPAQUE VERT	extern_wall	||<	external
4	60.0	0.	90.	Top-5	OPAQUE CEIL	roof	||<	external
5	60.0	0.	-90.	Base-6	OPAQUE FLOR	grnd_floor	||<	user def grnd profile 2
6	1.68	180.	0.	d	OPAQUE VERT	door	||<	external
7	14.4	0.	0.	Wall-8	OPAQUE VERT	intern_wall	||<	Wall-1:Living-room
8	14.4	0.	0.	Wall-4	OPAQUE VERT	intern_wall	||<	Wall-4:Dining-room
9	5.76	180.	0.	w	DCF767 VERT	dbl_glz	||<	external
10	2.40	270.	0.	w1	DCF767 VERT	dbl_glz	||<	external

Ventilation & infiltration is assessed via network analysis
and the associated network node is: Bed-room

Number of weekdays, Saturday and Sunday casual gains= 4

Day	Gain No.	Type labl	Period Hours	Sensible Magn.(W)	Latent Magn. (W)	Radiant Frac	Convec Frac
Wkd	1	OccuptW	0 - 9	350.0	175.0	0.50	0.50
Wkd	2	OccuptW	9 - 24	150.0	75.0	0.50	0.50
Wkd	3	LightsW	0 - 24	0.0	0.0	0.50	0.50
Wkd	4	EquiptW	0 - 24	100.0	50.0	0.50	0.50

Zone tube-1 (4) is composed of 8 surfaces and 12 vertices.It encloses a volume of 9.68m^3 of space, with a total surface area of 52.1m^2 & approx floor area of 6.05m^2.There is 6.0500m2 of exposed surface area. Flat roof is 100.00 % of floor area & avg U of 0.823 & UA of 4.9795

A summary of the surfaces in tube-1(4) follows:

Sur	Area	Azim	Elev	surface name	geometry type	construction loca	construction name	environment other side
	m^2	deg	deg					
1	18.4	179.	0.	Wall-1	OPAQUE VERT	earth-side	||<	user def grnd profile 1
2	1.60	90.	0.	Wall-2	OPAQUE VERT	earth-side	||<	user def grnd profile 1

```
  3  0.800     0.   0. end-1        OPAQUE VERT insul-frame  ||<
start-2:tube-2
  4  0.800   270.   0. Wall-4       OPAQUE VERT earth-side   ||<
user def grnd profile  1
  5  17.6    359.   0. Wall-5       OPAQUE VERT earth-side   ||<
user def grnd profile  1
  6  0.800   270.   0. Inlet        OPAQUE VERT earth-side   ||<
user def grnd profile  1
  7  6.05      0.  90. Top-7        OPAQUE CEIL earth-side   ||<
external
  8  6.05      0. -90. Base-8       OPAQUE FLOR earth-side   ||<
user def grnd profile  1


 Number of control periods:  1
 Number of surfaces = 8

 Period  1 start   0.00 finish  24.00
 User specified convection coefficients
 User supplied hc values
 Surface            Inside   Outside
 1 Wall-1       (VERT)     13.000    -1.000
 2 Wall-2       (VERT)     13.000    -1.000
 3 end-1        (VERT)     13.000    -1.000
 4 Wall-4       (VERT)     13.000    -1.000
 5 Wall-5       (VERT)     13.000    -1.000
 6 Inlet        (VERT)     13.000    -1.000
 7 Top-7        (CEIL)     13.000    -1.000
 8 Base-8       (FLOR)     13.000    -1.000

 Ventilation & infiltration is assessed via network analysis
 and the associated network node is: tube-1

Notes:
nothing happens in this zone in terms of occupants lights and small
power. There is not infiltration or ventilation.

 ____________________________________________________________________

Zone tube-2 ( 5) is composed of 14 surfaces and 24 vertices.It
encloses a volume of 10.4m^3 of space, with a total surface area of
56.2m^2 & approx floor area of 6.50m^2 There is 6.5000m2 of exposed
surface area.Flat roof is 100.00 % of floor area & avg U of 0.823 &
UA of 5.3499.

 A summary of the surfaces in tube-2( 5) follows:

 Sur| Area  |Azim|Elev| surface    | geometry | construction
|environment
    | m^2   |deg |deg | name       |type |loca| name         |other
side
  1  0.800   180.   0. start-2      OPAQUE VERT insul-frame  ||<
end-1:tube-1
  2  1.60     90.   0. Wall-2       OPAQUE VERT earth-side   ||<
user def grnd profile  1
  3  4.00      0.   0. Wall-3       OPAQUE VERT earth-side   ||<
user def grnd profile  1
  4  0.800   270.   0. Wall-4       OPAQUE VERT earth-side   ||<
user def grnd profile  1
```

```
  5  13.6    360.   0. Wall-5       OPAQUE VERT earth-side   ||<
user def grnd profile  1
  6  0.800    90.   0. Wall-6       OPAQUE VERT earth-side   ||<
user def grnd profile  1
  7  0.800     0.   0. end-2        OPAQUE VERT insul-frame  ||<
start-3:tube-3
  8  1.60    270.   0. Wall-8       OPAQUE VERT earth-side   ||<
user def grnd profile  1
  9  15.2    180.   0. Wall-9       OPAQUE VERT earth-side   ||<
user def grnd profile  1
 10  0.800    90.   0. Wall-10      OPAQUE VERT earth-side   ||<
user def grnd profile  1
 11  2.40    180.   0. Wall-11      OPAQUE VERT earth-side   ||<
user def grnd profile  1
 12  0.800   270.   0. Wall-12      OPAQUE VERT earth-side   ||<
user def grnd profile  1
 13  6.50      0.  90. Top-13       OPAQUE CEIL earth-side   ||<
external
 14  6.50      0. -90. Base-14      OPAQUE FLOR earth-side   ||<
user def grnd profile  1


 Number of control periods:  1
 Number of surfaces =14

 Period  1 start   0.00 finish  24.00
 User specified convection coefficients
 User supplied hc values
 Surface            Inside   Outside
 1 start-2      (VERT)     13.000    -1.000
 2 Wall-2       (VERT)     13.000    -1.000
 3 Wall-3       (VERT)     13.000    -1.000
 4 Wall-4       (VERT)     13.000    -1.000
 5 Wall-5       (VERT)     13.000    -1.000
 6 Wall-6       (VERT)     13.000    -1.000
 7 end-2        (VERT)     13.000    -1.000
 8 Wall-8       (VERT)     13.000    -1.000
 9 Wall-9       (VERT)     13.000    -1.000
10 Wall-10      (VERT)     13.000    -1.000
11 Wall-11      (VERT)     13.000    -1.000
12 Wall-12      (VERT)     13.000    -1.000
13 Top-13       (CEIL)     13.000    -1.000
14 Base-14      (FLOR)     13.000    -1.000

 Ventilation & infiltration is assessed via network analysis
 and the associated network node is: tube-2

Notes:
nothing happens in this zone in terms of occupants lights and small
power. There is not infiltration or ventilation.
```

Zone tube-3 (6) is composed of 12 surfaces and 20 vertices.It encloses a volume of 13.6m^3 of space, with a total surface area of 73.0m^2 & approx floor area of 8.50m^2. There is 8.5000m2 of exposed surface area.Flat roof is 100.00 % of floor area & avg U of 0.823 & UA of 6.9960.

A summary of the surfaces in tube-3(6) follows:

Sur	Area m^2	Azim deg	Elev deg	surface name	geometry type	loca	construction name	environment other side
1	0.800	180.	0.	start-3	OPAQUE	VERT	insul-frame	||< end-2:tube-2
2	0.800	90.	0.	Wall-2	OPAQUE	VERT	earth-side	||< user def grnd profile 1
3	17.6	180.	0.	Wall-3	OPAQUE	VERT	earth-side	||< user def grnd profile 1
4	3.20	90.	0.	Wall-4	OPAQUE	VERT	earth-side	||< user def grnd profile 1
5	6.40	360.	0.	Wall-5	OPAQUE	VERT	earth-side	||< user def grnd profile 1
6	0.800	270.	0.	end-3	OPAQUE	VERT	insul-frame	||< start-4:tube-4
7	5.60	180.	0.	Wall-7	OPAQUE	VERT	earth-side	||< user def grnd profile 1
8	1.60	270.	0.	Wall-8	OPAQUE	VERT	earth-side	||< user def grnd profile 1
9	17.6	0.	0.	Wall-9	OPAQUE	VERT	earth-side	||< user def grnd profile 1
10	1.60	270.	0.	Wall-10	OPAQUE	VERT	earth-side	||< user def grnd profile 1
11	8.50	0.	90.	Top-11	OPAQUE	CEIL	earth-side	||< external
12	8.50	0.	-90.	Base-12	OPAQUE	FLOR	earth-side	||< user def grnd profile 1

Number of control periods: 1
Number of surfaces =12

Period 1 start 0.00 finish 24.00
User specified convection coefficients
User supplied hc values

Surface		Inside	Outside
1 start-3	(VERT)	1.3000	-1.000
2 Wall-2	(VERT)	1.3000	-1.000
3 Wall-3	(VERT)	1.3000	-1.000
4 Wall-4	(VERT)	1.3000	-1.000
5 Wall-5	(VERT)	1.3000	-1.000
6 end-3	(VERT)	1.3000	-1.000
7 Wall-7	(VERT)	1.3000	-1.000
8 Wall-8	(VERT)	1.3000	-1.000
9 Wall-9	(VERT)	1.3000	-1.000
10 Wall-10	(VERT)	1.3000	-1.000
11 Top-11	(CEIL)	1.3000	-1.000
12 Base-12	(FLOR)	1.3000	-1.000

Ventilation & infiltration is assessed via network analysis
and the associated network node is: tube-3

Notes:
nothing happens in this zone in terms of occupants lights and small power. There is not infiltration or ventilation.

Zone tube-4 (7) is composed of 10 surfaces and 16 vertices.It encloses a volume of 12.4m^3 of space, with a total surface area of 66.7m^2 & approx floor area of 7.75m^2. There is 7.7500m2 of exposed surface area.Flat roof is 100.00 % of floor area & avg U of 0.823 & UA of 6.3787.

A summary of the surfaces in tube-4(7) follows:

Sur	Area	Azim	Elev	surface name	geometry type	construction loca	construction name	environment other side
	m^2	deg	deg					
1	0.800	90.	0.	start-4	OPAQUE VERT	insul-frame	||< end-3:tube-3	
2	11.2	360.	0.	Wall-2	OPAQUE VERT	earth-side	||< user def grnd profile 1	
3	0.800	90.	0.	Wall-3	OPAQUE VERT	earth-side	||< user def grnd profile 1	
4	11.2	180.	0.	Wall-4	OPAQUE VERT	earth-side	||< user def grnd profile 1	
5	0.800	90.	0.	end-4	OPAQUE VERT	insul-frame	||< start-5:tube-5	
6	12.0	360.	0.	Wall-6	OPAQUE VERT	earth-side	||< user def grnd profile 1	
7	2.40	270.	0.	Wall-7	OPAQUE VERT	earth-side	||< user def grnd profile 1	
8	12.0	180.	0.	Wall-8	OPAQUE VERT	earth-side	||< user def grnd profile 1	
9	7.75	0.	90.	Top-9	OPAQUE CEIL	earth-side	||< external	
10	7.75	0.	-90.	Base-10	OPAQUE FLOR	earth-side	||< user def grnd profile 1	

Number of control periods: 1
Number of surfaces =10

Period 1 start 0.00 finish 24.00
User specified convection coefficients
User supplied hc values

Surface		Inside	Outside
1 start-4	(VERT)	1.3000	-1.000
2 Wall-2	(VERT)	1.3000	-1.000
3 Wall-3	(VERT)	1.3000	-1.000
4 Wall-4	(VERT)	1.3000	-1.000
5 end-4	(VERT)	1.3000	-1.000
6 Wall-6	(VERT)	1.3000	-1.000
7 Wall-7	(VERT)	1.3000	-1.000
8 Wall-8	(VERT)	1.3000	-1.000
9 Top-9	(CEIL)	1.3000	-1.000
10 Base-10	(FLOR)	1.3000	-1.000

Ventilation & infiltration is assessed via network analysis and the associated network node is: tube-4

Notes:
nothing happens in this zone in terms of occupants lights and small power. There is not infiltration or ventilation.

Zone tube-5 (8) is composed of 10 surfaces and 16 vertices.It encloses a volume of 6.92m^3 of space, with a total surface area of 37.6m^2 & approx floor area of 4.32m^2. There is 4.3250m2 of exposed surface area. Flat roof is 100.12 % of floor area & avg U of 0.823 & UA of 3.5597.

A summary of the surfaces in tube-5(8) follows:

Sur	Area m^2	Azim deg	Elev deg	surface name	geometry type	loca	construction name	environment other side
1	6.56	180.	0.	Wall-1	OPAQUE	VERT	earth-side	||< user def grnd profile 1
2	2.41	86.	0.	Wall-2	OPAQUE	VERT	earth-side	||< user def grnd profile 1
3	6.40	0.	0.	Wall-3	OPAQUE	VERT	earth-side	||< user def grnd profile 1
4	0.800	270.	0.	end-5	OPAQUE	VERT	insul-frame	||< start-6:tube-6
5	5.60	180.	0.	Wall-5	OPAQUE	VERT	earth-side	||< user def grnd profile 1
6	0.800	270.	0.	Wall-6	OPAQUE	VERT	earth-side	||< user def grnd profile 1
7	5.60	360.	0.	Wall-7	OPAQUE	VERT	earth-side	||< user def grnd profile 1
8	0.800	270.	0.	start-5	OPAQUE	VERT	insul-frame	||< end-4:tube-4
9	4.32	0.	90.	Top-9	OPAQUE	CEIL	earth-side	||< external
10	4.32	0.	-90.	Base-10	OPAQUE	FLOR	earth-side	||< user def grnd profile 1

Number of control periods: 1
Number of surfaces =10

Period 1 start 0.00 finish 24.00
User specified convection coefficients
User supplied hc values

Surface		Inside	Outside
1 Wall-1	(VERT)	1.3000	-1.000
2 Wall-2	(VERT)	1.3000	-1.000
3 Wall-3	(VERT)	1.3000	-1.000
4 end-5	(VERT)	1.3000	-1.000
5 Wall-5	(VERT)	1.3000	-1.000
6 Wall-6	(VERT)	1.3000	-1.000
7 Wall-7	(VERT)	1.3000	-1.000
8 start-5	(VERT)	1.3000	-1.000
9 Top-9	(CEIL)	1.3000	-1.000
10 Base-10	(FLOR)	1.3000	-1.000

Ventilation & infiltration is assessed via network analysis and the associated network node is: tube-5

Notes:
nothing happens in this zone in terms of occupants lights and small power. There is not infiltration or ventilation.

Zone tube-6 (9) is composed of 10 surfaces and 16 vertices.It encloses a volume of 12.4m^3 of space, with a total surface area of 66.7m^2 & approx floor area of 7.75m^2. There is 7.7500m2 of exposed surface area. Flat roof is 100.00 % of floor area & avg U of 0.823 & UA of 6.3787.

A summary of the surfaces in tube-6(9) follows:

Sur	Area	Azim	Elev	surface name	geometry type	construction loca	construction name	environment other side
	m^2	deg	deg					
1	12.0	180.	0.	Wall-1	OPAQUE VERT	earth-side		||< user def grnd profile 1
2	0.800	90.	0.	start-6	OPAQUE VERT	insul-frame		||< end-5:tube-5
3	11.2	0.	0.	Wall-3	OPAQUE VERT	earth-side		||< user def grnd profile 1
4	0.800	90.	0.	Wall-4	OPAQUE VERT	earth-side		||< user def grnd profile 1
5	11.2	180.	0.	Wall-5	OPAQUE VERT	earth-side		||< user def grnd profile 1
6	0.800	90.	0.	Outlet	OPAQUE VERT	earth-side		||< user def grnd profile 1
7	12.0	0.	0.	Wall-7	OPAQUE VERT	earth-side		||< user def grnd profile 1
8	2.40	270.	0.	Wall-8	OPAQUE VERT	earth-side		||< user def grnd profile 1
9	7.75	0.	90.	Top-9	OPAQUE CEIL	earth-side		||< external
10	7.75	0.	-90.	Base-10	OPAQUE FLOR	earth-side		||< user def grnd profile 1

Number of control periods: 1
Number of surfaces =10

Period 1 start 0.00 finish 24.00
User specified convection coefficients
User supplied hc values

Surface		Inside	Outside
1 Wall-1	(VERT)	1.3000	-1.000
2 start-6	(VERT)	1.3000	-1.000
3 Wall-3	(VERT)	1.3000	-1.000
4 Wall-4	(VERT)	1.3000	-1.000
5 Wall-5	(VERT)	1.3000	-1.000
6 Outlet	(VERT)	1.3000	-1.000
7 Wall-7	(VERT)	1.3000	-1.000
8 Wall-8	(VERT)	1.3000	-1.000
9 Top-9	(CEIL)	1.3000	-1.000
10 Base-10	(FLOR)	1.3000	-1.000

Ventilation & infiltration is assessed via network analysis and the associated network node is: tube-6

Notes:
nothing happens in this zone in terms of occupants lights and small power. There is not infiltration or ventilation.

Villa floor area is 160.87m2, wall area is 86.880m2, window area is 18.720m2. Sloped roof area is 0.00m2, flat roof area is 160.88m2, skylight area is 0.00m2. There is 266.48m2 of outside surface area, 105.60m2 of which is vertical. Outside walls are 54.006 % of floor area & avg U of 0.677 & UA of 58.829. Flat roof is 100.00 % of floor area & avg U of 0.555 & UA of 89.231. Glazing is 11.637 % of floor & 17.727 % facade with avg U of 2.811 & UA of 52.616.

Multi-layer constructions used:

Details of opaque construction: external wall

Layer	Prim|db	Thick|(mm)	Conduc-|tivity	Density	Specif|heat	IR|emis	Solr|abs	Diffu|resis	R|m^2K/W	Descr
Ext	264	90.0	1.310	1918.	795.	0.90	0.85	5.	0.07	Sand-lime block
2	282	50.0	0.032	30.	1120.	0.90	0.65	30.	1.56	Insulation
3	301	200.0	1.640	2011.	910.	0.90	0.50	10.	0.12	Cement block
Int	302	20.0	1.000	2085.	840.	0.90	0.50	10.	0.02	Cement plaster

ISO 6946 U values (horiz/upward/downward heat flow)= 0.515 0.523 0.504 (partition) 0.492
Total area of extern_wall is 81.84

Details of opaque construction: internal wall

Layer	Prim|db	Thick|(mm)	Conduc-|tivity	Density	Specif|heat	IR|emis	Solr|abs	Diffu|resis	R|m^2K/W	Descr
Ext	302	20.0	1.000	2085.	840.	0.90	0.50	10.	0.02	Cement plaster
2	301	200.0	1.640	2011.	910.	0.90	0.50	10.	0.12	Cement block
Int	302	20.0	1.000	2085.	840.	0.90	0.50	10.	0.02	Cement plaster

ISO 6946 U values (horiz/upward/downward heat flow)= 3.012 3.312 2.689 (partition) 2.370
Total area of intern_wall is 81.60

Details of opaque construction: door

Layer	Prim|db	Thick|(mm)	Conduc-|tivity	Density	Specif|heat	IR|emis	Solr|abs	Diffu|resis	R|m^2K/W	Descr
1	69	25.0	0.190	700.	2390.	0.90	0.65	12.	0.13	Oak (radial)

ISO 6946 U values (horiz/upward/downward heat flow)= 3.316 3.682 2.928 (partition) 2.554
Total area of door is 5.04

```
Details of opaque construction: ground floor

Layer|Prim|Thick |Conduc-|Density|Specif|IR  |Solr|Diffu| R
|Descr
      |db  |(mm)  |tivity |       |heat  |emis|abs |resis|m^2K/W
 Ext   263  200.0     1.280  1460.   879. 0.90 0.85     5.  0.16
Common earth
    2   33  150.0     1.770  2297.   921. 0.90 0.65    19.  0.08
Concrete slab
    3  265   60.0     0.337  1800.   920. 0.90 0.85     5.  0.18
Sand
    4  266   20.0     1.000  2080.   840. 0.90 0.85     5.  0.02
Sand cement
 Int   152   20.0     1.104  2284.   800. 0.90 0.60    12.  0.02
Mozaic tiles
 ISO 6946 U values (horiz/upward/downward heat flow)=  1.595  1.675
1.499 (partition)  1.394
 Total area of grnd_floor is    120.00

Details of transparent construction: window      with DCF7671_06nb
optics.

Layer|Prim|Thick |Conduc-|Density|Specif|IR  |Solr|Diffu| R
|Descr
      |db  |(mm)  |tivity |       |heat  |emis|abs |resis|m^2K/W
 Ext   242    6.0     0.760  2710.   837. 0.83 0.05 19200.  0.01
Plate glass
    2    0   12.0     0.000     0.     0. 0.99 0.99     1.  0.17 air
0.17 0.17 0.17
 Int   242    6.0     0.760  2710.   837. 0.83 0.05 19200.  0.01
Plate glass
 ISO 6946 U values (horiz/upward/downward heat flow)=  2.811  3.069
2.527 (partition)  2.243

 Clear float 76/71,     6mm, no blind: with id of: DCF7671_06nb
 with 3 layers [including air gaps] and visible trn: 0.76
 Direct transmission @ 0, 40, 55, 70, 80 deg
   0.611 0.583 0.534 0.384 0.170
 Layer| absorption @ 0, 40, 55, 70, 80 deg
    1  0.157 0.172 0.185 0.201 0.202
    2  0.001 0.002 0.003 0.004 0.005
    3  0.117 0.124 0.127 0.112 0.077
 Total area of dbl_glz is     18.72

Details of opaque construction: roof

Layer|Prim|Thick |Conduc-|Density|Specif|IR  |Solr|Diffu| R
|Descr
      |db  |(mm)  |tivity |       |heat  |emis|abs |resis|m^2K/W
 Ext   152   20.0     1.104  2284.   800. 0.90 0.60    12.  0.02
Mozaic tiles
    2  303   20.0     0.940  2085.   840. 0.90 0.50    10.  0.02
Cement mortar
    3  128   20.0     0.940  2080.   840. 0.91 0.50    19.  0.02
Sand screed
    4  282   50.0     0.032    30.  1120. 0.90 0.65    30.  1.56
Insulation
    5  321    3.0     0.140   934.  1507. 0.90 0.50    10.  0.02
Water proofing
```

```
    6  128   20.0     0.940  2080.   840. 0.91 0.50    19.  0.02
Sand screed
    7   34   50.0     0.210   351.   879. 0.90 0.65    19.  0.24
Foam concrete
 Int    33  150.0     1.770  2297.   921. 0.90 0.65    19.  0.08
Concrete slab
 ISO 6946 U values (horiz/upward/downward heat flow)=  0.463  0.470
0.455 (partition)  0.445
 Total area of roof is    120.00

Details of opaque construction: earth-side

Layer|Prim|Thick |Conduc-|Density|Specif|IR  |Solr|Diffu| R
|Descr
      |db  |(mm)  |tivity |       |heat  |emis|abs |resis|m^2K/W
 Ext   263  250.0     1.280  1460.   879. 0.90 0.85     5.  0.20
Common earth
    2  263  250.0     1.280  1460.   879. 0.90 0.85     5.  0.20
Common earth
    3  263  250.0     1.280  1460.   879. 0.90 0.85     5.  0.20
Common earth
    4  263  250.0     1.280  1460.   879. 0.90 0.85     5.  0.20
Common earth
    5  262  100.0     0.520  2050.   184. 0.90 0.85     2.  0.19
Gravel based
 Int    32  100.0     1.400  2100.   653. 0.90 0.65    19.  0.07
Heavy mix concrete
 ISO 6946 U values (horiz/upward/downward heat flow)=  0.823  0.844
0.797 (partition)  0.766
 Total area of earth-side is    344.32

Details of opaque construction: insul-frame

Layer|Prim|Thick |Conduc-|Density|Specif|IR  |Solr|Diffu| R
|Descr
      |db  |(mm)  |tivity |       |heat  |emis|abs |resis|m^2K/W
 Ext    44    4.0   210.000  2700.   880. 0.82 0.72 19200.  0.00
Aluminium gray coted
    2  281   80.0     0.040    12.   840. 0.90 0.65    30.  2.00
Glass Fibre Quilt
 Int    44    4.0   210.000  2700.   880. 0.82 0.72 19200.  0.00
Aluminium gray coted
 ISO 6946 U values (horiz/upward/downward heat flow)=  0.461  0.467
0.452 (partition)  0.442
 Total area of insul-frame is      8.00
```

Table B.1: Sample of the synchronization of the multi-chiller control strategy for hot/humid climate.

Time (hr)	T_{amb} (°C)	T_{oc} (°C)	A/C (kW)	Culvert (kW)	Total (kW)	Culvert cooling contribution (%)	A/C (%)	Old Modularized A/C (%)	New Modularized A/C (%) (ESP-r)	Control strategy recommendation
0.5	22.80	21.54	-0.001	-0.36	-0.37	100	0	0	0	0
1.5	22.65	21.54	-0.001	-0.32	-0.32	100	0	0	0	0
2.5	22.30	21.54	-0.001	-0.22	-0.22	100	0	0	0	0
3.5	21.95	21.54	-0.001	-0.12	-0.12	99	1	0	0	0
4.5	21.70	21.54	-0.001	-0.05	-0.05	98	2	0	0	0
5.5	21.45	21.53	-0.001	0.02	0.02	0	100	0	0	0
6.5	21.50	21.53	-0.001	0.01	0.01	0	100	0	0	0
7.5	22.80	21.53	-0.001	-0.37	-0.37	100	0	0	0	0
8.5	24.75	21.52	-0.1	-0.93	-1.03	90	10	0	0	0
9.5	26.40	21.51	-0.51	-1.42	-1.93	74	26	3	3	25
10.5	27.75	21.5	-1.21	-1.81	-3.02	60	40	10	12	25
11.5	28.60	21.49	-1.78	-2.06	-3.84	54	46	17	20	25
12.5	29.15	21.5	-2.17	-2.21	-4.38	51	49	23	26	25
13.5	29.40	21.53	-2.42	-2.28	-4.70	48	52	26	30	50
14.5	29.40	21.57	-2.6	-2.27	-4.87	47	53	29	34	50
15.5	29.40	21.61	-2.84	-2.25	-5.09	44	56	33	38	50
16.5	29.15	21.66	-2.96	-2.17	-5.13	42	58	36	41	50
17.5	28.60	21.71	-2.88	-1.99	-4.87	41	59	36	41	50
18.5	27.75	21.75	-2.52	-1.74	-4.26	41	59	31	36	50

19.5	26.95	21.79	-1.94	-1.49	-3.43	43	57	23	26	50
20.5	26.15	21.84	-1.41	-1.25	-2.66	47	53	16	18	25
21.5	25.60	21.87	-1.11	-1.08	-2.19	49	51	12	14	25
22.5	25.60	21.91	-1.07	-1.07	-2.14	50	50	11	13	25
23.5	25.60	21.93	-1.05	-1.06	-2.11	50	50	11	13	25
24.5	21.40	22.78	-0.11	0.40	0.29	0	100	2	3	0
25.5	21.15	22.78	-0.05	0.47	0.42	0	100	1	1	0
26.5	20.75	22.77	0	0.58	0.58	0	100	0	0	0
27.5	20.25	22.75	0	0.72	0.72	0	100	0	0	0
28.5	19.80	22.74	0	0.85	0.85	0	100	0	0	0
29.5	19.45	22.73	0	0.95	0.95	0	100	0	0	0
30.5	19.35	22.71	0	0.97	0.97	0	100	0	0	0
31.5	20.25	22.69	0	0.71	0.71	0	100	0	0	0
32.5	21.95	22.67	-0.07	0.21	0.14	0	100	1	2	25
33.5	23.90	22.65	-0.39	-0.36	-0.75	48	52	4	5	25
34.5	25.30	22.62	-0.94	-0.78	-1.72	45	55	11	12	25
35.5	26.15	22.6	-1.4	-1.03	-2.43	42	58	17	19	25
36.5	26.70	22.59	-1.71	-1.19	-2.90	41	59	21	24	25
37.5	27.25	22.6	-1.97	-1.35	-3.32	41	59	25	28	50
38.5	27.25	22.63	-2.12	-1.34	-3.46	39	61	27	31	50
39.5	26.40	22.66	-2.06	-1.08	-3.14	34	66	28	33	25
40.5	25.85	22.69	-1.9	-0.91	-2.81	32	68	27	31	25
41.5	25.60	22.73	-1.66	-0.83	-2.49	33	67	23	27	25
42.5	25.85	22.76	-1.58	-0.89	-2.47	36	64	21	24	25
43.5	25.00	22.8	-1.19	-0.64	-1.83	35	65	16	19	25
44.5	23.60	22.82	-0.67	-0.23	-0.90	25	75	11	12	25

45.5	23.30	22.84	-0.56	-0.13	-0.69	19	81	10	11	25
46.5	23.30	22.86	-0.53	-0.13	-0.66	19	81	9	10	25
47.5	22.75	22.88	-0.42	0.04	-0.38	0	100	9	10	25
48.5	25.85	25.13	-1.64	-0.21	-1.85	11	89	31	35	25
49.5	25.65	25.13	-1.34	-0.15	-1.49	10	90	25	29	25
50.5	25.55	25.13	-1.21	-0.12	-1.33	9	91	23	27	25
51.5	25.45	25.13	-1.1	-0.09	-1.19	8	92	21	24	25
52.5	25.30	25.13	-1	-0.05	-1.05	5	95	20	23	25
53.5	25.15	25.13	-0.9	-0.01	-0.91	1	99	19	22	25
54.5	25.05	25.12	-0.82	0.02	-0.80	0	100	17	20	50
55.5	25.85	25.12	-1.13	-0.21	-1.34	16	84	20	23	25
56.5	27.25	25.12	-1.7	-0.62	-2.32	27	73	26	30	50
57.5	27.80	25.11	-2.16	-0.78	-2.94	26	74	33	38	50
58.5	27.80	25.11	-2.46	-0.78	-3.24	24	76	39	45	50
59.5	27.80	25.11	-2.6	-0.78	-3.38	23	77	42	48	50
60.5	27.80	25.11	-2.62	-0.78	-3.40	23	77	42	49	50
61.5	28.05	25.14	-2.85	-0.84	-3.69	23	77	46	53	50
62.5	28.30	25.16	-3.16	-0.91	-4.07	22	78	52	59	50
63.5	28.30	25.17	-3.33	-0.91	-4.24	21	79	55	63	50
64.5	28.30	25.19	-3.4	-0.90	-4.30	21	79	56	65	50
65.5	28.05	25.21	-3.33	-0.82	-4.15	20	80	56	64	50
66.5	27.50	25.23	-3.07	-0.66	-3.73	18	82	53	61	50
67.5	26.95	25.25	-2.66	-0.49	-3.15	16	84	47	54	50
68.5	26.70	25.27	-2.33	-0.41	-2.74	15	85	42	48	50
69.5	26.70	25.29	-2.15	-0.41	-2.56	16	84	38	44	50
70.5	26.40	25.3	-1.96	-0.32	-2.28	14	86	35	41	25

71.5	26.10	25.31	-1.82	-0.23	-2.05	11	89	34	39	25
72.5	26.7	27.45	-1.84	0.22	-1.62	0	100	39	44	50
73.5	26.95	27.44	-1.68	0.14	-1.54	0	100	35	41	75
74.5	27.1	27.43	-1.66	0.10	-1.56	0	100	35	40	75
75.5	26.8	27.42	-1.51	0.18	-1.33	0	100	32	36	50
76.5	26.35	27.42	-1.32	0.31	-1.01	0	100	28	32	50
77.5	26.05	27.41	-1.16	0.39	-0.77	0	100	24	28	50
78.5	26.5	27.41	-1.26	0.26	-1.00	0	100	26	30	50
79.5	26.95	27.41	-1.4	0.13	-1.27	0	100	29	34	75
80.5	26.15	27.41	-1.25	0.36	-0.89	0	100	26	30	50
81.5	26.4	27.4	-1.54	0.29	-1.25	0	100	32	37	50
82.5	27.2	27.4	-2.12	0.06	-2.06	0	100	45	51	75
83.5	28.05	27.39	-2.66	-0.19	-2.85	7	93	52	60	75
84.5	29.75	27.4	-3.33	-0.68	-4.01	17	83	58	67	75
85.5	30.6	27.39	-3.78	-0.93	-4.71	20	80	64	73	100
86.5	30.6	27.39	-3.99	-0.93	-4.92	19	81	68	78	100
87.5	30.3	27.4	-4.1	-0.84	-4.94	17	83	71	82	100
88.5	29.7	27.41	-4.07	-0.66	-4.73	14	86	74	85	100
89.5	29.4	27.44	-4.09	-0.57	-4.66	12	88	75	87	100
90.5	28.85	27.47	-3.92	-0.40	-4.32	9	91	75	86	100
91.5	28.3	27.5	-3.57	-0.23	-3.80	6	94	70	81	50
92.5	27.5	27.52	-3	0.01	-2.99	0	100	63	73	75
93.5	26.4	27.53	-2.37	0.33	-2.04	0	100	50	57	50
94.5	26.1	27.55	-2.14	0.42	-1.72	0	100	45	52	50
95.5	25.85	27.55	-2	0.49	-1.51	0	100	42	48	50
96.5	25.85	28.71	-2.18	0.83	-1.35	0	100	46	53	50

97.5	25.5	28.7	-1.82	0.93	-0.89	0	100	38	44	50
98.5	25.3	28.69	-1.64	0.98	-0.66	0	100	34	40	50
99.5	25.1	28.68	-1.5	1.04	-0.46	0	100	32	36	50
100.5	25.1	28.66	-1.4	1.03	-0.37	0	100	29	34	50
101.5	25.4	28.65	-1.42	0.94	-0.48	0	100	30	34	50
102.5	26.15	28.63	-1.57	0.72	-0.85	0	100	33	38	50
103.5	26.95	28.61	-1.82	0.48	-1.34	0	100	38	44	75
104.5	27.5	28.59	-2.16	0.32	-1.84	0	100	45	52	75
105.5	28.35	28.57	-2.76	0.06	-2.70	0	100	58	67	75
106.5	29.45	28.56	-3.46	-0.26	-3.72	7	93	68	78	75
107.5	28.35	28.55	-3.35	0.06	-3.29	0	100	70	81	75
108.5	26.15	28.56	-2.65	0.70	-1.95	0	100	56	64	50
109.5	25.6	28.56	-2.3	0.86	-1.44	0	100	48	56	50
110.5	26.15	28.57	-2.47	0.70	-1.77	0	100	52	60	50
111.5	27.8	28.59	-3.23	0.23	-3.00	0	100	68	78	75
112.5	28.9	28.6	-3.8	-0.09	-3.89	2	98	78	90	100
113.5	28.35	28.57	-3.72	0.06	-3.66	0	100	78	90	75
114.5	26.7	28.55	-3.16	0.54	-2.62	0	100	66	76	75
115.5	25.3	28.55	-2.47	0.94	-1.53	0	100	52	60	50
116.5	25	28.56	-2.04	1.03	-1.01	0	100	43	49	50
117.5	25	28.58	-1.83	1.04	-0.79	0	100	38	44	50
118.5	25	28.59	-1.73	1.04	-0.69	0	100	36	42	50
119.5	25	28.57	-1.68	1.03	-0.65	0	100	35	41	50
120.5	27.75	29.05	-2.49	0.38	-2.11	0	100	52	60	75
121.5	27.6	29.05	-2.2	0.42	-1.78	0	100	46	53	75
122.5	27.5	29.05	-2.09	0.45	-1.64	0	100	44	50	75

123.5	27	29.05	-1.86	0.59	-1.27	0	100	39	45	75
124.5	26.35	29.04	-1.6	0.78	-0.82	0	100	34	39	50
125.5	26.25	29.04	-1.5	0.81	-0.69	0	100	32	36	50
126.5	26.2	29.03	-1.42	0.82	-0.60	0	100	30	34	50
127.5	27.2	29.03	-1.7	0.53	-1.17	0	100	36	41	75
128.5	28.6	29.02	-2.22	0.12	-2.10	0	100	47	54	75
129.5	28.9	29	-2.68	0.03	-2.65	0	100	56	65	75
130.5	29.45	28.99	-3.28	-0.13	-3.41	4	96	66	76	75
131.5	30.85	28.98	-3.98	-0.54	-4.52	12	88	74	85	100
132.5	31.4	28.98	-4.35	-0.70	-5.05	14	86	79	90	100
133.5	31.1	28.99	-4.48	-0.61	-5.09	12	88	83	95	100
134.5	**31.4**	**29**	**-4.76**	**-0.69**	**-5.45**	**13**	**87**	**87**	**100**	**100**
135.5	30.85	29.01	-4.74	-0.53	-5.27	10	90	90	103	100
136.5	29.45	29.04	-4.3	-0.12	-4.42	3	97	88	101	100
137.5	28.9	29.07	-3.92	0.05	-3.87	0	100	82	95	100
138.5	28.6	29.08	-3.61	0.14	-3.47	0	100	76	87	75
139.5	28.3	29.1	-3.28	0.23	-3.05	0	100	69	79	75
140.5	28.3	29.12	-3.06	0.24	-2.82	0	100	64	74	75
141.5	28.3	29.12	-2.94	0.24	-2.70	0	100	62	71	75
142.5	28.05	29.11	-2.81	0.31	-2.50	0	100	59	68	75
143.5	27.5	29.11	-2.61	0.47	-2.14	0	100	55	63	75
144.5	25	28.09	-1.14	0.89	-0.25	0	100	24	28	50
145.5	25.15	28.08	-0.95	0.85	-0.10	0	100	20	23	50
146.5	25.3	28.07	-0.92	0.80	-0.12	0	100	19	22	50
147.5	25.5	28.05	-0.92	0.74	-0.18	0	100	19	22	50
148.5	25.6	28.04	-0.9	0.71	-0.19	0	100	19	22	50

149.5	25.65	28.03	-0.87	0.69	-0.18	0	100	18	21	50
150.5	25.65	28.02	-0.83	0.69	-0.14	0	100	17	20	50
151.5	25.8	28.01	-0.93	0.64	-0.29	0	100	20	22	50
152.5	26.15	28.01	-1.2	0.54	-0.66	0	100	25	29	50
153.5	26.5	28	-1.6	0.43	-1.17	0	100	34	39	50
154.5	26.95	28	-2.15	0.30	-1.85	0	100	45	52	75
155.5	27.5	27.99	-2.6	0.14	-2.46	0	100	55	63	75
156.5	28.05	27.99	-2.99	-0.02	-3.01	1	99	62	72	75
157.5	28.2	27.98	-3.21	-0.06	-3.27	2	98	66	76	75
158.5	28.05	27.99	-3.28	-0.02	-3.30	1	99	69	79	75
159.5	27.9	27.99	-3.29	0.03	-3.26	0	100	69	79	75
160.5	27.6	28	-3.22	0.12	-3.10	0	100	68	78	75
161.5	27.25	28.01	-3.12	0.22	-2.90	0	100	66	75	75
162.5	26.9	28.02	-2.9	0.32	-2.58	0	100	61	70	75
163.5	26.5	28.03	-2.46	0.44	-2.02	0	100	52	59	75
164.5	26.15	28.03	-2.08	0.54	-1.54	0	100	44	50	50
165.5	25.8	28.03	-1.82	0.65	-1.17	0	100	38	44	50
166.5	25.5	28.03	-1.68	0.73	-0.95	0	100	35	41	50
167.5	25.3	28.02	-1.56	0.79	-0.77	0	100	33	38	50
									Successful time-steps	146
									Total time-steps	168
									Cooling load match rate (%)	87

Table B.2: Synchronization of the multi-chiller control strategy for moderate climate.

Time (hr)	T_{amb} (°C)	T_{oc} (°C)	A/C (kW)	Culvert (kW)	Total (kW)	Culvert cooling contribution (%)	A/C (%)	Old Modularized A/C (%)	New Modularized A/C (%) (ESP-r)	Control strategy recommendation
0.5	11.10	16.66	-0.001	1.61	1.61	0	100	0	0	0
1.5	9.95	16.67	-0.001	1.95	1.94	0	100	0	0	0
2.5	9.05	16.66	-0.001	2.20	2.20	0	100	0	0	0
3.5	8.45	16.65	-0.001	2.37	2.37	0	100	0	0	0
4.5	8.10	16.63	-0.001	2.47	2.47	0	100	0	0	0
5.5	7.90	16.6	-0.001	2.52	2.52	0	100	0	0	0
6.5	8.10	16.57	-0.001	2.45	2.45	0	100	0	0	0
7.5	9.15	16.53	-0.001	2.14	2.14	0	100	0	0	0
8.5	10.70	16.49	-0.001	1.68	1.67	0	100	0	0	0
9.5	12.25	16.45	-0.001	1.22	1.21	0	100	0	0	0
10.5	13.35	16.41	-0.001	0.89	0.88	0	100	0	0	0
11.5	14.10	16.38	-0.001	0.66	0.66	0	100	0	0	0
12.5	14.85	16.36	-0.001	0.44	0.44	0	100	0	0	0
13.5	15.15	16.35	-0.001	0.35	0.35	0	100	0	0	0
14.5	15.10	16.36	-0.001	0.36	0.36	0	100	0	0	0
15.5	15.05	16.38	-0.001	0.38	0.38	0	100	0	0	0
16.5	14.85	16.39	-0.001	0.45	0.44	0	100	0	0	0
17.5	14.60	16.41	-0.001	0.52	0.52	0	100	0	0	0
18.5	14.35	16.43	-0.001	0.60	0.60	0	100	0	0	0

19.5	13.60	16.44	-0.001	0.82	0.82	0	100	0	0	0
20.5	12.65	16.46	-0.001	1.10	1.10	0	100	0	0	0
21.5	11.95	16.47	-0.001	1.31	1.31	0	100	0	0	0
22.5	11.45	16.48	-0.001	1.46	1.45	0	100	0	0	0
23.5	11.15	16.48	-0.001	1.54	1.54	0	100	0	0	0
24.5	16.90	18.1	-0.001	0.35	0.35	0	100	0	0	0
25.5	17.20	18.09	-0.001	0.26	0.26	0	100	0	0	0
26.5	17.35	18.09	-0.001	0.21	0.21	0	100	0	0	0
27.5	17.30	18.09	-0.001	0.23	0.23	0	100	0	0	0
28.5	17.05	18.09	-0.001	0.30	0.30	0	100	0	0	0
29.5	16.80	18.09	-0.001	0.37	0.37	0	100	0	0	0
30.5	16.75	18.1	-0.001	0.39	0.39	0	100	0	0	0
31.5	16.95	18.1	-0.001	0.33	0.33	0	100	0	0	0
32.5	17.25	18.11	-0.001	0.25	0.25	0	100	0	0	0
33.5	17.55	18.11	-0.001	0.16	0.16	0	100	0	0	0
34.5	17.95	18.11	-0.001	0.05	0.05	0	100	0	0	0
35.5	18.50	18.11	-0.001	-0.11	-0.11	99	1	0	0	0
36.5	19.05	18.11	-0.001	-0.27	-0.27	100	0	0	0	0
37.5	19.20	18.12	-0.001	-0.31	-0.31	100	0	0	0	0
38.5	19.00	18.13	-0.001	-0.25	-0.25	100	0	0	0	0
39.5	18.80	18.14	-0.001	-0.19	-0.19	99	1	0	0	0
40.5	18.35	18.16	-0.001	-0.05	-0.06	98	2	0	0	0
41.5	17.60	18.18	-0.001	0.17	0.17	0	100	0	0	0
42.5	16.85	18.19	-0.001	0.39	0.39	0	100	0	0	0
43.5	16.40	18.21	-0.001	0.52	0.52	0	100	0	0	0
44.5	16.15	18.22	-0.001	0.60	0.60	0	100	0	0	0

45.5	15.90	18.23	-0.001	0.67	0.67	0	100	0	0	0
46.5	15.70	18.23	-0.001	0.73	0.73	0	100	0	0	0
47.5	15.45	18.22	-0.001	0.80	0.80	0	100	0	0	0
48.5	19.50	20.7	-0.84	0.35	-0.49	0	100	16	17	50
49.5	19.00	20.71	-0.52	0.49	-0.03	0	100	10	11	25
50.5	18.70	20.7	-0.45	0.58	0.13	0	100	9	9	25
51.5	18.55	20.7	-0.41	0.62	0.21	0	100	8	9	25
52.5	18.55	20.68	-0.38	0.62	0.24	0	100	7	8	25
53.5	18.55	20.66	-0.36	0.61	0.25	0	100	7	7	25
54.5	18.90	20.64	-0.38	0.50	0.12	0	100	7	8	25
55.5	19.40	20.63	-0.46	0.36	-0.10	0	100	9	10	50
56.5	19.65	20.61	-0.64	0.28	-0.36	0	100	12	13	50
57.5	19.90	20.59	-0.99	0.20	-0.79	0	100	19	21	50
58.5	20.10	20.58	-1.39	0.14	-1.25	0	100	27	29	50
59.5	20.30	20.57	-1.71	0.08	-1.63	0	100	33	35	50
60.5	20.50	20.56	-1.89	0.02	-1.87	0	100	36	39	50
61.5	20.60	20.56	-2	-0.01	-2.01	0	100	38	41	50
62.5	20.60	20.56	-2.11	-0.01	-2.12	0	100	40	44	50
63.5	20.60	20.56	-2.24	-0.01	-2.25	0	100	43	46	50
64.5	20.55	20.56	-2.32	0.00	-2.32	0	100	44	48	50
65.5	20.40	20.56	-2.35	0.05	-2.30	0	100	45	49	50
66.5	20.25	20.56	-2.31	0.09	-2.22	0	100	44	48	50
67.5	20.05	20.57	-2.02	0.15	-1.87	0	100	39	42	50
68.5	19.70	20.57	-1.56	0.25	-1.31	0	100	30	32	50
69.5	19.35	20.57	-1.15	0.35	-0.80	0	100	22	24	50
70.5	19.10	20.57	-0.94	0.43	-0.51	0	100	18	19	25

71.5	18.90	20.57	-0.82	0.48	-0.34	0	100	16	17	25
72.5	25.6	24.44	-3.21	-0.34	-3.55	9	91	55	60	75
73.5	24.1	24.43	-2.52	0.10	-2.42	0	100	48	52	75
74.5	24	24.42	-2.34	0.12	-2.22	0	100	45	49	75
75.5	23.85	24.41	-2.18	0.16	-2.02	0	100	42	45	75
76.5	23.5	24.43	-1.99	0.27	-1.72	0	100	38	41	75
77.5	23.15	24.42	-1.81	0.37	-1.44	0	100	35	38	75
78.5	24.25	24.4	-2.11	0.04	-2.07	0	100	40	44	75
79.5	26.1	24.39	-2.83	-0.49	-3.32	15	85	46	50	75
80.5	27.25	24.37	-3.49	-0.83	-4.32	19	81	54	58	100
81.5	28.4	24.36	-4.21	-1.17	-5.38	22	78	63	68	100
82.5	29.3	24.34	-4.85	-1.44	-6.29	23	77	71	78	100
83.5	29.95	24.33	-5.28	-1.63	-6.91	24	76	77	84	100
84.5	30.6	24.35	-5.63	-1.81	-7.44	24	76	81	88	100
85.5	30.15	24.37	-5.67	-1.67	-7.34	23	77	84	91	100
86.5	28.7	24.4	-5.29	-1.24	-6.53	19	81	82	89	100
87.5	29.25	24.43	-5.38	-1.40	-6.78	21	79	82	89	100
88.5	**31.75**	**24.46**	**-6.03**	**-2.11**	**-8.14**	**26**	**74**	**85**	93	**100**
89.5	30.5	24.5	-5.7	-1.74	-7.44	23	77	83	91	100
90.5	27.3	24.52	-4.69	-0.80	-5.49	15	85	76	83	100
91.5	27.15	24.53	-4.38	-0.76	-5.14	15	85	71	77	100
92.5	28.3	24.55	-4.44	-1.09	-5.53	20	80	68	74	100
93.5	29.45	24.6	-4.62	-1.40	-6.02	23	77	68	74	100
94.5	32	24.63	-5.34	-2.13	-7.47	29	71	73	79	100
95.5	33	24.61	-5.64	-2.43	-8.07	30	70	75	82	100
96.5	25.65	24.57	-3.34	-0.31	-3.65	9	91	58	63	75

97.5	26	24.57	-3.2	-0.41	-3.61	11	89	54	59	75
98.5	26.3	24.56	-3.18	-0.50	-3.68	14	86	52	57	75
99.5	26.45	24.56	-3.15	-0.55	-3.70	15	85	51	56	75
100.5	26.45	24.56	-3.08	-0.55	-3.63	15	85	50	54	75
101.5	26.4	24.56	-2.98	-0.53	-3.51	15	85	48	52	75
102.5	26.4	24.57	-2.96	-0.53	-3.49	15	85	48	52	75
103.5	26.55	24.58	-3.11	-0.57	-3.68	15	85	50	55	75
104.5	26.8	24.59	-3.46	-0.64	-4.10	16	84	56	61	75
105.5	27.05	24.59	-3.98	-0.71	-4.69	15	85	64	70	75
106.5	27.35	24.6	-4.51	-0.80	-5.31	15	85	73	80	100
107.5	27.6	24.61	-4.83	-0.87	-5.70	15	85	78	85	100
108.5	27.85	24.62	-5	-0.93	-5.93	16	84	80	87	100
109.5	28.1	24.63	-5.18	-1.00	-6.18	16	84	83	90	100
110.5	28.3	24.64	-5.4	-1.06	-6.46	16	84	86	94	100
111.5	28.5	24.66	-5.62	-1.11	-6.73	17	83	90	97	100
112.5	28.5	24.68	-5.7	-1.11	-6.81	16	84	91	99	100
113.5	28.3	24.7	-5.66	-1.04	-6.70	16	84	91	99	100
114.5	28.1	24.72	-5.53	-0.98	-6.51	15	85	90	97	100
115.5	27.85	24.74	-5.16	-0.90	-6.06	15	85	84	91	100
116.5	27.5	24.76	-4.7	-0.79	-5.49	14	86	77	83	100
117.5	27.15	24.78	-4.34	-0.69	-5.03	14	86	72	78	75
118.5	27	24.8	-4.19	-0.64	-4.83	13	87	69	75	75
119.5	27	24.82	-4.12	-0.63	-4.75	13	87	68	74	75
120.5	26.6	25.57	-3.43	-0.30	-3.73	8	92	60	65	100
121.5	26.05	25.58	-3.02	-0.14	-3.16	4	96	55	60	100
122.5	25.6	25.59	-2.78	0.00	-2.78	0	100	53	58	75

123.5	25.2	25.6	-2.56	0.12	-2.44	0	100	49	53	75
124.5	24.85	25.61	-2.37	0.22	-2.15	0	100	45	49	75
125.5	24.5	25.61	-2.18	0.32	-1.86	0	100	42	45	75
126.5	24.15	25.6	-2.02	0.42	-1.60	0	100	39	42	75
127.5	24.35	25.6	-2.13	0.36	-1.77	0	100	41	44	75
128.5	25	25.59	-2.63	0.17	-2.46	0	100	50	55	75
129.5	25.65	25.58	-3.4	-0.02	-3.42	1	99	65	70	75
130.5	26.1	25.57	-4.08	-0.15	-4.23	4	96	75	82	100
131.5	26.3	25.56	-4.44	-0.21	-4.65	5	95	81	88	100
132.5	26.5	25.55	-4.63	-0.27	-4.90	6	94	83	91	100
133.5	26.7	25.55	-4.84	-0.33	-5.17	6	94	86	94	100
134.5	26.9	25.55	-5.07	-0.39	-5.46	7	93	90	98	100
135.5	**27.1**	**25.56**	**-5.24**	**-0.45**	**-5.69**	**8**	**92**	**92**	**100**	**100**
136.5	27.15	25.57	-5.25	-0.46	-5.71	8	92	92	100	100
137.5	27	25.57	-5.09	-0.41	-5.50	8	92	90	98	100
138.5	26.85	25.58	-4.8	-0.37	-5.17	7	93	85	92	100
139.5	26.7	25.59	-4.39	-0.32	-4.71	7	93	78	85	100
140.5	26.5	25.6	-4.03	-0.26	-4.29	6	94	72	79	100
141.5	26.3	25.61	-3.82	-0.20	-4.02	5	95	69	75	100
142.5	26.15	25.62	-3.7	-0.15	-3.85	4	96	68	74	100
143.5	26	25.63	-3.6	-0.11	-3.71	3	97	67	73	100
144.5	23.15	24.3	-1.48	0.33	-1.15	0	100	28	31	75
145.5	23.15	24.3	-1.25	0.33	-0.92	0	100	24	26	75
146.5	23.25	24.31	-1.21	0.31	-0.90	0	100	23	25	75
147.5	23.3	24.31	-1.17	0.29	-0.88	0	100	22	24	75
148.5	23.3	24.31	-1.11	0.29	-0.82	0	100	21	23	75

149.5	23.25	24.31	-1.04	0.31	-0.73	0	100	20	22	75
150.5	23.25	24.31	-0.99	0.31	-0.68	0	100	19	21	75
151.5	23.9	24.31	-1.2	0.12	-1.08	0	100	23	25	75
152.5	25.05	24.31	-1.77	-0.21	-1.98	11	89	30	33	75
153.5	26.2	24.32	-2.55	-0.54	-3.09	18	82	40	44	75
154.5	26.9	24.32	-3.19	-0.75	-3.94	19	81	49	54	75
155.5	27.05	24.32	-3.48	-0.79	-4.27	19	81	54	59	75
156.5	27.2	24.33	-3.65	-0.83	-4.48	19	81	57	62	75
157.5	27.15	24.35	-3.81	-0.81	-4.62	18	82	60	65	75
158.5	26.8	24.38	-3.94	-0.70	-4.64	15	85	64	69	75
159.5	26.45	24.42	-4.04	-0.59	-4.63	13	87	67	73	75
160.5	26.05	24.44	-3.93	-0.47	-4.40	11	89	67	73	75
161.5	25.55	24.47	-3.56	-0.31	-3.87	8	92	62	68	100
162.5	25.05	24.5	-3.05	-0.16	-3.21	5	95	55	60	50
163.5	24.75	24.52	-2.64	-0.07	-2.71	2	98	49	53	50
164.5	24.7	24.53	-2.47	-0.05	-2.52	2	98	46	50	50
165.5	24.65	24.55	-2.39	-0.03	-2.42	1	99	45	49	50
166.5	24.55	24.56	-2.31	0.00	-2.31	0	100	44	48	50
167.5	24.4	24.56	-2.23	0.05	-2.18	0	100	43	46	50
									Successful time-steps	148
									Total time-steps	168
									Cooling load match rate (%)	88

Appendix C : CAV A/C system in ESP-r

Synopsis

```
This is a synopsis of the Single-zone CAV A/C system model defined
in 3_room_Ac.cfg generated on Sat Sep 3 22:04:08 2011. The model is
located at latitude 24.70 with a longitude difference of 1.80 from
the local time meridian. The year used in simulations is 1988. The
site exposure is typical city centre and the ground reflectance is
0.20.

The climate used is: RIYADH - SAU and is held in:
/usr/esru/esp-r/climate/Hot_climate and uses hour centred solar
data.

There are currently 1 user defined ground temperature profiles.
Ground temperatures Jan-Dec:
14.0  17.0  20.0  26.0  26.0  26.0  26.0  26.0  26.0  26.0  22.0
15.0

Databases associated with the model:
 pressure distributions : pressc.db1
 materials              : /usr/esru/esp-r/databases/constr.db1
 constructions          : /usr/esru/esp-r/databases/multicon.db1
 plant components       : plantc.db1
 event profiles         : /usr/esru/esp-r/databases/profiles.db2.a
 optical properties     : optics.db2

 ____________________________________________________________

Zones control includes 3 functions.

The sensor for function 1 senses dry bulb temperature in Living-
room. The actuator for function 1 is the air point in Living-room.
There have been 1 day types defined.

Day type 1 is valid Fri-01-Jan to Sat-31-Dec, 1988 with 1 periods.
Per|Start|Sensing  |Actuating  | Control law       | Data
1  0.00 db temp   > flux      flux zone/plant     7.0 1.0 1.0
99000.0 99000.0 10.0 1.0
plant/zone coupling: source plant component 1 plant component node 1
coupling type mCp(0s-0a) sequential. Max heating 99000.00W max
cooling 99000.00W. Extract plant component 10 and extract node 1.

The sensor for function 2 senses dry bulb temperature in Dining-
room. The actuator for function 2 is the air point in Dining-room.
There have been 1 day types defined.

Day type 1 is valid Fri-01-Jan to Sat-31-Dec, 1988 with 1 periods.
Per|Start|Sensing  |Actuating  | Control law       | Data
1  0.00 db temp   > flux      flux zone/plant     8.0 1.0 1.0
99000.0 99000.0 11.0 1.0
```

plant/zone coupling: source plant component 1 plant component node 1 coupling type mCp(0s-0a) sequential. Max heating 99000.00W max cooling 99000.00W. Extract plant component 11 and extract node 1.

The sensor for function 3 senses dry bulb temperature in Bed-room. The actuator for function 3 is the air point in Bed-room. There have been 1 day types defined.

Day type 1 is valid Fri-01-Jan to Sat-31-Dec, 1988 with 1 periods.
Per|Start|Sensing |Actuating | Control law | Data
1 0.00 db temp > flux flux zone/plant 9.0 1.0 1.0 99000.0 99000.0 12.0 1.0
plant/zone coupling: source plant component 1 plant component node 1 coupling type mCp(0s-0a) sequential. Max heating 99000.00W max cooling 99000.00W. Extract plant component 12 and extract node 1.

Zone to contol loop linkages:
zone (1) Living-room << control 1
zone (2) Dining-room << control 2
zone (3) Bed-room << control 3

Plant control includes 1 loops.

The sensor for function 1 senses var in compt. 14:converge-2 @ node no. 1. The actuator for function 1 is plant component 4:cooling-coil @ node no. 1. There have been 1 day types defined.

Day type 1 is valid Fri-01-Jan to Sat-31-Dec, 1988 with 1 periods.
Per|Start|Sensing |Actuating | Control law | Data
1 0.00 dry bulb > flux PID flux control. -1.0 10000.0 0.0 25.0 4.0 0.0 0.0

The model includes a plant network.

The plant network contains 16 components from plantc.db1

Component: duct-1 (1) code 1, db reference 6
No Control data
Modified parameters for duct-1
Component total mass (kg) : 9.2500
Mass weighted average specific heat (J/kgK) : 500.00
UA modulus (W/K) : 14.000
Hydraulic diameter of duct (m) : 0.12500
Length of duct section (m) : 5.0000
Cross sectional face area (m^2) : 0.12270E-01

Component: mixing-box (2) code 2, db reference 1
No Control data
Modified parameters for mixing-box
Component total mass (kg) : 1.0000
Mass weighted average specific heat (J/kgK) : 500.00
UA modulus (W/K) : 3.5000

Component: duct-2 (3) code 3, db reference 6
No Control data
Modified parameters for duct-2
Component total mass (kg) : 9.2500
Mass weighted average specific heat (J/kgK) : 500.00
UA modulus (W/K) : 14.000

```
Hydraulic diameter of duct (m)                    :  0.12500
Length of duct section (m)                        :   5.0000
Cross sectional face area (m^2)                   :  0.12270E-01

Component: cooling-coil ( 4) code  4, db reference  4
Control data:    0.000
Modified parameters for cooling-coil
Component total mass (kg)                         :   15.000
Mass weighted average specific heat (J/kgK)       :   1000.0
UA modulus (W/K)                                  :   3.5000

Component: duct-3 ( 5) code  5, db reference  6
No Control data
Modified parameters for duct-3
Component total mass (kg)                         :   9.2500
Mass weighted average specific heat (J/kgK)       :   500.00
UA modulus (W/K)                                  :   14.000
Hydraulic diameter of duct (m)                    :  0.12500
Length of duct section (m)                        :   5.0000
Cross sectional face area (m^2)                   :  0.12270E-01

Component: supply-fan ( 6) code  6, db reference  3
Control data:    0.480
Modified parameters for supply-fan
Component total mass (kg)                         :   10.000
Mass weighted average specific heat (J/kgK)       :   500.00
UA modulus (W/K)                                  :   7.0000
Rated total absorbed power (W)                    :   200.00
Rated volume flow rate (m^3/s)                    :  0.20000
Overall efficiency (-)                            :  0.70000

Component: zone-1 ( 7) code  7, db reference  6
No Control data
Modified parameters for zone-1
Component total mass (kg)                         :   9.2500
Mass weighted average specific heat (J/kgK)       :   500.00
UA modulus (W/K)                                  :   14.000
Hydraulic diameter of duct (m)                    :  0.12500
Length of duct section (m)                        :   5.0000
Cross sectional face area (m^2)                   :  0.12270E-01

Component: zone-2 ( 8) code  8, db reference  6
No Control data
Modified parameters for zone-2
Component total mass (kg)                         :   9.2500
Mass weighted average specific heat (J/kgK)       :   500.00
UA modulus (W/K)                                  :   14.000
Hydraulic diameter of duct (m)                    :  0.12500
Length of duct section (m)                        :   5.0000
Cross sectional face area (m^2)                   :  0.12270E-01

Component: zone-3 ( 9) code  9, db reference  6
No Control data
Modified parameters for zone-3
Component total mass (kg)                         :   9.2500
Mass weighted average specific heat (J/kgK)       :   500.00
UA modulus (W/K)                                  :   14.000
Hydraulic diameter of duct (m)                    :  0.12500
Length of duct section (m)                        :   5.0000
```

```
Cross sectional face area (m^2)                    :  0.12270E-01

Component: return-zone-1 (10) code 10, db reference  6
No Control data
Modified parameters for return-zone-1
Component total mass (kg)                          :   9.2500
Mass weighted average specific heat (J/kgK)        :   500.00
UA modulus (W/K)                                   :   14.000
Hydraulic diameter of duct (m)                     :  0.12500
Length of duct section (m)                         :   5.0000
Cross sectional face area (m^2)                    :  0.12270E-01

Component: return-zone-2 (11) code 11, db reference  6
No Control data
Modified parameters for return-zone-2
Component total mass (kg)                          :   9.2500
Mass weighted average specific heat (J/kgK)        :   500.00
UA modulus (W/K)                                   :   14.000
Hydraulic diameter of duct (m)                     :  0.12500
Length of duct section (m)                         :   5.0000
Cross sectional face area (m^2)                    :  0.12270E-01

Component: return-zone-3 (12) code 12, db reference  6
No Control data
Modified parameters for return-zone-3
Component total mass (kg)                          :   9.2500
Mass weighted average specific heat (J/kgK)        :   500.00
UA modulus (W/K)                                   :   14.000
Hydraulic diameter of duct (m)                     :  0.12500
Length of duct section (m)                         :   5.0000
Cross sectional face area (m^2)                    :  0.12270E-01

Component: converge-1 (13) code 13, db reference  1
No Control data
Modified parameters for converge-1
Component total mass (kg)                          :   1.0000
Mass weighted average specific heat (J/kgK)        :   500.00
UA modulus (W/K)                                   :   3.5000

Component: converge-2 (14) code 14, db reference  1
No Control data
Modified parameters for converge-2
Component total mass (kg)                          :   1.0000
Mass weighted average specific heat (J/kgK)        :   500.00
UA modulus (W/K)                                   :   3.5000

Component: return-fan (15) code 15, db reference  3
Control data:    0.480
Modified parameters for return-fan
Component total mass (kg)                          :   10.000
Mass weighted average specific heat (J/kgK)        :   500.00
UA modulus (W/K)                                   :   7.0000
Rated total absorbed power (W)                     :   200.00
Rated volume flow rate (m^3/s)                     :  0.20000
Overall efficiency (-)                             :  0.70000

Component: humidifier (16) code 16, db reference  2
Control data:    0.004
Modified parameters for humidifier
```

```
 Component total mass (kg)                              :   25.000
 Mass weighted average specific heat (J/kgK)            :   1000.0
 UA modulus (W/K)                                       :   3.5000
 Rated effectiveness (-)                                :  0.85000
 Rated face velocity (m/s)                              :   1.0000
 Face area (m^2)                                        :  0.15000
 Mode of operation (-)                                  :   1.0000

 Nb of plant component connections: 19
 Con receiving component node type sending component node

1 mixing-box node 1 (from another component.) duct-1 node 1 details:
1.00    0.00    0.00

2 mixing-box node 1 (from another component.) return-fan node 1
details:     0.90    0.00    0.00

3 duct-2 node 1 (from another component.) humidifier node 1 details:
1.00    0.00    0.00

4 cooling-coil node 1 (from another component.) duct-2 node 1
details:     1.00    0.00    0.00

5 duct-3 node 1 (from another component.) cooling-coil node 1
details:     1.00    0.00    0.00

6 supply-fan node 1 (from another component.) duct-3 node 1 details:
1.00    0.00    0.00

7 zone-1 node 1 (from another component.) supply-fan node 1 details:
0.40    0.00    0.00

8 zone-2 node 1 (from another component.) supply-fan node 1 details:
0.30    0.00    0.00

9 zone-3 node 1 (from another component.) supply-fan node 1 details:
0.30    0.00    0.00

10 return-zone-1 node 1 (zone air or ambient.) zone-1 node 1
details:     1.00    1.00    0.00

11 return-zone-2 node 1 (zone air or ambient.) zone-2 node 1
details:     1.00    2.00    0.00

12 return-zone-3 node 1 (zone air or ambient.) zone-3 node 1
details:     1.00    3.00    0.00

13 converge-1 node 1 (from another component.) return-zone-1 node 1
details:     1.00    0.00    0.00

14 converge-1 node 1 (from another component.) return-zone-2 node 1
details:     1.00    0.00    0.00

15 converge-2 node 1 (from another component.) return-zone-3 node 1
details:     1.00    0.00    0.00

16 converge-2 node 1 (from another component.) converge-1 node 1
details:     1.00    0.00    0.00
```

```
17 return-fan node 1 (from another component.) converge-2 node 1
details:     1.00    0.00    0.00

18 duct-1 node 1 (zone air or ambient.) return-fan node 1 details:
0.10    0.00    0.00

19 humidifier node 1 (from another component.) mixing-box node 1
details:     1.00    0.00    0.00
```

Appendix D : Other Air Culvert models

- **(Loveday et al. 2006) model:**

  Where,

$$\varepsilon = 1 - e^{-UA/\dot{m}c_p} \quad \text{D.1}$$

  U is calculated from equation D.2 after plugging in parameters solved in equations D.3, D.4, and D.6.

$$U = 1/R_{tot.} \quad \text{D.2}$$

  Where,

$$R_{tot.} = R_s + R_c \quad \text{D.3}$$

  And,

$$R_s = \frac{\ln(r_1/r_2)}{2\pi Lk} \quad \text{D.4}$$

  Where,

$$k = 0.02442 + (10^{-4}(0.6992T_a)) \quad \text{D.5}$$

  But,

$$R_c = (1/2\pi \mathrm{r} \mathrm{L} \mathrm{h_c}) \quad \text{D.6}$$

  Where, $r = r_1/2$.

- **(Athienitis & Santamouris 2002) model:**

  Where,

$$a = VHwc\rho/[2f(H+w)\mathrm{h_c}] \quad \text{D.7}$$

- **(De Paepe & Janssens 2003) model:**

  Where,

$$NTU = \frac{\pi h_c D x}{\dot{m} c_p} \quad \text{D.8}$$

$$\epsilon = 1 - e^{-NTU} \quad \text{D.9}$$

Where,

$$\epsilon = \frac{T_{oc} - T_a}{T_g - T_a} \quad \text{D.10}$$

But,

$$\frac{NTU}{L} = Nu\pi \frac{k}{c_p \rho \dot{V}} \quad \text{D.11}$$

$$\Delta p = f \frac{L}{D} \rho \frac{V^2}{2} \quad \text{D.12}$$

$$J_{max.} = \frac{\Delta p_{max.}}{NTU_{min.}} \quad \text{D.13}$$